Pilot study into the molecular mechanisms of canine distemper virus infection

by

Tessa Rossi Schenone

Submitted in partial fulfilment of the requirements for the degree

Magister Scientiae

in the Faculty of Natural & Agricultural Sciences

Department of Biochemistry, Genetics and Microbiology

University of Pretoria

Pretoria

South Africa

19 July 2019

Supervisor: Prof Paulette Bloomer

Co-supervisor: Prof Andrew Leisewitz

Declaration

I, Tessa Rossi Schenone, declare that the dissertation, which I hereby submit for the degree Magister Scientiae at the University of Pretoria, is my own work and has not previously been submitted by me for a degree at this or any other tertiary institution.

Signature: …… Date: 19 July 2019

Ethics statement

The author, whose name appears on the title page of this dissertation, has obtained, for the research described in this work, the applicable research ethics approval from the Animal Ethics Committee of the University of Pretoria.

The author declares that she has observed the ethical standards required in terms of the University of Pretoria's Code of ethics for researchers and the Policy guidelines for responsible research.

Pilot study into the molecular mechanisms of canine distemper virus infection

by

Tessa Rossi Schenone

Supervisors: Prof Paulette Bloomer
Department of Biochemistry, Genetics and Microbiology
University of Pretoria

Prof Andrew Leisewitz
Department of Small Animal Clinical Studies
University of Pretoria

Department of Biochemistry, Genetics and Microbiology

Magister Scientiae

Summary

In order to understand how a disease should be prevented, treated and managed, one must understand both the host and the pathogen, and how they interact with and influence one another. Canine distemper virus (CDV) causes canine distemper, a multisystemic disease that can spread to infect the central nervous system resulting in profound nervous system clinical signs. A myriad of different host species are affected by this virus, with significant variation to be seen in how severely different hosts are affected and how rapidly the disease progresses, even within different individuals of the same host species. Although multiple studies have looked at the virus itself, fewer studies have focused on the host, and particularly the molecular mechanisms of the host response that may underlie the variation in host response to the same virus. In this project I looked at DNA polymorphisms in the SLAM and CD46 host receptors in wild canid and felid species and how this could result in amino acid and ultimately protein differences in these receptors crucial for viral entry into the cell. I found that the DNA and amino acid sequences of canid species grouped separately to those of felid species

in terms of sequence similarity, with small DNA sequence differences resulting in different amino acids between these species. These amino acid differences in turn may partially contribute to different host affinities for CDV at the receptor level by affecting the binding affinity between the virus and the host receptor. The V-domain of the signal lymphocyte activation molecule (SLAM) showed more sequence variability than the selected CD46 exons. Secondly, I compared the gene expression in the brain tissue of healthy dogs to that of dogs infected with CDV. Using RNA sequencing (RNA-Seq) a total of 768 differentially expressed genes were identified between healthy and infected dog brain tissues. Of these, 326 genes were not previously identified by microarray studies that evaluated gene expression associated with CDV infection. It is also worth mentioning that the gene expression differed between different lesion types (as defined histologically) of CDV infection, with certain genes differentially expressed only in each of the lesion types. The variation between lesion types was however smaller than the variation seen between the control versus infected dogs. By looking at both the host differences on a molecular level and studying the differential gene expression in two phases of canine distemper encephalitis, the host-specific differences and variable host affinity observed in CDV infections may be partially explained. This study contributes to improving our understanding of CDV, and the molecular mechanisms in different host species that underlie this disease and its variable manifestations.

Preface

This dissertation, entitled "Pilot study into the molecular mechanisms of canine distemper virus infection", communicates my research project and its most important findings. It was written to fulfil the requirements of the Magister Scientiae degree at the University of Pretoria.

This project formed part of a bigger CDV research project that was undertaken by multiple parties who expressed a keen interest in better understanding the various aspects of CDV, including the virus, the host and environmental factors that contribute to the disease or explains its different severities and varied manifestations. Although my project has quite a large scope for the degree that I am completing, it yielded very interesting information that can be used in future to continue more research into the molecular mechanisms underlying canine distemper virus infections. The target audience for this document and research is the scientific community in general, but more specifically anyone that has an interest in veterinary sciences, virology, epidemiology, host-virus interactions and molecular biology.

This document is formatted according to the editorial and referencing specifications of the scientific, peer reviewed journal *Veterinary Microbiology*. This journal was selected since it focuses specifically on microbes that cause disease in animals and the host response to these diseases. It has an impact factor of 2.09 and is focused at the target audience that this research is aimed at.

Chapter 1 gives a brief introduction about canine distemper virus, the pathology and immunology of the disease it causes and the different manifestations of canine distemper in different host species. This chapter also investigates some previous molecular studies conducted in this field, as well as the advantages of using newer techniques such as RNA sequencing compared to microarray techniques that were previously preferable.

Chapter 2 is the first research chapter, in which differences in the DNA sequences and the resulting amino acid sequences of selected regions of two important CDV receptor genes were studied in different wild canid and felid species. The potential effect of amino acid changes on the receptor protein structure was also evaluated in this chapter.

Chapter 3 focuses on gene expression differences in the brain tissues of healthy dogs compared to that of dogs with different lesion types of CDV infection. Enriched gene ontologies for the differentially expressed genes were also addressed, along with general trends observed for the gene expression patterns in different samples.

Chapter 4 integrates the major findings of the dissertation. The contribution of this study to the field of canine distemper virus research, limitations of the research and future research avenues that stem from this research is addressed.

Acknowledgements

I would like to thank my supervisor and co-supervisor, Prof Paulette Bloomer and Prof Andrew Leisewitz for the opportunity to undertake this project. It was a privilege to work with you both and to get exposure to new techniques and evolving knowledge on this topic. All the feedback and encouragement is much appreciated and the ongoing support through challenging times in the project made all the difference in the world. I was blessed to have been able to learn from such passionate, knowledgeable mentors.

I would like to acknowledge the University of Pretoria for providing the opportunity and the facilities for pursuing this degree. Thank you to Paulette and Andrew for the financial help during the years. I would also like to acknowledge the National Research Foundation (NRF) (grant reference number: CPRR130807726333) and the Institutional Research Theme in Animal Diseases and Zoonosis for bursary and research funding support.

I am indebted to my collaborators who provided me with biological samples, valuable information and invaluable additional data and insight regarding different aspects of canine distemper virus based on their own work. I am particularly grateful to all the veterinarians and assistants who undertook the challenging task of collecting blood samples from the various wild animal species. Thank you also to the SPCA and all the veterinarians and assistants that helped to harvest brain tissues from CDV-infected dogs, as well as healthy control dogs.

A very special thank you to Dr Sarah Clift from the Faculty of Veterinary Science for doing the immunohistochemistry analysis for this project and for continuously assisting me with better understanding the results and canine distemper itself. Not only did you make a significant contribution to the work presented in this dissertation, I also learned so much from you that made this project all the more interesting and enjoyable. Thank you so much to Carel van Heerden for his ongoing assistance with some of the RNA-Seq analysis and for helping me to understand the

bioinformatic analyses required for this project. I also thank Dr Charles Hefer (formerly from the ARC Biotechnology Platform) for his insightful comments that helped immensely to improve Chapter 3.

A word of thanks also to my fellow lab members for their moral support and helpful advice during this process, and for helping me find my academic feet. I have learned so much from this group and they have facilitated my academic and personal growth throughout my postgraduate studies. I would especially like to thank Amanda Maswanganye, who always listened patiently and provided encouragement through the ups and downs.

To my friends Gayle Wall, Kershney Naidoo, Kishen Mahesh, Jaco Maree and Narida Kotze – thank you so much for your tireless support, pep talks and scientific guidance.

To my mom, Carina, I will be eternally grateful for everything that you have sacrificed over the years to give me every opportunity in life and for always supporting me, believing in me and constantly reminding me that anything is possible. To my dad, Herman, who shares my love for science and understood the process better than most. I also have to thank my two great brothers, who always been there for me no matter what.

Last, but not least, to Oscar Rossi. Thank you for being my person, for being there through the frustrations and the joys and for always encouraging me to keep going and to keep learning. Your love for nature and your passion for knowledge is constantly inspiring me and motivated me to persevere until the very end.

Table of Contents

List of Tables

Table 3.3

Summary statistics of RNA-Seq alignment, listing the total number of reads (millions), the total number of mapped reads (percentage of the total number of reads) and the number of annotated mapped reads (millions and as a percentage of the total reads) for each of the twelve samples sequenced. The sample number indicated whether it is a CDV-infected or a control dog (+ for infected, - for control dogs), as well as the region of the brain the sample was taken from (MV: medullary velum and Cb: cerebellum). 120

List of Figures

Chapter 1

Chapter 3

List of Appendices

Appendices

Chapter 1

Canine distemper virus infection: the virus, hosts and current understanding of virus-host interactions

1. Introduction

Canine distemper virus (CDV) is a neurotropic virus affecting a wide range of susceptible species (Martella et al., 2008; Martinez-Gutierrez and Ruiz-Saenz, 2016). Although originally known as a disease affecting mostly dogs and similar canid species, in recent years the host range of CDV seems to be increasing significantly (Appel and Summers, 1995; Deem et al., 2000; Alexander et al., 2010). Several CDV outbreaks over the past three decades, and especially in the last 10 years, have been observed to affect feline species, not previously known to be susceptible to CDV infection (Appel et al., 1994; Terio and Craft, 2013; Martinez-Gutierrez and Ruiz-Saenz, 2016). With disease susceptibility varying not only between different species, but also between individuals of the same species, it is difficult to identify and diagnose canine distemper as there is no one manifestation of this disease (Martella et al., 2008; Amude et al., 2010; Lempp et al., 2014).

The virus itself has been extensively studied, with different genetic lineages identified and new strains detected and evaluated on an ongoing basis (Volz et al., 2013; Avila et al., 2015; Anis et al., 2018). A limited number of studies have however focused on the hosts and the molecular components that could influence the host-virus interactions (Ohishi et al., 2010; Noyce et al., 2013). With the advent of technologies such as DNA sequencing, and more recently RNA sequencing, it has become possible to study species at the molecular level to an extend that was previously unknown (Anders and Huber, 2010; Ozsolak and Milos, 2011; Li et al., 2014b). These technologies are making it possible to evaluate molecular mechanisms underlying various diseases and infections, as well as host susceptibility to these diseases and infections. Gene expression differences can be evaluated in different individuals, or under different conditions and at different times or stages of disease within individuals (Wang et al., 2009; Briggs et al., 2011; Albert et al., 2012; Qeska et al., 2014). This provides researchers with new insight into DNA differences, RNA differences, gene regulation and gene expression differences that underly diseases or infections (Wang et al., 2009; Ohishi et al., 2010; Noyce et al., 2013).

In addition to emerging technologies changing the way that disease and infection is studied, the model organisms used for research are also evolving to be more representative of the species in which specific diseases and infections occur (da Fontoura Budaszewski and von Messling, 2016). The use of domestic dogs (*Canis familiaris*) as a model species has increased since its molecular similarity to specifically humans has been proven useful for studying diseases and the molecular mechanisms underlying different disease manifestations and susceptibility (Mestas and Hughes, 2004; Parker et al., 2010). Canine distemper virus specifically is a disease affecting domestic dogs, but it has a close resemblance to the human measles disease (da Fontoura Budaszewski and von Messling, 2016). The demyelination associated with central nervous system infection of CDV is also very similar to human demyelinating diseases such as multiple sclerosis (MS) (Hodge and Wolfson, 1997; Lassmann, 2013). It for this reason that CDV in domestic dogs have been used as a study model for multiple sclerosis in humans (Hodge and Wolfson, 1997; Van der Star et al., 2012).

Making use of new emerging technologies, specifically RNA sequencing, and more accurate and representative model organisms in research, it is possible to better elucidate how a virus like canine distemper virus is continuously extending its host range and why there is such a significant difference in disease susceptibility between individuals and species (Costa et al., 2010; Roy et al., 2013; Ulrich et al., 2014b). It is however important to remember that neither the host nor the virus exists in isolation, and that virus-host interactions is merely one of many possible factors contributing to disease transmission and host susceptibility (Engering et al., 2013; Nguyen, 2014; Ruiz-Lopez et al., 2014; Williams et al., 2014b).

2. Canine distemper virus: Virus characteristics and diversity

Canine morbillivirus, the etiologic agent of distemper in dogs, belongs to the genus *Morbillivirus*, family *Paramyxoviridae* (Harder and Osterhaus, 1997; Martella et al., 2008). Other members of this genus are associated with high mortality rates in their hosts, including measles virus (MV), rinderpest virus (RPV), peste des petits ruminants virus (PPRV) and the more recently identified marine morbilliviruses, phocine distemper virus (PDV), dolphin morbillivirus (DMV) and porpoise morbillivirus (Chappius, 1995; Martella et al., 2008; Cosby, 2012). Canine distemper virus, the commonly used name for *Canine morbillivirus*, will be used to refer to this virus throughout this dissertation.

2.1 Virus structure and genome

Canine distemper virus contains a non-segmented, single negative-stranded RNA genome enclosed in a helical nucleocapsid, which in turn is enclosed in a lipid envelope (Fig. 1 a and b). Two glycoproteins are embedded in the virus envelope, the hemagglutinin (H) and fusion (F) proteins (Rivals et al., 2007; Martella et al., 2008; Sattler et al., 2014; Yuan et al., 2017). The RNA genome also encodes for a single-envelope-associated protein (M), two transcriptase-associated proteins (the phosphoprotein P and the large protein L) and the nucleocapsid protein (N) which encapsulates and protects the viral RNA. Two non-structural proteins, C and V, are derived from the P gene (Rivals et al., 2007; Anderson and von Messling, 2008; Martella et al., 2008; Cosby, 2012; Sattler et al., 2014; Avila et al., 2015; Yuan et al., 2017).

The H protein is the first protein that attached to receptors on the host cells during infection and it is therefore an important determinant of cellular tropism. Fusion of the virus cell with the host cell is mediated by the F protein. This protein causes the viral envelope to fuse with the host cell membrane, allowing entry of the nucleocapsid into the host cell (Plattet et al., 2005; Anderson and von Messling, 2008; Martella et al., 2008; Avila et al., 2015; Khosravi et al., 2015). The M protein provides an

interface between the virion core and the envelope. It interacts with the C terminals of both the H and F proteins to promote virus infectivity and budding from the host cell. The nucleoprotein, phosphoprotein and the large protein (three structural proteins of the nucleocapsid) and the viral RNA together forms the ribonucleoprotein replication complex (RNP). The large gene (L) encodes the RNA-dependent RNA polymerase. For viral RNA replication and transcription to occur, this protein needs to associate with the N protein through interaction with the P protein to form the enzymatically active RNA polymerase. Lastly, the C and V proteins are responsible for modulating the immune response by inhibiting the interferon system (Rivals et al., 2007; Anderson and von Messling, 2008; Martella et al., 2008; Anderson et al., 2012; Otsuki et al., 2013; Bringolf et al., 2017; Yuan et al., 2017).

The viral H protein attaches to different host cell receptors, primarily the signalling lymphocyte activation molecule (SLAM/CD150) and PVRL4 (nectin 4/poliovirus receptor-related 4) receptors (discussed in more detail later) (von Messling et al., 2001; Tatsuo and Yusuke, 2002; Delpeut et al., 2014a; Alves et al., 2015; Liszewski and Atkinson, 2015; Lin and Richardson, 2016). Upon binding of the viral H protein to these receptors, a conformational change occurs in the F protein, which allows fusion of the viral envelope with the host cell membrane. The nucleocapsid can then enter the host cell and once viral RNA-dependent RNA polymerase is expressed, negative-sense RNA is transcribed into positive-sense RNA, which can be translated into viral proteins (refer to Fig. 1 c for a schematic representation of this process) (Martella et al., 2008; Yuan et al., 2017). The negative-sense RNA is replicated while virus proteins are made, allowing new virus particles to be formed. New viral particles assemble near the cell membrane and are then released through budding in order to infect neighbouring cells (Martella et al., 2008; Bringolf et al., 2017).

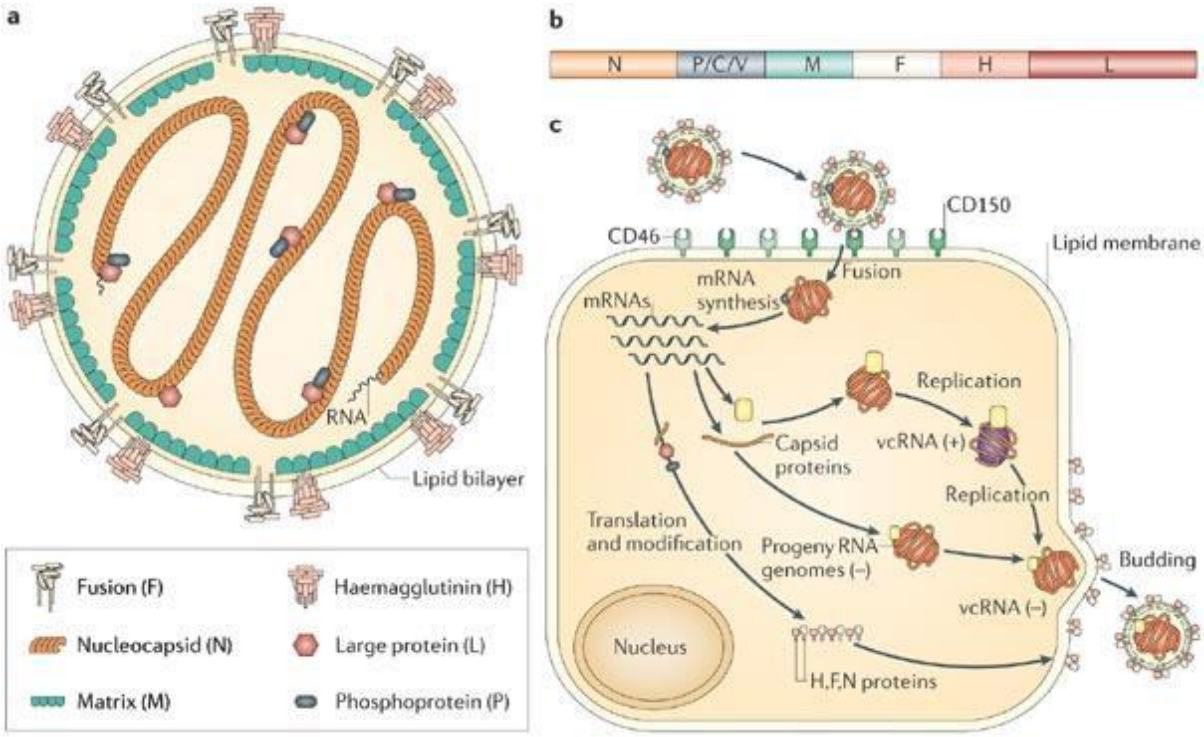

Fig. 1.1 a. A schematic representation of the structure of canine distemper virus, and the viral proteins with their relative positions in the virus particle. **b.** A simplified diagram showing the genes encoded for by the CDV RNA genome. **c.** Representation of the basic mechanism by which host cells are infected with CDV and how viral RNA is replicated and transcribed to be translated into viral protein (copyright permission obtained from Elsevier publishers) (Moss and Griffin, 2006).

2.2. Host range

Morbilliviruses can adapt to new cellular environments, allowing these viruses to infect species other than just their original host species. Canine distemper virus specifically infects a wide range of carnivore hosts, including domestic dogs. Evidence of CDV infection has been shown in mammalian species from the Canidae, Mustelidae, Procyonidae, Ursidae and Viverridae families (Appel and Summers, 1995; Barrett, 1999; Alexander et al., 2010; Beineke et al., 2015; Loots et al., 2016; Martinez-Gutierrez and Ruiz-Saenz, 2016). The disease has also been detected in captive and free-ranging large felids and in captive primates (Deem et al., 2000; Martella et al., 2008; Cosby, 2012; Nagao et al., 2012; Beineke et al., 2015; Feng et al., 2016a; Feng et al., 2016b; Loots et al., 2016;

Zhang et al., 2017). Canine distemper virus has spilled over between domestic and/or feral dog populations and wild species, leading to mass mortalities in several species, such as in the African wild dog (*Lycaon pictus*), bat-eared foxes (*Otocyon megalotis*), lions (*Panthera leo*), spotted hyenas (*Crocuta caspica*) and raccoon dogs (*Nyctereutes procyonoides*) (Deem et al., 2000; Alexander et al., 2010; Kapil and Yeary, 2011; Woodroffe et al., 2012; Beineke et al., 2015; Belsare and Gompper, 2015a; Viana et al., 2015; Marescot et al., 2018; Weckworth, 2018).

Various mechanisms contribute to host switching or adaptation of CDV to new hosts. For CDV to infect another species the specific cell entry receptors that allow the virus to bind to host cells must be present in the relevant cell types and tissues of the potential new host (Barrett, 1999; von Messling et al., 2001; von Messling et al., 2004; von Messling et al., 2006; Goller et al., 2010; Cosby, 2012; Beineke et al., 2015; Nikolin et al., 2016). The H protein is especially important in cross-species infection of morbilliviruses, as it is the main determinant for initial binding to the host cell entry receptors (Tatsuo and Yusuke, 2002; von Messling et al., 2004; von Messling et al., 2005; von Messling et al., 2006; Martella et al., 2008; Ke et al., 2015). It can also act as a predictor of zoonotic infection because of its role in the host-virus interaction (Bean et al., 2013; Volz et al., 2013; Weckworth, 2018).

Adaptation to a new host may or may not require the selection of virus H protein variants, depending on the degree of conservation of receptor proteins across host species (von Messling et al., 2001; Tatsuo and Yusuke, 2002). The antigenic region of the CDV H protein is crucial in eliciting the binding of B-cell and T-cell epitopes (Appel and Summers, 1995; Harder and Osterhaus, 1997; Barrett, 1999; Alexander et al., 2010; Beineke et al., 2015; Martinez-Gutierrez and Ruiz-Saenz, 2016). Any changes in this region can therefore change the severity of the immune response elicited, resulting in different disease presentation and severity in different host species (Martella et al., 2008; Sekulin et al., 2011; Sattler et al., 2014; Yuan et al., 2017).

Specific residues in the H protein of CDV have been implicated in SLAM receptor binding. Adaptations at these receptor-binding sites have been associated with the adaptation of CDV to hosts other than domestic dogs. Two residues in the receptor-binding region of the SLAM receptor, residues 530 and 549, have been shown to be under strong positive selection (Deem et al., 2000; Nikolin et al., 2012b; Sattler et al., 2014; Loots et al., 2016; Yi et al., 2016). Changes in these residues could affect the affinity of the interaction between the CDV H protein and SLAM receptors in different host species (Appel and Summers, 1995; von Messling et al., 2001; Tatsuo and Yusuke, 2002; Beineke et al., 2015; Lin and Richardson, 2016; Martinez-Gutierrez and Ruiz-Saenz, 2016).

Another factor that could potentially allow CDV to adapt to new hosts is recombination of its RNA genome, although this acts to a lesser extent in single-stranded negative-sense RNA viruses compared to other RNA viruses (Altizer et al., 2003; Yuan et al., 2017; Weckworth, 2018). Some recombination has been observed in the F gene of CDV, which could influence tropism by altering interactions of the F protein with host tissue-specific proteases (McCarthy et al., 2007; Anderson and von Messling, 2008; Cuthill and Charleston, 2013; Avila et al., 2015; Viana et al., 2015). Despite this observation, recombination levels in paramyxoviruses are generally low and it is therefore unlikely that this mechanism contributes significantly to host switching in CDV, except when it affects the glycoprotein genes (Cuthill and Charleston, 2013; Magiorkinis et al., 2013; Viana et al., 2015)7b). Antigenic drift (accumulation of mutations within the viral genes due to the decreased proofreading activity of viral RNA polymerases during replication) seems to be the most likely in contributing to changes in the genes most important in infecting novel hosts (Harder and Osterhaus, 1997; Cuthill and Charleston, 2013; Pybus et al., 2013; Volz et al., 2013).

It is however important to note that other viral proteins also play an important role in host switching, since a new host species can pose different barriers to viral replication, transcription and even virus maturity. The P protein is suggested to be essential for virulence, since it forms part of the RNA polymerase complex (Rivals et al., 2007; Martella et al., 2008; Nikolin et al., 2012a). Reduced virus

replication occurred *in vitro* when amino acid substitutions were made in the P, V and M proteins or by truncation of the C protein (Anderson and von Messling, 2008; Martella et al., 2008; Anderson et al., 2012; Otsuki et al., 2013; Bringolf et al., 2017).

Cuthill and Charleston (2013) showed that the success of host switching of a virus diminishes with phylogenetic distance between the current and new host. Small phylogenetic distances seem to present lower barriers to host switching, whereas these barriers potentially increase with increased phylogenetic distance (Harder and Osterhaus, 1997; McCarthy et al., 2007; Cosby, 2012; Cuthill and Charleston, 2013; Martinez-Gutierrez and Ruiz-Saenz, 2016). These observations could be related to evolutionary factors, such as co-evolution between hosts and their pathogens, although this correlation has not been conclusively proved (Kameo et al., 2012; Godfrey, 2013; Nguyen, 2014).

2.3 Phylogenetic relationships

The H gene of canine distemper virus has often been used in the characterization of field strains of CDV, since it shows the greatest genetic variation (about 10% amino acid variation) of the six structural CDV proteins (Ke et al., 2015; Liao et al., 2015). The current classification of distinct viral lineages is based on genetic variability and phylogenetic relationship of the H-protein, with twelve main lineages existing that follow a geographical pattern. These lineages include America I, America II, Asia I and II, South America I/Europe, Europe wildlife, South America II, South America III/Columbian, North America I and II, Arctic-like, Rockborn-like, South Africa and East Africa (Martella et al., 2008; Woma et al., 2010; Sarute et al., 2013; Budaszewski Rda et al., 2014; Panzera et al., 2014; Ke et al., 2015; Panzera et al., 2015; Nikolin et al., 2016). The greatest genetic diversity occurs between vaccine strains and other CDV lineages (von Messling et al., 2001; von Messling et al., 2004; Martella et al., 2008; Nikolin et al., 2012b; Ke et al., 2015). Individual variations in certain CDV strains, rather than properties inherent to given lineages, could account for differences in virulence and cell tropism observed for some strains (von Messling et al., 2001; von Messling et al., 2004; Martella et al., 2008; Woma et al., 2010; Nikolin et al., 2012b; Ke et al., 2015). Fig. 1.2

illustrates the phylogenetic relationships between CDV lineages determined according to H gene variation (Sarute et al., 2013).

Another study evaluated the effectiveness of using the signal peptide of the F protein (Fsp) region of the CDV genome for constructing phylogenetic relationships between lineages (Sarute et al., 2013). The dataset obtained from this study showed that strains clustered into the same lineages as those identified based on variation in the H gene. This region could therefore potentially be useful in rapidly identifying CDV field strains, since it is easier to amplify and it can successfully be compared between lineages (Sarute et al., 2013; Panzera et al., 2015).

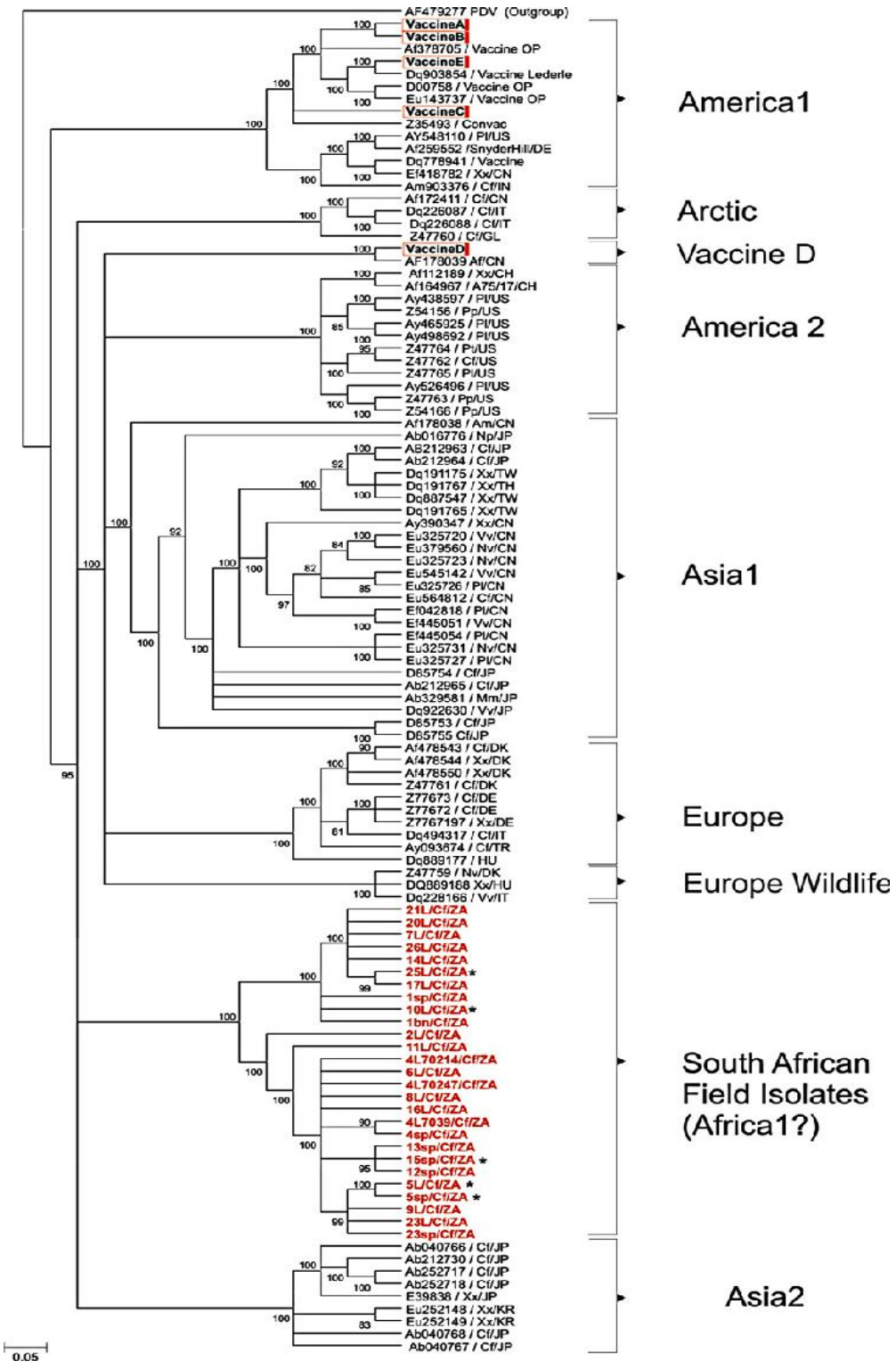

Fig. 1.2: A rooted cladogram of the complete H gene amino acid sequences of CDV and PDV (outgroup), as determined by Bayesian inference. The GenBank accession numbers/species from which the isolate was obtained/ countries of origin are indicated. South African isolates from dogs with a history of vaccination are indicated with an asterisk (copyright permission obtained from Elsevier publishers) (Panzera et al., 2015).

2.4 Transmission between animals

Canine distemper virus is an enveloped virus and it is quickly inactivated in the environment. This virus is therefore usually transmitted through direct animal-to-animal contact or by exposure of a host to infectious aerosol or respiratory secretions (coughing, sneezing, barking, licking) and other bodily excretions (urine and faeces) (Appel and Summers, 1995; Barrett, 1999; McCarthy et al., 2007; Alexander et al., 2010; Magiorkinis et al., 2013; Beineke et al., 2015). Virus-contaminated food and water bowls, garbage, compost piles and organic materials can also allow transmission of CDV between hosts. Some other disease-causing contacts include chasing, mating, fights, simultaneous and sequential feeding events at carcasses and grooming (McCarthy et al., 2007; Martella et al., 2008; Kapil and Yeary, 2011; Kameo et al., 2012; Beineke et al., 2015; Diaz et al., 2016).

Wildlife CDV cases increase during the summer and spring, since juveniles are more susceptible to infection (Weed and Gold, 2001; McCarthy et al., 2007; Tompkins et al., 2011; Kameo et al., 2012; Flacke et al., 2013; Magiorkinis et al., 2013). There is an age-related susceptibility of hosts to CDV infection, resulting from a decline in maternally derived immunity as animals mature (Amude et al., 2010; Maes et al., 2014; Diaz et al., 2016; Buragohain et al., 2017). This simply means that young pups are usually protected by passive immunity offered by maternal antibodies. Adult dogs, however, need the protection offered by vaccine immunization because they no longer have passive immunity (Beineke et al., 2009; Amude et al., 2010; Buragohain et al., 2017).

Persistence of canine distemper virus can occur in cases where multiple competent hosts occur in the same region or habitat (Iwatsuki et al., 1999; Almberg et al., 2010; Suzuki et al., 2015). This can pose a threat, especially dangerous to endangered species or species with small population sizes, as CDV infection can significantly decrease these population sizes (Appel and Summers, 1995; Van Moll et al., 1995; Alexander et al., 2010; Nikolin et al., 2012b; Beineke et al., 2015; Suzuki et al., 2015).

2.5 Recent epidemics

The transmission and epidemiology of CDV can be complex due to its wide host range. Domestic dogs have been considered to be the primary reservoir of CDV and it has been suggested that transmission occurs between free-ranging, unvaccinated dogs or incompletely vaccinated dogs and wildlife populations (Acosta-Jamett et al., 2011; Kapil and Yeary, 2011; Tompkins et al., 2011; Prager et al., 2012b; Ohishi et al., 2014; Viana et al., 2015; Weckworth, 2018). Cyclical outbreaks of distemper occur in various canid hosts as a result, and increasingly in non-canid hosts too (McCarthy et al., 2007; Tompkins et al., 2011; Kameo et al., 2012; Flacke et al., 2013; Suzuki et al., 2015).

Canine distemper has contributed to population declines in various carnivore species, including grey wolves, coyotes, pumas, sea otters, and African wild dogs. The last wild population of black footed ferrets was wiped out in 1985 due to CDV infection (Chappius, 1995; McCallum and Dobson, 1995; Timm et al., 2009; Kapil and Yeary, 2011; Woodroffe et al., 2012; Beineke et al., 2015). Both the African wild dog Conservation Trust and the Zambian Wildlife Authority are developing conservation management strategies for critically endangered species that may be increasingly threatened by CDV infection. Some of the focus species include African wild dogs, African lions, bat-eared foxes, and leopards (McCarthy et al., 2007; Alexander et al., 2010; Prager, 2010; Tompkins et al., 2011; Prager et al., 2012b; Viana et al., 2015).

Thousands of seals (*Phoca sibirica*) in Lake Baikal died in 1987 as a result of a CDV strain most closely related to a CDV strain isolated from dogs and ferrets in Germany (McCarthy et al., 2007; Siebert et al., 2013). An outbreak in North American large captive cat species caused multiple deaths in 1991, and similarly in the lion population from the Serengeti Park in 1993 (Appel et al., 1994; McCarthy et al., 2007; Kameo et al., 2012; Suzuki et al., 2015; Martinez-Gutierrez and Ruiz-Saenz, 2016; Sadler et al., 2016; Weckworth, 2018). During the outbreak in the Serengeti Park, multiple other canid species were also infected, including the spotted hyena (*Crocuta crocuta*) and the bat-eared fox (*Otocyon megalotis*) (Haas et al., 1996; Carpenter et al., 1998; Cleaveland et al., 2000;

Goller et al., 2010; Nikolin et al., 2016). Feral dogs living in the surrounding area are often unvaccinated and experience periodic CDV outbreaks and may therefore have been the primary reservoir for this outbreak (Cleaveland et al., 2000). Hyenas and possibly foxes were likely the amplifying species, spreading CDV to various carnivores throughout the park (Haas et al., 1996; Carpenter et al., 1998; Cleaveland et al., 2000; Goller et al., 2010).

Although CDV is not clinically recognised in domestic cats, various cases have been reported where large felids proved to be susceptible to the virus (Appel et al., 1994; Harder et al., 1995; Nagao et al., 2012; Terio and Craft, 2013; Avendano et al., 2016; Zhang et al., 2017; Sulikhan et al., 2018; Weckworth, 2018). African lions of the Serengeti are the most extensively studied, mainly as a result of the aforementioned outbreak (Harder et al., 1995; Carpenter et al., 1998; Nikolin et al., 2016). A Brazilian study focused on two state parks with the aim of determining the prevalence of CDV in wild felid populations, including jaguars, tigers and pumas (Appel et al., 1994; Konjević et al., 2011; Nagao et al., 2012; Seimon et al., 2013; Terio and Craft, 2013; Avendano et al., 2016; Zhang et al., 2017; Sulikhan et al., 2018).There seems to be a correlation between infected wild felids and their proximity and association with unvaccinated, infected domestic dogs in surrounding regions (Cleaveland et al., 2000; Terio and Craft, 2014).

A number of CDV outbreaks have occurred in Rhesus monkeys (*Macaca culatta*) at a monkey breeding farm in China in 2006. Of the more than 10 000 monkeys that contracted the disease, over 4 250 died (Sakai et al., 2013; Feng et al., 2016a). This high mortality suggests that CDV has increased virulence in monkeys. Characterising strains from these outbreaks are especially important, since adaptation of the virus to non-human primate receptors poses a potential threat of adaptation of CDV to human cell receptors (Sakai et al., 2013; Feng et al., 2016a).

2.6 Vaccination and prevention

At present there is no cure for canine distemper, but current vaccines have proved to be quite effective in providing protection against CDV in domestic dogs if properly administered (Chappius, 1995; Belsare and Gompper, 2015b; Bi et al., 2015). Most vaccine strains were isolated in the 1930s and have not changed in the past 60 years, even though there is potential for antigenic variants of CDV to emerge (Belsare and Gompper, 2015b). Several different vaccine strains have been used to elicit long-lasting protective immunity in dogs, most of these are of the America-1 (Onderstepoort) lineage and it is not known if these strains continue to circulate in nature (Chappius, 1995; Martella et al., 2008; Sato et al., 2011; Belsare and Gompper, 2015b).

The two main vaccines currently used are modified live vaccines (MLV) and recombinant canary pox vectored canine distemper virus vaccines (CDV) (Chappius, 1995; Sato et al., 2011; Belsare and Gompper, 2015b). The recombinant vaccine has the advantage of being effective and safe for use, without the introduction of a live virus that could replicate and spread to other susceptible hosts. The virus vector used for the recombinant vaccine does not replicate efficiently in mammalian cells and it is also more likely to produce immunity in puppies that have not cleared maternal antibodies (Chappius, 1995; Sato et al., 2011; Belsare and Gompper, 2015b). There is concern that new genetic variants of CDV may be associated with changes in pathogenesis or immune evasion in dogs vaccinated with current vaccines (Chappius, 1995; Sato et al., 2011; Wilson et al., 2014; Belsare and Gompper, 2015b; Wahldén et al., 2018). Ongoing surveillance, studies of genetic and antigenic drift in circulating strains and molecular analysis of emerging CDV variants is necessary to ensure that vaccines remain potent and effective in preventing CDV infection (Chappius, 1995; Demeter et al., 2010; Sato et al., 2011; Buczkowski et al., 2012; Belsare and Gompper, 2015b; Yi and Cheng, 2015).

Unfortunately, when used in wildlife animals some vaccine strains retain their pathogenicity, making large-scale vaccination of wild animals impractical (Chappius, 1995; Demeter et al., 2010; Sato et al., 2011; Belsare and Gompper, 2015b). Other problems associated with current CDV vaccines are

the potential of vaccine strains to retain their pathogenicity when administered in conjunction with canine adenovirus-type 1 (Durchfeld et al., 1990; Martella et al., 2011; Sato et al., 2011; Kapil and Neel, 2015; de Fontoura Budaszewski et al., 2016). Vaccine strains may also revert to their initial virulence during immune depression induced by stress or infection with concomitant diseases (Sato et al., 2011; Buczkowski et al., 2012).

In recent year, a number of studies have evaluated the immunogenic effectiveness of different DNA vaccines, with most of these vaccines making use of a vector containing the CDV nucleocapsid, fusion and hemagglutinin genes. Some of these DNA vaccines have elicited a significant immune response both in mice, mink and in domestic dogs, with at least three studies showing robust protective immunity provided by DNA vaccines (Cherpillod et al., 2000; Jensen et al., 2009; Nielsen et al., 2012).

In young pups, lingering passive immunity of maternal origin poses a problem to vaccination in that it could prevent active immunisation upon administration of the vaccine (Martella et al., 2008; Wilson et al., 2014; Belsare and Gompper, 2015b). To overcome this problem, pups should be vaccinated at 6-8 weeks of age and again after 2-4 weeks (Martella et al., 2008; Wilson et al., 2014; Belsare and Gompper, 2015b; Kapil and Neel, 2015). Although vaccine-induced disease is always suspected in dogs that develop distemper shortly after vaccination, vaccine failures are mostly attributable to incorrect vaccination protocols or to vaccine alteration after improper storage (Chappius, 1995; Belsare and Gompper, 2015b).

Hygiene measures should be used along with immunisation to ensure prevention of CDV infection (Chappius, 1995; Belsare and Gompper, 2015b). Unvaccinated puppies should be kept away from other dogs and infected dogs should be completely isolated to prevent spread of the virus. Efficient disinfection protocols in the environment, especially in kennels and shelters, are especially important (Chappius, 1995; Belsare and Gompper, 2015b; Yi and Cheng, 2015). Benzalkonium chloride can be used to inactivate canine distemper virus if used for 10 minutes at room temperature. Disinfection

with 70% ethanol is also effective in inactivating CDV (Martella et al., 2008; Morens et al., 2011; Carvalho de Lima and Lallo, 2013; Engering et al., 2013).

Treatment strategies focus on treating the clinical signs of distemper and preventing secondary bacterial infections, rather than curing the disease. Antiviral drugs are not commercially available, but CDV replication can be inhibited by using the purine nucleoside analogue Ribovirin (Martella et al., 2008). It has also been suggested that retinoic acid could decrease the extent of immune depression that results from distemper and flavonoids and phenolic acids have also been proposed as substances that inhibit CDV *in vitro* (Carvalho de Lima and Lallo, 2013).

2.7 Interest in CDV

Even though vaccine-based prophylaxis has thus far been successful in controlling distemper disease, the incidence of CDV-related disease seems to be increasing in canine and carnivore populations worldwide (Haas et al., 1996; Harder and Osterhaus, 1997; Barrett, 1999; Deem et al., 2000; Goller et al., 2010; Martella et al., 2010; Cottrell et al., 2013; Di Sabatino et al., 2014; Beineke et al., 2015; Feng et al., 2016b). Several cases of CDV disease in vaccinated animals and reported increasing emergence of new CDV strains in recent years bring the efficacy of current vaccines and characterisation of circulating strains into question (Demeter et al., 2010; Martella et al., 2011; Sato et al., 2011; Connolly et al., 2013; Belsare and Gompper, 2015b; Park et al., 2015; Wahldén et al., 2018).

Canine distemper is also constantly emerging in new hosts, increasingly in various feline species, and re-emerging in populations where it was previously thought to no longer occur (Appel et al., 1994; Konjević et al., 2011; Nagao et al., 2012; Seimon et al., 2013; Terio and Craft, 2013; Gilbert et al., 2014; Avendano et al., 2016; Weckworth, 2018). Uncontrolled trading of pets, along with poor veterinary care and poor hygiene practices in many developing countries all contribute to increasing the potential for the spread of the virus from domestic dogs into (often threatened) wildlife

populations (Barrett, 1999; Deem et al., 2000; Alexander et al., 2010; Nikolin et al., 2012b; Beineke et al., 2015; Loots et al., 2016; Martinez-Gutierrez and Ruiz-Saenz, 2016).

Canine distemper virus infection has received a lot of attention in recent years for its value as a model for morbillivirus infection in other animals, and in humans. Specifically, it mimic measles virus infection in humans and it has been recognised as a good model for the inflammation and demyelination processes resulting from multiple sclerosis in humans (Sips et al., 2007; Chinnakannan et al., 2013; Lassmann, 2013; de Vries et al., 2014; Mahad et al., 2015; da Fontoura Budaszewski and von Messling, 2016; Lassmann and Bradl, 2017). One hypothesis regarding the aetiology of MS proposes that exposure to CDV increases the risk of MS (Sips et al., 2007; Lassmann and Bradl, 2017).

There is marked geographic variations in the prevalence of MS, and it has been suggested that MS has a long latency period following a critical event likely during childhood or early adolescence. It is therefore possible that one or more environmental exposures during this time may predispose an individual to developing MS later in life (Hodge and Wolfson, 1997; Lassmann, 2013; Lassmann and Bradl, 2017). The possible viral aetiology of MS stems from the fact that individuals are exposed to numerous viruses, including ones that cause demyelination and inflammatory responses, during childhood (Sips et al., 2007; Tselis, 2011; Lassmann and Bradl, 2017). Evidence for the role of virus infection in MS pathogenesis is however indirect and limited and further studies are required to confirm this proposed link (Sips et al., 2007; Tselis, 2011; Mahad et al., 2015; Lassmann and Bradl, 2017).

3. The host: Known host responses and pathogenesis

3.1 Viral infection

Canine distemper virus usually infects its host through the nasal or oral route (Beineke et al., 2009). The lymphoid cells, along with circulating B and T cells, are therefore usually the first to be infected and this is where initial virus replication takes place. This includes tissues of the spleen, thymus, mucosa associated lymphoid tissue (MALT) and lymph nodes (von Messling et al., 2006; Nielsen et al., 2009; Amude et al., 2010; Buragohain et al., 2017). Monocytes and macrophages located along the respiratory epithelium and tonsils are the mains cells targeted by CDV for primary viral replication (von Messling et al., 2004; Beineke et al., 2009; Langedijk et al., 2011). Some hosts may show a delayed disease progression, with the virus persisting in the central nervous system (CNS) following initial infection. This can result in the nervous form of distemper which manifests in overt CNS clinical signs (Bonami et al., 2007; Carvalho et al., 2012).

After the initial rapid replication phase of the virus, the virus is disseminated to various hematopoietic tissues through the lymph and blood vessels. Some of the initial tissues affected by the initial viremic spread includes the thymus, spleen, lymph nodes, bone marrow, MALT, and macrophages in the lamina propria of the gastrointestinal tract and hepatic Kupffer cells (von Messling et al., 2004; Beineke et al., 2009; Nielsen et al., 2009; Langedijk et al., 2011). This stage of disease is usually associated with the immunosuppression so characteristic of CDV infection, with a decreased number of white blood cells and a transient fever often occurring in this stage (Krakowka et al., 1987b; Tipold et al., 2001; von Messling et al., 2004; Beineke et al., 2009).

This is followed by the second viremia, during which high fever, parenchymal and tissue cell infection usually occurs throughout the body (Krakowka et al., 1987b; Schobesberger et al., 2005; Beineke et al., 2009; Pillet and von Messling, 2009). A very wide range of cells and tissues throughout the body is therefore affected by CDV, ranging from cells in the respiratory system, endocrine system,

gastrointestinal and urinary tracts, lymphoid tissues, CNS and vasculature to fibroblasts, thrombocytes and lymphoid cells. Bronchial, endothelial, epithelial and neuroectodermal cells are also affected by canine distemper virus infection (Krakowka et al., 1987b; Grőne et al., 2000; Schobesberger et al., 2005; Beineke et al., 2009; Pillet and von Messling, 2009; Bregano et al., 2010; Perrone et al., 2010; Buragohain et al., 2017).

The signalling lymphocyte activation molecule (SLAM/CD150) cell receptor, found on lymph nodes and multiple other organs, is the primary receptor to which the CDV H protein binds to initiate infection (von Messling et al., 2001; Tatsuo and Yusuke, 2002). The recognition of SLAM receptors by the viral protein is essential for lymphocyte infection and subsequent viral dissemination and induction of immunosuppression (Tatsuo and Yusuke, 2002; von Messling et al., 2006; Ohishi et al., 2010; Khosravi et al., 2015; Sawatsky et al., 2018). This explains the lymphotropism associated with CDV infection. It is also interesting to note that SLAM expression is markedly upregulated upon CDV infection, which could increase virus entry and replication within the host cells (von Messling et al., 2006; Ohishi et al., 2010; Ludlow et al., 2014; Khosravi et al., 2015; Sawatsky et al., 2018).

There are two other important receptors that are involved in the initial interactions with CDV surface antigen that should also be mentioned. The first of these is the cluster of differentiation 46 (CD46) receptor. This receptor is a complement regulatory protein and a membrane cofactor and acts as an inhibitory complement receptor, inhibiting complement activation via the classical pathway (Liszewski and Atkinson, 2015; Lin and Richardson, 2016). Nectin-4 (poliovirus-receptor-like 4 or PVRL-4) is the second of these receptors. It is expressed on various epithelial cells and has been shown to function as a receptor for CDV to gain entry into the cell (Delpeut et al., 2014a, b; Lin and Richardson, 2016).

3.2 Clinical signs and disease progression

Successful infection of a host with CDV depends on the immune response of the host. In many cases the host can launch a sufficiently strong immune response to the initial CDV infection, which can clear the virus rapidly from the host's system (Nielsen et al., 2009; Amude et al., 2010; Buragohain et al., 2017). However, if a weak immune response is present in the host, successful CDV infection is more likely to occur. The respiratory lymphoid tissues form the initial site for primary viral replication, after which the virus is spread to different organs throughout the body through the lymphatic system (von Messling et al., 2004; Nielsen et al., 2009; Amude et al., 2010; Buragohain et al., 2017). Some mild clinical signs may develop following the initial viremic spread, including nausea, lethargy and nasal discharge. These initial clinical signs are usually quite non-specific and can be characteristic of various virus infections and canine distemper is therefore seldom diagnosed during these early stages (Martella et al., 2008; Amude et al., 2010; Buragohain et al., 2017). Clinical signs also vary between individuals, as well as between different dog breeds and between different species, which further complicates diagnosis (Appel and Summers, 1995; Basso et al., 2015; Beineke et al., 2015; Loots et al., 2016).

The typical incubation period of CDV ranges from one to four weeks, but it could also be longer than four weeks. Initial clinical signs include lethargy, dehydration, anorexia and weight loss. This can later be followed by more pronounced clinical manifestations, with clinical signs varying depending on which organ is most severely affected (Beineke et al., 2009; Nielsen et al., 2009; Carvalho et al., 2012). One of the most characteristic signs of CDV infection is the virus-induced immunosuppression, which is characterised by a sudden, rapid decrease in CD4+ lymphocytes that can last up to several weeks (Krakowka et al., 1987b; von Messling et al., 2004; Beineke et al., 2009; Chinnakannan et al., 2013). T-cells are typically more severely affected by this immunosuppression compared to B cells (Krakowka et al., 1987b).

The mechanisms underlying CDV-induced immunosuppression has not been elucidated yet, although different possible mechanisms have been proposed (Krakowka et al., 1987b; Beineke et al., 2009). One of the proposed mechanisms is that the viral N protein has immunosuppressive activity, similar to what has been shown for measles virus (Krakowka et al., 1987b; Schobesberger et al., 2005; Beineke et al., 2009; Chinnakannan et al., 2013; Haralambieva et al., 2013; Sugai et al., 2013; Pan et al., 2014; Svitek et al., 2014). Three to six days after CDV infection, transient fever associated with initial viremia reaches a peak. Clinical signs that may be associated with this stage include loss of appetite, ocular and nasal discharge and inflammation of the tonsils (Krakowka et al., 1987b; Beineke et al., 2009; Pillet and von Messling, 2009). Cell-associated viremia is responsible for the further spread of CDV to the epithelial cells of other organs, approximately six to nine days post infection (Martella et al., 2008; Amude et al., 2010; Carvalho et al., 2012).

Within approximately 10 days after infection, respiratory, intestinal and dermatological signs will appear due to the epithelial localisation of the virus (Beineke et al., 2009; Amude et al., 2010). As the disease progresses, intracytoplasmic eosinophilic inclusion bodies can be observed in the epithelial cells of the skin, bronchi, intestinal tract, urinary tract, bile duct, salivary glands, adrenal glands, CNS, lymph nodes and spleen (Krakowka et al., 1987b; Beineke et al., 2009; Amude et al., 2010). Secondary bacterial infections can occur due to the immunosuppressive effect of the virus, exacerbating clinical signs (Nguyen, 2014). Nasal discharge, coughing, dyspnoea, pneumonia, diarrhoea, vomiting and dermal pustules can be observed. Hyperkeratosis of the foot pads and nose are very common clinical signs in CDV infected dogs (Martella et al., 2008; Beineke et al., 2009; Langedijk et al., 2011; Carvalho et al., 2012; Nguyen, 2014).

If the virus spreads to the central nervous system, neurological signs can be observed approximately from 20 days post infection onwards (Amude et al., 2010; Lempp et al., 2014; Takenaka et al., 2016). Neurological signs may include circling, head tilting, nystagmus, partial or complete paralysis, convulsions and/or dementia. Other typical signs of this stage of CDV infection include chewing gum

movements, ataxia and muscle convulsions (Amude et al., 2010; Lempp et al., 2014; Takenaka et al., 2016). Neurological signs may be delayed in cases where chronic CDV-induced demyelination occurs, with clinical signs only manifesting 40 to 50 days after infection. Canine distemper virus can persist in the CNS, with the disease progressively developing and with worsened clinical signs occurring over an extended period of time (Summers and Appel, 1985; Rima et al., 1987; Vandevelde and Zurbriggen, 1995; Bonami et al., 2007; Rudd et al., 2010; Pan et al., 2013).

3.3 General immune responses

The severity of CDV infection is determined both by the humoral and cell-mediated immune responses, with both contributing to the outcome of the viral infection (Markus et al., 2002; Beineke et al., 2009; Perrone et al., 2010). One of the first serological signs of CDV is the presence of anti-CDV IgM in the host within the first two weeks after infection (Beineke et al., 2009; Perrone et al., 2010). The virus can effective be cleared from the host's system if enough anti-viral nucleoprotein antibodies are produced and if sufficient immune responses are launched to specifically target the envelope protein of the virus. High specificity of the immunoglobulins produced in response to virus infection, specifically those targeted against the viral envelope proteins, is crucial in preventing development of CNS lesions in infected dogs (Iwatsuki et al., 1995; Grŏne et al., 2000; von Messling et al., 2004; Schobesberger et al., 2005; Beineke et al., 2009; Nielsen et al., 2009; Bregano et al., 2010; Perrone et al., 2010; Elia et al., 2015).

Intracellular and extracellular spread of the virus is prevented by the production of neutralising antibodies by the immune system, although prolonged exposure to these antibodies can result in the internalization of viral surface antigens, causing them to disappear from the membrane of infected cells (Iwatsuki et al., 1995; Nielsen et al., 2009; Elia et al., 2015). This can result in inadequate activation of the complement-mediated humoral cytotoxicity due to decreased antigen recognition (Iwatsuki et al., 1995; Beineke et al., 2009; Nielsen et al., 2009; Amude et al., 2010; Elia et al., 2015).

Canine distemper infection causes a combination of endoplasmic reticulum (ER) stress, calreticulin (CRT) fragmentation and re-localisation on the cell surface that contributes to the cytotoxic effects and cell dysfunctions associated with CDV infection (Markus et al., 2002; Beineke et al., 2009; Brunner et al., 2012). Firstly, the viral glycoproteins (H and F proteins) accumulate in the ER of infected cells, triggering ER stress. This in turn causes increased expression of the ER chaperone protein calnexin and the pro-apoptotic transcription factor CHOP/GADD 153. Another ER chaperone protein, CRT is fragmented by CDV and the vasostatin fragment is re-localised on the surface of infected and neighbouring uninfected cells (Tipold et al., 2001; Markus et al., 2002; Schobesberger et al., 2005; Beineke et al., 2009; Brunner et al., 2012).

Cell-mediated immune responses also play a crucial role in determining whether viral clearance will take place or if the virus will persist in the host. A T cell-mediated CDV-specific response is triggered by exposure to CDV, independent of the antibody titre (Krakowka et al., 1987b; Beineke et al., 2009; Shen et al., 2011). The persistence of natural killer (NK) cells and macrophage function form an essential part of antiviral lymphocyte-mediated cytotoxicity (Krakowka et al., 1987b; Beineke et al., 2009; Chinnakannan et al., 2013). A virus-specific humoral immune response can be detected throughout the lifetime of a dog exposed to CDV, while a cellular immune response can only be detected for a short period of time in infected dogs (Beineke et al., 2009).

Canine distemper virus infection can suppress cytokine production in lymphoid cells, especially if a high viral load and viremia is associated with the infection (Markus et al., 2002; Schobesberger et al., 2005; Beineke et al., 2009). A decrease in cytokine expression in blood leukocytes are observed in such cases (Markus et al., 2002; Beineke et al., 2009). The CDV V protein is important for regulating the interferon response during infection, with this protein interfering with the phosphorylation of interferon-receptor-associated kinases Tyk2 and Jak1. This controls the interferon (IFN) signalling pathway by blocking type I and type II IFN-induced gene transcription, which also inhibits downstream-activated pathways (Beineke et al., 2009; Chinnakannan et al., 2013; Svitek et al., 2014).

3.4 Immunosuppression

Canine distemper is usually associated with lymphoid depletion and significant immunosuppression, due to the fact that it is a lymphotropic virus (Krakowka et al., 1987b). Immunosuppression is associated with the loss of lymphocytes, which causes reduces efficacy of both the humoral and cellular immune responses (Krakowka et al., 1987b; Markus et al., 2002; Schobesberger et al., 2005). Various circulating immune cells are therefore depleted, specifically CD4+ T helper cells, CD8+ cytotoxic T cells and CD21+ B cells (Krakowka et al., 1987b; Grőne et al., 2000; Markus et al., 2002; von Messling et al., 2004; Schobesberger et al., 2005). Hosts have an increased susceptibility to secondary infections because of this immunosuppression, with secondary infections potentially worsening the outcome of the CDV infection (Krakowka et al., 1987b; von Messling et al., 2004; Schobesberger et al., 2005).

Although the precise mechanism by which CDV induces immunosuppression is not yet understood, some of the contributing factors have been identified through studies in naturally and experimentally infected hosts (Krakowka et al., 1987b; Schobesberger et al., 2005; Beineke et al., 2009; Perrone et al., 2010; Chinnakannan et al., 2013). Various mechanisms could function together to cause the reduced immune cell circulation. These mechanisms may include the impaired cellular output from lymphoid organs and apoptosis of peripheral blood leukocytes, as well as virus-independent mechanisms of apoptosis causing the death of uninfected lymphocytes (Krakowka et al., 1987b; Schobesberger et al., 2005; Pillet and von Messling, 2009; Bregano et al., 2010; Brunner et al., 2012; Coughlin et al., 2013).

Diminished immune function during the early stages of disease is promoted directly through virus-induced apoptosis resulting from over-activation of the innate immune system during the initial viremia (Schobesberger et al., 2005; Pillet and von Messling, 2009; Bregano et al., 2010). Since viral antigen is located in T-cell-dependent areas, CD4+ lymphocytes are usually the first cells to be affected, followed by CD8+ cells loss. It is very likely that mechanisms other than direct viral

infection of lymphoid tissues cause immunosuppression, as only a portion of cells are infected by CDV and immunological depletion frequently persists even after viral clearance from the lymphoid tissues (Krakowka et al., 1987b; Grőne et al., 2000; Schobesberger et al., 2005; Beineke et al., 2009; Pan et al., 2014). Repopulation of lymphoid tissues require the reconstitution of CD3-, CD4- and CD8-expressing lymphocytes, and the immune system may therefore not recover completely following CDV infection (Krakowka et al., 1987b; Schobesberger et al., 2005).

It is known that SLAM recognition is essential for lymphocyte infection, viral dissemination and for the induction of immunosuppression (Martella et al., 2008; Volz et al., 2013). One way in which CDV potentially impairs cell function of infected cells, and even target these cells for apoptosis, is by relying on the fact that SLAM expression is normally increased upon activation of T and B lymphocytes, monocytes and dendritic cells (Schobesberger et al., 2005; Coughlin et al., 2013; Pan et al., 2014). Antigen presentation may also be impaired during CDV infection, since SLAM is expressed on dendritic cells. This could lead to a less efficient anti-viral immune response (Krakowka et al., 1987b; Coughlin et al., 2013).

Virus proteins and host cell population both modulate the host response and thus together contributes to the extended persistence of immunosuppression. Canine distemper virus infection of monocytes inhibits interleukin 1 (IL-1) function and impairs antigen presentation (Krakowka et al., 1987b; Grőne et al., 2000; Markus et al., 2002; Coughlin et al., 2013). This in turn leads to decreased B cell differentiation, decreased plasma cell formation and decreased immunoglobulin production. This, along with the increased E2 in mononuclear suppressor cell populations, causes immunosuppression in uninfected cells (Krakowka et al., 1987b; Markus et al., 2002; Pan et al., 2014).

T helper cell function is decreased a result of reduced antigen presentation and this contributes to disturbed germinal centre formation and reduced class switching from IgM to IgG (Krakowka et al., 1987b; Pan et al., 2014). The interaction of the viral N protein with B lymphocytes further contributes to immunosuppression by decreasing IL-12 production (Krakowka et al., 1987b; Pan et al., 2014).

The viral V protein also plays an important part in debilitating the immune system by acting as interferon antagonist, as previously discussed, and by inhibiting the cytokine response activation (Krakowka et al., 1987b; Markus et al., 2002; Chinnakannan et al., 2013). Fig. 1.3 shows some mechanisms of immunosuppression, mainly focusing on impaired antigen presenting functions of cells (Beineke et al., 2009).

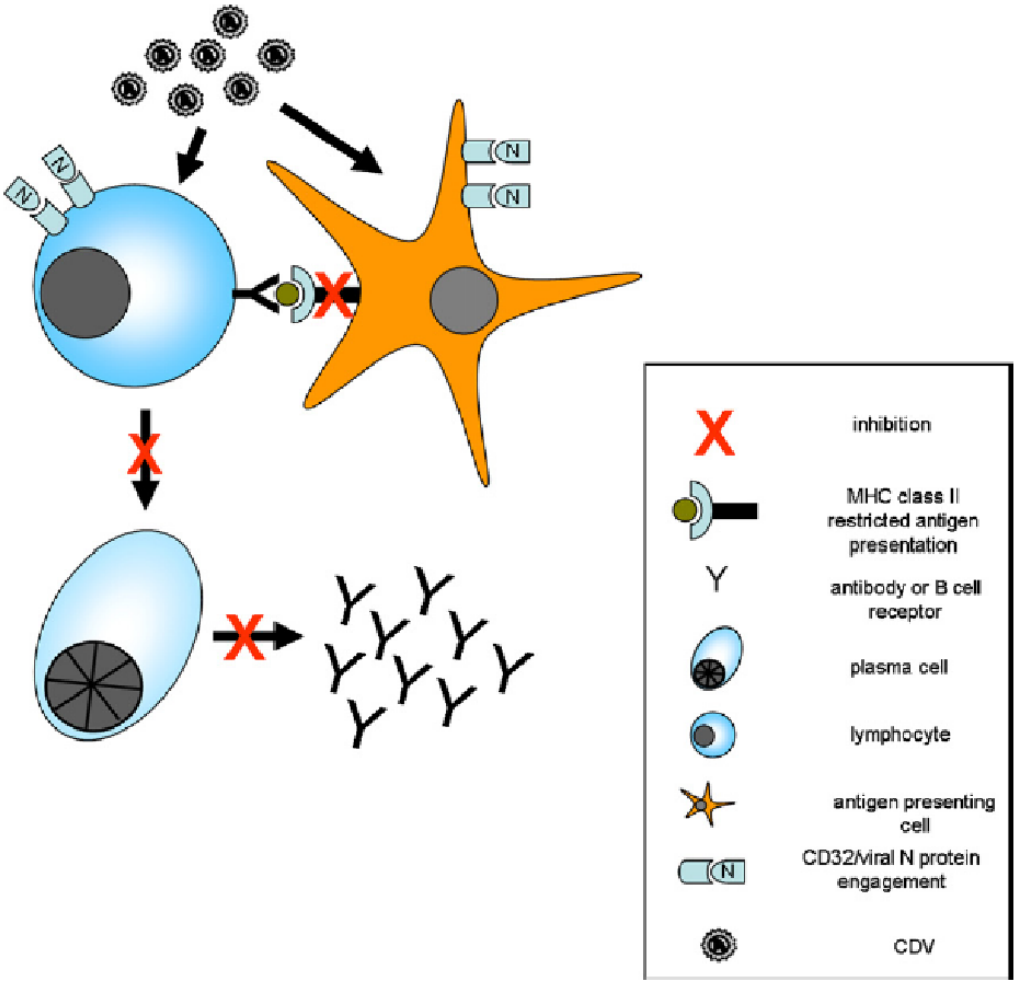

Fig. 1.3 Mechanisms of immunosuppression in CDV-infected dogs. Viral infection and the viral N protein/ CD32 engagement leads to diminished antigen presentation as well as disturbed dendritic cell and B cell maturation within germinal centres. Subsequently, plasma cell formation and immunoglobulin production is significantly reduced (copyright permission obtained from Elsevier publishers) (Beineke et al., 2009).

3.5 Pathology of non-nervous tissues

Different clinical and pathological signs of CDV infection can be detected in different organs of the body following the initial viremic spread, including cytoplasmic and intranuclear inclusion bodies and viral antigen presence in various tissues (Nielsen et al., 2009; Amude et al., 2010; Behera et al., 2014; Buragohain et al., 2017). The infection of different tissues by the virus is characterised by different clinical signs, as well as different disease severities. For example, infection of the respiratory tract is often associated with mucopurulent rhinitis, interstitial pneumonia and necrotizing bronchiolitis. If the virus has spread to the gastrointestinal tract (GIT), depletion of Peyer's patches may be observed (Martella et al., 2008; Amude et al., 2010; Elia et al., 2015). Pustular dermatitis may also be observed on the thighs and abdomen, or on the ear pinnae in some cases. Multinucleated syncytial cells may be seen in affected tissues (Martella et al., 2008; Beineke et al., 2009; Behera et al., 2014; Buragohain et al., 2017). Another possible indication of CDV infections is hyperkeratosis of the footpads and nasal planum, as CDV can disrupt the differentiation of keratinocytes (Cornwell et al., 1965; Martella et al., 2008; Beineke et al., 2009).

Lymphoid tissues often show lymph node swelling, depletion of MALT and reduced thymus size when infected with CDV. A depletion of T and B cell compartments and enlargement of reticular cells are also sometimes observed in infected lymph nodes (Krakowka et al., 1987b; Wünschmann et al., 2000; Beineke et al., 2009). Syncytial formation and cell death of immune cells in acute distemper infection can result in the complete loss of secondary lymphoid follicles. The amount of CDV antigen in the affected organ determines the extent of lymphoid depletion, with more antigen being associated with more extensive lymphoid depletion (Krakowka et al., 1987b; Wünschmann et al., 2000; Schobesberger et al., 2005; Beineke et al., 2009; Perrone et al., 2010). In dogs with persistent CDV infection, or those recovering from infection, there is some repopulation of lymphoid tissues and increased presence of germinal centres in lymphoid tissues (Krakowka et al., 1987b; Wünschmann et al., 2000; Beineke et al., 2009; Perrone et al., 2010).

The detrimental effect of CDV on lymphoid tissues can be observed for an extended period of time, with reduced CD-5 and IgG expressing cells and virus antigen in dendritic cells observed even after clearance of CDV from lymphoid tissues (Krakowka et al., 1987b; Wünschmann et al., 2000; Schobesberger et al., 2005; Beineke et al., 2009; Perrone et al., 2010). Dendritic cells act as the primary carrier of the virus during chronic CDV infection, possibly because virus infection could prevent terminal differentiation of these cells into effector cells. This delays the repopulation of peripheral lymphoid tissues, causing a persistent immunosuppressive effect on the host (Krakowka et al., 1987b; Beineke et al., 2009; Coughlin et al., 2013).

3.6 Central nervous system infection

Canine distemper virus can spread to the central nervous system if the virus is not cleared shortly after infection takes place (Vandevelde and Zurbriggen, 1995; Beineke et al., 2009; Carvalho et al., 2012). This can result in the manifestation of neurological signs, with the extent of infection and the occurrence of CNS lesions depending on the CDV strain, as well as the age and the immune status of the infected animal. Clinical signs are usually delayed in cases where the virus has spread to the central nervous system (Beineke et al., 2009; Rudd et al., 2010; Carvalho et al., 2012; Pan et al., 2013).

Localisation of CDV in the CNS results in acute demyelination, and although some dogs may recover and display lifelong residual signs of persistence, most dogs with nervous signs (signs of CNS infection) usually die within two to four weeks after infection (Rudd et al., 2010; Carvalho et al., 2012; Pan et al., 2013). Demyelination (loss of myelin surrounding neurons) causes prominent lesions in the brain of infected dogs, with different degrees of demyelination observed depending on the severity and progression of viral infection (Vandevelde and Zurbriggen, 2005; Beineke et al., 2009; Pan et al., 2013).

Demyelination associated with acute infection is not related to inflammation, but rather due to decreased myelin synthesis in CDV-infected oligodendrocytes. This is caused by metabolic dysfunction and virus-induced activation of microglial cells, with no perivascular cuffing observed (Vandevelde and Zurbriggen, 1995, 2005; Bonami et al., 2007; Beineke et al., 2009; Bregano et al., 2010). If CDV persists in CNS tissues, the inflammatory reaction resulting from CDV-specific immune responses results in demyelination and demyelination in this case is therefore associated with the presence of inflammatory cells (Vandevelde and Zurbriggen, 1995, 2005; Beineke et al., 2009; Carvalho et al., 2012; Pan et al., 2013; Spitzbarth et al., 2016). Although the exact mechanisms underlying chronic demyelination has not yet been elucidated, one of the possible causes is the increased inflammatory reaction caused by the interactions between macrophages and virus-induced antibodies (Rima et al., 1987; Markus et al., 2002; Beineke et al., 2009; Carvalho et al., 2012). Perivascular cuffing with lymphocytes, plasma cells and monocytes are a feature in areas of chronic demyelination. Signs of chronic CDV infection in the CNS include myoclonus, nystagmus, ataxia, postural reaction deficits and tetra paresis or paralysis. Neurological signs often occur in the absence of systemic clinical signs (Vandevelde and Zurbriggen, 1995; Wünschmann et al., 1999; Vandevelde and Zurbriggen, 2005; Carvalho et al., 2012).

3.6.1 Neuroinvasion and neurotropism of CDV

Neuroinvasion of CDV occurs mainly through the hematogenous route, with spread along the cerebrospinal fluid (CSF) pathway as reflected by infection of the ependymal and subependymal white matter (Krakowka, 1989; Vandevelde and Zurbriggen, 1995; Rudd et al., 2006; Bonami et al., 2007; Rudd et al., 2010; Spitzbarth et al., 2016). Canine distemper virus spreads to the CNS through an initial cell free viremia, followed by cell-associated spread. Lymphocyte-bound viruses and free viruses both invade vascular endothelial cells in the meninges, choroid plexus cells and the ependymal cells. The virus therefore enters the brain through the cerebrospinal fluid (CSF) (Krakowka et al., 1987a; Krakowka, 1989; Techangamsuwan et al., 2011). Canine distemper virus

mainly targets astrocytes in the brain, with spread in astrocytes not requiring infectious particles. The spread occurs cell to cell through intercellular fusion activity, mediated by the viral F protein. It is very likely that CDV might make use of gap junctions to spread to the astrocytes syncytial network, since viral spread between neighbouring cells occur in very short intervals of time (Summers and Appel, 1985; Krakowka et al., 1987a; Krakowka, 1989; Rudd et al., 2010; Techangamsuwan et al., 2011; Pan et al., 2013).

Approximately 6 days post infection viral antigen can be detected in CNS capillaries and venular endothelia. This is followed by viral spread to astrocytic foot process and pericytes at about 8 days post infection (Krakowka, 1989; Vandevelde and Zurbriggen, 1995, 2005; Beineke et al., 2009; Pan et al., 2013; Ulrich et al., 2014a; Spitzbarth et al., 2016). Productive infection of the choroid plexus epithelium can be observed at approximately 10 days post infection, with the release of progeny viruses into the CSF and ependymal infection characterizing this phase. Canine distemper virus seems to enter the CNS in a sequential fashion, with a brief phase of grey matter disease preceding the development of demyelinating leukoencephalitis (DL) in the white matter (Krakowka, 1989; Vandevelde and Zurbriggen, 1995, 2005; Rudd et al., 2006; Carvalho et al., 2012; Pan et al., 2013; Ulrich et al., 2014a; Spitzbarth et al., 2016). During the early phase of infection, lesions can be observed in the region beneath the pia mater, along with CDV antigen positive cells in the pia mater itself and in subjacent grey matter (Summers and Appel, 1985; Techangamsuwan et al., 2011; Carvalho et al., 2012; Pan et al., 2013; Ulrich et al., 2014b).

A significantly bigger amount of CDV RNA relative to viral protein present in the grey matter reflect impaired viral translation, indicating that this method is potentially used because it allows virus infection and spread without immune system detection (Bregano et al., 2010; Rudd et al., 2010; Stimmer et al., 2010; Carvalho et al., 2012; Pan et al., 2013; Ulrich et al., 2014a; Ulrich et al., 2014b). Persistence of the virus in the CNS is therefore mediated by this reduced viral protein production and

by non-cytolytic infection (Krakowka et al., 1987a; Stimmer et al., 2010; Carvalho et al., 2012; Pan et al., 2013). Fig. 1.4 illustrates the spread of CDV in the CNS (Summers and Appel, 1985).

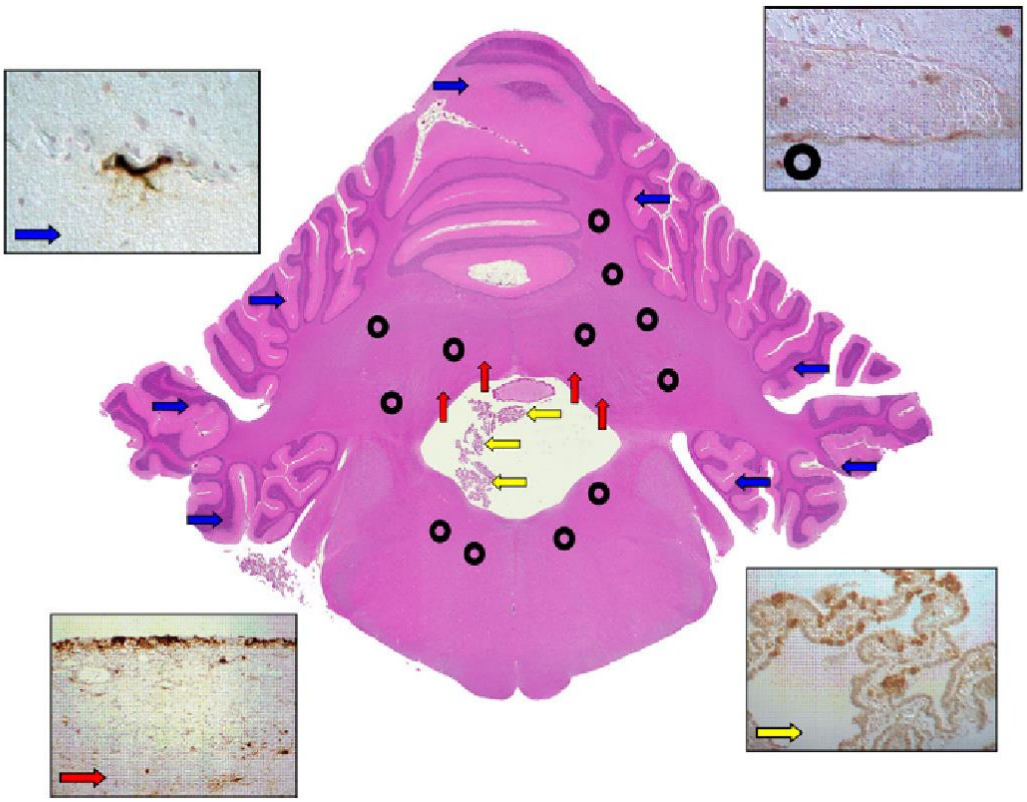

Fig. 1.4 Canine distemper virus (CDV) spread within the CNS with a cross-section view of the cerebellum. Blue arrows: viral spread via infected meningeal cells; black circles: viral spread via infected leukocytes and endothelial cells; yellow arrows: viral spread via infected choroid plexus epithelial cells; red arrows: viral spread via infected ependymal cells. Insets display detection of CDV antigen with a CDV-N-specific monoclonal antibody using the ABC detection method (copyright permission obtained from Elsevier publishers) (Beineke et al., 2009).

The range of CNS cell targeted by CNS infection include oligodendrocytes, astrocytes, microglia, neurons, ependymal cells, choroid plexus cells and aldynoglia (Rudd et al., 2010; Carvalho et al., 2012; Pan et al., 2013). The stage of cellular differentiation of oligodendrocytes could affect the

susceptibility of these cells to CDV infection, with bipolar oligodendrocyte precursor cells which express galactocerobroside seemingly having a higher susceptibility to some CDV strains than mature oligodendrocytes. Oligodendrocytes usually occur in chronic lesions, with demyelination preceding oligodendrocyte loss (Krakowka et al., 1987a; Vandevelde and Zurbriggen, 1995; Rudd et al., 2010; Techangamsuwan et al., 2011; Carvalho et al., 2012; Pan et al., 2013). Contradictory results in oligodendrocyte infection studies emphasizes the need for more studies into the infection process in this cell population (Krakowka et al., 1987a; Krakowka, 1989; Vandevelde and Zurbriggen, 1995; Rudd et al., 2010; Techangamsuwan et al., 2011; Carvalho et al., 2012; Pan et al., 2013).

Astrocytes is the main cell population infected by CDV, making up 95% of all infected cells. Mature astrocytes appear to be less susceptible to infection compared to immature astrocytes (Vandevelde and Zurbriggen, 2005; Rudd et al., 2006; Carvalho et al., 2012; Pan et al., 2013). These cells are especially affected during early CNS infection, with vimentin-positive astrocyte-like cells commonly harbouring the pathogen in advanced lesions (Krakowka, 1989; Vandevelde and Zurbriggen, 1995; Beineke et al., 2009; Bregano et al., 2010; Carvalho et al., 2012).

Central nervous system lesions resulting from CDV infection is usually characterised by infiltrating microglia, macrophages and T lymphocytes, which results in neuronal death and neuronophagia. Perivascular cuffing and intranuclear inclusion bodies are often observed in lesions in neurons and astrocytes (Rima et al., 1987; Krakowka, 1989; Vandevelde and Zurbriggen, 1995, 2005; Pan et al., 2013).

3.6.2 Pathology of CNS distemper

Demyelinating leukoencephalitis (DL) represents the most common CNS manifestation of distemper, with lesions forming in the cerebellar and sometimes cerebral white matter and even in the spinal cord (Summers and Appel, 1985; Beineke et al., 2009; Carvalho et al., 2012). The cerebellar velum, cerebellar peduncles and optic tracts are most often affected by these lesions (Vandevelde and

Zurbriggen, 2005; Carvalho et al., 2012; Spitzbarth et al., 2016). Demyelinating leukoencephalitis lesion progression can be divided into different stages: acute lesions, subacute non-inflammatory lesions, subacute inflammatory lesions, chronic lesions and sclerotic lesions (Vandevelde and Zurbriggen, 2005; Carvalho et al., 2012; Pan et al., 2013; Ulrich et al., 2014b; Spitzbarth et al., 2016).

Focal vacuolisation of the white matter is characteristic of acute lesions, with mild gliosis with few activated astrocytes and macrophages. Vacuolisation results from intramyelin oedema of the subependymal white matter and can be observed as early as 24 days after virus infection (Beineke et al., 2009; Carvalho et al., 2012; Pan et al., 2013; Spitzbarth et al., 2016). These vacuoles proceed to grow in size and number, eventually forming demyelinated plaques characterised by micro- and astrogliosis and the formation of multinucleated giant cells. Mononuclear infiltration is rare during this phase of disease (Krakowka et al., 1987a; Vandevelde and Zurbriggen, 1995; Beineke et al., 2009; Carvalho et al., 2012; Pan et al., 2013; Spitzbarth et al., 2016). However, immune cells can already be observed in acute and subacute non-inflammatory stages of disease. Prominent inflammation and reduced viral protein expression are typically observed during chronic changes (Markus et al., 2002; Rudd et al., 2006; Bregano et al., 2010; Techangamsuwan et al., 2011; Carvalho et al., 2012; Pan et al., 2013).

3.6.2.1 Immunopathology of demyelinating leukoencephalitis

Demyelinating leukoencephalitis resulting from CDV CNS infection occurs as two-staged event. Initially, direct virus-mediated processes contribute to demyelinating leukoencephalitis, with the second phase (plague progression) probably caused by an autoimmune response (Vandevelde and Zurbriggen, 1995; Markus et al., 2002; Vandevelde and Zurbriggen, 2005; Pan et al., 2013; Ulrich et al., 2014b). The number of inflammatory cells present in the CNS increases as the disease progresses, with a low number of inflammatory cells present during the early stages of CNS infection. A significant increase in the influx of blood-borne inflammatory cells takes place as the disease progresses. Cluster of differentiation (CD) 8+ cells are the first lymphocytes which infiltrated the

CNS, mediated by microglia-derived chemokines such as IL-8 (Rima et al., 1987; Markus et al., 2002; Beineke et al., 2009; Bregano et al., 2010; Pan et al., 2013; Spitzbarth et al., 2016). This indicates that antibody-independent cytotoxicity may be involved in both viral clearance and initial lesion development (Vandevelde and Zurbriggen, 2005; Carvalho et al., 2012; Ulrich et al., 2014a; Spitzbarth et al., 2016).

Immune-mediated processes contributing to and associated with an increase in major histocompatibility complex II (MHC II) molecule expression and increased virus protein expression in the CNS are associated with chronic demyelination (Summers and Appel, 1985; Bonami et al., 2007; Bregano et al., 2010; Rudd et al., 2010; Techangamsuwan et al., 2011; Carvalho et al., 2012). Canine distemper virus-induced activation of macrophages in the CNS are triggered in part by non-viral antigens, with overactive macrophages contributing to virus-mediated demyelination in chronic lesions and myelin loss in early lesions. This is partially accomplished by the release of proteolytic enzymes that have myelin damaging effects (Markus et al., 2002; Vandevelde and Zurbriggen, 2005; Beineke et al., 2009; Ulrich et al., 2014b; Spitzbarth et al., 2016). Virus-induced stimulation of macrophages is also accompanied by upregulation of MHCII and adhesion molecule expression, which promotes the release of toxic factors by cells expressing these molecules. This subsequently leads to increased phagocytic activity and oxygen radical production (Wünschmann et al., 1999; Markus et al., 2002; Carvalho et al., 2012; Pan et al., 2013).

The precise role of self-reactive immunity in demyelination remains to be determined, but it is known that the human immune response contributes to the destruction of oligodendrocytes (Rudd et al., 2010; Pan et al., 2013). Autoreactive T cells play a role in the induction of myelin-specific cellular immunity via epitope spreading secondary to myelin damage in the CNS. Approximately seven weeks after infection, there is an influx of CD4+ cells, B cells and CD8+ cells into brain lesions. This is accompanied by a significant intrathecal antibody production by plasma cells (Wünschmann et al., 1999; Rudd et al., 2010; Pan et al., 2013). The intralesional increase in both antibodies and immune

cells is indicative of complement-dependent antibody mediated cytotoxicity and antibody-dependent T-cell cytotoxicity acting in concert to accelerate myelin destruction (Wünschmann et al., 1999; Rudd et al., 2010; Carvalho et al., 2012; Pan et al., 2013).

A prominent upregulation of various pro-inflammatory cytokines has been observed in early CNS lesions, including IL-6, IL-8, IL-12 and TNF-α. Interleukin-8 attracts T cells, promoting antiviral cytotoxicity and exacerbating CNS lesions (Wünschmann et al., 1999; Markus et al., 2002; Rudd et al., 2010; Carvalho et al., 2012; Pan et al., 2013). Tumour necrosis factor-α is expressed mainly in astrocytes and attracts other inflammatory cells to CNS lesions, which in turn causes increased synthesis of more cytokines and thus contributes to pathogenesis of early demyelination. The inappropriate response of anti-inflammatory cytokines along with the increased expression of pro-inflammatory cells cytokines may therefore contribute to the initiation and progression of CDV infection in the CNS (Rima et al., 1987; Wünschmann et al., 1999; Markus et al., 2002; Vandevelde and Zurbriggen, 2005; Rudd et al., 2010; Carvalho et al., 2012; Pan et al., 2013; Ulrich et al., 2014b; Spitzbarth et al., 2016). Fig. 1.5 illustrates some of the proposed immune mechanisms underlying the pathogenesis of chronic lesions in demyelinating distemper (Beineke et al., 2009).

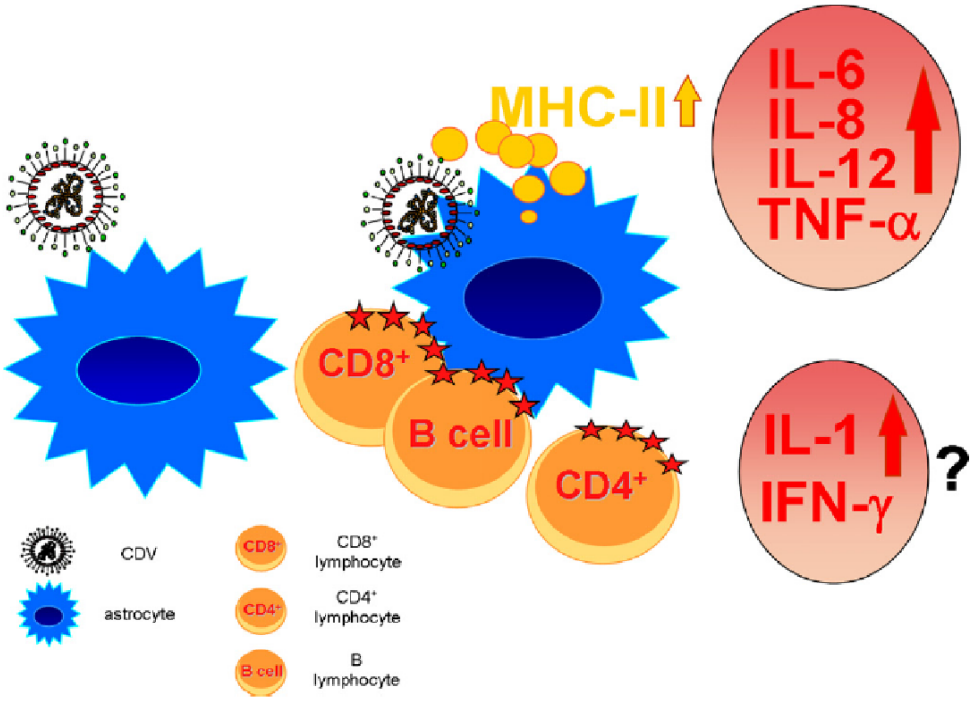

Fig. 1.5 Schematic presentation of the proposed pathogenesis of chronic lesions in demyelinating distemper leukoencephalitis. Following virus infection, reduced viral protein expression can be noticed, coinciding with an increased influx of CD8+, CD4+ and B cells (influx of these molecules are represented by the red stars on the molecules in the representation). Upregulated MHC II expression (showed by the presence of yellow circles surrounding astrocytes) is also observed in resident brain cells, accompanied by a significant increase in the expression of IL-6, IL-8, IL-12 and TNF-α. Thus far the precise role of IL-1 and IFN-ϒ in demyelinating leukoencephalitis has not been elucidated (copyright permission obtained from Elsevier publishers) (Beineke et al., 2009).

3.6.2.2 Crossing the blood-brain-barrier

Disruption of the blood-brain-barrier is essential for the influx of inflammatory cells that contribute to lesion progression (Krakowka, 1989; Vandevelde and Zurbriggen, 1995, 2005). Although only a few studies have looked at the potential mechanisms underlying the crossing of CDV into the blood-brain-barrier, with these studies reaching different conclusions regarding how this may be achieved (Krakowka et al., 1987a; Krakowka, 1989; Carvalho et al., 2012; Spitzbarth et al., 2016).

Astrocytes are the major source of extracellular matrix (ECM) proteins and cell mediator molecules, playing a significant role in maintaining the structural integrity of the CNS. Canine distemper virus targets these cells, which forms a significant part of the blood-brain-barrier, during CNS infection (Krakowka, 1989; Vandevelde and Zurbriggen, 1995, 2005; Pan et al., 2013). The receptor CD44 is expressed on astrocyte cells and is responsible for inducing chemokines and cytokine activation and therefore initiates and perpetuates inflammatory processes. If CDV binds to these receptors, it causes a significant increase in inflammatory responses, which contributes to lesion formation in demyelinating leukoencephalitis (Vandevelde and Zurbriggen, 2005; Beineke et al., 2009; Carvalho et al., 2012; Pan et al., 2013). Astrocytes release matrix metalloproteinases (MMPs) in response to virus infection, which results in cleaving of the ECM and thus opens the blood-brain-barrier and affects myelin in the CNS (Krakowka et al., 1987a; Krakowka, 1989; Rudd et al., 2006; Beineke et al., 2009; Spitzbarth et al., 2016).

Antiviral antibodies have been shown to promote entry of CDV into the brain and reticuloendothelial tissues, with infection of the CNS endothelium preceding invasion of virus positive and negative leukocytes into CNS tissues (Krakowka et al., 1987a; Rima et al., 1987; Krakowka, 1989; Vandevelde and Zurbriggen, 1995; Wünschmann et al., 1999; Rudd et al., 2006; Carvalho et al., 2012; Spitzbarth et al., 2016). Based on this, platelets have been implicated in the initiation of endothelial infection by this virus. Canine distemper virus infected dogs are thrombocytopenic, and platelets contain IgG-virus complexes on their membranes, which further supports this hypothesis (Rima et al., 1987; Carvalho et al., 2012; Spitzbarth et al., 2016). Increased capillary permeability is associated with thrombocytopenia and this could permit direct access of astrocytic foot processes to plasma and leukocyte-bound infectious virus-antibody complexes. In this case viral antibody is not protective, but rather acts to facilitate entry of the virus into CNS tissues (Summers and Appel, 1985; Rima et al., 1987; Wünschmann et al., 1999; Vandevelde and Zurbriggen, 2005; Techangamsuwan et al., 2011; Spitzbarth et al., 2016).

3.7 Persistence and outcome of disease

Multiple factors contribute to the distemper disease severity and outcome, including the strain of the virus, the age and immune status of the animal and the host species involved. Disease manifestation can range from almost no clinical signs to severe disease, with nervous distemper typically being the most severe manifestation of CDV infection (Vandevelde and Zurbriggen, 1995, 2005; Spitzbarth et al., 2016). Spread of CDV to the CNS typically occurs when the initial immune response launched by the host is insufficient to clear the virus from the system, and if the disease progresses to this stage, it could result in the death of the host (Markus et al., 2002; Bregano et al., 2010; Carvalho et al., 2012; Pan et al., 2013).

Neurological disease can persist if there is delayed or diminished antibodies against the viral N protein. A lack of complement-fixing antibodies in response to the viral envelope proteins can also contribute to persistence (Vandevelde and Zurbriggen, 2005; Rudd et al., 2006; Carvalho et al., 2012). Since virus neutralising antibodies modulate the expression of viral antigen, prolonged exposure to these antibodies can further promote viral persistence (Vandevelde and Zurbriggen, 1995; Beineke et al., 2009; Chinnakannan et al., 2013; Pan et al., 2013).

Chronic encephalomyelitis of mature dogs (old dog encephalitis, ODE) occurs when CDV persists in nervous tissues of dogs following infection (Rima et al., 1987; Rudd et al., 2006; Bonami et al., 2007). This typically occurs in dogs with a complete vaccination history, and a range of clinical signs reflecting progressive cortical derangement is associated with it. Multifocal perivascular and parenchymal lymphoplasmacytic encephalitis lesions are found in the cerebral hemispheres in ODE (Krakowka et al., 1987a; Rima et al., 1987; Beineke et al., 2009).

4. Co-infection of other pathogens with CDV infection

Primary pathogen infections resulting in a compromised immune system often make hosts more susceptible to infection by other parasites and can allow different pathogens to co-exist in the host (Nguyen, 2014). Co-infection or secondary infections can make effective diagnosis and treatment of the disease-causing pathogen difficult as it can worsen or alter clinical signs (Aguiar et al., 2012; Nguyen, 2014; Jardine et al., 2018).

Co-infection in a host or in different host populations are influenced by direct competition for resources and/or attachment sites, as well as by indirect competition via host immune responses (Engering et al., 2013; Jamieson et al., 2013). The order of infection (timing of establishment) can change the host's susceptibility to co-infection and could influence the disease outcome. Different hosts can experience different orders of infection due to genetic variability in host or parasite populations, making it difficult to predict disease outcome (Engering et al., 2013; Nguyen, 2014). Different parasite taxa that infect a host can result in different interactions between the taxa, further affecting host susceptibility to disease (Engering et al., 2013; Liu et al., 2013; Ruiz-Lopez et al., 2014).

Co-circulating pathogens in a given area could also increase the probability of co-infection in susceptible hosts (McCarthy et al., 2007; Berentsen et al., 2013). For example, outbreaks of canine distemper virus in African lion populations in the Serengeti National Park were found to be strongly influenced by the interaction between wild carnivore populations, as well as between these populations and domestic dog populations in surrounding areas (McCarthy et al., 2007; Prager et al., 2012a; Berentsen et al., 2013). Rabies also persists in the Serengeti ecosystem and infects similar hosts, increasing the probability of these two pathogens co-infecting the same host and potentially altering disease outcomes (McCallum and Dobson, 1995; Prager et al., 2012a).

Strong interactions between parasite species may translate into effects at the level of the host population. One example of this was during unusually deadly canine distemper virus outbreaks in lions (de Almeida Curi et al., 2010; Prager, 2010; Tompkins et al., 2011; Viana et al., 2015; Weckworth, 2018). Within pride mortality rates were positively correlated with the proportion of individuals showing high intensity *Babesia* infections, suggesting that that co-infection was a major contributing factor during fatal epidemics (Williams et al., 2014a).

5. Diagnosis

Clinical signs associated with canine distemper resemble clinical signs of various other canine diseases, complicating the diagnosis of CDV (Si et al., 2010; Silva et al., 2014; Wang et al., 2017a). Diagnostic routines should therefore focus on excluding canine parvovirus, coronavirus, respiratory viruses, bacterial and internal parasite infections as possible causes of respiratory and gastrointestinal signs (Martella et al., 2008; Amude et al., 2012; Nguyen, 2014; Headley et al., 2018). Rabies should also be ruled out as part of the diagnostic procedure, as the neurological signs resulting from CDV infection are often mistakenly thought to be due rabies infection (Chappius, 1995; Amude et al., 2010; Yang et al., 2013).

There are currently five basic diagnostic methods that are commonly used to diagnose CDV infection. Each test has its advantages and limitations, with some being more effective than others. Immunofluorescence assay (IFA) of ante-mortem specimens detects CDV inclusion bodies in cells from conjunctival scrapes, buffy coat (peripheral blood lymphocytes), urine sediment, uro-epithelial cytology, transtracheal washes, cerebrospinal fluid and biopsies of the footpads or nose (An et al., 2008; Gray et al., 2012). This test is most reliable within three weeks of initial infection. The disadvantage is that the virus often persists in the CNS for 60 days or longer, not necessarily causing acute disease (Beineke et al., 2009; Carvalho et al., 2012).

Various serological tests can also be used in diagnosing CDV. ELISA (enzyme-linked immunosorbent assay) is usually used to detect IgM antibodies in serum (Martella et al., 2008; Litster et al., 2012). Presence of IgM is indicative of recent CDV exposure, either by infection or vaccination and may last for 3 months (Beineke et al., 2009). IgG antibodies can be measured through serial titres on 2 samples taken two weeks apart. If the titre is increased more than 4-fold between samples, it is usually indicative of CDV infection (Martella et al., 2008; Beineke et al., 2009). Since vaccine-induced antibodies do not cross the blood-brain-barrier, anti-CDV antibodies in cerebrospinal fluid are highly indicative of CDV infection. Unfortunately, if distemper antibodies occur in the CSF, CNS infection is confirmed (Beineke et al., 2009; Soma et al., 2013). Initial infection by CDV is not necessarily detected with this method (Beineke et al., 2009; de Camargo et al., 2016).

Cell culture is not a very effective way for easy and rapid CDV diagnosis. Virus isolation takes up to 3 weeks or at the very least a few days. The origin of the specimen, as well as its quality, could limit the results obtained from this diagnostic method (Martella et al., 2008; Beineke et al., 2009). Post-mortem specimens are usually examined with conventional stains, IFA and immunohistochemistry (IHC) to study histopathology and detect viral antigen and are typically performed on various tissues including the spleen, tonsils, lymph nodes, stomach, kidney, lung, duodenum, bladder and brain tissues (Martella et al., 2008; Beineke et al., 2009).

Reverse transcriptase-polymerase chain reaction (RT-PCR) can be used to detect the virus in various bodily fluids, including respiratory secretions, CSF, faeces, urine, whole blood, and conjunctival or ocular samples (Silva et al., 2014; Wang et al., 2017a). It should however be kept in mind that vaccination with the modified live CDV vaccine can interfere with PCR detection testing for up to 4 weeks, which could result in false positives (Martella et al., 2008; Wilkes et al., 2014; Nemeth et al., 2018). More recent studies have made use of different variations of a nested RT-PCR approach to detect canine transcripts. Molecular detection methods are continuously being optimised to detect the

presence of CDV more efficiently and to determine the extent of viral infection (Si et al., 2010; Di Francesco et al., 2011; Alcalde et al., 2013; Maes et al., 2014).

One of the most challenging aspects of diagnostic testing is that testing for anti-CDV antibodies does not distinguish between antibodies produced in response to CDV vaccination and those induced as a result of infection by CDV (Wang et al., 2011; Soma et al., 2013; Jensen et al., 2015). An animal that becomes infected and clears the infection itself through mounting an adequate immune response will return a positive antibody titre despite being disease free (Soma et al., 2013). Since CDV has a single, monotypic serotype, serological techniques are unable to distinguish between different CDV genotypes (Elia et al., 2006; Maes et al., 2014). The most effective way to distinguish between wild type strains and vaccine strains is still by sequencing of the H gene or the whole virus genome of an isolated strain, which can be quite time consuming (Martella et al., 2008; Maes et al., 2014).

6. Emergence of CDV in wild felid species

The recent emergence of CDV in a wide range of wild felid species, distributed across wide geographical ranges, has resulted in a significant number of mortalities (Appel et al., 1994; Terio and Craft, 2013; Gilbert et al., 2014). It is known that canine distemper has variable outcomes in different individuals and species, and these recent felid CDV infections seem to indicate that wild felid species are probably more susceptible to severe CDV infection compared to some canid hosts (Terio and Craft, 2013; Weckworth, 2018).

Recent CDV outbreaks in felids have affected various Siberian tiger (*Panthera tigris altaica*) populations and Amur tiger (*Panthera tigris*) populations (Konjević et al., 2011; Nagao et al., 2012; Seimon et al., 2013; Terio and Craft, 2013; Gilbert et al., 2014; Zhang et al., 2017). Even though CDV has been previously been detected in African lion populations, recent outbreaks have been associated with increased mortality rates in these populations (Weckworth, 2018). Far eastern leopards (*Panthera pardus orientalis*) and mountain lions (*Puma concolor*) have also been affected

by CDV infections (Foley et al., 2013; Sulikhan et al., 2018). A study previously performed in North America (Appel et al., 1994) has suggested that CDV is epizootic among lions, tigers and leopards in the region.

Residue G530 and Y530 in the SLAM receptor binding domain of the H gene has been identified as residues crucial for binding of the viral H protein to the host cell (Terio and Craft, 2013; Ohishi et al., 2014). These residues are therefore important in determining cell tropism and binding affinity (McCarthy et al., 2007; Viana et al., 2015). One possibility is thus that changes in these crucial residues could have contributed to the adaptation of CDV to wild felid host cells (McCarthy et al., 2007). Unique amino acid changes were found in the H gene sequence of one the CDV strain isolated in Amur tigers, with mutations including V538 – I, T548 – M and D570 – N (Seimon et al., 2013). Since these are not mutations commonly found it other strains, the authors suggested that these changes may have contributed to the spill over of CDV into this new host (Seimon et al., 2013; Gilbert et al., 2014).

It is however unlikely that variation within the H gene alone is responsible not only for the adaptation to of CDV to wild felid hosts, but also the increased severity of distemper observed in these relatively new hosts (Foley et al., 2013; Terio and Craft, 2013). Interaction of felid species with other wildlife reservoir species may well be a more important factor contributing to pathogen spill over (Tompkins et al., 2011; Suzuki et al., 2015; Viana et al., 2015). Genetic differences between hosts, specifically in immune response and virus receptor genes, as well as host population density and social interactions are major contributing factors in establishing pathogen infection in new host species (Malpica et al., 2006; Tompkins et al., 2011; Magiorkinis et al., 2013; Suzuki et al., 2015; Viana et al., 2015). A combination of all these factors need to be investigated in the pursuit of improving understanding of CDV spill over into new host species.

7. The dog as model organism

7.1 Advantages of studying infection in natural hosts

Various animal models, most notably murine models, have been used to improve our understanding of host responses to pathogen infection. Although mice have proven very useful to model certain human diseases, it should be noted that there are limitations that prevent data from certain studies done on mice to be extrapolated to human conditions (Mestas and Hughes, 2004). There are simple considerations such as the fact that humans and mice diverged from each other 65 to 75 million years ago, they have evolved separately and have adapted to different ecological niches. These two species also differ in their size, lifespan and the environment in which occur. Moreover, despite some similarities between the immune systems of mice and humans (and other mammals), there are also significant differences in the innate and adaptive immune responses between these two species and they often differ significantly when it comes to complex multicomponent processes (Mestas and Hughes, 2004; Bean et al., 2013).

One such difference is the lack of correlation in the transcriptional responses between mice in humans, further emphasised by recent genomics studies. In addition to this, some phenotypic markers used to discriminate immune cell populations in mice are absent in humans and mouse models often incompletely reproduce human disease phenotypes (O'Brien, 1999; Mestas and Hughes, 2004; Martella et al., 2008; Ludlow et al., 2014). Another complicating factor is that various diseases need to be induced experimentally in mice, which raises multiple ethical issues and has the disadvantage of not being naturally occurring as it would be in a non-model host (Bean et al., 2013). Experimental infections often do not reflect disease progression resulting from natural infection. The relatively easy genetic manipulation of mice will keep making this species invaluable in improving biology's understanding of immunological processes, but the data from such studies should be interpreted in the light of the possible limitations of this model species (O'Brien, 1999; Mestas and Hughes, 2004).

Various host factors could contribute to variability in disease presentation in different hosts. Antigen receptors have evolved through natural selection processes over many generations and may be very different in different species (Malpica et al., 2006; Bean et al., 2013). The immune system is also shaped by the co-evolution of a host with its pathogens (Altizer et al., 2003; Bean et al., 2013). Evolution of unique immune mechanisms associated with the control of viral replication may allow one host to efficiently coexist with a virus, while a susceptible species will develop severe disease when exposed to the same pathogen (Kameo et al., 2012b).

Understanding the immune systems of wild and domesticated animal hosts is crucial for understanding the disease mechanisms involved in zoonotic infections. By studying immunology in the natural host one can aim to explain how infection with the same pathogen can result in vastly different outcomes in different species (Mestas and Hughes, 2004; Bean et al., 2013). There are various ways in which natural and spill over hosts can be studied to better understand their immunological complexity. Comparative genomics has proved to be an extremely powerful tool in identifying genetic determinants underlying phenotypical differences between species (Ekblom and Galindo, 2011). With whole genome sequences becoming more readily available, it is possible to perform comparative analyses to identify candidate genes for disease-susceptibility or disease-resistance phenotypes during infection with zoonotic viruses (Ekblom and Galindo, 2011; Ludlow et al., 2014). The identification of key differences in immune pathways between susceptible and non-susceptible hosts might offer insights for the development of disease intervention strategies (O'Brien, 1999; Parker et al., 2010; Ludlow et al., 2014).

Other factors that would also need to be further researched are the influence of population genetics on host-pathogen interactions and the role of environmental factors, food supply, co-infections, interactions between species and changes in demographics in influencing disease prevalence and spread (Boulouis et al., 2005; Engering et al., 2013; Liu et al., 2013; Williams et al., 2014b; Headley et al., 2018; Marescot et al., 2018). Studying viruses and other pathogens infections in their natural

hosts will be the first step in determining the role of these other factors in disease (Martella et al., 2008).

7.2 Advantages of the dog as model organism

Domestic dogs have more naturally occurring medically evaluated diseases than any other species, with the exception of humans (Pedersen, 1999; Parker et al., 2010). Over 400 hereditary canine diseases have known equivalent human diseases, and similarities between dog and human physiology, disease presentation and clinical responses make the dog a suitable study model for pathogen infections that occur in other canids, as well as for the study of human diseases (Parker et al., 2006; Parker et al., 2010; Bean et al., 2013).

Domestication of dogs from grey wolves is an event that began at least 30 000 years ago, with continual artificial selection since domestication contributing to the development of isolated populations or breeds of dogs (Vila et al., 1997; Perri, 2016; Pendleton et al., 2018). One of the reasons why dogs are afflicted with so many diseases is as a result of years of selective inbreeding to obtain purebred dog populations, predisposing various breeds to inherited diseases (Pedersen, 1999; Starkey et al., 2005; Parker et al., 2010).

In 2003 whole-genome shotgun sequencing was used to sequence the dog genome for the first time, with an improved assembly and annotation of this genome released in 2014 (Ostrander and Comstock, 2004; Hoeppner et al., 2014). The complete assembled dog genome was constructed from 7.6-fold sequence coverage and is estimated to cover approximately 96-98% of the canine genome. Initially 20 439 genes encoding 32 548 transcripts were annotated. Extended analyses of other dog genomes lead to the identification of 974 400 putative SNPs, with a higher degree of sequence conservation being observed when comparing the dog and human than when human sequences are compared to those of mice (Ostrander and Comstock, 2004; Wayne and Ostrander, 2007; Hoeppner et al., 2014).

There are many advantages to using the dog as a model organism for disease studies. Various conditions are naturally occurring in dogs and are similar in biology, histologically and in clinical course to similar diseases observed in humans. Dogs also have a physiology more suited to gross comparison with the human than other traditional model organisms, like the mouse model (O'Brien, 1999; Mestas and Hughes, 2004; Ostrander, 2012). Dogs also share a common environment with man, making it likely that the aetiology of canine diseases is similar to those of their human equivalents. Multifactorial diseases can therefore be studied more effectively in dogs than in humans (Ostrander and Comstock, 2004; Starkey et al., 2005; Parker et al., 2010; Bean et al., 2013).

Mapping of disease genes is simplified by the natural history and structure of different breeds and the availability of detailed genealogical records (Ostrander and Comstock, 2004; Starkey et al., 2005; Akey et al., 2010). Dogs also have a relatively condensed life span, allowing collection of samples for molecular analysis from multiple generations, allowing for detection of recombination between disease and marker alleles (Parker et al., 2006; Parker et al., 2010; Bean et al., 2013). Canine families also tend be large, increasing the statistical power of linkage analyses (Ostrander and Comstock, 2004; Hoeppner et al., 2014). Mapping of complex diseases can also be simplified in dogs due to some breeds being enriched for a small number of disease alleles, making a significant number of diseases breed specific. Linkage disequilibrium also tends to be more extensive in dogs, making it possible to use fewer markers for whole-genome association studies (Ostrander and Comstock, 2004; Parker et al., 2004; Starkey et al., 2005; Wayne and Ostrander, 2007; Hoeppner et al., 2014).

Although the canine genome annotation can still be improved and there are still a number of challenges to overcome, there is a large extent of canine disease and immune orthologs that correspond to similar orthologs in humans (Ostrander and Comstock, 2004; Lindblad-Toh et al., 2005; Hoeppner et al., 2014). There are also advantages to using dogs to study diseases occurring in other similar hosts, not just humans. Since dogs are often naturally infected by pathogens occurring in other canid hosts, it eliminates the ethical dilemmas associated with the experimental infection of

animal model organisms (O'Brien, 1999; Mestas and Hughes, 2004; Bean et al., 2013). Canine distemper virus infection, for example, can therefore be studied in dogs rather than in the currently used ferret model (von Messling et al., 2003; Parker et al., 2010; Ludlow et al., 2014; da Fontoura Budaszewski and von Messling, 2016). Dogs also develop clinical signs of disease more quickly than some other hosts, allowing progression of disease to be studied (Ostrander and Comstock, 2004; Ostrander, 2012; Bean et al., 2013; Hoeppner et al., 2014).

The availability of a complete genome sequence will enable high-resolution gene expression studies and the efficient identification of alleles conferring susceptibility to diseases (Carninci et al., 2005; Hoeppner et al., 2014). It will also enable the development of universal whole-genome SNP markers for association studies in different breeds, further promoting identification of disease-associated genes and variation in alleles of these genes (Ostrander and Comstock, 2004; Starkey et al., 2005; Wayne and Ostrander, 2007).

8. Molecular studies done on canine distemper virus and associated host responses

8.1 DNA-based methods

Although various immunohistochemical and histopathological studies have been performed on different host tissues infected with CDV, very few studies have focused on genetic differences underlying different host responses and susceptibility to CDV (Cornwell et al., 1965; Van Moll et al., 1995; Wünschmann et al., 2000; Rudd et al., 2010; Techangamsuwan et al., 2011; Carvalho et al., 2012; Pan et al., 2013; Maes et al., 2014; McGavin, 2014). Although some studies have identified receptors important in the binding of CDV to host cells and have characterised the functionally important sites within these receptors, genetic differences in other genes involved in generating the immune response have rarely been studied (Tatsuo and Yusuke, 2002; Bieringer et al., 2013; Delpeut et al., 2014a; Alves et al., 2015).

The authors of a recent, extensive study aimed to explore the contribution of variation in previously identified host candidate genes to different mortality patterns observed in European harbour seal populations in response to PDV (phocine distemper virus – the closest relative to CDV) infection (McCarthy et al., 2011). In this study the variation in eight genes were evaluated: genes encoding the CD46 and SLAM receptors, the RARα (involved in disease physiology) and TLR2 (detection of pathogen associated molecular pattern molecules) genes, as well as the gene encoding IFNG, and genes encoding immune modulatory interleukins 1, 8 and 10 (McCarthy et al., 2007b). Although no variation was found in the protein coding domains of the SLAM and CD46 receptors of harbour seals, various SNPs were detected in the second intron of SLAM. Single nucleotide polymorphisms were also detected in IL8 p2 and exon 1 of RARα. Further analysis of the polymorphisms detected in the SLAM and RARα genes showed that these two genes are probably not involved in the immune resistance to PDV in the studied harbour seal populations (McCarthy et al., 2011).

It should however be mentioned that this study made use of the existing domestic dog genome gene sequences for most of the genes they were trying to detect variation in, as there were no existing sequence data for these genes in seals at the time (McCarthy et al., 2011; Maes et al., 2014; Ohishi et al., 2014). Although the authors failed to find a significant relationship between especially the SLAM and RARα genes and PDV disease susceptibility, a subtle or different role of these genes and their involvement in disease susceptibility could not be ruled out. This study was especially significant since it was the first genetic association study for morbillivirus disease susceptibility in a non-model organism and despite the negative results, various new questions could be raised as a result of this study (McCarthy et al., 2011; Bean et al., 2013; Liu and Harada, 2013). This further emphasised the need to evaluate host responses to morbillivirus infection in natural hosts more extensively in order to better understand disease susceptibility and resistance (O'Brien, 1999; Bean et al., 2013).

Since the SLAM receptor is one of the primary receptors involved in the initial binding of the CDV-H protein to the host cell, it comes as no surprise that this is one of the best studied genes in host-pathogen interactions (von Messling et al., 2001; Tatsuo and Yusuke, 2002; Bieringer et al., 2013; Lin and Richardson, 2016). Another recent study aimed to detect variations in the SLAM receptor in carnivores (Ohishi et al., 2014). Various families within the suborders Carniformia and Feliformia were included in the study. Within the SLAM receptor, 34 amino acid residues involved in the binding of CDV to the cell were identified. The SLAM receptor of the domestic dog was similar to that of members of the suborder Carniformia, meaning these hosts probably have similar susceptibility to dog CDV (Ohishi et al., 2010; Ohishi et al., 2014).

When looking at differences between the SLAM receptors of families within Carniformia compared to felid families, nine amino acid positions were identified that could potentially alter the susceptibility of felids to CDV. Four amino acid changes (at positions 72, 76, 82, and 129) in the domestic cat (*Felis catus*) and three positions (72, 82, and 129) in lions (*Panthera leo persica*) were associated with charge alterations within the SLAM receptor. A positively charged threonine residue at position 76 in the SLAM receptor of domestic cats could explain the lowered affinity of this receptor for the CDV-H protein (Ohishi et al., 2010; Ohishi et al., 2014).

Host susceptibility to CDV may therefore be affected by genes involved in the recognition of the virus, as well as genes involved in subsequent immunological responses (Ohishi et al., 2010; Pybus et al., 2013; Ohishi et al., 2014). This study extended the information available for the crucial SLAM receptor and emphasised the importance of evaluating molecular variation between and even within host species to better understand disease susceptibility (Ohishi et al., 2010; Pybus et al., 2013; Ohishi et al., 2014). Studying the host responses in natural hosts rather than in model organisms, in which immune responses may be significantly different to that of natural hosts, will improve our understanding of various molecular mechanisms underlying disease susceptibility, progression and recovery (Wayne and Ostrander, 2007; Bean et al., 2013).

8.2 RNA-based methods

8.2.1 Microarray versus RNA-Sequencing

The two most common techniques currently used to assess differential gene expression, especially when comparing diseased and healthy states in organisms, are microarrays and RNA-Sequencing (RNA-Seq). Most gene expression studies thus far have relied largely on array-based approaches and microarray-based studies have been extensively developed, evaluated and improved over many years (Conway and Schoolnik, 2003; Thomson et al., 2005; Noel et al., 2014; Wang et al., 2017b). With the rapid evolution of high throughput sequencing approaches, RNA-Seq has become more commonly utilized and it is already recognised for the valuable information that can obtained from it (Wang et al., 2009; Costa et al., 2010; Mooney et al., 2013). However, since RNA-Seq is still a relatively new method compared to microarray technology, there is still a lot of uncertainty and debate about which technology is currently best to use in expression studies, taking their respective challenges and limitations into account (Ozsolak and Milos, 2011; Vijay et al., 2013; Wang et al., 2014; Wimmer et al., 2018).

Microarray studies have enabled the simultaneous evaluation of the expression of thousands of genes in a single genome and this technology has been invaluable in global gene expression studies (Conway and Schoolnik, 2003; Noel et al., 2014; Wang et al., 2017b). Standardisation of statistical analysis and normalisation of microarray data is improved on an ongoing basis, but it is better established than for most high throughput sequencing approaches since it has been used for longer (Noel et al., 2014; Ari and Arikan, 2016; Wimmer et al., 2018). As with any technology, microarrays also have limitations. Microarrays measure only the relative quantities of transcripts and suffer from significant background fluorescence and cross-hybridisation problems. This limited dynamic range of detection could result in underestimation of low-abundance transcripts (Conway and Schoolnik, 2003; Noel et al., 2014; Ari and Arikan, 2016). Another limitation is that microarray chips are made up of a predefined set of genes, and only the activity of previously identified genes are therefore

measured. There are also inconsistencies between data obtained from different microarray platforms, which can be attributed to the lack of universal standards among the different platforms. Reproducibility of results is therefore a problem (Thomson et al., 2005; Noel et al., 2014; Ari and Arikan, 2016; Wang et al., 2017b). Different methods of target RNA preparation and differences in data analyses also further contribute to poor reproducibility of results among different experiments and different laboratories (Conway and Schoolnik, 2003; Marioni et al., 2008; Dong and Chen, 2013; Wang et al., 2017b).

As the cost of high throughput sequencing decreases and access to instrumentation increases, RNA-Seq is becoming viable option for molecular expression studies. Some of the advantages of RNA-Seq over microarray include the quantitation of transcripts, the fact that it has a better dynamic range, and has additional capabilities of detecting expressed single nucleotide variants (SNVs) and translocations (Wang et al., 2009; Costa et al., 2010; Ari and Arikan, 2016). Ribonucleic acid sequencing also produces more accurate data on transcript sequences and requires less RNA than microarray approaches (Marioni et al., 2008; Consortium, 2014; Ari and Arikan, 2016). Microarrays are limited to a predefined set of usually well-annotated genes, while RNA-Seq allows for detection of alternative splice variants and better detection of novel transcripts (Marioni et al., 2008; Dong and Chen, 2013). Genes expressed at very low and very high levels are more likely to be detected by RNA-Seq due to the absence of significant background signal, more relaxed limits for quantification and a greater range of expression levels. An additional benefit of high throughput sequencing techniques include biological and technical reproducibility (Ozsolak and Milos, 2011; Dillies et al., 2013; Consortium, 2014; Han et al., 2015; Ari and Arikan, 2016). It is however important to take into consideration that internal standards for data quality, reliability and reproducibility are still being established (Mortazavi et al., 2008; Kvam et al., 2012; Dillies et al., 2013).

One study made use of both RNA-Seq and microarray analysis to evaluate gene expression changes associated with B-cell lymphomas in the domestic dog (Mooney et al., 2013). Their main aim was to

disentangle the variation among the gene expression profiles for the different technologies, thereby not only doing an expression profile for this cancer but also comparing these two commonly used approaches for gene expression profiling. In addition to identifying differentially expressed genes between normal and disease-affected lymph nodes in dogs, the authors also concluded that although RNA-Seq may provide more sensitive detection of transcripts than microarrays, microarray observations have greater statistical power for identifying genome-wide differential expression. The authors went further to report statistical methods for treating the combined data of the two different approaches as a means for supporting biological discovery from the different platforms. According to this study, it is currently more advantageous to use microarray and RNA-Seq as complementary technologies, rather than as competing approaches (Mooney et al., 2013).

8.2.2 Relevant RNA studies performed

Differences in gene expression between normal and abnormal tissues inform our understanding of disease. As already mentioned, the domestic dog is a clinically relevant model for the study of human diseases (Mestas and Hughes, 2004; Parker et al., 2010; Ostrander, 2012; Bean et al., 2013). It is also a natural host for a range of diseases affecting various wildlife populations. Studying gene expression in domestic dogs could therefore be very important to improve our understanding of a wide range of disease conditions, as well as disease progression and variation in host susceptibility to specific infections and diseases (O'Brien, 1999; Parker et al., 2010; Bean et al., 2013; Hoffman et al., 2018).

With this in mind, a study was performed in which the gene expression of 10 normal canine tissues was catalogued as a baseline for future expression studies and cross-species analyses (Briggs et al., 2011). The lack of a comprehensive functional assessment of canine gene expression in normal tissues limits our understanding of diseased states in this model organism. The authors made use of the Affymetrix Canine GeneChip platform to develop a publicly accessible gene expression profile database from these ten normal canine organs. One of the advantages of their experimental design was that it included tissues from both pure bred and mixed breed dogs of both sexes and of varying

ages. It also included a number of biological repeats for each organ. Thus, although their sample size in terms of the number of dogs was fairly small, each organ within the individual dogs were sampled extensively (Briggs et al., 2011).

Apart from their good experimental design, this study yielded results that will have significant applications in post-genomics research projects. One significant finding was that each tissue has a specific gene expression profile, allowing organs and tissues to be distinguished based on unique expression data associated with that tissue/organ. Brain-specific transcripts were also annotated during this study, emphasising that gene identifiers can now be linked to previously unknown probe sets with more confidence than possible in the past (Briggs et al., 2011). This will give a more complete and functional view of genes involved in disease development and progression in future. The database containing the gene expression profiles and related annotations for normal canine tissues will therefore advance the dog as a model species in medical research as it will also enable inter-species comparisons of common diseases (Emilsson et al., 2008; Briggs et al., 2011). Various future studies will benefit from this characterisation of normal canine tissues and it will make genomic characterisation of diseased states in dogs less expensive and more expedient (Lindblad-Toh et al., 2005; Wayne and Ostrander, 2007; Bean et al., 2013; Hoeppner et al., 2014; Hoffman et al., 2018).

Subsequent RNA-Seq studies have focused on gene expression differences between the brain tissues of domestic and wild animals (Albert et al., 2012), the brain transcriptome of dogs with an emphasis on the hypothalamus and cerebral cortex (Roy et al., 2013) and gene expression in the brain tissues of dogs affected by meningoencephalitis (Greer et al., 2010). Other RNA-Seq studies specifically done in dogs include gene expression studies associated with cardiomyopathy (Friedenberg et al., 2016), differential gene expression in head and neck carcinomas (Liu et al., 2015) and the study evaluating gene expression differences associated with B-cell lymphomas that was previously mentioned (Mooney et al., 2013).

One specific study, performed by Ulrich et al. (2014), has contributed significantly to an increased understanding of molecular mechanisms underlying the host response of dogs specifically to canine distemper virus infection (Ulrich et al., 2014b). This study made use of microarray analysis to evaluate the molecular pathogenesis of CDV leukoencephalitis in domestic dogs and to identify pathways that are intimately associated with demyelination. The authors made use of an extremely varied sample, with 12 control dogs and 14 diseased dogs of different breeds, ages and sexes and dogs with different stages of CDV leukoencephalitis. Transcriptional changes associated with CDV leukoencephalitis were dominated by the gene ontologies "immunoglobulin mediated immune response" and "complement activation, classical pathway." This supports the hypothesis proposed by Vandevelde et al. (1995) suggesting that locally produced antibodies and complement is involved in the pathogenesis of demyelination in chronic inflammatory leukoencephalitis (Vandevelde and Zurbriggen, 1995, 2005).

Other up-regulated genes corresponded with the gene ontologies "positive regulation of T-cell mediated cytotoxicity," which correspond to immunohistochemistry findings of diffuse infiltration of the CNS by CD8+ lymphocytes (Wünschmann et al., 1999; Wünschmann et al., 2000). Genes that showed significant downregulation belonged to the gene ontology terms "intermediate filament bundle assembly" and "regulation of neuron differentiation." The main conclusion made by the authors, based on the gene expression profiling results, is that CDV leukoencephalitis follows a biphasic mode of demyelination previously proposed by other authors (Markus et al., 2002; Beineke et al., 2009; Lempp et al., 2014; Ulrich et al., 2014b). This biphasic mode of demyelination is presumably characterised by an initial non-apoptotic oligodendrocyte dystrophy, which is later followed by an intrathecally synthesised immunoglobulin- and complement-mediated autoimmunity (Grőne et al., 2000; Beineke et al., 2009; Lempp et al., 2014; Ulrich et al., 2014b).

The results from these studies will be useful in subsequent transcriptomic and other post-genomic studies. The database of canine normal tissue gene expression provides a good foundation to which

diseased states can be compared and it will also be useful for cross-species comparisons of gene expression profiles associated with certain tissues and organs (Weis et al., 2007; Wang et al., 2009; Briggs et al., 2011). The study performed by Ulrich et al. (2014) was a bit more limited as a result of the varied sample selection. Some of the transcriptional changes observed may have resulted from differences between dog breeds, ages and even sexes and it may not necessarily reflect expression differences only in response to CDV infection. It will however serve as a valuable comparative study and the results serve as a sound baseline for similar future studies (Ulrich et al., 2014b).

8.2.3 RNA preservation and normal gene expression in different tissues

Since RNA is a less stable molecule than DNA, there are various important considerations when attempting an RNA-based approach to study molecular differences between diseased and healthy states (Weis et al., 2007; Costa et al., 2010). The stability of RNA varies for different RNA molecules and this should be taken into consideration even for different mRNA molecules in different tissues. There are also multiple tissue-specific differences in gene expression, and even differences between different areas of the same tissue, that are unrelated to disease or an abnormal host response (Morozova and Marra, 2008; Rapaport et al., 2013; Hedegaard et al., 2014; Wang et al., 2014). It is therefore important to know how much of the detected variation results from the disease being studied and to what extent the variation is just normal variation (Briggs et al., 2011; Albert et al., 2012; Wang et al., 2014).

A recent review paper looked at some of the factors affecting RNA stability and how this influence sampling of specifically brain tissue for RNA-based expression studies (Weis et al., 2007). Ribonucleic acid molecules are generally characterised by a relatively short life span, with enzymes such as ribonucleases or RNases being responsible for rapid degradation of RNA *in vivo*. This enzymatic activity may continue for a time after the death of the organism. Other post-mortem factors can also increase the degradation of RNA in tissues, such as chemical (e.g. changes in pH) and temperature-related changes (Weis et al., 2007; Wang et al., 2009; Naumova et al., 2013). Even before

an animal dies there are factors that could alter gene expression, such as the severity of disease, trauma, drugs administered and stress. Various qualitative and quantitative changes may therefore occur in the transcriptome composition as a result of RNA degradation either before or after the death of the animal (Weis et al., 2007; Costa et al., 2010; Dong and Chen, 2013; Naumova et al., 2013). It has been shown that an increase in the post-mortem interval (PMI – time following death) is associated with increased RNA degradation. By the PMI of 48 hours, about 12% of the mRNAs show a twofold decrease in abundance. It has been suggested that isolation and freezing of the tissue of interest for RNA studies within 36 hours after the death of the animal would reduce this effect (Weis et al., 2007; Naumova et al., 2013; Wimmer et al., 2018). Studies making use of RNAlater to store tissues for RNA-based expression studies typically store these tissues at -80°C until the samples are processed (Weis et al., 2007; Briggs et al., 2011; Mooney et al., 2013; Ulrich et al., 2014b).

The gene expression profile of canine brain tissue is clearly distinct from other tissues and is characterised by a high level of gene expression, as well as a higher transcriptome complexity compared to other tissues (Weis et al., 2007; Greer et al., 2010; Briggs et al., 2011). In humans it has been shown that in the transcriptome of brain tissue there are especially high enrichment for regulatory elements, with non-coding RNAs and a particular set of microRNAs (miRNAs) making up an important part of the brain-specific transcriptome. An unusually high level of alternative splicing events has also been reported in human brain tissue, with highly distinct splicing patterns compared to other tissues (Wang et al., 2009; Naumova et al., 2013). Apart from the brain having a distinct transcriptome, variation in gene expression across brain regions can also be observed and is related to both functional and anatomical differences in its substructures. Various anatomical brain substructures have different cell compositions and therefore cell-specific differences in gene expression (Naumova et al., 2013; Takahashi et al., 2013).

When using RNA as raw material for a gene expression study, it is therefore important to take the above-mentioned factors into consideration and to allow for normal differences within and between

tissues. The conditions preceding and following the death of an animal should be reported as extensively as possible and the tissues should be stored appropriately as soon as possible following its isolation to prevent RNA degradation (Ozsolak and Milos, 2011; Naumova et al., 2013).

8.2.4 RNA Sequencing Analysis

RNA sequencing has become increasingly popular as a high-throughput, cost-effective approach for transcriptome profiling (Wang et al., 2009; Costa et al., 2010; Ozsolak and Milos, 2011; Han et al., 2015). RNA-Seq has the advantages that it can be performed without prior knowledge of a genome or sequences, it has multiple applications (e.g. *de novo* assembly, detection of low abundance transcripts and detection of alternatively spliced transcripts) and it does not have the technical biases inherent to microarray technology (Ozsolak and Milos, 2011; Vijay et al., 2013; Consortium, 2014; Han et al., 2015).

To quantify gene expression from RNA-Seq data, the reads can either be aligned to the reference genome of a model organism or de novo assembly can be used to reconstruct the transcriptome sequences if there is no reference genome to use (Dong and Chen, 2013; Vijay et al., 2013; Liu et al., 2014). Based on the alignment, the number of mapped reads is calculated, and this is used to estimate the relative expression levels of genes. Statistical methods are subsequently applied to test whether differences between groups are significant or not (Mortazavi et al., 2008; Kvam et al., 2012; Rapaport et al., 2013; Ari and Arikan, 2016). Refer to Fig. 1.6 below for a general workflow of differential gene expression analysis of RNA-Seq data.

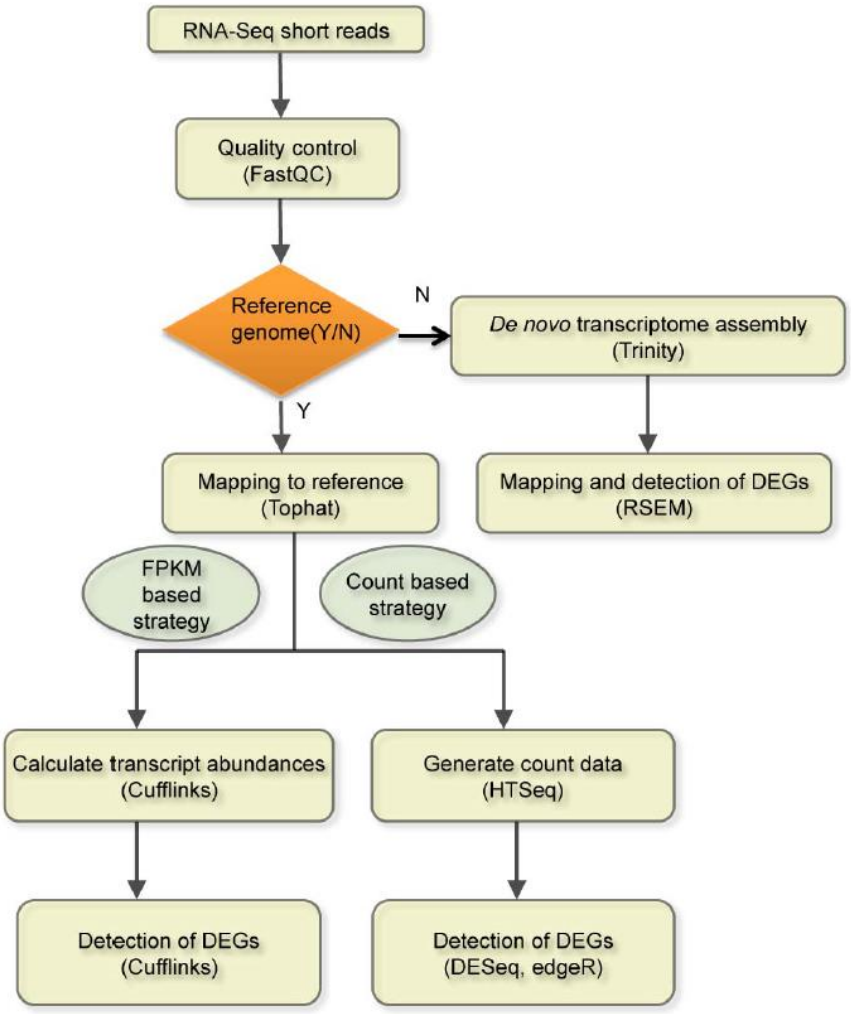

Fig. 1.6 The general workflow of differential gene expression analysis for RNA-Seq data (Zhang et al., 2014).

Despite some initial claims that RNA-Seq would be able to produce unbiased, ready-to-analyse gene expression data, accurate quantification of gene expression remains challenging (Li et al., 2014b; Ari and Arikan, 2016). Some of the difficulties faced in the study design and analysis of RNA-Seq data include biases inherent to this technology (variability in library preparation, biases in sequence quality for specific nucleotides and read positions and error rate); nucleotide composition and different gene and transcript lengths lead to biases in abundance measures; the effects of number of replicates and the sequencing depth on the data and normal biological variation between groups can also make it challenging to distinguish real biological differences between groups. Different splice variants and

overlapping transcripts can further complicate differential expression analysis (Robinson and Oshlack, 2010; Ozsolak and Milos, 2011; Dillies et al., 2013; Vijay et al., 2013; Li et al., 2014b; Liu et al., 2014; van Dijk et al., 2014; Ari and Arikan, 2016).

A Poisson distribution, where the mean is equal to the variance, fit well to data from studies in which there are few biological replicates (Trapnell et al., 2012; Sorenson and Delorenzi, 2013; Seyednasrollah et al., 2015). Overdispersion, where the variation in data is underestimated, is seen when more biological replicates are included in studies. Statistical tests which were based on Poisson assumptions therefore does not control for this error (Kvam et al., 2012; Dillies et al., 2013; Zhang et al., 2014). The Negative Binomial (NB) distribution has been proposed as a solution as it can deal with the overdispersion problem. The NB distribution has been included as the preferred approach in most newer methodologies that are used to model feature counts for RNA-Seq data (Mortazavi et al., 2008; Kvam et al., 2012; Dillies et al., 2013; Zhang et al., 2014). Even with the development of a number of tools utilising the NB distribution for differential expression analysis, no consensus has yet been reached regarding which method is optimal and how reproducibility, accuracy and robustness can be ensured with each of these tools (Marioni et al., 2008; Kvam et al., 2012; Han et al., 2015; Wimmer et al., 2018).

Three of the most popular tools that are currently used in RNA-Seq differential expression analyses are Cuffdiff2, DESeq and edgeR. Cufflinks can be more difficult to use due to the fact that it does not make use of count matrices and requires BAM files (the binary version of sequence alignment data) as its input (Dillies et al., 2013; Rapaport et al., 2013; Li et al., 2014a; Zhang et al., 2014). These large binary files make comparisons involving Cufflinks-Cuffdiff2 more cumbersome compared to methods like DESeq and edgeR that make use of count matrices as input, which simplifies comparative analysis (Trapnell et al., 2012; Rapaport et al., 2013; Li et al., 2014a; Zhang et al., 2014).

Compared to Cuffdiff2 and DESeq, edgeR performs better in its ability to uncover true positives. This means that edgeR will always detect more differentially expressed genes (DEGs), but this may

also introduce more false positives. Including more biological or technical replicates allows all three tools to perform better in detecting DEGs, emphasising the importance of including biological replicates in RNA-Seq studies (Rapaport et al., 2013; Vijay et al., 2013; Li et al., 2014a; Liu et al., 2014). The number of biological replicates required for a study depends significantly on the variability between biological replicates and when no or very few replicates are available, the use of edgeR is recommended (Robinson and Oshlack, 2010; Liu et al., 2014; Seyednasrollah et al., 2015).

Although the impact of sequencing depth on RNA-Seq data is not as critical as the number of biological replicates, it has been shown that Cuffdiff2 is the most sensitive to sequencing depth and DESeq is the least sensitive in this regard (Robinson et al., 2010; Wang et al., 2010; Kvam et al., 2012; Trapnell et al., 2012; Zhang et al., 2014; Seyednasrollah et al., 2015). A sequencing depth of approximately 20 M for each sample is recommended for species for which genomic information is available when Cuffdiff2 is used. If there is not a lot of molecular data available for the sample a similar depth and more biological replicates are required. In cases where the sequencing depth between groups is unbalanced, DESeq is most sensitive to these imbalances (Robinson et al., 2010; Wang et al., 2010; Liu et al., 2014; Seyednasrollah et al., 2015).

Cuffdiff2 is not recommended when the sequencing depth is low and for differential expression analysis at gene level resolution (Anders and Huber, 2010; Anders and Wolfgang, 2012; Alamancos et al., 2014; Ari and Arikan, 2016). If false positives are a concern, it is recommended that DESeq be used. It is preferable that DESeq is not used in cases where the sequencing depth is unbalanced between groups. EdgeR has the advantage that it can tolerate both the unbalanced library sizes and low sequencing depth relatively well (Robinson et al., 2010; Wang et al., 2010; Sorenson and Delorenzi, 2013; Liu et al., 2014; Seyednasrollah et al., 2015).

Each method had its own strengths and limitations and there is no single method that is clearly superior for differential expression analysis. The analysis method used should be suitable for the specific RNA-Seq dataset and study design and should take overall performance of each tool into

account (Zhang et al., 2014; Seyednasrollah et al., 2015; Ari and Arikan, 2016; Hrdlickova et al., 2017).

9. Conclusion

From the literature it is clear that CDV is a complex disease not only the myriad of ways that it manifests and progresses in different individuals and species, but also in the wide host range it affects and the various factors potentially contributing to different host susceptibility to this disease (Martella et al., 2008; Beineke et al., 2015; Viana et al., 2015; Loots et al., 2016). Genetic drift in the viral genome, genetic differences in host receptors genes, gene expression differences in the host both prior to and following CDV infection, environmental factors and ecosystem interactions are all contributing factors to the varied susceptibility of CDV that is observed (Martella et al., 2008; Ohishi et al., 2010; Engering et al., 2013; Noyce et al., 2013; Ulrich et al., 2014b; Avila et al., 2015; Yuan et al., 2017).

Studies done in the past have mostly focused on evaluating different strains of CDV, especially the strains and variants causing epidemics and although these differences to contribute in part to the disease being different in different outbreaks and regions, it seems to play a limited role (Liao et al., 2015; Panzera et al., 2015). Genetic lineages of CDV tend to group together according to geographic regions, with small variations in especially the H-gene of CDV often resulting in new outbreaks and epidemics (Goller et al., 2010; Monne et al., 2011; Liao et al., 2015; Panzera et al., 2015). Some studies have looked at the genetic differences in different host receptor genes, including the SLAM, CD46 and nectin-4 genes. Specific regions within these genes have been showed to be more variable and some regions have been shown to be important in the binding affinity of the receptor to the CDV haemagglutinin protein (Ohishi et al., 2010; McCarthy et al., 2011; Noyce et al., 2013).

The use of predictive protein modelling has also proved useful in evaluating binding affinity between host cell receptors and the CDV host-binding proteins like the H-protein (Ohishi et al., 2010).

Ultimately how variations in the DNA relates to amino acid changes and subsequent structural changes in the protein determines if a change affects host-virus binding affinity. Despite the increase in available information with regard to molecular changes potentially underlying different CDV susceptibility, a lot remains unknown about the exact reason for why some species become infected, some species are especially severely affected and why others seem to not be susceptible to the disease at all (Appel and Summers, 1995; Alexander et al., 2010; Martinez-Gutierrez and Ruiz-Saenz, 2016).

The spread of CDV to the CNS and its progression to demyelinating leukoencephalitis is one of the interesting aspects of canine distemper and the mechanism, or mechanisms, underlying this process has not yet been fully elucidated (Vandevelde and Zurbriggen, 2005; Bonami et al., 2007; Carvalho et al., 2012). In recent years, gene expression studies have been helpful in better understanding some gene expression changes in the brain tissues of dogs infected with CDV and with different stages of demyelinating leukoencephalitis (Ulrich et al., 2014b). The main conclusion made from these studies is that CDV leukoencephalitis follows a biphasic mode of demyelination (Markus et al., 2002; Beineke et al., 2009; Lempp et al., 2014; Ulrich et al., 2014b), which is characterised by an initial oligodendrocyte dystrophy which is followed by an intrathecally synthesised immunoglobulin- and complement-mediated autoimmunity (Grőne et al., 2000; Beineke et al., 2009; Lempp et al., 2014; Ulrich et al., 2014b). This is similar to what has been observed in some multiple sclerosis gene expression studies, a demyelinating disease similar to canine distemper (Gandhi et al., 2010; Riveros et al., 2010; Mahad et al., 2015).

Various molecular techniques are evolving and being developed to study molecular changes on the DNA, RNA and protein levels respectively. Microarrays have been popular for gene expression studies, specifically for organisms for which gene and/or genome information is available (Conway and Schoolnik, 2003; Thomson et al., 2005; Noel et al., 2014; Wang et al., 2017b). In recent years RNA-Seq has been increasingly used to study gene expression and has the advantage over microarrays that it can be used even if little or no genome information is available. Some other

advantages of RNA-Seq over microarrays include its ability to detect novel gene expression (it is not limited to known genes) and RNA-Seq analysis can also be used to splice variants and expression differences for different splice variants of a gene (Alamancos et al., 2014; Ari and Arikan, 2016). Although it is a new technique for which standardisation still needs to be improved, this hypothesis-free approach is becoming increasingly popular for studies comparing gene expression between diseased and healthy states (Auer and Doerge, 2010; Dillies et al., 2013; Ari and Arikan, 2016).

One of the challenges facing RNA-Seq is the different analysis methods and approaches and the advantages and limitations associated with each of these. The Cuffdiff2 approach for detecting differentially expressed genes have been used most often, but a newer platform, DESeq offers certain advantages over Cuffdiff2 (Wang et al., 2010; Kvam et al., 2012; Vijay et al., 2013; Hrdlickova et al., 2017). Specifically, it seems to detect differential gene expression with more accuracy in studies where sequencing depth may be limited (Wang et al., 2010; Zhang et al., 2014). The balance between sequencing depth and biological replicates is another issued that is often debated in the context of RNA-Seq studies, although the majority of studies thus far propose increasing the number of biological replicates rather than the sequencing depth (Ozsolak and Milos, 2011; Liu et al., 2014; Ari and Arikan, 2016).

Combining advances in molecular biology, including the use of more accurate model organisms and technologies such as RNA-Seq and predictive protein modelling, host-virus interactions and gene expression in different hosts and during different stages of canine distemper can be studied more effectively and elaborately than before. This makes it possible for research to no longer be limited to just the virus or just the host, but to study both together. To ultimately understand the various mechanisms that underly CDV infection, disease progression and susceptibility it is essential to not consider any factors in isolation but to evaluate differences, especially molecular differences, at different levels (DNA, RNA and protein level).

Based on the information gained from the literature, the research discussed in the following two chapters could be planned. The first part of this research entails evaluating host receptor differences at the DNA level and using predictive protein modelling to predict which amino acid changes may potentially have the most significant impact on protein structure and the host-virus binding affinity. The second part of the following research focuses on gene expression differences within the CNS tissues of domestic dogs that are infected with CDV compared to their healthy counterparts.

Chapter 2

Variation in the Signalling Lymphocyte Activation Molecule (SLAM) and Cluster of Differentiation (CD46) receptors in different carnivore species of South Africa

Abstract

Canine distemper virus (CDV) is highly contagious, with an expanding host range and high mortality rates in wildlife species, including endangered species such as the African wild dog (*Lycaon pictus*). Significant differences in host susceptibility and disease manifestation have been observed in CDV infection, within and across species, but the underlying mechanisms for this remain unclear. This study aimed to better understand disease susceptibility by evaluating virus-host interactions in species from Canidae, Felidae and Hyaenidae families. Regions of two receptors involved in CDV binding and subsequent infection, SLAM and CD46, were amplified and sequenced to detect nucleotide and amino acid sequence changes. The secondary protein structures of the amino acid sequences were predicted to determine the possible effects of amino acid changes in host-virus binding affinity. Family-specific nucleotide and amino acid changes were observed in both receptors, with the V-domain of SLAM showing more variation than the selected exons in CD46. Most amino acid changes resulted in changes on the surfaces and in the grooves of secondary protein structures. These changes affected the predicted secondary structure of both receptors and could alter the binding affinity of the host receptors to virus proteins. Varying disease susceptibility can therefore be explained in part by molecular differences in the receptors involved in primary virus-host interactions. Understanding molecular mechanisms that contribute to host specificity of viruses expands our knowledge regarding the spread of highly infectious diseases and could assist in the improvement of prevention and treatment strategies.

1. Introduction

Canine distemper virus (CDV) is a single strand, non-segmented, negative sense RNA Morbillivirus belonging to the *Paramyxoviridae* family (Martella et al., 2008). It is the causative agent of canine distemper, a highly contagious systemic disease that is transmitted between susceptible hosts through aerosols and direct contact with contaminated body fluids (mucus, ocular discharge and excretions) (Behera et al., 2014).

Initial infection occurs in respiratory organs and then moves into the lymphoid system, where it is spread to other organs (Iwatsuki et al., 1999; Carvalho et al., 2012). Clinical signs vary between individuals within a species and between different species, with initial disease stages including fever, nausea and respiratory signs. The virus can also cross the blood-brain barrier and cause neurological signs and demyelination in the brain of some individuals (Vandevelde and Zurbriggen, 1995, 2005). In other cases, the virus persists for a long period of time without progression to severe neurological clinical signs (Beineke et al., 2009). The most notable symptom is however the severe immunosuppression accompanied by lymphopenia (Carvalho et al., 2012; Takenaka et al., 2016).

Canine distemper virus occurs in various canid species, especially *Canis familiaris* (domestic dogs), and a range of other species across different mammalian families (Appel and Summers, 1995; Barrett, 1999). The virus host range is increasing and has recently expanded to include multiple felid species, including *Panthera leo* (lions) and *Panthera tigris* (tigers) (Appel et al., 1994). Interestingly, CDV has not caused disease in *Felis catus* (domestic cats), despite their close proximity to dogs who could act as reservoir species for the virus (Viana et al., 2015). It has also not been observed in *Acinonyx jubatus* (cheetahs) thus far (Seimon et al., 2013; Terio and Craft, 2013). The disease susceptibility and severity vary significantly between species and between individuals within species, with felid species apparently more susceptible to infection (Deem et al., 2000; Martinez-Gutierrez and Ruiz-Saenz, 2016). *Lycaon pictus* (African wild dog) has also been infected with this disease, which has

significant implications for conservation of this endangered species (McCallum and Dobson, 1995; Prager et al., 2011; Prager et al., 2012b).

A modified live vaccine for CDV has been available since the 1950s, but proper vaccination does not always occur, especially in the South African context where many feral dogs are allowed to roam between residential and wildlife areas (Chappius, 1995). The efficacy of this vaccine in wild carnivores has long been debated due to the potential reversion to virulence, with the use of live attenuated vaccines not recommended unless there is no recombinant equivalent vaccine available (Chappius, 1995; Belsare and Gompper, 2015b). Although the vaccine has effectively induced immunity in some susceptible species, including *Mustela lutreda* (mink) populations, it has also been shown to cause disease in some felid species specifically (Belsare and Gompper, 2015b, a; Ramsay et al., 2016).

There are currently nine different CDV lineages, with one lineage specific to South Africa (Panzera et al., 2015). Differences in the viral hemagglutinin protein, the main protein involved in virus binding to host cells, are characteristic of different lineages in different geographical locations (Ke et al., 2015; Liao et al., 2015). A recent study showed that CDV circulating in South African wildlife falls within the Southern African lineage, with two possible sub-genotypes circulating which corresponds to the northern and the southern regions of South Africa (Loots et al., 2018).

The signalling lymphocyte activation molecule (SLAM), expressed on immune cells throughout the body, is the primary receptor for morbilliviruses. SLAM has an immunoglobulin-like variable domain (V-domain) and a constant domain in its extracellular surface (von Messling et al., 2001; von Messling et al., 2004; von Messling et al., 2005; Loots et al., 2018). This receptor is essential for CDV to establish infection in a host and has been shown to be variable among host species (von Messling et al., 2005; von Messling et al., 2006). Another receptor involved in CDV infection is the Cluster of differentiation 46 (CD46) receptor. This molecule is involved in the complement immune response, regulating the pro-inflammatory response and thereby changing the extent to which the

inflammatory response affects the host cells (Liszewski and Atkinson, 2015). The exact role of this secondary receptor in CDV infection is not clear (McCarthy et al., 2011).

Studies evaluating mechanisms underlying the different host responses seen in CDV infection have been limited to investigating the virus genes involved in binding to host cells (Otsuki et al., 2013; Sattler et al., 2014) and studies focusing on the SLAM receptor (Plattet et al., 2005; Sattler et al., 2014; Alves et al., 2015) and other immune response genes (McCarthy et al., 2007; McCarthy et al., 2011). Since receptors are one of the primary locations where host-virus interactions occur, they could contribute to differences in species' susceptibility to CDV infection. The aim of this study was therefore to assess amino acid variation and its potential effects on virus-host protein interactions, in the SLAM and CD46 receptors of different carnivore species of South Africa, but also material from some extralimital species.

2. Materials and Methods

2.1 *Blood samples*

Blood samples were collected from various species of the Canidae, Felidae and Hyaenidae families from different locations. For the Canidae family, blood was collected from *Lycaon pictus* (African wild dog) and *Canis africanis* (dog breed unique to Southern Africa). For the Felidae family, blood was collected from *Panthera leo* (lion), *Panthera tigris* (tiger), *Panthera pardus* (leopard), *Neofelis nebulosa* (clouded leopard), *Acinonyx jubatus* (cheetahs) and *Leptailurus serval* (serval). Samples were also collected from *Crocuta crocuta* (spotted hyena).

2.2 DNA extraction

Genomic DNA was extracted from whole blood using a commercial DNA extraction kit (DNeasy Blood and Tissue Extraction Kit, Qiagen, Hilden, Germany) according to the manufacturer's protocol for purification of total DNA from Animal Blood and Cells. Extractions made use of 100µl of blood from each of the samples. To confirm that high-molecular weight genomic DNA was successfully extracted, all extractions were visualized on 1% agarose gels using GelRed (Biotium) staining.

2.3 Amplification of SLAM V-domain and selected regions of the CD46 receptor gene

Primers that were previously designed for the SLAM V-domain (Ohishi et al., 2014) were used to amplify this region from DNA extracted from all species. The primers were used in the following combinations: SLAM-DF1 and SLAM-DR2 (primer set 1), Car-F1 and Cado-RI (primer set 2), Car-F2 and Cado-RI (primer set 3) and Car-F3 and Car-R1 (primer set 4). Primers designed for various exons and introns of the CD46 gene (McCarthy et al., 2011) were used to amplify regions of the gene from all species. The primers for this receptor gene were used in the following combinations: CD46F1 and CD46 R1 (primer set 1, targeting exon 2-3), CD4 F2 and CD46 R2 (primer set 2, targeting exon 4) and CD46 F3 and CD46 R3 (primer set 3, targeting exon 5). Refer to Table 2.1 for the complete list of primers.

An initial PCR amplification reaction for each primer set was performed using a single representative sample from each species. Initial reagent concentrations used were as follows: 1 × reaction buffer, 2.5 mM $MgCl_2$, 2.5 mM dNTPs, 10 µM of each of the primers and 0.5 U *Taq* DNA Polymerase (Whitehead Scientific). SABAX water was used to make up the reaction to a volume of 20 µl and a negative control (master mix without any DNA added to it) was included for each PCR batch. Initial amplifications with SLAM primers were carried out in a thermal cycler under the following conditions: 96ºC for 1 min; 30 cycles of 96ºC for 20 sec, 57ºC for 30 sec and 72ºC for 1 min, followed by a final extension at 72ºC for 10 min. Initial amplifications with CD46 primers were carried out under the following conditions: 95ºC for 1 min; 35 cycles of 95ºC for 45 sec, 56ºC/50ºC/52ºC for 45 sec (for primer sets 1-3 respectively) and 72ºC for 1 minute, followed by a final extension at 72ºC for 10 minutes. Amplified products were visualised on 1% agarose gels, along with the negative control and a 100bp molecular marker (to ensure the correct amplicon fragments were obtained) using GelRed staining.

Due to failure of DNA amplification in the majority of the species under the initial conditions, species-specific optimisation was done to determine the concentrations and conditions which resulted in successful amplification (a single DNA band of the correct size) for each individual species. During optimization all reagent concentrations were varied. The range of concentrations used were as follows: $MgCl_2$ concentrations varied between 0.5 and 2.5 mM; primer concentrations ranged from 7 to 25 µM; DNA concentrations varied between 20 and 40 ng; *Taq* polymerase concentrations were between 0.2 and 0.7 U and dNTPs were used at concentrations between 2.5 mM. Annealing temperatures used ranged from 57ºC to 61ºC for SLAM primers and temperatures for CD46 amplification ranged from 54ºC to 60ºC for primer set 1, 48ºC to 54ºC for primer set 2, and 50ºC to 57ºC for primer set 3.

The SLAM-DF1 and SLAM-DR2 primer set amplified the SLAM V-domain across all the species and only this primer set was therefore used to amplify the SLAM V-domain for downstream applications. Table 2.2 shows the species-specific amplification conditions used in the final PCR reactions (after optimisation).

Table 2.1

Primers used in this study to amplify the signalling lymphocyte activation molecule (SLAM) V-domain and part of the cluster of differentiation 4 (CD46) genes

Primer name	**Sequence**	**Nucleotide position**
SLAM*	GenBank: NM001003084	
Forward		
SLAM-DF1	5'-GTGAGAGCTTGATGAATTGC-3'	77-95
Car-F1	5'-GTGAGAGCTTGATGAATTGC-3'	78-96
Car-F2	5'-TGGGAAGAAATTTGCTGCTG-3'	116-135
Car-F3	5'-AAGGCATAAGTAAGAGCATG-3'	149-165
Reverse		
SLAM-DR2	5'-GCTTCAGCTGCAGACAAAAG-3'	388-408
CADO-RI	5'-TCATAGAGCTTCAGCTGCAG-3'	390-408
Car-R1	5'-TTCAGCTGCAGACAAAAGTG-3'	397-417
CD46**	GenBank: D84105	
Forward		
CD46 F1	5'-TGTGATCGTCCAGCATACATC-3'	Exon 2-3
CD46 F2	5'-ACTTCCAGACCCCGAAAATG-3'	Exon 4
CD46 F3	5'-AGCGGAGTACAGTGCATACCA-3'	Exon 5
Reverse		
CD46 R1	5'-TACGAGGACTACCTGGCCATT-3'	Exon 2-3
CD46 R2	5'-TTAAGACACATCGGCATCTCA-3'	Exon 4
CD46 R3	5'-CCTTTGCATGTATACCCATGA-3'	Exon 5

*Primers from Ohishi et al. (2014); **Primers from McCarthy et al. (2011)

Table 2.2

Reagent concentrations and cycling conditions for species-specific SLAM V-domain amplification

Species	**Optimised reagent concentrations**	**Optimised annealing temperatures**
Domestic dog *Canis africanis* African wild dog	1.0 mM $MgCl_2$ 20 µM SLAM-DF1 20 µM SLAM-DR2	58ºC for 30 seconds
Lion Serval Tiger	2.5 mM $MgCl_2$ 15 µM SLAM-DF1 15 µM SLAM-DR2	60ºC for 30 seconds
Leopard	2.2 mM $MgCl_2$ 20 µM SLAM-DF1 20 µM SLAM-DR2	59ºC for 30 seconds
Cheetah	2.7 mM $MgCl_2$ 22 µM SLAM-DF1 22 µM SLAM-DR2	57ºC for 30 seconds
Hyena	1.0 mM $MgCl_2$ 20 µM SLAM-DF1 20 µM SLAM-DR2 35 ng DNA	59ºC for 30 seconds

Table 2.3

Reagent concentrations and cycling conditions for species-specific CD46 exon 2-3 domain amplification

Species	**Optimised reagent concentrations**	**Optimised annealing temperatures**
Domestic dog *Canis africanis* African Wild dog Lion	1.5 mM $MgCl_2$ 18 µM CD46-F1 18 µM CD46-R1	57ºC for 45 seconds
Leopard Hyena	2.0 mM $MgCl_2$ 20 µM CD46-F1 20 µM CD46-R1 30 ng DNA	58ºC for 45 seconds
Tiger Serval	2.5 mM $MgCl_2$ 22 µM CD46-F1 22 µM CD46-R1	59ºC for 45 seconds
Cheetah	2.2 mM $MgCl_2$ 20 µM CD46-F1 20 µM CD46-R1 30 ng DNA	59.5ºC for 45 seconds

The primer set for exon 2-3 amplification (CD46 F1 and R1) yielded the highest concentration and quality amplicons and amplified this region of the CD46 gene across all the species. Only this primer set was therefore used to amplify part of the CD46 gene for downstream applications. DNA from the clouded leopard was not successfully amplified under any of these conditions and was therefore excluded from further analyses. Table 2.3 shows the species-specific amplification conditions used in the final PCR reactions (after optimisation).

2.4 DNA sequencing of the amplified SLAM V-domain and exon 2-3 of the CD46 receptor gene

Polymerase chain reaction products were cleaned up prior to sequencing by ethanol precipitation in which absolute EtOH, ddH_2O and 3M NaAc was added to each of the PCR products, followed by centrifugation for 20 minutes at 13 000 g. After removing the supernatant and drying the pellet, the amplified products were resuspended in 5 × TE buffer. Approximately 30 ng of amplicon DNA was used in a standard, quarter ABI Dye Terminator sequencing reaction and capillary gel separated on an ABI 3500XL sequencer (Thermo Fisher Scientific, Carlsbad, USA). All sequences were generated at the DNA Sanger sequencing facility in the Faculty of Natural and Agricultural Sciences, University of Pretoria. Sequences were verified by forward and reverse comparison. Refer to Table 2.4 below for a list of the samples that were sequenced.

2.5 SLAM V-domain and CD46 exon 2-3 sequence analysis

All sequences were manually edited in CLCBio v.7.7.3 **(**https://www.qiagenbioinformatics.com/**)** and each sequence was compared to available sequences in GenBank in a BLASTn and BLASTp analysis (Altschul et al., 1990; States and Gish, 1994). The SLAM V-domain and CD46 exon 2-3 gene sequences for the domestic cat (*Felis catus*) were also downloaded from GenBank for inclusion in further analysis (Table 5).

Table 2.4

List of species for which part of the SLAM V-domain and exon 2-3 of the CD46 receptor gene was sequenced

Animal	**Scientific name**	***N***
Suborder Caniformia		
Family Canidae		
Domestic dog	*Canis lupus familiaris*	2
African hunting dog	*Canis africanis*	4
African wild dog	*Lycaon pictus*	2
Suborder Feliformia		
Family Felidae		
Domestic cat	*Felis catus*	GenBank: AB828001 (Ohishi *et al*. 2014)
Lion	*Panthera leo*	8
Tiger	*Panthera tigris*	3
Leopard	*Panthera pardus*	2
Cheetah	*Acinonyx jubatus*	12
Serval	*Leptailurus serval*	2
Family Hyaenidae		
Spotted hyena	*Crocuta crocuta*	2

All sequences were aligned in MEGA 6.06 (Tamura et al., 2013) using the ClustalW alignment tool with default parameters. Sequences were then translated into amino acid sequences using the universal code for nuclear DNA available in MEGA 6.06 and evaluated for premature stop codons that could be indicative of sequencing errors or pseudogenes.

After obtaining a complete dataset with a total of 38 sequences, a reduced data set with one representative sequence for each species was constructed for further analysis. The number and positions of nucleotide variations between different species were calculated and the effect of nucleotide differences on the amino acid sequence (synonymous and non-synonymous amino acid changes) was subsequently evaluated.

2.6 Homology modelling of SLAM 3D protein structures

Three-dimensional (3D) structures of the obtained protein sequences were modelled using the Swiss-Model online modelling workspace (Guex et al., 2009). The protein data base (PDB) (Berman et al., 2003) entries for human NTB-A (2IF7) and marSLAM in complex with the measles virus hemagglutinin protein (3ALX: A-D chains) were used as template structures for the SLAM V-domain sequence modelling (Cao et al., 2006; Hashiguchi et al., 2011). The two N-terminal domains of the human CD46 (membrane cofactor protein) molecule (1CKL: A-B chains) were used as template structures for modelling of CD46 targeted sequences (Casasnovas et al., 1999). Only 3D structures modelled with a 90% or higher confidence were used. Individual atoms of the generated 3D models were visualised in the Visual Molecular Dynamics (VMD 1.9.3) programs and changes in bonding affinity as a result of amino acid changes were evaluated (http://www.ks.uiuc.edu/).

3. Results

3.1 DNA extraction and PCR amplification of target genes

DNA was successfully extracted from all blood samples (44 samples in total), with DNA concentrations varying between 90 ng/µl and 200 ng/µl (refer to fig. 2.1 for GelRed visualisations of DNA extractions). A few outlier samples yielded 10-15 ng/µl and 220-240 ng/µl DNA respectively.

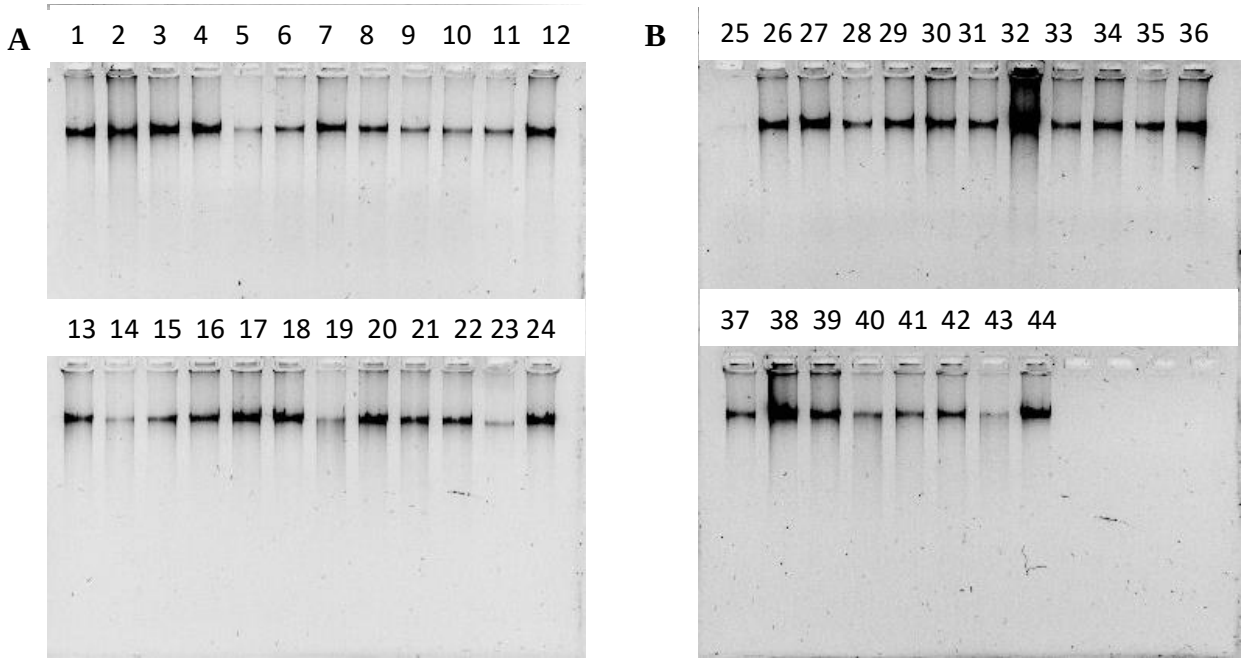

Fig. 2.1 DNA extractions stained with GelRed for visualisation under UV light. **A.** DNA extractions from the first 24 species samples: 1. lion 2. African wild dog 3. leopard 4. spotted hyena 5. serval 6. cheetah 7. cheetah 8. cheetah 9. tiger 10. serval 11. cheetah 12. leopard 13. lion 14. cheetah 15. cheetah 16. cheetah 17. lion 18. leopard 19. lion 20. serval 21. tiger 22. cheetah 23. lion 24. cheetah **B.** DNA extractions from samples 25-44. All DNA extractions were successful. 25. cheetah 26. cheetah 27. cheetah 28. tiger 29. cheetah 30. lion 31. tiger 32. African wild dog 33. African wild dog 34. African wild dog 35. cheetah 36. cheetah 37. lion 38. lion 39. African wild dog 40. *Canis africanis* 41. *Canis africanis* 42. *Canis africanis* 43. *Canis africanis* 44. spotted hyena.

SLAM V-domain amplification under the initial conditions specified by the authors who designed the respective primers did not yield successful amplification products, with multiple DNA bands being observed for SLAM primer set 1 and primer set 3 across species. Primer set 2 and 4 failed to amplify the SLAM V-domain in most species. In the case of CD46 target region amplification, primer set 1 resulted in non-specific amplification in most species, while primer set 2 only successfully amplified exon 2-3 of this gene in domestic dogs. Primer set 3 failed to yield any amplicons. Further optimisation was therefore necessary for targeted regions of both receptors.

Optimisation for all SLAM and CD46 primers was done by altering the $MgCl_2$, primer, DNA and *Taq* polymerase concentrations each in turn and by either increasing or decreasing the annealing temperature for each of the primer sets. Only primer set 1 (SLAM DF-1 and SLAM-DR2) for the SLAM V-domain resulted in successful amplification (a single, clear, high concentration DNA band of the correct size) of the target region across all the species, therefore only this primer set was used in subsequent amplification steps and for sequencing purposes, as it covers the majority of the SLAM V-domain targeted in this study. The amplicons obtained were on average 300 bp long. The primer set designed to cover exon 2-3 of the CD46 gene (primer set 1) yielded successful amplicons of approximately 220 bp and was used in subsequent amplification steps and sequencing.

DNA from the clouded leopard could not be successfully amplified in any of these cases and was therefore excluded from further analyses. One lion sample, one leopard sample, four cheetah samples, one African wild dog and one serval sample were also excluded due to very low PCR amplicon concentrations and multiple failed amplifications under optimised conditions.

3.2 Nucleotide sequences and deduced amino acid residues in carnivore species

For both SLAM V-domain sequences and CD46 exon 2-3 sequences only high-quality sequences were used for sequence comparisons. A total number of 38 sequences made up the initial dataset. Nucleotide variation between species was assessed and upon finding no differences between different samples of the same species within this data set a reduced data set with one representative sample from each species was constructed and used for further analysis. The nucleotide and amino acid sequences in both cases separated into three main groups: Caniformia (I), Feliformia (II) and Hyaenidae (III). No premature stop codons occurred in the deduced amino acid sequences.

3.2.1 SLAM V-domain

Nucleotide variation between species is shown in Fig. 2.2 below (only region containing variable sites shown), with non-synonymous changes reflecting in the amino acid sequence being considered as important contributors to potential differences in virus-receptor affinity between hosts.

Variable positions in the SLAM V-domain amino acid sequence (Fig. 2.3) occurred between residues 60 and 85. Domestic cats have a valine residue at position 63, where other species had a glycine residue at this position. Caniformia species had a glycine residue at position 66, whereas other species had an alanine residue. A change from glycine in other species to valine was also seen in lions at position 75. Caniformia species shared an arginine residue with hyenas and lions at position 77. Caniformia differed from all other species at position 79 too, with a glycine residue being present rather than a threonine residue. Leopards had a unique change at position 84, with a leucine in other species changing to a serine residue in leopards.

	15				20					25					30					35				40					45				50					55				60					65				70			
Domestic dog	T	C	C	C	T	G	T	C	T	C	C	C	T	G	G	C	C	G	A	T	G	G	A	T	T	C	C	A	G	G	G	G	C	T	T	C	C	T	C	T	C	C	C	T	G	C	G	C	T	G	C	C	T	G	C	T	G	G	T	C
Canis africanis	.	.	.	.	.	.	.	.	.	.	.	.	.	.	.	.	.	.	.	.	.	.	.	.	.	.	.	.	.	.	.	.	.	.	.	.	.	.	.	.	.	.	.	.	.	.	.	.	.	.	.	.	.	.	.	.	.	.	.	.
African Wild Dc	.	.	.	.	.	.	.	.	.	.	.	.	.	.	.	.	.	.	.	.	.	.	.	.	.	.	.	.	.	.	.	.	.	.	.	.	.	.	.	.	.	.	.	.	.	.	.	.	.	.	.	.	.	.	.	.	.	.	.	.
Domestic cat	.	.	.	.	.	.	.	.	.	.	.	.	.	.	.	.	.	.	.	.	T	.	G	.	.	.	.	.	.	C	C	.	.	.	.	.	.	.	.	.	.	.	.	.	.	.	.	.	.	.	.	.	.	.	.	.	.	.	.	.
Lion	.	.	.	.	.	.	.	.	.	.	.	.	.	.	.	.	.	.	.	.	.	.	G	.	.	.	.	.	.	C	C	.	.	.	.	.	.	.	.	.	.	.	.	.	.	.	.	.	.	.	.	.	.	.	.	.	.	T	.	.
Cheetah	.	.	.	.	.	.	.	.	.	.	.	.	.	.	.	.	.	.	.	.	.	.	G	.	.	.	.	.	.	C	C	.	.	.	.	.	.	.	.	.	.	.	.	.	.	.	.	.	.	.	.	.	.	.	.	.	.	.	.	.
Leopard	.	.	.	.	.	.	.	.	.	.	.	.	.	.	.	.	.	.	.	.	.	.	G	.	.	.	.	.	.	C	C	.	.	.	.	.	.	.	.	.	.	.	.	.	.	.	.	.	.	.	.	.	.	.	.	.	.	.	.	.
Tiger	.	.	.	.	.	.	.	.	.	.	.	.	.	.	.	.	.	.	.	.	.	.	G	.	.	.	.	.	.	C	C	.	.	.	.	.	.	.	.	.	.	.	.	.	.	.	.	.	.	.	.	.	.	.	.	.	.	.	.	.
Serval	.	.	.	.	.	.	.	.	.	.	.	.	.	.	.	.	.	.	.	.	.	.	G	.	.	.	.	.	.	C	C	.	.	.	.	.	.	.	.	.	.	.	.	.	.	.	.	.	.	.	.	.	.	.	.	.	.	.	.	.
Hyena	.	.	.	.	.	.	.	.	.	.	.	.	.	.	.	.	.	.	.	.	.	.	G	.	.	.	.	.	.	C	C	.	.	.	.	.	.	.	.	.	.	.	.	.	.	.	.	.	.	.	.	.	.	.	.	C	.	.	.	.
	75				80					85					90					95				100					105				110					115				120					125													
Domestic dog	C	T	C	G	C	C	C	T	G	G	C	G	T	C	C	A	A	G	C	T	G	A	G	C	T	G	T	G	G	G	A	C	A	G	G	T	G	A	G	A	G	C	T	T	G	A	T	G	A	A	T	T	G						
Canis africanis	.	.	.	.	.	.	.	.	.	.	.	.	.	.	.	.	.	.	.	.	.	.	.	.	.	.	.	.	.	.	.	.	.	.	.	.	.	.	.	.	.	.	.	.	.	.	.	.	.	.	.	.	.						
African Wild Dc	.	.	.	.	.	.	.	.	.	.	.	.	.	.	.	.	.	.	.	.	.	.	.	.	.	.	.	.	.	.	.	.	.	.	.	.	.	.	.	.	.	.	.	.	.	.	.	.	.	.	.	.	.						
Domestic cat	.	.	.	A	A	.	G	.	A	C	.	.	.	.	.	.	.	.	.	.	.	.	.	.	.	.	.	.	.	.	.	.	.	.	.	.	.	.	.	.	.	.	.	.	.	.	.	.	.	.	.	.	.						
Lion	.	.	.	C	A	.	.	.	A	C	A	.	.	.	.	.	.	.	.	.	.	.	.	.	.	.	.	.	.	.	.	.	.	.	.	.	.	.	.	.	.	.	.	.	.	.	.	.	.	.	.	.	.						
Cheetah	.	G	.	A	A	.	G	.	A	C	.	.	.	.	.	.	.	.	.	.	.	.	.	.	.	.	.	.	.	.	.	.	.	.	.	.	.	.	.	.	.	.	.	.	.	.	.	.	.	.	.	.	.						
Leopard	.	.	.	A	A	.	.	.	A	C	.	.	.	.	.	.	.	.	.	.	.	.	.	T	C	.	.	.	.	.	.	.	.	.	.	.	.	.	.	.	.	.	.	.	.	.	.	.	.	.	.	.	.						
Tiger	.	G	.	A	A	.	G	.	A	C	.	.	.	.	.	.	.	.	.	.	.	.	.	.	.	.	.	.	.	.	.	.	.	.	.	.	.	.	.	.	.	.	.	.	.	.	.	.	.	.	.	.	.						
Serval	.	.	.	A	A	.	.	.	A	C	.	.	.	.	.	.	.	.	.	.	.	.	.	.	.	.	.	.	.	.	.	.	.	.	.	.	.	.	.	.	.	.	.	.	.	.	.	.	.	.	.	.	.						
Hyena	.	.	.	.	A	.	.	.	A	C	.	.	.	.	.	.	.	.	.	.	.	.	.	.	.	.	.	.	.	.	.	.	.	.	.	.	.	.	.	.	.	.	.	.	.	.	.	.	.	.	.	.	.						

Fig. 2.2 Nucleotide sequence variation in the sequenced V-domain of the SLAM receptor. The sequences were aligned without gaps, with the nucleotide bases identical to that of the domestic dog reference sequence indicated with a dot. This sequence reflects part of the coding reading frame of the SLAM V-domain exonic region.

					60					65					70					75					80				85						
Domestic dog	F	P	V	S	L	A	D	G	F	Q	G	L	P	L	P	A	L	P	A	G	P	R	P	G	V	Q	A	E	L	W	D	R	E	L	D	E	L
Canis africanis	.	.	.	.	.	.	.	.	.	.	.	.	.	.	.	.	.	.	.	.	.	.	.	.	.	.	.	.	.	.	.	.	.	.	.	.	.	.
African Wild Dog	.	.	.	.	.	.	.	.	.	.	.	.	.	.	.	.	.	.	.	.	.	.	.	.	.	.	.	.	.	.	.	.	.	.	.	.	.	.
Domestic cat	.	.	.	.	.	.	.	V	V	.	A	.	.	.	.	.	.	.	.	.	.	Q	R	T	.	.	.	.	.	.	.	.	.	.	.	.	.	.
Lion	.	.	.	.	.	.	.	.	V	.	A	.	.	.	.	.	.	.	.	V	.	P	.	T	.	.	.	.	.	.	.	.	.	.	.	.	.	.
Cheetah	.	.	.	.	.	.	.	.	V	.	A	.	.	.	.	.	.	.	.	.	.	Q	R	T	.	.	.	.	.	.	.	.	.	.	.	.	.	.
Leopard	.	.	.	.	.	.	.	.	V	.	A	.	.	.	.	.	.	.	.	.	.	Q	.	T	.	.	.	.	S	.	.	.	.	.	.	.	.	.
Tiger	.	.	.	.	.	.	.	.	V	.	A	.	.	.	.	.	.	.	.	.	.	Q	R	T	.	.	.	.	.	.	.	.	.	.	.	.	.	.
Serval	.	.	.	.	.	.	.	.	V	.	A	.	.	.	.	.	.	.	.	.	.	Q	.	T	.	.	.	.	.	.	.	.	.	.	.	.	.	.
Hyena	.	.	.	.	.	.	.	.	V	.	A	.	.	.	.	.	.	.	.	.	.	.	.	T	.	.	.	.	.	.	.	.	.	.	.	.	.	.

Fig. 2.3 Deduced amino acid sequence of the variable domain of the SLAM receptor. Variable sites occurred between position 60-85 (amino acid residue numbers corresponding to the nucleotide sequence in Fig. 2.2, with dots indicating residues that are the same as those in the domestic dog).

Variable positions in the SLAM V-domain amino acid sequence (Fig. 2.3) occurred between residues 60 and 85. Domestic cats have a valine residue at position 63, where other species had a glycine residue at this position. Caniformia species had a glycine residue at position 66, whereas other species had an alanine residue. A change from glycine in other species to valine was also seen in lions at position 75. Caniformia species shared an arginine residue with hyenas and lions at position 77. Caniformia differed from all other species at position 79 too, with a glycine residue being present rather than a threonine residue. Leopards had a unique change at position 84, with a leucine in other species changing to a serine residue in leopards.

3.2.2 CD46 nucleotide sequences and deduced amino acid residues in carnivore species

Sequence alignment of the CD46 exons showed some nucleotide variation between species, as shown in Fig. 2.4 below. Non-synonymous changes that occurred as a result of these differences and differences between the amino acid sequences of different species are shown in Fig. 2.5. The most notable differences include unique residues in African wild dogs (tyrosine, not serine, at position 70) domestic cats (histidine at position 72), cheetahs (glycine at position 74), lions (arginine instead of

leucine at position 77) and a change from arginine to tyrosine at position 88 in hyenas. Caniformia species share a cysteine at position 82, compared to other species that have a serine at this location. Cats and cheetahs share a lysine residue at position 85 and leopards, tigers and servals share a glutamine residue at position 72.

					80					85					90					95				100				105				110				115				120				125			
Domestic dog	G	G	C	G	A	G	G	A	G	T	C	C	T	C	C	C	G	G	C	C	G	G	C	T	C	G	T	C	G	G	C	T	C	C	C	G	C	T	G	G	G	C	A	C	C	T	G	C	A	A
African Wild Dog	.	.	.	.	.	.	.	.	.	.	A	.	.	.	.	.	.	.	.	.	.	.	.	.	.	.	.	.	.	.	.	.	.	.	.	.	.	.	.	.	.	.	.	.	.	.	.	.	.	.	.
Canis africanis	.	.	.	.	.	.	.	.	.	.	.	.	.	.	.	.	.	.	.	.	.	.	.	.	.	.	.	.	.	.	.	.	.	.	.	.	.	.	.	.	.	.	.	.	.	.	.	.	.	.	.
Domestic cat	.	.	.	.	.	T	.	.	.	.	.	.	.	.	.	.	A	C	.	.	.	.	.	.	.	.	.	.	.	.	.	.	.	.	.	.	.	.	.	.	.	.	.	.	.	C	.	.	.	.	.
Lion	.	.	.	.	.	T	.	.	.	.	.	.	.	.	.	.	.	.	.	.	.	.	.	.	.	.	.	.	.	G	.	.	.	.	.	.	.	.	.	.	.	.	.	.	.	C	.	.	.	.	.
Cheetah	.	.	.	.	.	T	.	.	.	.	.	.	.	.	.	.	.	.	.	.	.	.	G	.	.	.	.	.	.	.	.	.	.	.	.	.	.	.	.	.	.	.	.	.	.	C	.	.	.	.	.
Leopard	.	.	.	.	.	T	.	.	.	.	.	.	.	.	.	.	A	.	.	.	.	.	.	.	.	.	.	.	.	.	.	.	.	.	.	.	.	.	.	.	.	.	.	.	.	C	.	.	.	.	.
Tiger	.	.	.	.	.	T	.	.	.	.	.	.	.	.	.	.	A	.	.	.	.	.	.	.	.	.	.	.	.	.	.	.	.	.	.	.	.	.	.	.	.	.	.	.	.	C	.	.	.	.	.
Serval	.	.	.	.	.	T	.	.	.	.	.	.	.	.	.	.	A	.	.	.	.	.	.	.	.	.	.	.	.	.	.	.	.	.	.	.	.	.	.	.	.	.	.	.	.	C	.	.	.	.	.
Hyena	.	.	.	.	.	T	.	.	.	.	.	.	.	.	.	.	.	.	.	.	.	.	.	.	.	.	.	.	.	.	.	.	.	.	.	.	.	.	.	.	.	.	.	.	.	C	.	.	.	.	.

					130					135					140					145				150				155				160				165				170				175			
Domestic dog	G	A	T	G	A	C	G	G	C	G	T	C	C	C	G	C	G	C	A	C	C	G	C	G	C	A	C	C	C	G	C	G	G	T	C	C	C	T	G	C	T	G	C	C	C	C	C	T	G	A
African Wild Dog	.	.	.	C	.	.	.	.	.	.	.	.	.	.	.	.	.	.	.	.	.	.	.	.	.	.	.	.	.	.	.	.	.	.	.	.	.	.	.	.	.	.	.	.	.	.	.	.	.	.	.
Canis africanis	.	.	.	.	.	.	.	.	.	.	.	.	.	.	.	.	.	.	.	.	.	.	.	.	.	.	.	.	.	.	.	.	.	.	.	.	.	.	.	.	.	.	.	.	.	.	.	.	.	.	.
Domestic cat	.	.	.	.	.	A	.	.	.	.	.	.	.	.	.	.	.	.	.	.	.	.	.	.	.	.	.	.	.	.	.	.	.	.	.	.	.	.	.	.	.	.	.	.	.	.	.	.	.	.	.
Lion	.	.	.	.	.	.	.	.	.	.	.	.	.	.	.	.	.	.	.	.	.	.	.	.	.	.	.	.	.	.	.	.	.	.	.	.	.	.	.	.	.	.	.	.	.	.	.	.	.	.	.
Cheetah	.	.	.	.	.	A	.	.	.	.	.	.	.	.	.	.	.	.	.	.	.	.	.	.	.	.	.	.	.	.	.	.	.	.	.	.	.	.	.	.	.	.	.	.	.	.	.	.	.	.	.
Leopard	.	.	.	.	.	.	.	.	.	.	.	.	.	.	.	.	.	.	.	.	.	.	.	.	.	.	.	.	.	.	.	.	.	.	.	.	.	.	.	.	.	.	.	.	.	.	.	.	.	.	.
Tiger	.	.	.	.	.	.	.	.	.	.	.	.	.	.	.	.	.	.	.	.	.	.	.	.	.	.	.	.	.	.	.	.	.	.	.	.	.	.	.	.	.	.	.	.	.	.	.	.	.	.	.
Serval	.	.	.	.	.	.	.	.	.	.	.	.	.	.	.	.	.	.	.	.	.	.	.	.	.	.	.	.	.	.	.	.	.	.	.	.	.	.	.	.	.	.	.	.	.	.	.	.	.	.	.
Hyena	.	.	.	.	.	.	.	.	.	.	.	.	.	A	C	.	.	.	.	.	.	.	.	.	.	.	.	.	.	.	.	.	.	.	.	.	.	.	.	.	.	.	.	.	.	.	.	.	.	.	.

					180					185					190					195				200				205				210				215				220				225			
Domestic dog	G	C	C	C	C	T	C	C	T	G	T	T	C	G	C	C	G	C	G	C	T	G	C	T	C	T	C	A	G	C	C	T	C	T	C	C	G	G	G	G	C	T	T	C	C	T	A	A	T	G	C	T	C	C
African Wild Dog	.	.	.	.	.	.	.	.	.	.	.	.	.	.	.	.	.	.	.	.	.	.	.	.	.	.	.	.	.	.	.	.	.	.	.	.	.	.	.	.	.	.	.	.	.	.	.	.	.	.	.	.	.	.
Canis africanis	.	.	.	.	.	.	.	.	.	.	.	.	.	.	.	.	.	.	.	.	.	.	.	.	.	.	.	.	.	.	.	.	.	.	.	.	.	.	.	.	.	.	.	.	.	.	.	.	.	.	.	.	.	.
Domestic cat	.	.	.	.	.	.	.	.	.	.	.	.	.	A	.	.	.	.	.	.	.	.	.	.	.	.	.	.	.	.	.	.	.	.	.	.	.	.	.	.	.	.	.	.	.	.	.	.	.	.	.	.	.	.
Lion	.	.	.	.	.	.	.	.	.	.	.	.	.	A	.	.	.	.	.	.	.	.	.	.	.	.	.	.	.	.	.	.	.	.	.	.	.	.	.	.	.	.	.	.	.	.	.	.	.	.	.	.	.	.
Cheetah	.	.	.	.	.	.	.	.	.	.	.	.	.	A	.	.	.	.	.	.	.	.	.	.	.	.	.	.	.	.	.	.	.	.	.	.	.	.	.	.	.	.	.	.	.	.	.	.	.	.	.	.	.	.
Leopard	.	.	.	.	.	.	.	.	.	.	.	.	.	A	.	.	.	.	.	.	.	.	.	.	.	.	.	.	.	.	.	.	.	.	.	.	.	.	.	.	.	.	.	.	.	.	.	.	.	.	.	.	.	.
Tiger	.	.	.	.	.	.	.	.	.	.	.	.	.	A	.	.	.	.	.	.	.	.	.	.	.	.	.	.	.	.	.	.	.	.	.	.	.	.	.	.	.	.	.	.	.	.	.	.	.	.	.	.	.	.
Serval	.	.	.	.	.	.	.	.	.	.	.	.	.	A	.	.	.	.	.	.	.	.	.	.	.	.	.	.	.	.	.	.	.	.	.	.	.	.	.	.	.	.	.	.	.	.	.	.	.	.	.	.	.	.
Hyena	.	.	.	.	.	.	.	.	.	.	.	.	.	A	.	.	.	.	.	.	.	.	.	.	.	.	.	.	.	.	.	.	.	.	.	.	.	.	.	.	.	.	.	.	.	.	.	.	.	.	.	.	.	.

Fig. 2.4 Nucleotide sequence variation in the exon 2-3 of the CD46 receptor. These sequences were aligned without gaps, with the nucleotide bases identical to that of the domestic dog indicated with a dot. Only the variable part of the 435 bp sequence is shown.

				70					75					80					85					90			
Domestic dog	G	E	E	S	S	R	P	A	R	R	L	P	L	G	T	C	K	M	T	A	S	R	A	P	R	T	R
African Wild Dog	.	.	.	Y	.	.	.	.	.	.	.	.	.	.	.	.	.	I	.	.	.	.	.	.	.	.	.
Canis africanis	.	.	.	.	.	.	.	.	.	.	.	.	.	.	.	.	.	.	.	.	.	.	.	.	.	.	.
Domestic cat	.	D	.	.	.	H	.	.	.	.	.	.	.	.	.	S	.	.	K	.	.	.	.	.	.	.	.
Lion	.	D	.	.	.	.	.	.	.	.	R	.	.	.	.	S	.	.	.	.	.	.	.	.	.	.	.
Cheetah	.	D	.	.	.	.	.	G	.	.	.	.	.	.	.	S	.	.	K	.	.	.	.	.	.	.	.
Leopard	.	D	.	.	.	Q	.	.	.	.	.	.	.	.	.	S	.	.	.	.	.	.	.	.	.	.	.
Tiger	.	D	.	.	.	Q	.	.	.	.	.	.	.	.	.	S	.	.	.	.	.	.	.	.	.	.	.
Serval	.	D	.	.	.	Q	.	.	.	.	.	.	.	.	.	S	.	.	.	.	.	.	.	.	.	.	.
Hyena	.	D	.	.	.	.	.	.	.	.	.	.	.	.	.	S	.	.	.	.	.	T	.	.	.	.	.

Fig. 2.5 Deduced amino acid sequence of exon 2-3 of the CD46 receptor (only part of the sequence shown). Variable sites occurred between position 68-90 (amino acid residues corresponding to nucleotide sequence regions shown in Fig. 2.4), with dots indicating residues that are the same as those in domestic dogs.

3.2.3 *Three dimensional models of carnivore SLAM V-domain interfaces*

The 3D models of the SLAM V-domain consisted of two β sheets, with the front sheet most likely providing the binding interface to canine distemper virus (Fig. 2.6) (Ohishi et al., 2010). Anti-parallel β-sheets and the loop structures connecting them form this binding interface. The amino acid changes noted in the previous section all occurred in regions previously determined to be binding sites in the receptor's structure and these residues are possibly involved in the interaction with the virus.

The sequenced region of the SLAM gene yielded the same conformation for domestic dogs, the African wild dog and *Canis africanis* (all Canidae species), with the same orientation of β-sheets and folding of connecting loops being observed. Hyena SLAM V-domain has a more open structural conformation, with loss of some of the overlap between loops. In Felidae species a similar pattern to that seen in the hyena is observed, with a much more open conformation with increased surface area compared to Canidae species. Servals are the only exception to this, where the protein conformation

is the same as that seen in Canidae. Cheetahs have a slightly more tightly wound conformation than other felid species, but still lacks overlapping loop regions that form the tighter conformation of the template SLAM molecule (Fig. 2.6 and Fig. 2.7).

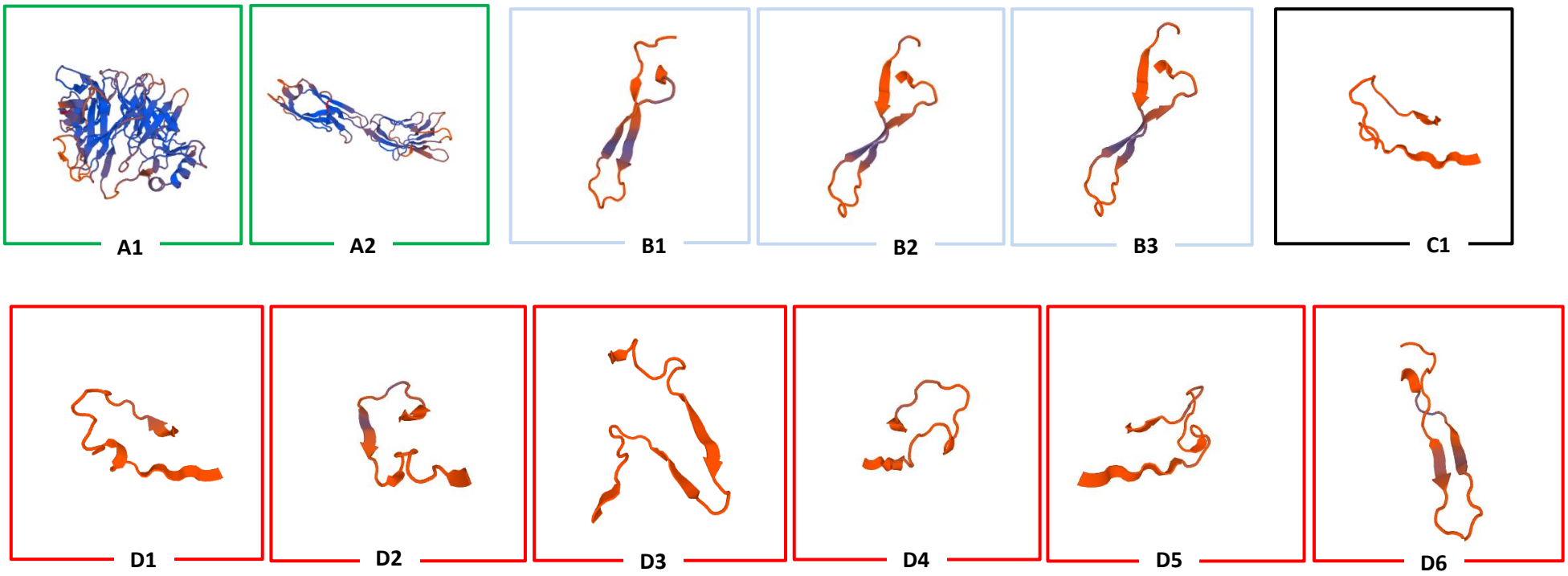

Fig. 2.6 Secondary protein structure of the V-domain of the SLAM receptor, modelled using the online SwissModel tool. A. Ribbon models of the two protein templates with known structures (A1. 2IF7 and A2. 3ALX). B. Ribbon model showing the secondary structure of different Caniformia species. B1. *Canis lupus familiaris* (domestic dog), B2. *Canis africanis* (African hunting dog), B3. *Lycaon pictus* (African wild dog). C. Ribbon model showing the secondary structure of Hyaenidae species. C1. *Crocuta crocuta* (spotted hyena). D. Ribbon model showing the secondary structure of different Feliformia species. D1. *Felis catus (domestic cat)*, D2. *Panthera leo* (lion), D3. *Panthera pardus* (leopard), D4. *Panthera tigris* (tiger), D5. *Acinonyx jubatus* (cheetah), D6. *Leptailurus serval* (serval).

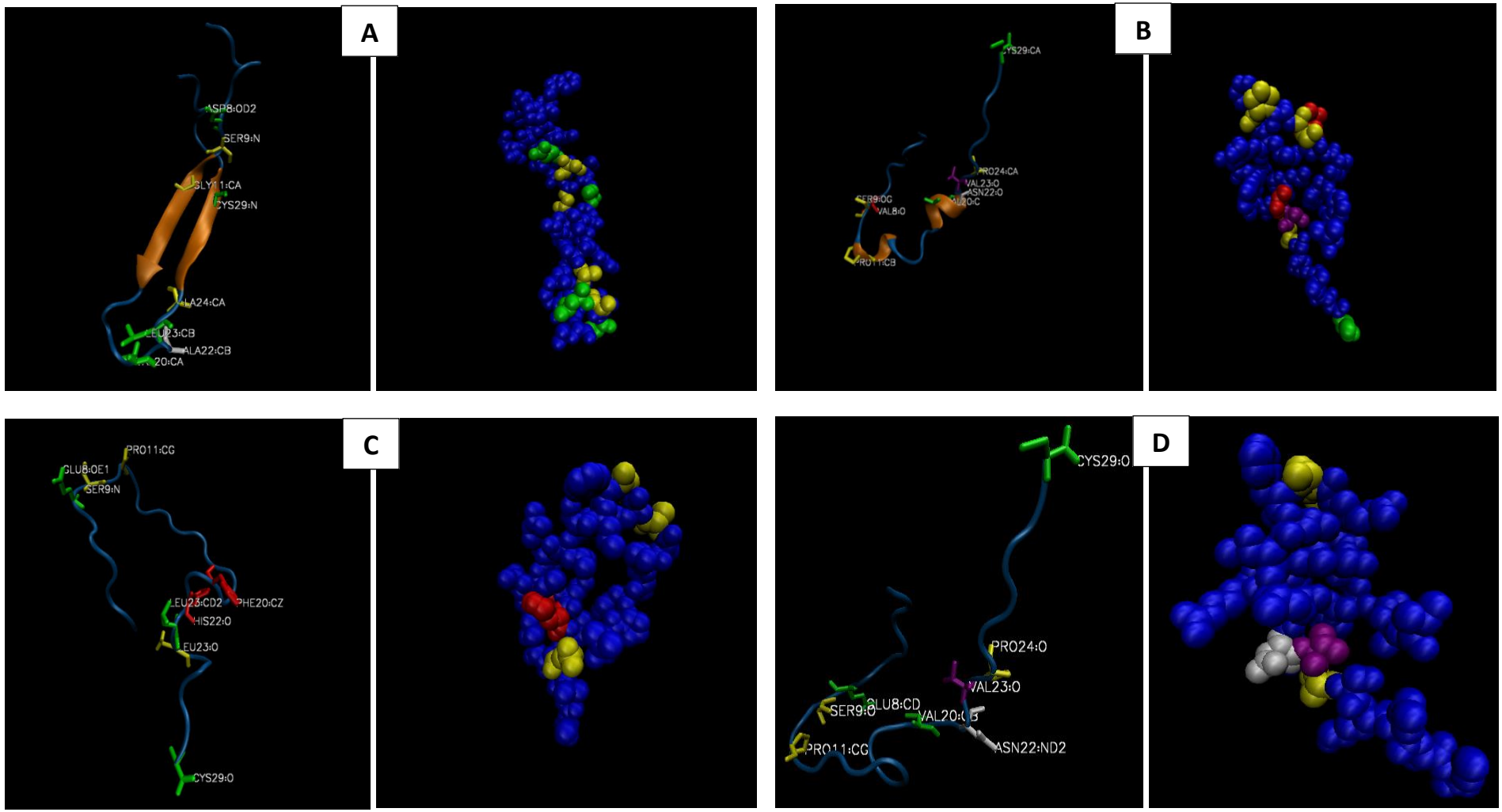

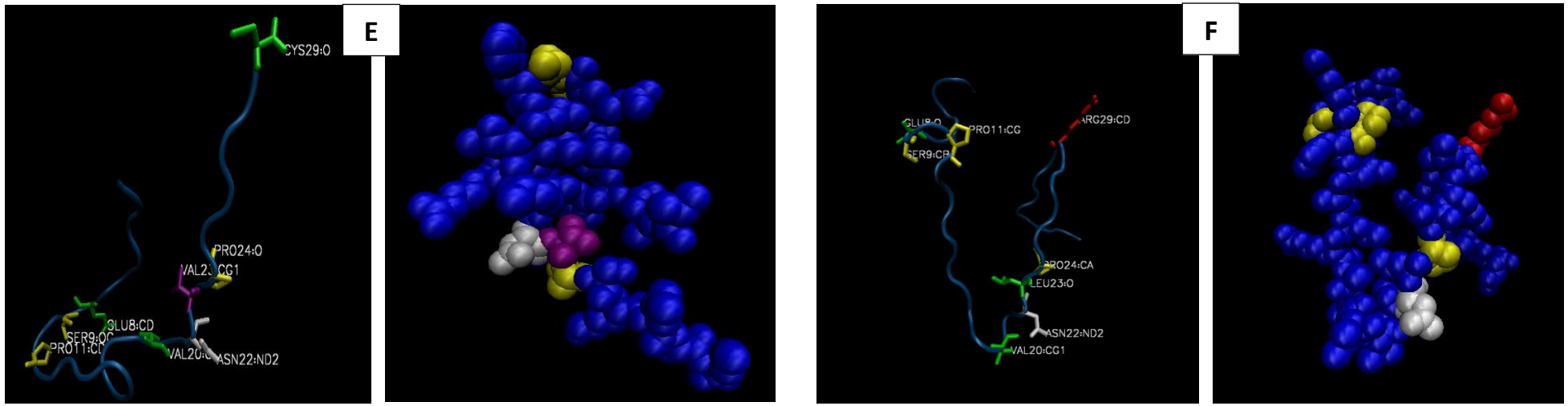

Fig. 2.7 Secondary structure diagrams (left) along with solid protein structures (right) indicating residue changes in the V-domain of the SLAM receptor between and within families. The secondary structure shows the general location of residue changes and the conformation of the protein, while the solid diagrams give an indication of the space occupied by the protein. Orange is used to indicate helices in the secondary structure diagrams, with blue regions showing loops and coils. Individual colour differences indicate amino acid residue differences. Structure for A. Domestic dog, B. Domestic cat, C. Lion, D. Cheetah, E. Tiger, F. Leopard. Green indicates positions where the residue is the same as that of the reference (domestic dog), yellow indicates residues that differ between Canidae and other species, white indicates residues that differ between species, purple indicates differences in residues shared by two or more species and red indicates species-specific changes. Most residue changes occur on the outer surface and in the grooves of the predicted protein V-domain, with very few changes located more towards the interior of the protein structure

3.3.4 Three dimensional models of carnivore exon 2-3 region of the CD46 gene

The 3D models of the CD46 domain consisted of β sheets folded onto each other and connected with loop structures to form two globular domains which together forms the binding surface for morbilliviruses (refer to Fig. 2.8 below).

Differences in the conformation of the CD46 protein can be observed for different Canidae species. In the domestic dog one of the domains necessary for binding is tightly formed, with part of the second domain partially present relative to the protein template structures that were used. In *Canis africanis* a looser, more open structure can be seen, with neither domain properly formed nor connecting loops as tightly wound to form domains as in the template structure. In the hyena, both domains involved in virus binding are partially formed, with increased surface area being observed in this conformation. Felid species appear to have a CD46 conformation very similar to that seen for the hyena, with one domain having a relatively open conformation and increased surface area, and both domains more completely formed than seen in Canidae species.

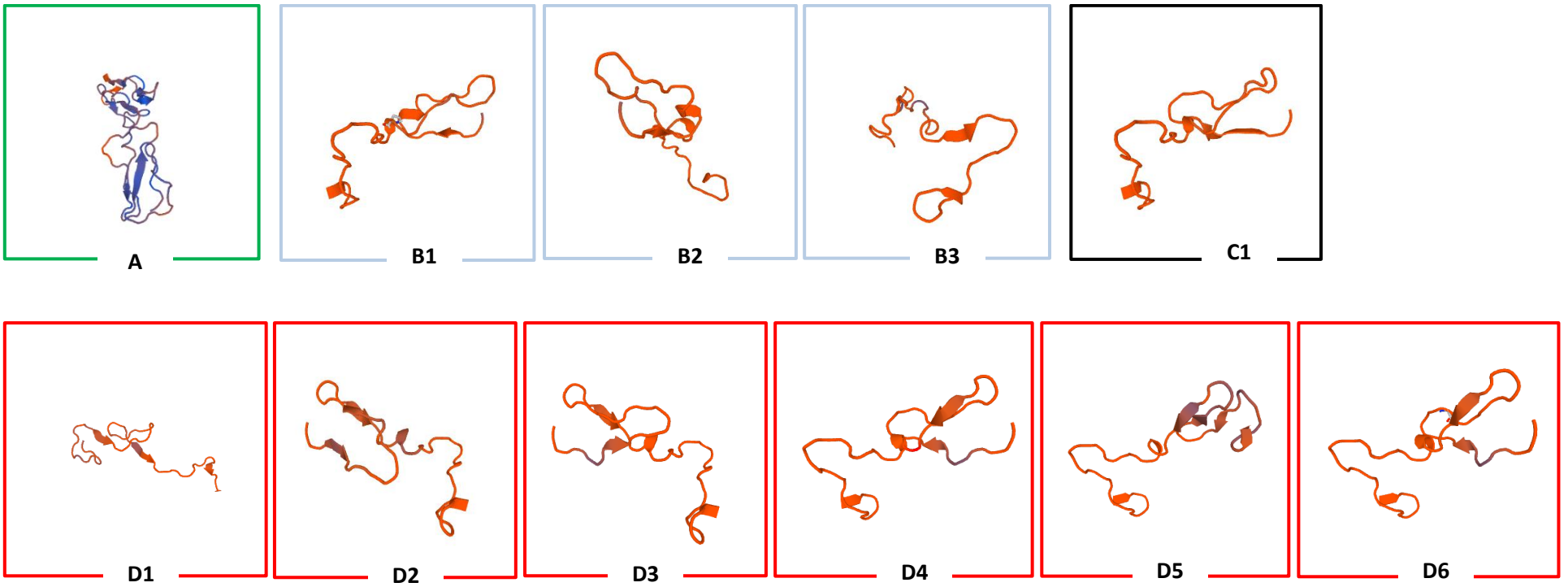

Fig. 2.8 Secondary protein structure of exon 2-3 of the CD46 receptor, modelled using the online SwissModel tool. A. Ribbon models of the protein template with known structures (1CKL). B. Ribbon model showing the secondary structure of different Caniformia species. B1. *Canis lupus familiaris* (domestic dog), B2. *Canis africanis* (African hunting dog), B3. *Lycaon pictus* (African wild dog). C. Ribbon model showing the secondary structure of Hyaenidae species. C1. *Crocuta crocuta* (spotted hyena). D. Ribbon model showing the secondary structure of different Feliformia species. D1. *Felis catus* (domestic cat), D2. *Panthera leo* (lion), D3. *Panthera pardus* (leopard), D4. *Panthera tigris* (tiger), D5. *Acinonyx jubatus* (cheetah), D6. *Leptailurus serval* (serval).

Individual residue changes in the secondary and overall protein structure of exon 2-3 of the CD46 receptor gene, between and within species, are shown in Fig. 2.9. More species-specific residue changes are observed in these predicted structures compared to the SLAM V-domain region, but the overall conformational changes between the different families are more limited than seen in the SLAM receptor. The helices seen in the template structures are present in most species. Most residues that differ between species is located toward the terminals and in the grooves of the protein structure, but the residue shared between the domestic cat, cheetah and tiger is located more towards the interior of the protein, with only a section of it appearing on the surface of the receptor region. The predicted structure for African wild dog shows a closer resemblance to the more open conformation seen in most of the felid species and in the hyena, but varies more when compared to domestic dogs and *Canis africanis* structures.

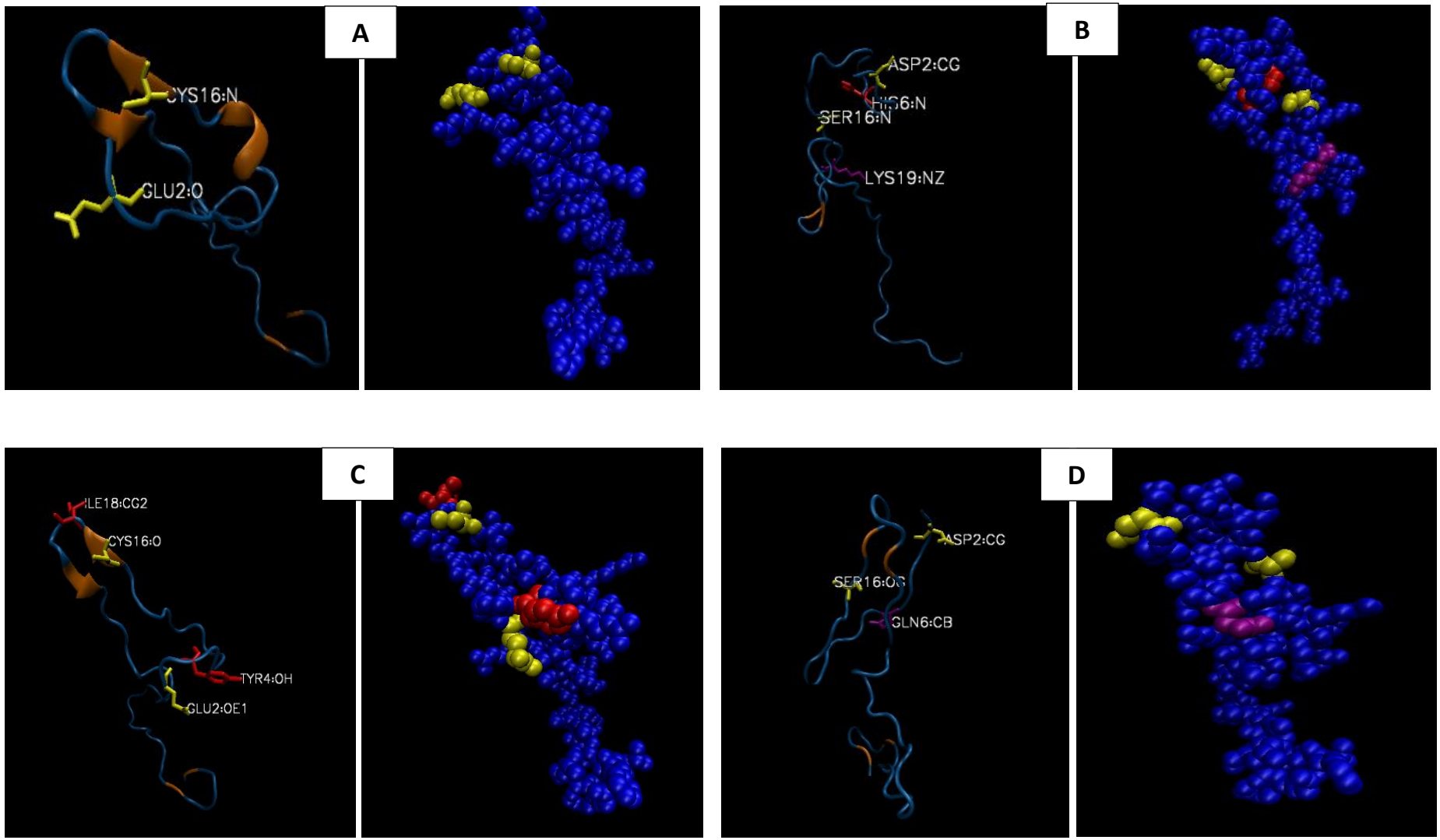

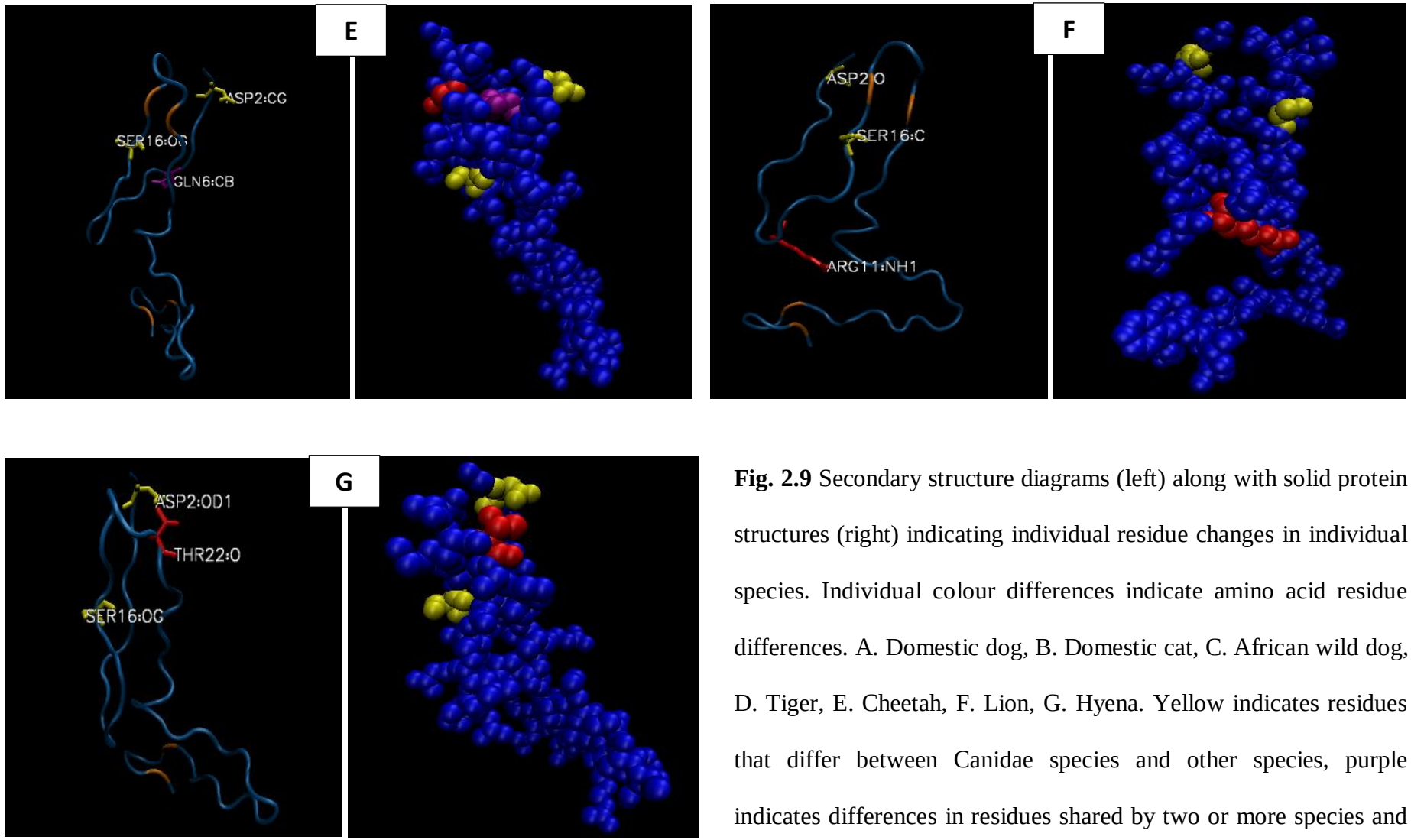

Fig. 2.9 Secondary structure diagrams (left) along with solid protein structures (right) indicating individual residue changes in individual species. Individual colour differences indicate amino acid residue differences. A. Domestic dog, B. Domestic cat, C. African wild dog, D. Tiger, E. Cheetah, F. Lion, G. Hyena. Yellow indicates residues that differ between Canidae species and other species, purple indicates differences in residues shared by two or more species and red indicates species-specific changes.

4. Discussion

In order to better understand the mechanisms underlying the host range (Harder and Osterhaus, 1997; Barrett, 1999; Martinez-Gutierrez and Ruiz-Saenz, 2016) and differences in the disease severity seen in CDV infection, many different factors can be considered, ranging from changes in the genome and proteins of the virus itself (Nikolin et al., 2012a; Sattler et al., 2014; Nikolin et al., 2016), to environmental factors that favour disease (Engering et al., 2013; Liu et al., 2013) and host mechanisms involved in establishing virus infection and controlling disease progression (Van Moll et al., 1995; Beineke et al., 2009; Beineke et al., 2015).

One of the first interfaces where the host and virus interact is at the level of host receptors and receptors therefore play an important role in determining host specificity (von Messling et al., 2004; Malpica et al., 2006). Signalling lymphocyte activation molecule SLAM is the main receptor targeted by the majority of morbilliviruses, including CDV (Tatsuo and Yusuke, 2002; Bieringer et al., 2013; Ohishi et al., 2014). Another receptor involved in CDV infection is the CD46 receptor, although less is known about its exact role in establishing infection (Liszewski and Atkinson, 2015). Specific residues in these receptors have previously been shown to be involved in the host-virus interaction (Hashiguchi et al., 2011; McCarthy et al., 2011; Lin and Richardson, 2016). Changes in these residues can result in changes in the protein's structure and conformation, potentially changing the binding affinity for CDV. Ohishi et al. (2010) made use of protein modelling in their studies to indicate the positions of residue changes, thereby improving the understanding of the effect of the specific changes on the affinity of the host cell to virus proteins. Protein modelling has also been used to predict interaction between the measles virus (a closely related virus) and its receptor in humans (Hashiguchi et al., 2011).

The amino acid variation in the SLAM receptor V-domain grouped the species that were sequenced into the carnivore families that they represent – Canidae, Felidae and Hyaenidae. Three amino acid changes (four nucleotide changes) separated Canidae from the Felidae and Hyaenidae families. The

species-specific variation was limited, with the lion being the exception with a more unique sequence, with two amino acids (valine at position 75 and proline at position 77) not found in any other species used in this study. The amino acid residue (arginine, R) shared between domestic cats, cheetahs and tigers was especially interesting, since CDV does not seem to cause disease in domestic cats and cheetahs but can cause severe illness in tigers (Appel et al., 1994; Kameo et al., 2012; Seimon et al., 2013; Gilbert et al., 2014).

The secondary receptor structure for these three species were similar to each other despite the apparent different susceptibilities. The secondary protein structures were also similar in all Canidae species, but differed significantly between Canidae and Felidae species, and even between Felidae species (except for servals that had similar structure to that seen in Canidae species). Hyaenidae sequences were more similar to Felidae sequences than to Canidae sequences, with the predicted protein conformations also showing this pattern. More than one residue change in a given sequence (compared to the reference sequence) together contributed to changes in protein structures more often than when a single residue was altered.

In the case of the CD46 receptor, more intra-family amino acid changes were observed than inter-family changes. Only two amino acid residues (three nucleotide changes) separated the Canidae species from Felidae and Hyaenidae. The changes in the African wild dog were the most interesting, with a tyrosine residue at position 70 and an isoleucine residue at position 84 being limited to this species. These residues resulted in a conformational change in the predicted protein structure, causing the structural characteristics and overall conformation to look more like the predicted proteins of felids, rather than the structures seen for dogs and *Canis africanis* samples. In general, the Felidae species all had a similar secondary protein structure, except for the cheetah receptor which had a different structural conformation. In the majority of the species the overall structure of the receptor was more conserved than for the SLAM receptor, with the helices being retained in most species and only some loop overlap lost.

Hashiguchi et al. (2011) found that residues in four main SLAM sites are involved in the interaction between host cells and measles virus: site 1: 77, 90; site 2: 61, 63; 3: 127-131 and 4: 75,119). The differences found in the present study corresponded to these findings, with three of the eight variable residues occurring at positions 63, 75 and 77 respectively and all other changes occurring within 2-4 positions from these sites. When McCarthy et al. (2011) investigated variation in different immune response genes they found no variation in the CD46 gene in the European harbor seal (*Phoca vitulina*). In the carnivore species used in this study, variation between species and within different families was detected. These observations support past suggestions that the molecular mechanisms underlying CDV infection differ in different species (Ohishi et al., 2010; McCarthy et al., 2011; Noyce et al., 2013; Pybus et al., 2013).

In both receptors, the majority of the structural changes occur towards the outside (surface) of the protein or in the grooves of the proteins. Since these regions have been shown to be more likely to interact with virus proteins (Luscombe et al., 2000; Luscombe and Thornton, 2002), residue changes here are more likely to affect host susceptibility by altering the affinity of the host cell to virus proteins. Changes in charge and hydrophobicity will also have a more significant effect than changes that involve residues with similar chemical characteristics (Luscombe and Thornton, 2002; Ohishi et al., 2010; Ohishi et al., 2014). The difference in disease susceptibility seen in the different carnivores used in this study could in part be due to amino acid differences that change the affinity with which the host receptors bind to CDV proteins.

From this study it can be concluded that the amino acid sequences for exon 2-3 of CD46 is more variable than for the SLAM V-domain, but the same region of CD46 is more constrained with regard to its protein conformation. Changes in the V-domain of SLAM resulted in changes in the secondary structure and spatial conformation of the receptor more often compared to CD46, but only when the alterations occurred in sites that typically interact with virus components. Amino acid changes occurred more often in species that had high mortality rates in epidemics, namely African wild dogs,

hyenas, lions and tigers. There was variation in the receptors of cheetahs, with some of the residue changes corresponding to residues found in domestic cats, but some also overlapping with species that are susceptible to CDV, such as the tiger. This is significant, since CDV does not cause disease in domestic cats and has not been documented in cheetahs thus far. Canine distemper virus does however affect tigers, which are phylogenetically related to lions. A different mechanism may therefore be responsible for the resistance to CDV infection seen in cheetahs and cats.

This study provides information about variation in two of the receptors involved in CDV binding for different carnivore species found naturally or in captivity in South Africa. From this study it can be concluded that there are differences between different carnivore species in the SLAM V-domain and in exon 2-3 of the CD46 receptor gene and these changes cause different extents of changes in the secondary structure and overall spatial conformation of receptor proteins. Most of these changes occur on regions of the proteins that contribute to host-virus binding, thereby potentially changing the way in which proteins interact with each other. This variation is one of the molecular mechanisms that could influence host specificity and susceptibility by altering the affinity with which host cells bind to viral proteins.

Comparative predictive modelling relies on establishing an evolutionary relationship between the sequence of the protein of interest and other members of the protein family, whose structures have been solved experimentally by X-ray or NMR. For this reason, the major limitation of this technique is the availability of homologous templates. Only regions of the protein corresponding to an identified template can be modelled accurately (Bordoli et al., 2009; Guex et al., 2009). As experimental protein structures are often available only for individual structural domains, it is often not possible to infer the correct relative domain orientation in a model. Modelling oligomeric proteins, such as complexes composed of more than one polypeptide chain, may be straightforward in cases where the complex of interest is similar to a homologous complex of known structure. However, this situation is

relatively rare, as most experimental structures in the PDB consist of individual proteins rather than complexes (Humphrey et al., 1996; Bordoli et al., 2009; Kiefer et al., 2009).

Modelling complexes from individual components is rarely successful without integrating additional information about the assembly. Comparative protein modelling techniques rely on structural information from the template to derive the structure of the target (Guex et al., 2009). Large structural changes, caused by mutations, insertions, deletions and fusion proteins, are therefore, in general, not expected to be modelled accurately by comparative techniques (Humphrey et al., 1996; Guex et al., 2009; Biasini et al., 2014). Nonetheless, homology models of a protein under investigation can provide a valuable tool for the interpretation of sequence variation and the design of mutagenesis experiment to elucidate the biological function of proteins (Bordoli et al., 2009; Guex et al., 2009). The reliability of different protein modelling methods can be objectively evaluated by examining the quality of predictions made during blinded tests. Emphasis is also placed on the analysis of the results of automated prediction servers whose accuracy has significantly increased over the last years (Humphrey et al., 1996; Arnold et al., 2006; Biasini et al., 2014; Kelley et al., 2015).

By making use of protein modelling and electrostatic potential calculations, it is possible to predict the way in which proteins will interact with each other and this can provide valuable insight into the host specificity and host range expansions of various pathogens. Protein docking can also be used to study the interactions of the virus proteins with host proteins in silico (Guven-Maiorov et al., 2019). Ultimately this approach is useful in determining how a given species can be influenced by a disease such as canine distemper and how disease circulation could be prevented. Cell lines expressing the SLAM receptor and/or the CD46 receptor with the observed amino acid changes could be infected with the virus and cell changes monitored to confirm that these changes do in fact change the way the virus proteins interact with host receptors.

Chapter 3

Differential gene expression in the brain tissue of domestic dogs with and without canine distemper virus infection

Abstract

Gene expression studies are useful to determine how differences in gene regulation and expression levels may relate to disease pathogenesis during different stages of disease development. RNA sequencing (RNA-Seq) is increasing in popularity because it allows a hypothesis-free way of evaluating large-scale gene expression and can allow for detection of novel genes or splice-variants of known genes. Canine distemper virus infection in dogs can manifest in various ways, with varying severity of clinical signs and a variety of histopathological manifestations which largely relate to the duration of infection. This pilot study made use of RNA-Seq to determine which genes are differentially expressed in the central nervous system (CNS) tissues of dogs infected with two histologically distinct lesion types of CDV compared to healthy control dogs. In total 768 differentially expressed genes were identified, of which 326 were not identified in previous microarray-based studies. The majority of differentially expressed genes was shared between the two CDV lesion types and mild subacute samples yielded the largest number of uniquely expressed genes. Enriched ontology terms included mitotic cell cycle and regulation of protein metabolic processes in upregulated genes. Precursor metabolites were the predominant ontology in downregulated genes. There are significant differences in the gene expression profiles of CNS tissues of CDV infected dogs compared to healthy dogs and both lesion types of CDV had genes that were only differentially expressed in the specific subtype. This study contributes to improved understanding of molecular mechanisms underlying disease in the CNS resulting from CDV infection.

1. Introduction

Canine distemper virus (CDV) is a highly contagious neurotropic measles-like virus causing canine distemper in dogs and various other carnivore species (Martella et al., 2008). The virus that causes a multisystemic disease can have a mortality rate of up to 50%, depending on the strain of the virus, the immune status and age of the host and environmental factors that may play a role (Malpica et al., 2006; McCarthy et al., 2007). Initial CDV infection is oronasal, with the first viremic spread causing lymphopenia and immunosuppression as it infects lymphoid tissues (Iwatsuki et al., 1999; Takenaka et al., 2016). If a sufficient immune response is launched by the host recovery from infection is possible (Beineke et al., 2009). Alternatively, a second viremic spread to multiple organs and tissues takes place, which can cause chronic persistent or late-onset encephalitis if the virus reaches the central nervous system (CNS) (Amude et al., 2010; Amude et al., 2012).

Central nervous system lesions observed in CDV-induced leukoencephalitis in experimental and natural infection can be classified into distinct lesion types. Acute lesions, occurring around 16-24 days post infection (p.i.), are characterized by the focal accumulation of CDV antigen in glial cells (Appel et al., 1974; Appel and Summers, 1995; Takenaka et al., 2016). It can eventually be accompanied by vacuolization of the white matter and mild gliosis. At day 26-32 p.i. subacute lesions occur, which are primarily characterised by demyelination but without inflammation. Finally, subacute to chronic lesions may form as the infection progresses (day 29-63 p.i.). This subtype is characterized by a reduced number of CDV antigen-positive cells and distinct lymphohistioplasmacytic perivascular cuffs several layers thick (Summers et al., 1984; Krakowka et al., 1987a; Krakowka et al., 1987b).

Different mechanisms that potentially underlie demyelination have been proposed. These include virus-induced damage of oligodendrocytes, activated astrocytes and microglia or macrophages that release tumour necrosis factor-α or damage caused by humoral and cell-mediated immunity (Vandevelde and Zurbriggen, 1995, 2005). Bystander damage due to activated microglia or

macrophages releasing myelotoxic reactive oxygen species and proteolytic enzymes have also been described as the underlying mechanism. Since CDV is a demyelinating disease naturally occurring in dogs, it has been proposed as a model to study the pathogenesis of demyelination in subacute sclerosing panencephalitis and multiple sclerosis in humans (Vandevelde and Zurbriggen, 2005; Ulrich et al., 2014a; Ulrich et al., 2014b).

In the past, CDV was even suggested to be a possible etiological agent for MS due to a correlation in the incidence and prevalence of MS in dog owners (Hodge and Wolfson, 1997; Sips et al., 2007; Lassmann, 2013). Aside from CDV infection and resulting demyelination occurring in dogs, dogs also share the same environments as humans and are more similar to humans in biology than some other model species (e.g. mice) (Parker et al., 2010; Maes et al., 2014). It may therefore be a very useful model species to shed light on the molecular pathogenesis of both CDV and other demyelinating diseases of the CNS (Pedersen, 1999; Ostrander, 2012; Pedersen et al., 2014).

Canine distemper virus in domestic dogs produces clinical signs similar to the systemic clinical signs seen in humans infected with measles virus, a closely related morbillivirus (Haralambieva et al., 2013). Both viruses are neurotropic, although the frequency and time course of the neurological effects differ (Haralambieva et al., 2013). The measles virus vaccine used in humans has also been shown to produce an amnestic immune response to canine distemper virus in measles-immunized pups (Hodge and Wolfson, 1997; da Fontoura Budaszewski and von Messling, 2016).

Over the last several years, multiple studies have been performed to better understand the genome and transcriptome of the domestic dog (Wayne and Ostrander, 2007; Briggs et al., 2011; Albert et al., 2012; Mooney et al., 2013; Roy et al., 2013; Hoeppner et al., 2014). Genes associated with certain diseases, specifically cancers, that overlap between dogs and humans have been the focus of several investigations, with one study specifically focusing on the normal transcriptome in various organs of dogs (Parker et al., 2006; Briggs et al., 2011; Mooney et al., 2013; Raddatz et al., 2014). Dogs are becoming increasingly popular model organisms as multiple studies have illustrated the poor

transcriptional overlap between mouse models and human inflammatory diseases (Mestas and Hughes, 2004; Parker et al., 2010; Bean et al., 2013; Hoffman et al., 2018).

Despite this myriad of different molecular biology and specifically gene expression studies, only one study has focused on gene expression changes in the CNS of dogs with CDV-induced demyelination and the potential molecular mechanisms underlying it (Ulrich et al., 2014b). This was a microarray-based study that evaluated genes differentially expressed in the different leukoencephalitis lesion types observed in dogs infected with CDV compared to healthy control dogs. The authors identified 442 differentially expressed genes across 720 probe sets. Many up-regulated genes were classified by the gene ontology terms "viral replication" and "humoral immune response," while down-regulated genes were related to "metabolite and energy generation." Multiple myelin-associated genes were selectively down-regulated in chronic CDV leukoencephalitis, while genes relating to the innate and humoral immune response were significantly up-regulated. The main conclusion was that the transcriptional changes in CDV-leukoencephalitis support a biphasic mode of demyelination with an initial non-apoptotic oligodendrocyte dystrophy followed by a later wave of intrathecally-synthesized immunoglobulin and complement mediated autoimmunity (Ulrich et al., 2014b).

Genome-wide expression analyses have become very popular to elucidate disease mechanisms, to identify causative genes and in suggesting potential therapeutic targets for specific diseases (Carninci et al., 2005; Qian et al., 2013; Qeska et al., 2014). Ulrich et al. (2014) laid the foundation for understanding the molecular mechanisms underlying CDV infection in the CNS of dogs. However, with the advent of RNA sequencing, it became possible to detect low-abundance and novel transcripts, as well as alternative splice variants and allele-specific expression of transcripts with increased sensitivity. This is especially useful in species for which very little genomic information is known (Ozsolak and Milos, 2011; Vijay et al., 2013; Han et al., 2015; Ari and Arikan, 2016; Hrdlickova et al., 2017).

RNA-Sequencing is a model free method that allows us to better understand the transcriptomic landscape underlying various diseases and its increased sensitivity gives it a significant advantage over traditional microarray experiments (Marioni et al., 2008; Auer and Doerge, 2010; Ari and Arikan, 2016). Gene expression can then be correlated to disease by combining gene expression studies with clinical information. To progress from gene expression to disease risk, it is especially important to ensure that gene expression measurements are performed in tissues and cell types with biological relevance to the trait or disease of interest (Chen et al., 2008; Dermitzakis, 2008). More robust correlations can also be made by combining data from various data sets and ranking genes according to significant correlations with clinical traits (Emilsson et al., 2008).

RNA-Sequencing has been used to elucidate the mechanisms underlying the IFN-dependent antiviral immunity in MeV-infected brain tissues to promote the understanding of vaccine-induced immune responses (Kim et al., 2013). It was also used to study genetic variants affecting the regulation of transcription and mRNA processing in MS (Gandhi et al., 2010). In the latter study the importance of studying genetic variance in tissues associated with pathogenesis was reinforced and showed that there was dysregulation of T cell gene expression in MS and its specific lesion types compared to healthy controls (Emilsson et al., 2008; Gandhi et al., 2010). This method of studying gene expression has also been used to determine which transcription factors play an important role in the pathogenesis of various lesion types of MS (Riveros et al., 2010). Another study used RNA-Seq to analyse gene expression in the brain tissue of Greyhounds with meningoencephalitis (Greer et al., 2010).

The aim of this non-hypothesis driven pilot study was to use RNA-Seq to identify CNS genes that are differentially expressed between healthy dogs and dogs infected with CDV, to better understand this complicated neurotropic viral disease.

2. Materials and methods

2.1 Ethics statement

Ethical approval for this study was obtained and a tissue collection protocol approved before the study commenced (University of Pretoria Animal Ethics Committee V034-14). No animals were artificially infected during this study and animals from which samples were collected were euthanized. Canine distemper virus infected dogs were euthanized at the owners request due to poor prognosis and the infectious risk the dogs posed in their home environments. Control dogs were euthanized because they were feral and no longer wanted. All the tissues used was collected by one of the investigators (Andrew Leisewitz) at the Onderstepoort Veterinary Academic Hospital (OVAH) or at various participating private veterinary practices close to the OVAH.

2.2 Experimental design and sampling

Brain tissues were collected from CDV infected and healthy dogs of different breeds, ages and sexes (Table 3.1). All tissues were collected within an hour of death. Portions of the brain collected included a left and right portion of the mid cerebrum, cerebellum, hypothalamus and medullary velum. Half of each of these portions were immediately fixed in 10% buffered formalin. The other half was immediately fixed in twice the tissue volume of iced RNAlater (RNAlater RNA Stabilization Reagent, Qiagen) and stored at 4 °C for at least 72 hours before being archived at -80°C for no longer than six months before being subjected to the RNA extraction procedures.

Table 3.1

Description of dogs with canine distemper virus infection (CDV) and controls from which brain tissues were collected.

Animal number	Breed	Sex	Age (months)	RNA Sequencing Code	CDV Classification
CDV-positive samples					
CDV 3	Jack Russel Terrier	F	10	CDV+I1	Moderate-severe chronic
CDV 6	German Shepherd	M	Unknown (middle aged adult)	CDV+I2	Mild-subacute
CDV 7	Siberian Husky	F	Unknown (middle aged adult)	Not sequenced	Mild-subacute
CDV 10	Boerboel	M	4	CDV+I3	Moderate-severe chronic
CDV 14	Mixed breed	M	24	CDV+I4	Mild-subacute
Control samples					
Control 1	Jack Russel Terrier	F	180	CDV-C1	Not infected
Control 2	Yorkshire Terrier	M	7	Not sequenced	Not infected
Control 3	Boston Terrier	M	42	Not sequenced	Not infected
Control 4	Mixed breed	F	10	CDV-C2	Not infected
Control 5	Border Collie	M	12	Not sequenced	Not infected
Control 6	Corgi	F	24	Not sequenced	Not infected
Control 7	Pitbull	M	12	Not sequenced	Not infected
Control 8	Labrador	F	24	Not sequenced	Not infected

For the current study, only the cerebellum and medullary velum of infected and healthy dogs were immunohistologically compared to confirm the presence or absence of CDV infection (refer to Fig 3.1 below). Based on histopathological findings dogs with CDV were classified into two groups: (1) Moderate-severe chronic infection (with moderate multifocal demyelination and associated astrogliosis and mononuclear inflammation) and (2) mild-subacute infection (with mild multifocal demyelination, mild astrogliosis and scant inflammation).

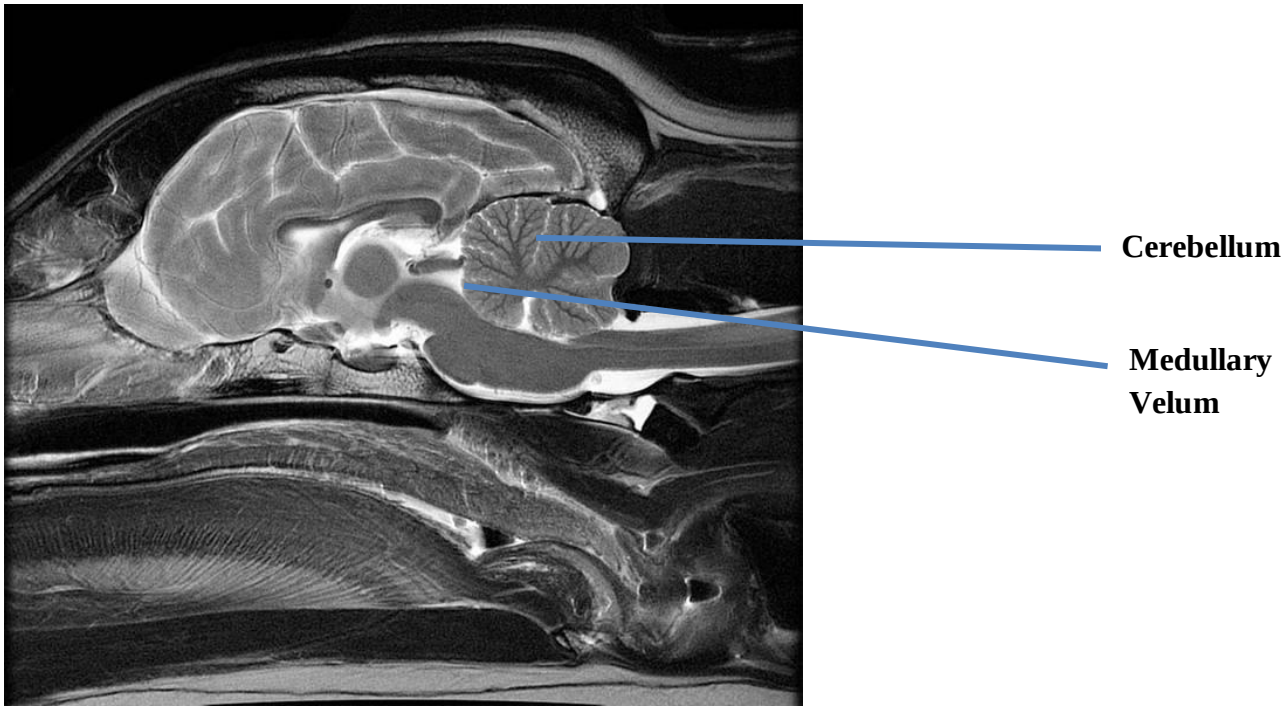

Fig. 3.1 Magnetic resonance imaging image showing the sagittal plane of the brain of the dog. Samples taken from the cerebellum and the medullary velum were used for RNA-Seq purposes, as these regions contained the highest concentration of CDV (image curtesy of the Canine Brain MRI Atlas initiative hosted by the University of Minnesota; http://vanat.cvm.umn.edu/mriBrainAtlas/ accessed June 2018).

Healthy dogs were from here-on referred to as group 1, dogs with moderate-severe chronic infection as group 2 and those with mild-subacute infection as group 3.

2.3 Histology and Immunohistochemistry

All histology and immunohistochemistry work were performed by a specialist veterinary pathologist (Dr Sarah Clift, Section of Veterinary Pathology, Faculty of Veterinary Science, University of Pretoria). Immunohistochemistry was performed for all control and cases that were clinically suspicious for CDV infection. The presence or absence of CDV infection was thus confirmed for cases included in the study. Brain samples (no bigger than $5mm^3$) were fixed for 24-48 hours in 10% neutral buffered formalin, paraffin-embedded and sectioned at 4µm. The cerebellar and medullary velum sections were routinely stained with haematoxylin and eosin (HE) and Luxol fast blue-cresyl violet (LFB) for myelin according to optimized laboratory protocols. Immunohistochemistry (IHC) was performed using a mouse monoclonal anti-CDV nucleoprotein antibody (Code No. DV2-12, Custom Monoclonals International, W. Sacramento, CA, USA) to confirm CDV infection (Fig. 3.1). Heat-induced epitope retrieval was performed on the tissue sections (microwaved at 96 ^oC in Citrate buffer, pH of 6) for 14 minutes after which sections were incubated for 2 hours with the monoclonal mouse anti-CDV antibody (dilution 1:80).

Sections were then processed using the EnVision polymer-based immunodetection system (code no. K5007, DakoCytomation, Denmark) according to specific kit instructions. A Vector NovaRED substrate system (Code No. SK4800, Vector Laboratories, Burligame, USA) was used for development of colour (red brown) in the tissue sections. The tissue sections were routinely mounted, and cover slipped for light microscopic examination using an Olympus BX43 microscope.

2.4 RNA extraction and quantification

Total RNA was isolated from the frozen brain specimens using the RNeasy Lipid Tissue Mini Kit (Qiagen, Hilden, Germany), according to manufacturer specified protocols and treated with DNase. The quality and integrity of the RNA was determined using the Experion^{TM} Automated Electrophoresis System (Bio-Rad). The 1:2 ratio of 28S and 18S RNAs was also confirmed by peak estimation with the bioanalyzer. Samples were considered to be of high quality if they contained intact RNA that yielded a RIN value (RNA integrity number) of more than 8 and if samples contained at least 1.5 µg RNA per sample total RNA.

2.5 RNA Sequencing

RNA sequencing was only performed for a total of twelve samples from six dogs. Samples from the cerebellum and the medullary velum of four CDV positive dogs and two control dogs were submitted to the Central Analytical Facilities (CAF) at Stellenbosch University for RNA sequencing.

RNA-Sequencing libraries were generated for the control and diseased samples according to standard procedures using ION Proton library preparation kits (performed by CAF). Samples were enriched for mRNA by capture on poly-T covered magnetic beads, followed by chemical fragmentation and the remaining mRNA was used as templates for cDNA synthesis. Double-stranded cDNA was blunt-ended and paired-end ION Proton sequencing adapters were ligated to the cDNA. Libraries were sequenced on the ION Proton platform by CAF, using one sequencing lane per sample; 100bp were sequenced from both ends of each fragment. Samples were processed together throughout RNA extraction and library preparation to minimize potential batch effects.

2.6 RNA Sequencing Analysis

2.6.1 Quality check and filtering

ION Proton reads were processed by trimming adapter sequences, merging overlapping read pairs and keeping only reads with >51bp length (after merging and adapter trimming). FastQC v.0.11.5 was used to calculate the per base sequence quality and per sequence quality scores. Only sequences with Phred scores >20 were included in downstream analyses.

2.6.2 Read mapping and gene expression quantitation

Paired-end reads were mapped to the dog reference genome, canFam2 (Lindblad-Toh et al., 2005), using Bowtie v.2.2.9 (http://bowtie-bio.sourceforge.net/index.shtml) (Langmead and Salzberg, 2012) and Tophat v.0.12.9 (http://tophat. cbcb.umd.cdu/) (Trapnell et al., 2009; Trapnell et al., 2010; Trapnell et al., 2012; Kim et al., 2013). Initially Bowtie was used to map all reads to the reference genome, allowing for a maximum mismatch of 1bp. All reads that did not map to the reference genome at first were re-mapped using Tophat. Tophat infers that reads may span a splice junction when several segments of a read maps to regions far apart from each other on the genome. Mapped reads were assembled into transcripts for each sample based on the reference assembly, with fragment bias and multi-read correction. Assembled transcripts were merged into a single assembly based on the reference input, and transcript assemblies for each dog were grouped into affected and unaffected (four dogs and two dogs respectively). The 12 different transcript data sets were merged into a single data set for differential expression analysis.

Gene expression was quantified from the merged assembly file of mapped reads (from Tophat) using the HTSeq-count (http://www-huber.ensbl.de/user/anders/HTSeq/doc/count.html) (Anders and Wolfgang, 2012; Anders et al., 2014) and Cufflinks software packages. HTSeq-count (v.0.6.1p2) was used to obtain the integer counts of mapped reads per gene, while the default parameters in Cufflinks (v.2.2.1) were used to obtain FPKM (fragments per kilobase of exon per million mapped fragments) expression values, based on the library size distributions and sequence composition bias corrections.

Read mapping and gene quantification was performed separately for each transcriptome assembly. Gene models defined in the Ensembl89 database were used to run both programs (Aken et al., 2016). No gene annotations were modified or excluded during quantification, and genetic variation was not used to correct the expression levels and differences between samples.

2.6.3 Differential gene expression analysis

Differentially expressed genes were identified in DESeq v. 1.6.1, based on normalized integer count data (Anders and Huber, 2010; Anders and Wolfgang, 2012). Size factors that took the total number of reads in different samples into account were calculated and a dispersion parameter was then determined for each gene, to take the biological variation between samples into account. DESeq then fitted a negative binomial distribution to the counts of each gene. The *q*-value was calculated to determine the significance of differential gene expression between the comparative groups. Pairwise comparisons only made use of genes with >0 counts in >50% of samples.

Genes that were not called present in at least two of the twelve samples were removed. This value was chosen because the control group had four samples from only two different dogs. Presence in four samples were not required because the two samples taken from the same dog artificially reduce the variance and this prevented genes that might have been present in normal but not diseased dogs from being discarded. The number of reads mapped to each gene and variance among samples were used to normalize transcript abundances to the overall read depth. A heatmap of the differentially expressed transcripts that mapped to known genes was generated using the online heatmapping tool, Heatmapper (Babicki et al., 2016).

Three main comparisons were performed using the assembled transcriptomes to evaluate differential gene expression. Gene expression between moderate severe chronic samples were compared to control samples (group 2 compared to group 1). Gene expression in mild subacute samples were compared to control samples (group 3 compared to group 1)), and lastly, gene expression in moderate severe chronic samples were compared to mild subacute samples (group 2 compared group 3).

Gene ontology enrichment was performed using the R package GOSeq, which can correct for biases in the power to detect differential gene expression due to different expression levels (Young et al., 2010). The median expression level for each gene across all the samples was used to control for transcript length and mRNA abundance differences between genes. GO enrichment was performed for the differentially expressed genes using the DAVID (v6.8) functional annotation tool (david.abcc.ncifcrf. gov.edu/-exu1/VirusSeq.html) and making use of GO terms from the Ensembl89 database (Huang da et al., 2009; Aken et al., 2016). The identified differentially expressed genes were checked for significantly overrepresented functional terms in the various gene ontology categories by employing a modified Fisher's exact test (EASE score) in the DAVID (v6.8) functional annotation clustering algorithm (Huang da et al., 2009a, b).

3 Results

3.2 Histological and immunological changes in CDV infection of the central nervous system

According to the basic classification system used by Ulrich et al. (2014), dogs with natural CDV infection in the present study were allocated to one of two groups, a subacute and a chronic CDV infection group. This was based on the results of the IHC and the histopathology that was observed in the sections of cerebellum and anterior medullary velum.

CDV-specific positive labelling consisted of red-brown cytoplasmic granular to diffuse as well as intranuclear (inclusion body) staining in astrocytes, microglia, microvascular endothelial cells, Purkinje cells, ependymal cells, mononuclear inflammatory cells, occasional neurons, choroid plexus epithelial cells and oligodendrocytes. There was also no evidence of canine distemper viral antigen using the abovementioned IHC staining method in the control dogs. No significant histopathology or myelin degeneration (as seen with LFB staining) was observed in the examined sections of cerebellum and anterior medullary velum from the control group. Also, canine distemper viral antigens were not observed in any of the other control brain sections not included for RNA-Seq.

In the chronic CDV infection group (which included the two remaining CDV-positive cases), the histopathology, although still multifocal, was moderate in severity, as was the myelin degeneration. The most severe histopathology was still observed in the paraventricular white matter as well as in the white matter of the cerebellar folia. In addition to the demyelination, other significant microscopic lesions included marked astrogliosis with prominent intranuclear inclusion bodies in astrocytes and microglial cells. There was also associated outspoken perivascular mononuclear inflammation and occasional foci of malacia with neovascularization (Fig. 3.2, B1). Immunohistochemistry for CDV antigens revealed multifocal widespread positive labelling of target cells in the white matter, including Gitter cells in the malacic foci, but there was also increased positive labelling of cells in the cerebellar cortex (Fig. 3.2, B2). There was far less positive labelling in the leptomeninges of the brain sections in the chronic infection group compared to the subacute infection group (Fig. 3.2, B3).

In the subacute CDV infection group (which included three of the five CDV-positive cases), the histopathology and myelin degeneration was mild and multifocal, most obvious in the paraventricular white matter. Histopathology included mild multifocal astrogliosis associated with scarce demyelination and very mild perivascular as well as leptomeningeal mononuclear inflammation (Fig. 3.2, C1). In these cases, IHC for CDV antigens revealed widespread positive labelling, especially in the paraventricular white matter (Fig. 3.2, C2), white matter of the cerebellar folia and the leptomeninges. There was only scarce multifocal positive labelling of cells in the grey matter of the cerebellum. The extent of IHC positive labelling in the white matter of the brain sections in this group far exceeded the severity of the histopathology that was observed (Fig. 3.2, C3). Cerebellum from a validated CDV-positive dog was used as the positive tissue control for illustration purposes. For negative tissue control purposes, the cerebellum from two healthy dogs that were euthanised were stained with HE, LFB and subjected to CDV IHC in the same way as the brain samples from the CDV-positive dogs.

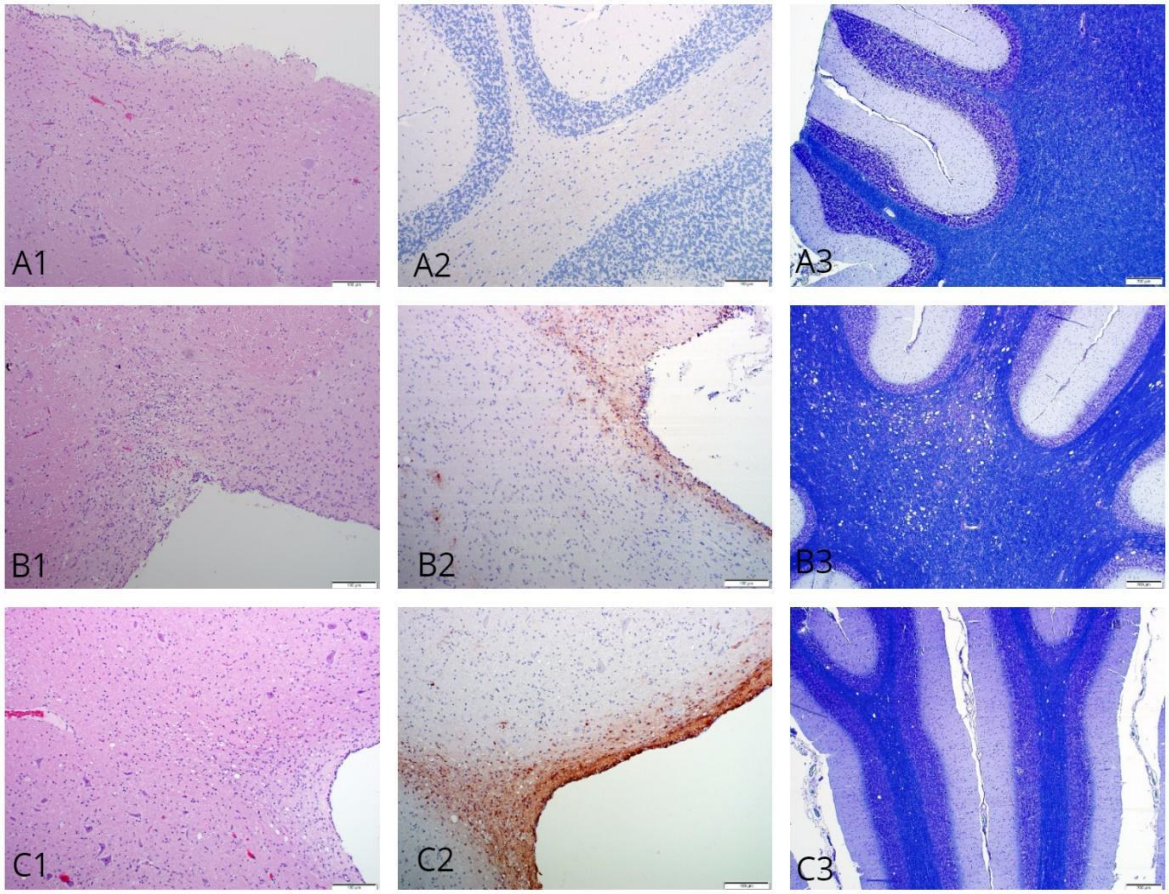

Fig. 3.2 Histomorphological and immunohistochemical characteristics for the two different lesion types of CDV leukoencephalitis used in this study. **A)** The cerebellum of the non-infected control dogs displayed no histological lesions and no detection of CDV antigen by immunohistochemistry/IHC. (A1. H&E stain, A2. No evidence of CDV antigen labelling via IHC and A3. LFB stain for myelin showing no myelin defects). **B)** H&E (B1), IHC (B2) and LFB (B3) comparison in the cerebellum of dogs with moderate-severe chronic CDV infection. B1. Focally extensive paraventricular malacia with myelin degeneration and neovascularization was evident. B2. Large amounts of CDV antigen were detected within astrocytes, microglia, Gitter cells, microvascular endothelial cells, and occasional neurons within the paraventricular region. B3. Focal area of demyelination (areas of decreased LFB staining) associated with astrogliosis. **C)** H&E (C1), IHC (C2) and LFB (C3) comparison in the cerebellum of dogs with mild-subacute CDV infection. C1. Mild vacuolization of the white matter with mild associated astrogliosis. C2. Ample strong CDV-specific positive labelling is present in the paraventricular white matter. C3. Multifocal demyelination in the cerebellar white matter as evidenced by multifocal vacuolization/spongiosis. H&E and IHC stains viewed at 10× magnification and LFB stain at 4× magnification.

3.3 RNA Sequencing

Details for the samples that were used for RNA-Seq are shown in Table 3.2, including the respective RNA quality values. Only RNA samples with a quality score (RIN value) above 8 were sequenced to ensure that good quality reads could be obtained.

Paired-end reads of approximately 100 bp were obtained from all samples. Between 12.9 million and 22.4 million reads (mean 19.4 million reads) were generated for each sample, representing a total of 23.6 billion bases; 79.8% of the total bases were included, with a mean read length of 94 bases (ranging from 63 – 109 bases). Table 3.3 shows the summary statistics for the RNA-Seq alignment. More than 80% of all reads were mapped across all the samples, of which more than 65% were annotated mapped reads in all samples. The total number of reads, as well as the total number of mapped reads were higher in samples from the cerebellum of each dog compared to that of the medullary velum from the same dog.

The results obtained from FastQC are shown in Fig.3.3. Quality scores were calculated across bases for the data set before and after filtering. Only sequences with a final Phred score above 20 was used in reads that were 100bp long, with filtering significantly increasing overall sequence quality (Fig 3.3). Overrepresented *k*-mers are also shown, with the CACCA k-mer being enriched most frequently in sequences (Fig. 3.4). The per sequence GC content is also shown (Fig. 3.5), with the mean GC content being lower than the predicted GC content. Lastly, the distribution of sequence composition is shown in Fig. 3.6.

Table 3.2

Details regarding RNA quality for total RNA extracted from brain tissue collected from healthy and infected dogs and used for RNA sequencing. The letters "M" and "C" were used in addition to the assigned sequencing code to denote whether the brain tissue was sampled from the medullary velum or from the cerebellum.

Dog breed	**Cerebellum** **[RNA] (RIN values)**	**Medullary Velum** **[RNA] (RIN values)**	**RNA sequencing code**
CDV positive samples			
CDV 3: Jack Russel Terrier	8.2	8.3	CDV+I1
CDV 6: German Shepherd	8.4	8.2	CDV+I2
CDV 7: Siberian Husky	7.8	7.7	Not sequenced
CDV 10: Boerboel	8.6	8.4	CDV+I3
CDV 14: Mixed breed	8.2	8.1	CDV+I4
Control samples			
CDV 1: Jack Russel Terrier	9.3	9.0	CDV-C1
CDV 2: Yorkshire Terrier	8.3	8.2	Not sequenced
CDV 3: Boston Terrier	8.4	8.2	Not sequenced
CDV 4: Mixed breed	8.4	8.3	CDV-C2
CDV 5: Border Collie	8.5	8.3	Not sequenced
CDV 6: Corgi	7.9	8.0	Not sequenced
CDV 7: Pitbull	8.3	8.4	Not sequenced
CDV 8: Labrador	8.5	8.3	Not sequenced

Table 3.3

Summary statistics of RNA-Seq alignment, listing the total number of reads (millions), the total number of mapped reads (percentage of the total number of reads) and the number of annotated mapped reads (millions and as a percentage of the total reads) for each of the twelve samples sequenced. The sample number indicated whether it is a CDV-infected or a control dog (+ for infected, - for control dogs), as well as the region of the brain the sample was taken from (MV: medullary velum and Cb: cerebellum).

Sample number	Brain tissue	Total number of reads (millions)	Number of mapped reads (millions)	Mapped reads (% of total)	Number of annotated mapped reads (millions)	Number of annotated mapped reads (% of total)
CDV+I1 Cb	Cerebellum	19987	17688.5	88.5	13814.7	78.1
CDV+I1 MV	Medullary Velum	18643	15865.2	85.1	10693.1	67.4
CDV+I2 Cb	Cerebellum	19453	17040.8	87.6	12473.9	73.2
CDV+I2 MV	Medullary Velum	19178	16723.2	87.2	11756.4	70.3
CDV+I3 Cb	Cerebellum	21536	19770	91.8	16567.3	83.8
CDV+I3 MV	Medullary Velum	20742	18584.8	89.6	15183.8	81.7
CDV+I4 Cb	Cerebellum	17147	14472.1	84.4	9508.2	65.7
CDV+I4 MV	Medullary Velum	15426	12973.3	84.1	8445.6	65.1
CDV-C1 Cb	Cerebellum	22481	21267	94.6	18289.6	86
CDV-C1 MV	Medullary Velum	22231	20963.8	94.3	17945	85.6
CDV-C2 Cb	Cerebellum	19623	17307.5	88.2	13253.7	76.6
CDV-C2 MV	Medullary Velum	18769	16272.7	86.7	11016.6	67.7

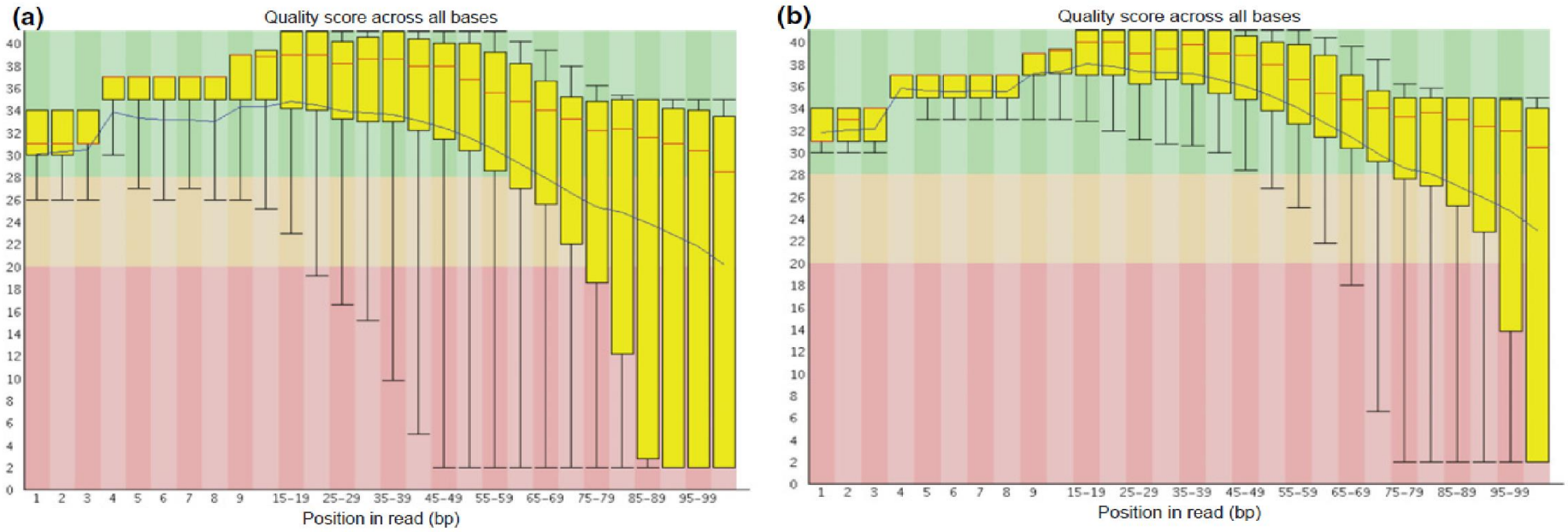

Fig. 3.3 Distribution of quality scores across bases for the assembled data set, (a) before filtering and (b) after filtering was applied. The position in reads are indicated on the x-axis and the quality scores on the y-axis, with the black line indicating the mean quality score and the red line the median within each of the quality scores.

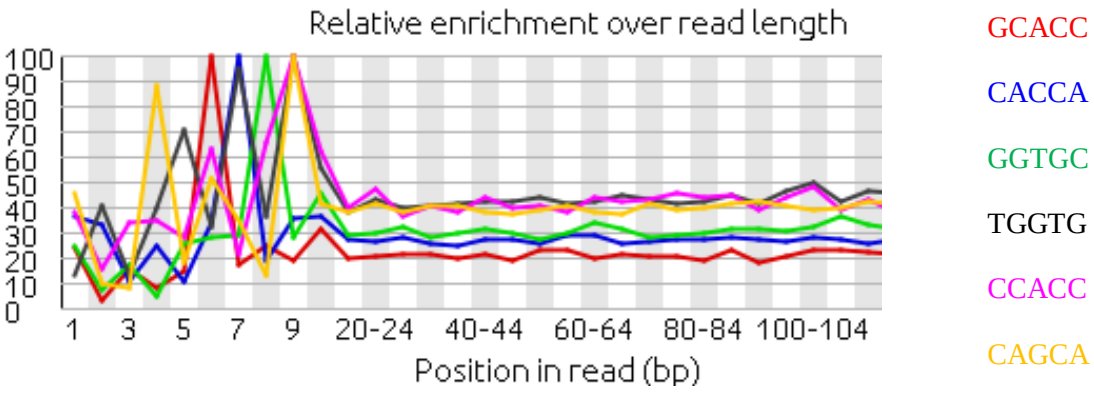

Fig. 3.4 Relative enrichment level of *k*-mers over read position for the RNA-Seq data set. The CACCA *k*-mer was enriched in most sequences, with most enrichment occurring between the first base and the twenty fourth base of sequences.

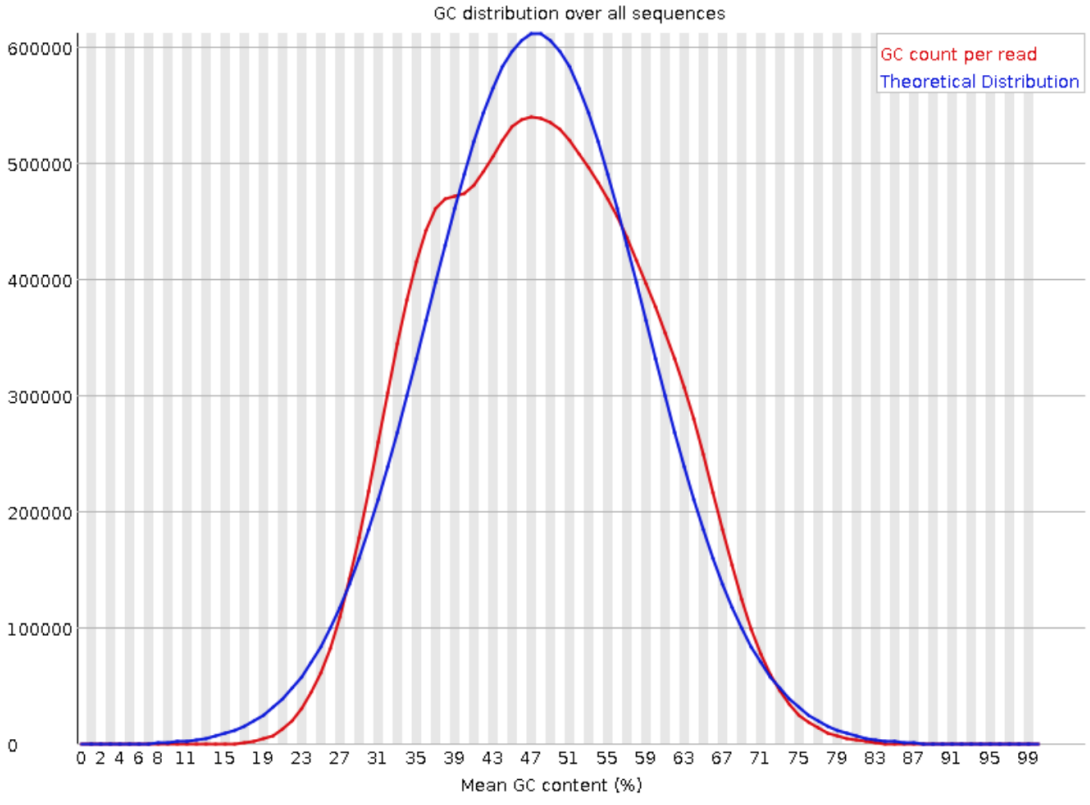

Fig. 3.5 This graph shows the GC distribution over all sequences and the mean GC content (%) of the sequences. A theoretical distribution is compared the GC count per read, with the overall GC content being less than the theoretical prediction.

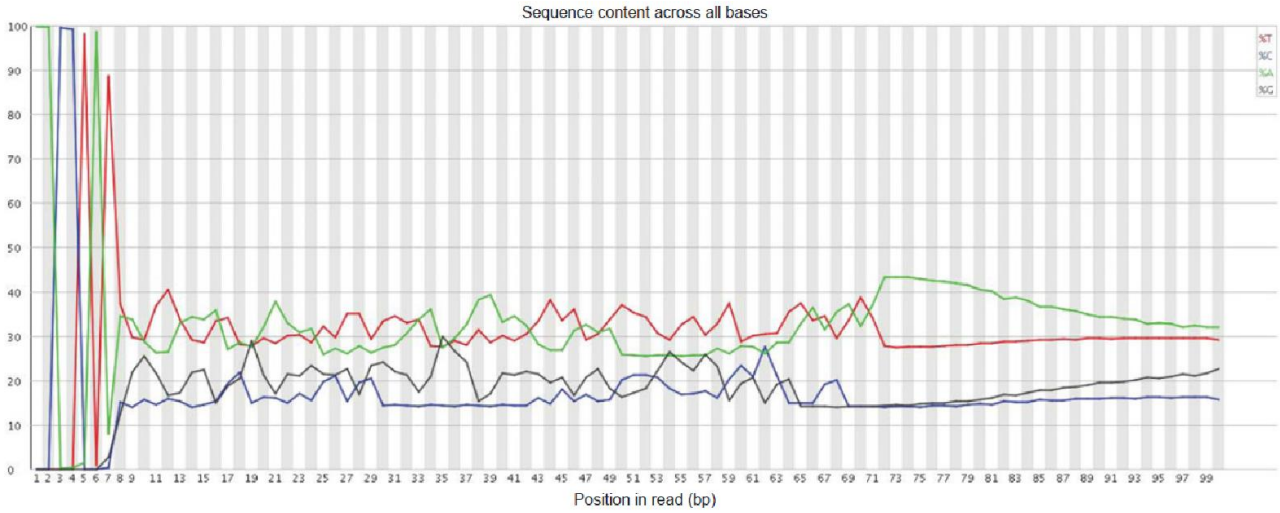

Fig 3.6 The distribution of sequence composition across bases for the ION Proton RNA-Seq data set. Sequence content is reflected on the y-axis, with the position in the reads being shown on the x-axis.

Differential gene expression

Differential gene expression analysis yielded a total of 768 genes that were differentially expressed between the three different comparisons that were done between samples (p-value < 0.05). The Venn-diagram in Fig. 3.7 illustrates the number of genes that were differentially expressed in the mild-subacute infected group compared to the healthy group, the genes that were differentially expressed between the moderate-severe chronic group compared to the control group and the shared genes that were upregulated or downregulated respectively between all the groups.

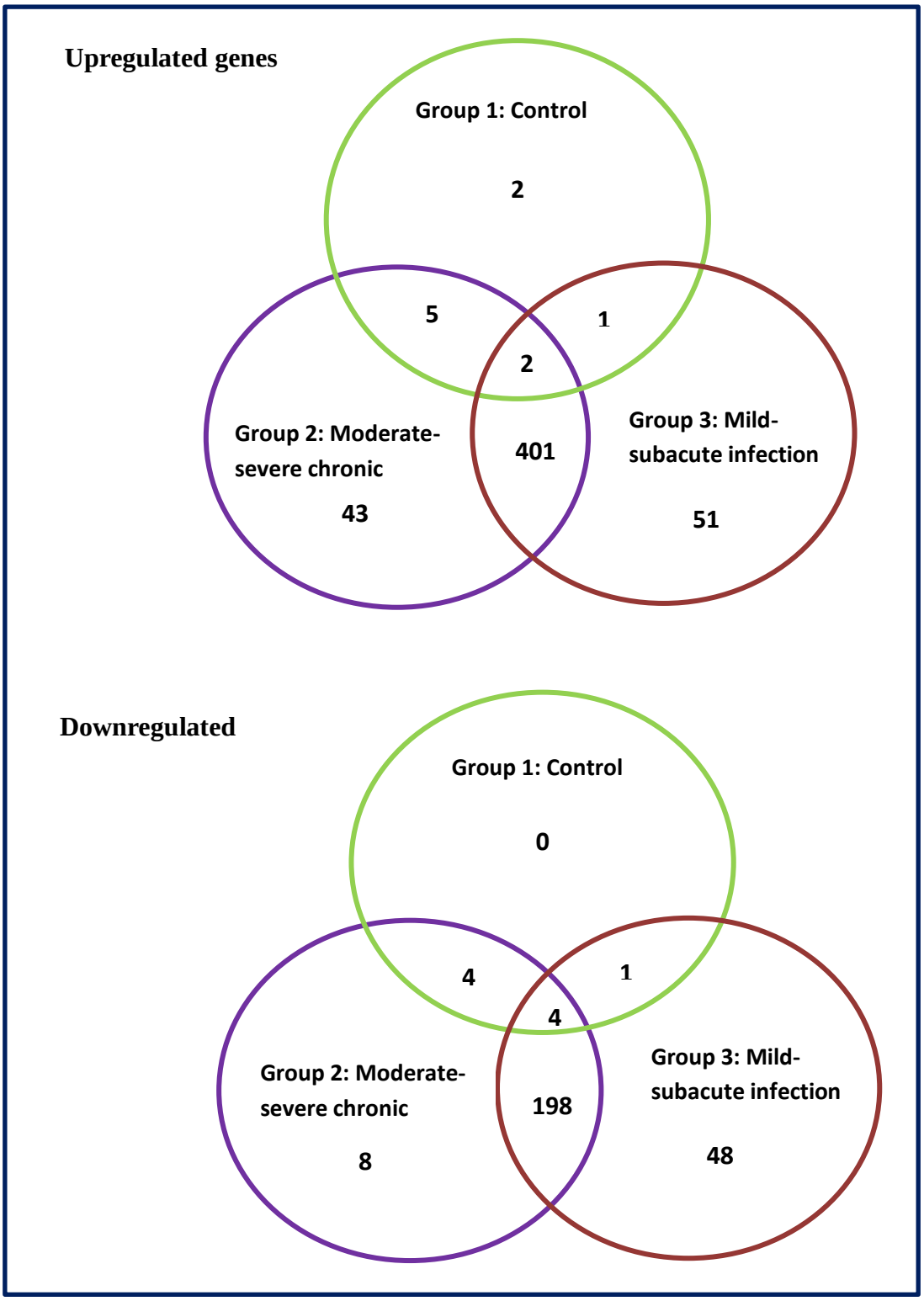

Fig. 3.7 Venn diagram comparing the number of differentially expressed genes in central nervous system tissues from healthy dogs compared to CDV infected dogs and between the defined lesion types of CDV leukoencephalitis. The majority of the differentially expressed genes are shared between samples with moderate-severe chronic infection and those with mild-subacute CDV

Most of the genes differentially expressed between diseased dogs and control dogs are shared between the two CDV lesion types (>80%). Only two of the differentially expressed genes were specific to control dogs, where they are downregulated compared to the same genes in CDV-infected dogs. Five upregulated genes were shared between group 1 and 2, and 1 between group 1 and 3. Only two genes were upregulated when comparing moderate severe chronic infection to control samples, mild subacute infection to control dogs and the two diseased subtype samples to each other. Five genes were downregulated across all these comparisons. Samples from dogs with mild subacute infection had the largest number of uniquely expressed genes.

Genes that were upregulated in group 1 and group 2 were CNS1S1 (casein alpha S1), TREML 4 (triggering receptor expressed on myeloid cell-like 4), MSR 1 (macrophage scavenger receptor 1), CB///CFB (complement component 2///complement factor B) and BAZ2B (bio domain adjacent to zinc finger domain, 2B).

The only differentially expressed gene shared between group 1 and group 3 was LOC606869 (similar to Ig heavy chain V-111 region VH26 precursor). Two genes were upregulated in group 1, 2 and 3. These were DPP4 (dipeptidyl-peptidase 4) and LOC100856330 (transcription factor EC-like).

Genes that were downregulated between group 1 and 2 included LRMP (lymphoid-restricted membrane protein), PLA267 (phospholipase A2, group V11, plasma), CD274 (CD274 molecule) and GPNMB (glycoprotein – transmembrane). The only gene down regulated in between group 3 & 1 was ADCY5 (adenylate cyclase 5).

Four genes were downregulated between all three groups: CPE (carboxypeptidase E), CRIL (complement component 3b/4b receptor 1-like), CRABP1 (cellular retinoic acid binding protein 1) and CRP (C-reactive protein, pentraxin-related).

In the comparison between control samples and diseased samples, three distinct clusters could be identified (Fig. 3.8). Cluster one shows the genes that are differentially expressed in control samples

compared to diseased samples. Clusters two and three show the genes that are differentially expressed in moderate severe chronic and mild subacute infection compared to the control samples respectively. The control samples were distinct from the CDV-infected samples, while the histologically distinct subgroups of CDV leukoencephalitis showed overlap in the genes that were differentially expressed.

In the comparison between moderate severe chronic samples and control samples, 263 genes were downregulated and 505 were upregulated. When mild subacute samples were compared to control samples it was found that 283 genes were downregulated, and 485 genes were upregulated. More genes were therefore downregulated in mild subacute samples and a larger number of genes were upregulated in moderate severe chronic samples when compared to control samples. Comparing the chronic samples to the subacute samples yielded 466 downregulated genes and 302 upregulated genes.

Two genes were upregulated in control samples but not in either of the lesion types of CDV infected samples. This included ACSBG1 (acetyl-CoA synthase, bubblegum family member I) and AZGP1 (alpha-2-glycoprotein 1, zinc-binding). In CDV-infected samples ubiquitination factors, interferon components, lectin proteins, chemokines and integrin genes formed part of the most highly upregulated genes. Downregulated genes in the CDV-infected samples included various protein kinases, ataxin, genes involved in ion channel formation and solute carriers. Major histocompatibility class I and class II components were also downregulated in both CDV lesion types, along with tumour necrosis factor and complement system components. In mild subacute infections, acetylcholinesterase was significantly downregulated compared to chronic infected samples and controls. The G-protein coupled receptors were significantly downregulated in mild subacute infections relative to chronically infected and control samples.

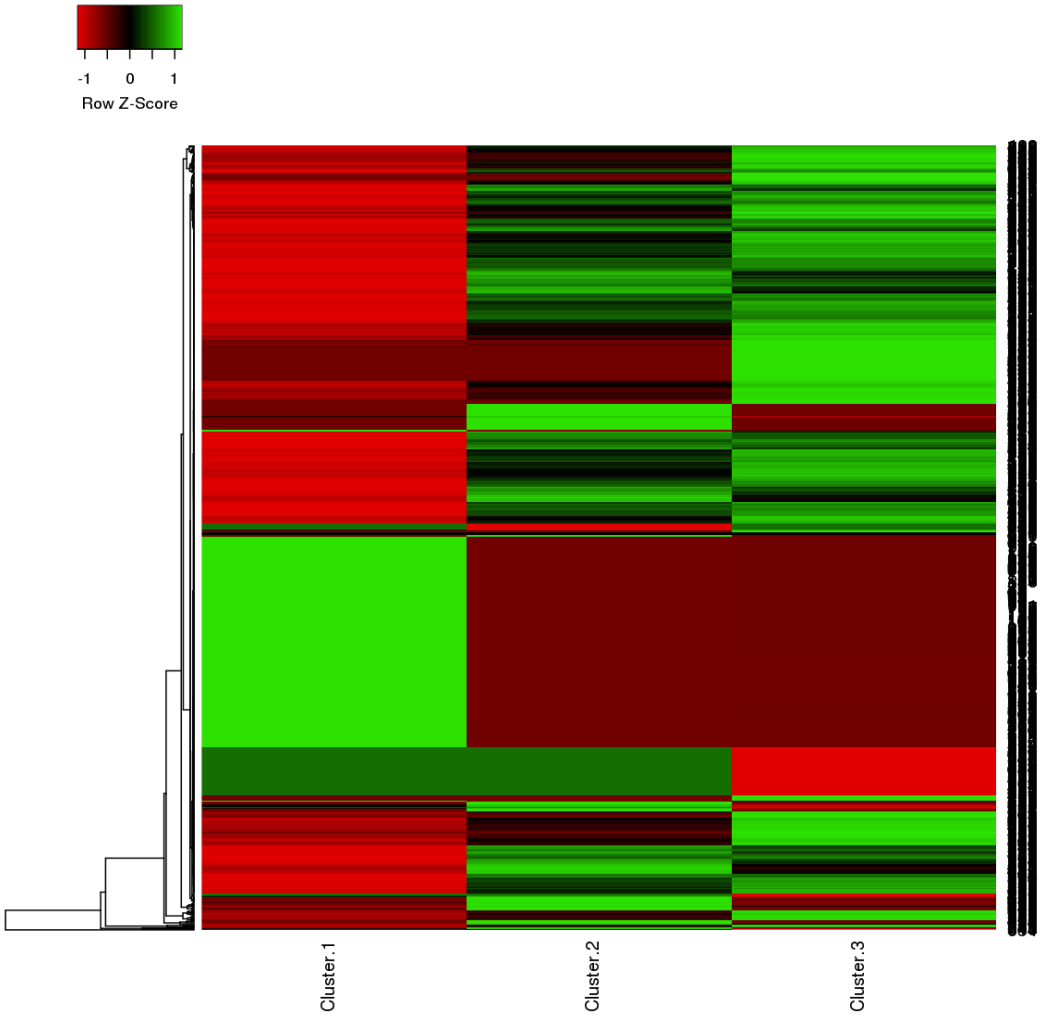

Fig 3.8 Heatmap displaying the expression profile of the 768 differentially expressed genes between the three groups of dog samples used in this study. Cluster one compares control samples to diseased samples and cluster 2 and 3 represents chronic infected samples and subacute affected samples compared to control samples respectively. Green illustrates upregulated genes, while red illustrates downregulated genes.

3.4 Gene ontology

Ten processes were significantly up- or downregulated when gene ontologies of diseased samples were compared to control samples. The term “generation of precursor metabolites and energy” was severely downregulated in diseased samples. Differentially expressed genes belonged to the following ontologies: (1) Biological process: regulation of protein metabolic processes, regulation of

immune response, immune response and viral reproductive processes and (2) Cellular component: Central nervous system development and mitotic cell cycle. Generation of precursor metabolites was the most overrepresented gene ontology among downregulated genes. Fig. 3.9 illustrates the gene ontology terms that were enriched in the diseased samples relative to the control samples.

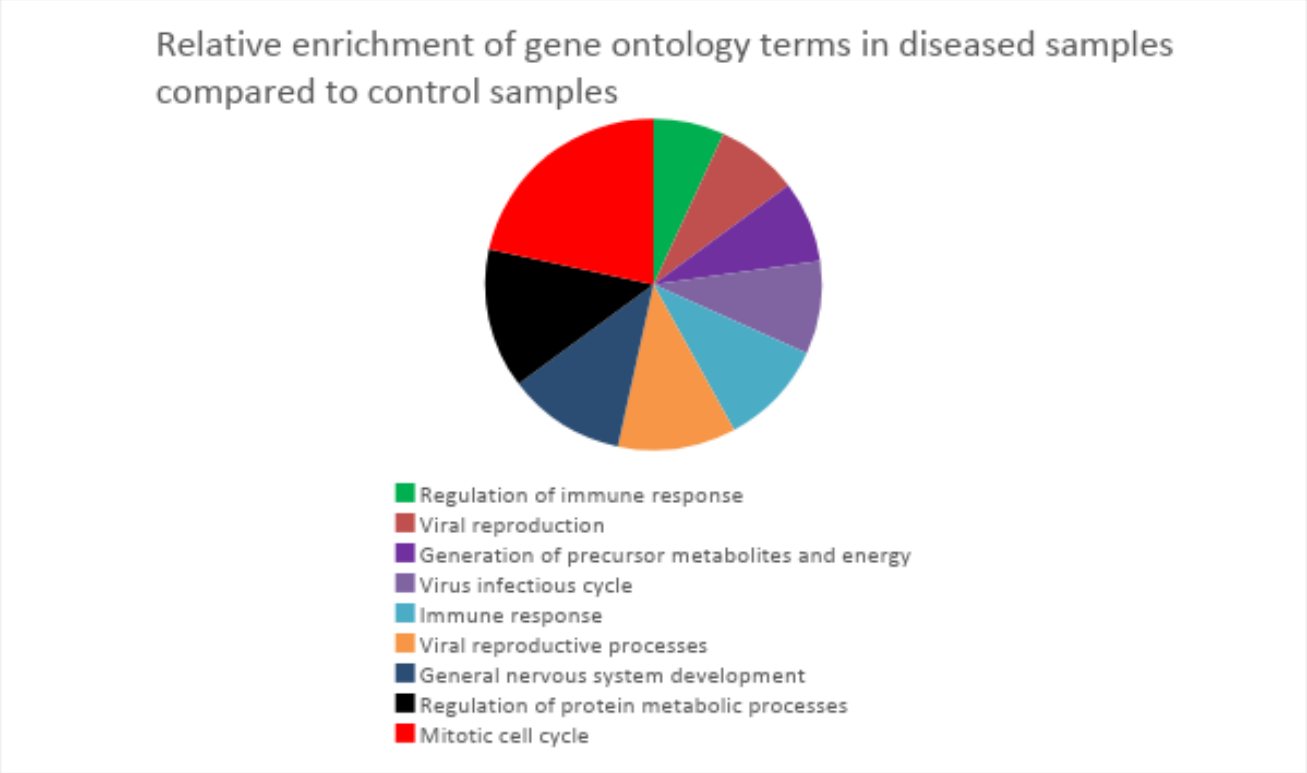

Fig. 3.9 Chart illustrating the gene ontology terms overrepresented by differentially expressed genes in CDV lesion types as a percentage relative to control samples. The ontology most represented in upregulated genes were mitotic cell cycle processes, while generation of precursor metabolites and energy was identified as the enriched gene ontology in downregulated genes.

4 Discussion

Previous RNA studies that evaluated the gene expression in the CNS of domestic dogs infected with CDV made use of microarrays (Ulrich et al., 2014b). The authors did detect 720 gene probes that were differentially expressed in the CNS tissues of dogs with different stages and severities of CDV and concluded that CDV-leukoencephalitis follows a biphasic mode of demyelination. However, this study was limited by the use of only known genes that were used for the microarray and the detection of low abundance transcripts would have been challenging with this approach. Another limitation was the limited sampling of dogs affected by each of the different CDV stages and the controls that were used, with inconsistencies in dog breeds and ages being used (Liu et al., 2014; Ulrich et al., 2014b; Wang et al., 2014).

The RNA-Seq data presented in this dissertation made use of brain tissue samples that were collected from dogs infected with CDV and from healthy control dogs. Histopathology results showed two distinct lesion types of CDV in the CNS tissues, moderate-severe chronic infection and mild-subacute infection. Myelin degradation and multifocal lesions were present in both lesion types, with the severity and distribution of lesions differing between them. No histological lesions or CDV antigen were present in control samples. Samples from the cerebellum and medullary velum were used to extract total RNA to be submitted for RNA-Seq and the resulting sequences were evaluated to detect differentially expressed genes.

A total of 768 differentially expressed genes were identified when comparing the CDV-infected samples to healthy control samples. The infected samples were clearly distinct from the control samples and the majority of differentially expressed genes were present in both moderate-severe chronic infection and mild-subacute infection. Various immune response genes were upregulated, including chemokines and components involved in interferon response.

Downregulated genes included genes involved in regulating pathway signalling cascades, most notably various protein kinases. This could explain the downregulation of downstream genes that

may be important in maintaining cell function and integrity (Svitek et al., 2014). Interestingly, MHC class I and II components were downregulated. MHC class II molecules are often upregulated in response to viral infection (Beineke et al., 2009; Greer et al., 2010; Mahad et al., 2015). Components of the complement system were upregulated in both lesion types of CDV, which in part explains the inflammation associated with neurological CDV infection (Pedersen, 1999; Beineke et al., 2009; Liszewski and Atkinson, 2015).

Acetylcholinesterase, the main catalyst for breaking down acetylcholine, is significantly downregulated in mild subacute infections compared to other samples. Acetylcholine is important in neurotransmission and the downregulation could impair normal neurological functions (Pan et al., 2013b). Metabolic and energy generating processes could be affected by the downregulation of G-protein coupled receptors (Qian et al., 2013) in samples with mild subacute CDV infection. In control samples ACSBG1 and AZGP1 genes were upregulated. Acyl-CoA synthase plays an important role in the metabolism of very long-chain fatty acids in the brain and in myelinogenesis. AZGP1 is a glycoprotein involved in energy metabolism. Its downregulation has been associated with weight loss in some disease conditions, such as certain cancers. It is to be expected that these two genes would be differentially expressed in CDV-infected samples compared to the controls, as these processes could be affected by CDV-infection.

Ontologies classifying upregulated genes included mitotic cell cycle processes, immune response and regulation of protein metabolic processes. Downregulated genes were classified by the ontologies metabolite and energy generation and generation of precursor molecules. Since CDV leukoencephalitis is a neurodegenerative disease it follows logically that normal metabolic processes are impaired in infected individuals. Both moderate-severe chronic infection and mild subacute infection is characterized by inflammation and the increase in immune response components is therefore not unexpected (Amude et al., 2010; Takenaka et al., 2016).

Compared to the expression study performed by Ulrich *et al*. (2014), an additional 326 differentially expressed genes were identified in the present study. The gene ontologies describing upregulated genes were similar to those identified by Ulrich *et al*., with the exception of mitotic cell cycle processes which were significantly upregulated in the RNA-Seq data set. The predominant gene ontologies describing downregulated genes in the dataset in this study is different from the intermediate filament bundle assembly and regulation of neuron differentiation ontologies which described the most significant portion of the downregulated genes in the microarray data set (Ulrich et al., 2014c).

The results from this study represent a starting point to better understand the gene expression changes associated with different lesion types of canine distemper-associated leukoencephalitis. Making use of RNA-Seq to assess gene expression, it was possible to identify differentially expressed genes and their related gene ontologies that could not be identified from a previous microarray-based study. Immune response genes, metabolites and metabolism regulating genes, as well as genes involved in normal cell division processes appear to play an important role in CDV-induced leukoencephalitis. The differential expression of especially immune response genes, specifically complement-activation transcripts, is in accordance with the biphasic demyelination process proposed by various previous studies (Vandevelde and Zurbriggen, 2005; Beineke et al., 2009; Pan et al., 2013; Ulrich et al., 2014b).

Chapter 4

Concluding remarks

The first aim of this study was to determine if there are genetic differences in the V-domain of the SLAM receptor gene and in the CD46 receptor gene of different Canidae, Felidae and Hyenidae species. Part of this aim was also to determine if these genetic differences resulted in amino acid changes, and if these amino acid changes could potentially affect the virus-host binding affinity at these two receptors. The second aim of this research was to evaluate gene expression differences in the brain tissues of domestic dogs affected by different stages and severities of neurological CDV infection by making use of RNA-Seq. Overall, the research presented here aimed to increase the understanding of some of the molecular mechanisms that could underly CDV infection and disease progression.

Different domestic and wildlife species were included for studying nucleotide and amino acid variation in host receptor genes. The sample set included species that are known to be susceptible to CDV infection, such as the domestic dog and species that seem to be especially susceptible to CDV and in which disease progression tends to be more rapid and severe, including African wild dogs, lions and tigers. Cheetah samples, a species in which CDV has not yet been detected, were also included. This allowed the study to look at a range of species and to evaluate differences between mildly susceptible and very susceptible species, as well as species that are not known to be affected by CDV.

Nucleotide and amino acid sequenced could be grouped together according to families (Canidae, Felidae and Hyenidae) from which they came for both of the receptors studied. Exon 2-3 of the CD46 receptor contained more non-synonymous changes across species compared to the V-domain of the SLAM receptor. Predicted protein structures for CD46 were more conserved in their variability, with very few significant structural changes occurring compared to the predicted SLAM protein structures. Non-synonymous amino acid changes occurred on the surface or in the grooves of predicted protein structures. These regions are known to interact with virus proteins more often than regions located towards the interior of the protein structure.

From the DNA study it was seen that species-specific nucleotide and amino acid differences in the CD46 and SLAM receptors correlated with protein structure changes which could affect the interaction of host cells with viral proteins. Most non-synonymous changes occurred in regions of the protein which are involved in interacting with proteins on virus cells and these family-specific changes could contribute to the difference in host susceptibility observed during CDV epidemics. Amino acid changes shared between cheetahs and the domestic cat could potentially partially explain why these species appear to be non-susceptible to CDV infection. Likewise, amino acids shared among different canid species could contribute to their susceptibility, with unique amino acid changes in species such as the African wild dog potentially playing a role in how severely this species is affected by CDV infections.

The DNA data gathered from this study contributed to the existing DNA sequence data available for the SLAM and CD46 genes of various species. Nucleotide and amino acid changes identified added to the information gained by previous studies regarding these two receptor genes and promoted the understanding of the potential effect of amino acid changes on host-virus interactions and binding affinity (Tatsuo and Yusuke, 2002; Ohishi et al., 2010; McCarthy et al., 2011; Liszewski and Atkinson, 2015).

The sample size for some species used in the DNA study was small, skewing the data set and making it difficult to detect individual sequence differences within certain different species. It is also important to take note that predictive protein modelling was used, and the obtained models may not necessarily reflect the true structure of the relevant protein. Complete chemical interactions should be analysed before conclusive remarks regarding binding affinity can be made.

Immunohistopathology showed that CDV-infected samples could be grouped into two lesion types, namely moderate-severe chronic infection and mild-subacute infection. From RNA-Seq analysis, 768 differentially genes differentially expressed in brain tissue between dogs infected with CDV and healthy controls, with the majority of differentially expressed genes found in both lesion types of

CDV infections. Two genes were uniquely expressed in healthy brain tissues, alpha-2-glycoprotein 1, zinc-binding and acyl-CoA synthetase bubblegum family member A. These genes are involved in energy metabolism and in the metabolism of very long-chain fatty acids and in myelinogenesis respectively. Upregulated genes in diseased samples were described by the gene ontologies mitotic cell cycle processes, immune response and regulation of protein metabolic processes. The majority of downregulated genes belonged to the metabolite and energy generation and generation of precursor molecules ontologies. Both chronic infection and subacute infection were characterized by an upregulation in genes involved in inflammation and components which form part of the immune response.

This was the first study in which RNA-Seq was used to evaluate and compare gene expression differences in the central nervous system tissues of dogs infected with CDV. The data presented here is therefore novel and contributes baseline information to the field of gene expression relating to CDV infection in neurological tissues. It also supports a biphasic demyelination mode that has been previously been proposed by other authors (Vandevelde and Zurbriggen, 2005; Beineke et al., 2009; Ulrich et al., 2014b) and there were notable differences between the samples from the two infected groups compared to the control group samples.

It is however important to note that very stringent parameters were used during the filtering and quality steps in this study, and less stringent parameters may allow for the detection of more genes and specifically more novel genes. Alternative splicing analysis was also not carried out for this data set and more in-depth alternative splicing analysis has the potential to reveal various splice variants.

This project was a starting point in providing insight into different mechanisms potentially underlying CDV infection at a molecular level. The data from this research opens up many avenues that can be pursued by future studies to improve our understanding of CDV and the disease and susceptibility differences associated with this disease.

It would be worth evaluating the virus-host protein interactions more closely, looking at different chemical bonds and interactions that could form between the different protein and receptor molecules. Additional *in situ* predictions to determine the effect of different nucleotide and amino acid changes on host-virus bonding affinity would also be interesting to examine further. Eventually, the ideal would be to make the studied changes to tissue culture cells and directly study disease susceptibility between wild type cells and the virus compared to mutated cells and CDV.

Comparative predictive modelling relies on establishing an evolutionary relationship between the sequence of the protein of interest and other members of the protein family, whose structures have been solved experimentally by X-ray or NMR. For this reason, the major limitation of this technique is the availability of homologous templates (Bordoli et al., 2009; Guex et al., 2009). Modelling complexes from individual components is rarely successful without integrating additional information about the assembly. Comparative protein modelling techniques rely on structural information from the template to derive the structure of the target (Guex et al., 2009). Large structural changes, caused by mutations, insertions, deletions and fusion proteins, are therefore, in general, not expected to be modelled accurately by comparative techniques (Humphrey et al., 1996; Guex et al., 2009; Biasini et al., 2014). Nonetheless, homology models of a protein under investigation can provide a valuable tool for the interpretation of sequence variation and the design of mutagenesis experiment to elucidate the biological function of proteins (Bordoli et al., 2009; Guex et al., 2009).

Including DNA sequences for the SLAM V-domain and the relevant parts of the CD46 gene of the jackal and mongoose would also be informative in determining if this could be a potential reservoir species, specifically in the South African context. This could give new insight into how CDV is spread between wildlife species and between wildlife and domestic species. Sampling of wildlife species does however remain difficult and sampling will need to be continued on an ongoing basis when opportunities for this present itself, such as during CDV outbreaks in which wildlife species are involved.

In terms of gene expression, more extensive data analysis, including the evaluation of KEGG pathways and additional gene ontology analysis must be performed. Less stringent filtering parameters can also be used to allow for the detection of novel genes or alternative gene transcripts. Looking into alternative splice variants could potentially yield interesting insights to the various molecular mechanisms underlying CDV infection and the effect this could have on disease outcomes in different individuals and different host species.

This project just touched the surface of CDV at a molecular level. Many aspects remain to be studied and ultimately, it is essential to remember that neither the virus, the host, the environment, populations and/or ecosystems exist in isolation. Although only a glance at this interesting virus and its hosts was obtained from this research, the results contribute valuable information to the field of CDV research and create many avenues for prospective research.

References

Acosta-Jamett, G., Chalmers, W.S., Cunningham, A.A., Cleaveland, S., Handel, I.G., Bronsvoort, B.M., 2011. Urban domestic dog populations as a source of canine distemper virus for wild carnivores in the Coquimbo region of Chile. Vet. Microbiol. 152, 247-257.

Aguiar, D.M., Amude, A.M., Santos, L.G.F., Ribeiro, M.G., Ueno, T.E.H., Megid, J., Paes, A.C., Alfieri, A.F., Alfieri, A.A., Gennari, S.M., 2012. Canine distemper virus and Toxoplasma gondii co-infection in dogs with neurological signs. Arq. Bras. Med. Vet. Zoo. 64, 221-224.

Aken, B.L., Ayling, S., Barrell, D., Clarke, L., Curwen, V., Fairley, S., Fernandez Banet, J., Billis, K., Garcia Giron, C., Hourlier, T., Howe, K., Kahari, A., Kokocinski, F., Martin, F.J., Murphy, D.N., Nag, R., Ruffier, M., Schuster, M., Tang, Y.A., Vogel, J.H., White, S., Zadissa, A., Flicek, P., Searle, S.M., 2016. The Ensembl gene annotation system. Database 2016.

Akey, J.M., Ruhe, A.L., Akey, D.T., Wong, A.K., Connelly, C.F., Madeoy, J., Nicholas, T.J., Neff, M.W., 2010. Tracking footprints of artificial selection in the dog genome. P. Natl. Acad. Sci. USA 107, 1160-1165.

Alamancos, G., Agirre, E., Eyras, E., 2014. Methods to study splicing from high-throughput RNA Sequencing data. Spliceosomal Pre-mRNA Splicing: Methods and Protocols, 357-397.

Albert, F.W., Somel, M., Carneiro, M., Aximu-Petri, A., Halbwax, M., Thalmann, O., Blanco-Aguiar, J.A., Plyusnina, I.Z., Trut, L., Villafuerte, R., Ferrand, N., Kaiser, S., Jensen, P., Paabo, S., 2012. A comparison of brain gene expression levels in domesticated and wild animals. Plos Genet. 8, e1002962.

Alcalde, R., Kogika, M.M., Fortunato, V.A.B., M., C.B., Lopes, L.R., Paiva, P.B., Durigon, E.L., 2013. Canine distemper virus: detection of viral RNA by Nested RT-PCR in dogs with clinical diagnosis. Braz. J. Vet. Res. Anim. Sci. 50, 74-76.

Alexander, K.A., McNutt, J.W., Briggs, M.B., Standers, P.E., Funston, P., Hemson, G., Keet, D., van Vuuren, M., 2010. Multi-host pathogens and carnivore management in southern Africa. Comp. Immunol. Microb. 33, 249-265.

Almberg, E.S., Cross, P.C., Smith, D.W., 2010. Persistence of canine distemper virus in the Greater Yellowstone Ecosystem's carnivore community. Ecol. Appl. 20, 2058-2074.

Altizer, S., Harvell, D., Friedle, E., 2003. Rapid evolutionary dynamics and disease threats to biodiversity. Trends Ecol. Evol. 18, 589-596.

Altschul, S.F., Gish, W., Miller, W., Myers, E.W., Lipman, D.J., 1990. Basic Local Alignment Search Tool. J Mol. Biol. 215, 403-410.

Alves, L., Khosravi, M., Avila, M., Ader-Ebert, N., Bringolf, F., Zurbriggen, A., Vandevelde, M., Plattet, P., 2015. SLAM- and nectin-4-independent noncytolytic spread of canine distemper virus in astrocytes. J. Virol. 89, 5724-5733.

Amude, A.M., Alfieri, A.F., Alfieri, A.A., 2010. Clinical courses and neurological signs of canine distemper virus infection in dogs. Curr. Res. Technol. Educ. Top. Appl. Microbiol. Microb. Biotech.

Amude, A.M., Alfieri, A.A., Arias, M.V.B., Alfieri, A.F., 2012. Clinical syndromes of nervous distemper in dogs initially presented without conventional evidences of CDV infection. Semina: Ciências Agrárias 33, 2347-2358.

An, D.J., Kim, T.Y., Song, D.S., Kang, B.K., Park, B.K., 2008. An immunochromatography assay for rapid antemortem diagnosis of dogs suspected to have canine distemper. J. Virol. Methods 147, 244-249.

Anders, S., Huber, W., 2010. Differential expression analysis for sequence count data. Genome Biol. 11.

Anders, S., Wolfgang, H., 2012. Differential expression of RNA-Seq data at the gene level: the DESeq package DESeq Package 1.

Anders, S., Pyl, P.T., Huber, W., 2014. HTSeq – A Python framework to work with high-throughput sequencing data. Bioinformat. Adv. Access.

Anderson, D.E., von Messling, V., 2008. Region between the canine distemper virus M and F genes modulates virulence by controlling fusion protein expression. J. Virol. 82, 10510-10518.

Anderson, D.E., Castan, A., Bisaillon, M., von Messling, V., 2012. Elements in the canine distemper virus M 3' UTR contribute to control of replication efficiency and virulence. Plos One 7, e31561.

Anis, E., Newell, T.K., Dyer, N., Wilkes, R.P., 2018. Phylogenetic analysis of the wild-type strains of canine distemper virus circulating in the United States. Virol. J. 15, 118.

Appel, M., Sheffy, B.E., Percy, D.H., Gaskin, J.M., 1974. Canine Distemper Virus in Domesticated Cats and Pigs. Am. J. Vet. Res. 35, 803-806.

Appel, M.J., Yates, R.A., Foley, G.L., Bernstein, J.J., Santinelli, S., Spelman, L.H., Miller, L.D., Arp, L.H., Anderson, M., Barr, M., 1994. Canine distemper epizootic in lions, tigers, and leopards in North America. J. Vet. Diagn. Invest. 6, 277-288.

Appel, M.J.G., Summers, B.A., 1995. Pathogenicity of morbilliviruses for terrestrial carnivores. Vet. Microbiol. 44, 187-191.

Ari, Ş., Arikan, M., 2016. Next-Generation Sequencing: Advantages, Disadvantages, and Future. 109-135.

Arnold, K., Bordoli, L., Kopp, J., Schwede, T., 2006. The SWISS-MODEL workspace: a web-based environment for protein structure homology modelling. Bioinformatics 22, 195-201.

Auer, P.L., Doerge, R.W., 2010. Statistical design and analysis of RNA sequencing data. Genetics 185, 405-416.

Avendano, R., Barrueta, F., Soto-Fournier, S., Chavarria, M., Monge, O., Gutierrez-Espeleta, G.A., Chaves, A., 2016. Canine Distemper Virus in Wild Felids of Costa Rica. J. Wildlife Dis. 52, 373-377.

Avila, M., Khosravi, M., Alves, L., Ader-Ebert, N., Bringolf, F., Zurbriggen, A., Plemper, R.K., Plattet, P., 2015. Canine distemper virus envelope protein interactions modulated by hydrophobic residues in the fusion protein globular head. J. Virol. 89, 1445-1451.

Babicki, S., Arndt, D., Marcu, A., Liang, Y., Grant, J.R., Maciejewski, A., Wishart, D.S., 2016. Heatmapper: web-enabled heat mapping for all. Nucleic Acids Res. 44, W147-153.

Barrett, T., 1999. Morbillivirus infections, with special emphasis on morbilliviruses of carnivores. Vet. Microbiol. 69, 3-13.

Basso, C.R., de Camargo Tozato, C.C., Araujo, J.P., Pedrosa, V.A., 2015. A fast and highly sensitive method for the detection of canine distemper virus by the naked eye. Anal. Methods 7, 2264-2267.

Bean, A.G., Baker, M.L., Stewart, C.R., Cowled, C., Deffrasnes, C., Wang, L.F., Lowenthal, J.W., 2013. Studying immunity to zoonotic diseases in the natural host - keeping it real. Nat. Rev. Immunol. 13, 851-861.

Behera, S.K., Bordoloi, G., Behera, P., 2014. Clinico-Hemato-Biochemical and therapeutic study of canine distemper: a report from North-Eastern part of India. Indian J. Field Vets. 9, 18-20.

Beineke, A., Puff, C., Seehusen, F., Baumgärtner, W., 2009. Pathogenesis and immunopathology of systemic and nervous canine distemper. Vet. Immunol. Immunop. 127, 1-18.

Beineke, A., Baumgärtner, W., Wohlsein, P., 2015. Cross-species transmission of canine distemper virus—an update. Curr. Top. Microbiol. 1, 49-59.

Belsare, A.V., Gompper, M.E., 2015a. A model-based approach for investigation and mitigation of disease spillover risks to wildlife: Dogs, foxes and canine distemper in central India. Ecol. Model. 296, 102-112.

Belsare, A.V., Gompper, M.E., 2015b. To vaccinate or not to vaccinate: lessons learned from an experimental mass vaccination of free-ranging dog populations. Anim. Consev. 18, 219-227.

Berentsen, A.R., Dunbar, M.R., Becker, M.S., M'Soka, J., Droge, E., Sakuya, N.M., Matandiko, W., McRobb, R., Hanlon, C.A., 2013. Rabies, canine distemper, and canine parvovirus exposure

in large carnivore communities from two Zambian ecosystems. Vector-Borne Zoonot. 13, 643-649.

Berman, H.M., Henrick, K., Nakamura, H., 2003. Announcing the worldwide Protein Data Bank Nat. Struct. Biol. 10, 980.

Bi, Z., Xia, X., Wang, Y., Mei, Y., 2015. Development and characterization of neutralizing monoclonal antibodies against canine distemper virus hemagglutinin protein. Microbiol. Immunol. 59, 202-208.

Biasini, M., Bienert, S., Waterhouse, A., Arnold, K., Studer, G., Schmidt, T., Kiefer, F., Gallo Cassarino, T., Bertoni, M., Bordoli, L., Schwede, T., 2014. SWISS-MODEL: modelling protein tertiary and quaternary structure using evolutionary information. Nucleic Acids Res. 42, W252-258.

Bieringer, M., Han, J.W., Kendl, S., Khosravi, M., Plattet, P., Schneider-Schaulies, J., 2013. Experimental adaptation of wild-type canine distemper virus (CDV) to the human entry receptor CD150. Plos One 8, e57488.

Bonami, F., Rudd, P.A., von Messling, V., 2007. Disease duration determines canine distemper virus neurovirulence. J. Virol. 81, 12066-12070.

Bordoli, L., Kiefer, F., Arnold, K., Benkert, P., Battey, J., Schwede, T., 2009. Protein structure homology modeling using SWISS-MODEL workspace. Nat. Protoc. 4, 1-13.

Boulouis, H.J., Chang, C.C., Henn, J.B., Kasten, R.W., Chomel, B.B., 2005. Factors associated with the rapid emergence of zoonotic Bartonella infections. Vet. Res. 36, 383-410.

Bregano, L.C., Agostinho, S.D., Roncatti, F.T.L.B., Pires, M.C., Garcia, A.F., Gameiro, R., Luvizotto, M.C.R., Cardoso, T.C., 2010. Expression of pro-and-anti-apoptotic antigens in the cerebellum of dogs naturally infected with canine distemper virus. Braz. J. Vet. Pathol. 3, 80-85.

Briggs, J., Paoloni, M., Chen, Q.R., Wen, X., Khan, J., Khanna, C., 2011. A compendium of canine normal tissue gene expression. Plos One 6, e17107.

Bringolf, F., Herren, M., Wyss, M., Vidondo, B., Langedijk, J.P., Zurbriggen, A., Plattet, P., 2017. Dimerization Efficiency of Canine Distemper Virus Matrix Protein Regulates Membrane-Budding Activity. J. Virol. 91.

Brunner, J.M., Plattet, P., Doucey, M.A., Rosso, L., Curie, T., Montagner, A., Wittek, R., Vandelvelde, M., Zurbriggen, A., Hirling, H., Desvergne, B., 2012. Morbillivirus glycoprotein expression induces ER stress, alters Ca2+ homeostasis and results in the release of vasostatin. Plos One 7, e32803.

Buczkowski, H., Parida, S., Bailey, D., Barrett, T., Banyard, A.C., 2012. A novel approach to generating morbillivirus vaccines: negatively marking the rinderpest vaccine. Vaccine 30, 1927-1935.

Budaszewski Rda, F., Pinto, L.D., Weber, M.N., Caldart, E.T., Alves, C.D., Martella, V., Ikuta, N., Lunge, V.R., Canal, C.W., 2014. Genotyping of canine distemper virus strains circulating in Brazil from 2008 to 2012. Virus Res. 180, 76-83.

Buragohain, M., Goswami, S., Kalita, D.J., 2017. Clinicopathological findings of canine distemper virus infection in dogs. J. Entomol. Zoo. 5, 1817-1819.

Cao, E., Ramagopal, U.A., Fedorov, A., Fedorov, E., Yan, Q., Lary, J.W., Cole, J.L., Nathenson, S.G., Almo, S.C., 2006. NTB-A receptor crystal structure: insights into homophilic interactions in the signaling lymphocytic activation molecule receptor family. Immunity 25, 559-570.

Carninci, P., Kasukawa, T., Katayama, S., Gough, J., Frith, M.C., Maeda, N., 2005. The Transcriptional Landscape of the Mammalian Genome. Science 309, 1559-1563.

Carpenter, M.A., Appel, M.J.G., Roelke-Parker, M.E., Munsond, L., Hofere, H., Easte, M., O'Brien, S.J., 1998. Genetic characterization of canine distemper virus in Serengeti carnivores. Vet. Immunol. Immunop. 65, 259-266.

Carvalho de Lima, R.S., Lallo, M.A., 2013. Public survey of knowledge concerning canine distemper and protective measures. Res. Vet. Sci. 20, 213-215.

Carvalho, O.V., Botelho, C.V., Ferreira, C.G., Scherer, P.O., Soares-Martins, J.A., Almeida, M.R., Silva, A.J., 2012. Immunopathogenic and neurological mechanisms of canine distemper virus. Adv. Virol. 2012, 163860.

Casasnovas, J.M., Larvie, M., Stehle, T., 1999. Crystal structure of two CD46 domains reveals an extended measles virus-binding surface. EMBO J. 18, 2911-2922.

Chappius, G., 1995. Control of canine distemper. Vet. Microbiol. 44, 351-358.

Chen, Y., Zhu, J., Lum, P.Y., Yang, X., Pinto, S., MacNeil, D.J., Zhang, C., Lamb, J., Edwards, S., Sieberts, S.K., Leonardson, A., Castellini, L.W., Wang, S., Champy, M.F., Zhang, B., Emilsson, V., Doss, S., Ghazalpour, A., Horvath, S., Drake, T.A., Lusis, A.J., Schadt, E.E., 2008. Variations in DNA elucidate molecular networks that cause disease. Nature 452, 429-435.

Cherpillod, P., Tipolda, A., Griot-Wenka, M., Cardozoa, C., Schmida, I., Fatzera, R., Schobesberger, M., 2000. DNA vaccine encoding nucleocapsid and surface proteins of wild type canine distemper virus protects its natural host against distemper. Vaccine 18, 2927-2936.

Chinnakannan, S.K., Nanda, S.K., Baron, M.D., 2013. Morbillivirus v proteins exhibit multiple mechanisms to block type 1 and type 2 interferon signalling pathways. Plos One 8, e57063.

Cleaveland, S., Appel, M.J.G., Chalmers, W.S.K., Chillingworth, C., Kaaree, M., Dye, C., 2000. Serological and demographic evidence for domestic dogs as a source of canine distemper virus infection for Serengeti wildlife. Vet. Microbiol. 72, 217-227.

Connolly, M., Thomas, P., Woodroffe, R., Raphael, B.L., 2013. Comparison of oral and intramuscular recombinant canine distemper vaccination in African wild dogs (*Lycaon pictus*). J. Zoo Wildlife Med. 44, 882-888.

Consortium, S.M.-I., 2014. A comprehensive assessment of RNA-seq accuracy, reproducibility and information content by the Sequencing Quality Control Consortium. Nat. Biotechnol. 32, 903-914.

Conway, T., Schoolnik, G.K., 2003. Microarray expression profiling: capturing a genome-wide portrait of the transcriptome. Mol. Microbiol. 47, 879-889.

Cornwell, H.J.C., Campbell, R.S.F., Vantsis, J.T., Penny, W., 1965. Studies in Experimental Canine Distemper I. Clinico-pathological findings. J. Comp. Pathol. 75, 3-17.

Cosby, S.L., 2012. Morbillivirus cross-species infection: is there a risk for humans? Future Virol. 7, 1103-1113.

Costa, V., Angelini, C., De Feis, I., Ciccodicola, A., 2010. Uncovering the complexity of transcriptomes with RNA-Seq. J. Biomed. Biotechnol. 2010, 853916.

Cottrell, W.O., Keel, M.K., Brooks, J.W., Mead, D.G., Phillips, J.E., 2013. First report of clinical disease associated with canine distemper virus infection in a wild black bear (Ursus americana). J. Wildlife Dis. 49, 1024-1027.

Coughlin, M.M., Bellini, W.J., Rota, P.A., 2013. Contribution of dendritic cells to measles virus induced immunosuppression. Rev. Med. Virol. 23, 126-138.

Cuthill, J.H., Charleston, M.A., 2013. A simple model explains the dynamics of preferential host switching among mammal RNA viruses. Evolution 67, 980-990.

da Fontoura Budaszewski, R., von Messling, V., 2016. Morbillivirus Experimental Animal Models: Measles Virus Pathogenesis Insights from Canine Distemper Virus. Viruses 8.

de Almeida Curi, N.H., Araújo, A.S., Campos, F.S., Lobato, Z.I.P., Gennari, S.M., Marvulo, M.F.V., Silva, J.C.R., Talamoni, S.A., 2010. Wild canids, domestic dogs and their pathogens in Southeast Brazil: disease threats for canid conservation. Roy. Soc. Ch. 19, 3513-3524.

de Camargo, T.C., Ferreira, Z.V., Rodrigues, B.C., Pessoa, A.J., 2016. Canine distemper virus detection by different methods of One-Step RT-qPCR. Ciência Rural 46, 1601-1606.

de Fontoura Budaszewski, R., Streck, A.F., Nunes Weber, M., Maboni Siqueira, F., Muniz Guedes, R.L., Wageck Canal, C., 2016. Influence of vaccine strains on the evolution of canine distemper virus. Infect. Genet. Evol. 41, 262-269.

de Vries, R.D., Ludlow, M., Verburgh, R.J., van Amerongen, G., Yuksel, S., Nguyen, D.T., McQuaid, S., Osterhaus, A.D., Duprex, W.P., de Swart, R.L., 2014. Measles vaccination of nonhuman primates provides partial protection against infection with canine distemper virus. J. Virol. 88, 4423-4433.

Deem, S.L., Spelman, L.H., Yates, R.A., Montali, R.J., 2000. Canine distemper in terrestrial carnivores: A review. J. Wildlife Med. 31, 441-451.

Delpeut, S., Noyce, R.S., Richardson, C.D., 2014a. The V domain of dog PVRL4 (nectin-4) mediates canine distemper virus entry and virus cell-to-cell spread. Virology 454-455, 109-117.

Delpeut, S., Noyce, R.S., Richardson, C.D., 2014b. The tumor-associated marker, PVRL4 (nectin-4), is the epithelial receptor for morbilliviruses. Viruses 6, 2268-2286.

Demeter, Z., Palade, E.A., Hornyak, A., Rusvai, M., 2010. Controversial results of the genetic analysis of a canine distemper vaccine strain. Vet. Microbiol. 142, 420-426.

Dermitzakis, E.T., 2008. From gene expression to disease risk. Nat. Gen. 40, 492-493.

Di Francesco, C.E., Di Francesco, D., Di Martino, B., Speranza, R., Santori, D., Boari, A., Marsilio, F., 2011. Detection by hemi-nested reverse transcription polymerase chain reaction and genetic characterization of wild type strains of Canine distemper virus in suspected infected dogs. J. Vet. Diagn. Invest. 24, 107-115.

Di Sabatino, D., Lorusso, A., Di Francesco, C.E., Gentile, L., Di Pirro, V., Bellacicco, A.L., Giovannini, A., Di Francesco, G., Marruchella, G., Marsilio, F., Savini, G., 2014. Arctic lineage-canine distemper virus as a cause of death in Apennine wolves (Canis lupus) in Italy. Plos One 9, e82356.

Diaz, N.M., Mendez, G.S., Grijalva, C.J., Walden, H.S., Cruz, M., Aragon, E., Hernandez, J.A., 2016. Dog overpopulation and burden of exposure to canine distemper virus and other pathogens on Santa Cruz Island, Galapagos. Prev. Vet. Med. 123, 128-137.

Dillies, M.A., Rau, A., Aubert, J., Hennequet-Antier, C., Jeanmougin, M., Servant, N., Keime, C., Marot, G., Castel, D., Estelle, J., Guernec, G., Jagla, B., Jouneau, L., Laloe, D., Le Gall, C.,

Schaeffer, B., Le Crom, S., Guedj, M., Jaffrezic, F., French StatOmique, C., 2013. A comprehensive evaluation of normalization methods for Illumina high-throughput RNA sequencing data analysis. Brief Bioinform. 14, 671-683.

Dong, Z., Chen, Y., 2013. Transcriptomics: advances and approaches. Sci. China Life Sci. 56, 960-967.

Durchfeld, B., Baumgärtner, W., Herbst, W., Brahm, R., 1990. Vaccine-associated Canine Distemper Infection in a Litter of African Hunting Dogs (Lycaonpictus). J. Vet. Med. 37, 203-212.

Ekblom, R., Galindo, J., 2011. Applications of next generation sequencing in molecular ecology of non-model organisms. Heredity 107, 1-15.

Elia, G., Decaro, N., Martella, V., Cirone, F., Lucente, M.S., Lorusso, E., Di Trani, L., Buonavoglia, C., 2006. Detection of canine distemper virus in dogs by real-time RT-PCR. J. Virol. Methods 136, 171-176.

Elia, G., Camero, M., Losurdo, M., Lucente, M.S., Larocca, V., Martella, V., Decaro, N., Buonavoglia, C., 2015. Virological and serological findings in dogs with naturally occurring distemper. J. Virol. Methods 213, 127-130.

Emilsson, V., Thorleifsson, G., Zhang, B., Leonardson, A.S., Zink, F., Zhu, J., Carlson, S., Helgason, A., Walters, G.B., Gunnarsdottir, S., Mouy, M., Steinthorsdottir, V., Eiriksdottir, G.H., Bjornsdottir, G., Reynisdottir, I., Gudbjartsson, D., Helgadottir, A., Jonasdottir, A., Jonasdottir, A., Styrkarsdottir, U., Gretarsdottir, S., Magnusson, K.P., Stefansson, H., Fossdal, R., Kristjansson, K., Gislason, H.G., Stefansson, T., Leifsson, B.G., Thorsteinsdottir, U., Lamb, J.R., Gulcher, J.R., Reitman, M.L., Kong, A., Schadt, E.E., Stefansson, K., 2008. Genetics of gene expression and its effect on disease. Nature 452, 423-428.

Engering, A., Hogerwerf, L., Slingenbergh, J., 2013. Pathogen-host-environment interplay and disease emergence. Emerg. Microbes Infect. 2, e5.

Feng, N., Liu, Y., Wang, J., Xu, W., Li, T., Wang, T., Wang, L., Yu, Y., Wang, H., Zhao, Y., Yang, S., Gao, Y., Hu, G., Xia, X., 2016a. Canine distemper virus isolated from a monkey efficiently

replicates on Vero cells expressing non-human primate SLAM receptors but not human SLAM receptor. BMC Vet. Res. 12, 160.

Feng, N., Yu, Y., Wang, T., Wilker, P., Wang, J., Li, Y., Sun, Z., Gao, Y., Xia, X., 2016b. Fatal canine distemper virus infection of giant pandas in China. Sci. Rep. 6, 27518.

Flacke, G., Becker, P., Cooper, D., Szykman Gunther, M., Robertson, I., Holyoake, C., Donaldson, R., Warren, K., 2013. An Infectious Disease and Mortality Survey in a Population of Free-Ranging African Wild Dogs and Sympatric Domestic Dogs. Int. J. Biodiversity 2013, 1-9.

Foley, J.E., Swift, P., Fleer, K.A., Torres, S., Girard, Y.A., Johnson, C.K., 2013. Risk factors for exposure to feline pathogens in California mountain lions (Puma concolor). J. Wildlife Dis. 49, 279-293.

Friedenberg, S.G., Chdid, L., Keene, B., Sherry, B., Motsinger-Reif, A., Meurs, K.M., 2016. Use of RNA-seq to identify cardiac genes and gene pathways differentially expressed between dogs with and without dilated cardiomyopathy. Am. J. Vet. Res. 77, 693-699.

Gandhi, K.S., McKay, F.C., Cox, M., Riveros, C., Armstrong, N., Heard, R.N., Vucic, S., Williams, D.W., Stankovich, J., Brown, M., Danoy, P., Stewart, G.J., Broadley, S., Moscato, P., Lechner-Scott, J., Scott, R.J., Booth, D.R., Consortium, A.N.M.S.G., 2010. The multiple sclerosis whole blood mRNA transcriptome and genetic associations indicate dysregulation of specific T cell pathways in pathogenesis. Hum. Mol. Genet. 19, 2134-2143.

Gilbert, M., Miquelle, D.G., Goodrich, J.M., Reeve, R., Cleaveland, S., Matthews, L., Joly, D.O., 2014. Estimating the potential impact of canine distemper virus on the Amur tiger population (Panthera tigris altaica) in Russia. Plos One 9, e110811.

Godfrey, S.S., 2013. Networks and the ecology of parasite transmission: A framework for wildlife parasitology. In.t J. Parasitol. Parasites Wildlife 2, 235-245.

Goller, K.V., Fyumagwa, R.D., Nikolin, V., East, M.L., Kilewo, M., Speck, S., Muller, T., Matzke, M., Wibbelt, G., 2010. Fatal canine distemper infection in a pack of African wild dogs in the Serengeti ecosystem, Tanzania. Vet. Microbiol. 146, 245-252.

Gray, L.K., Crawford, C., Levy, J.K., Dubovi, E., 2012. Comparison of two assays for detection of antibodies against canine parvovirus and canine distemper virus in dogs admitted to a Florida animal shelter. J. Am. Vet. Med. Acc. 240, 1084-1087.

Greer, K.A., Daly, P., Murphy, K.E., Callanan, J.J., 2010. Analysis of gene expression in brain tissue from Greyhounds with meningoencephalitis. Am. J. Vet. Res. 71, 547-554.

Grőne, A., Alldinger, S., Baumgärtner, W., 2000. Interleukin-1b, -6, -12 and tumor necrosis factor-a expression in brains of dogs with canine distemper virus infection. J. Neuroimmunol. 110, 20-30.

Guex, N., Peitsch, M.C., Schwede, T., 2009. Automated comparative protein structure modeling with SWISS-MODEL and Swiss-PdbViewer: a historical perspective. Electrophoresis 30 Suppl 1, S162-173.

Guven-Maiorov, E., Tsai, C.-J., Ma, B., Nussinov, R. 2019. Interface-Based Structural Prediction of Novel Host-Pathogen Interactions, In: Sikosek, T. (Ed.) Computational Methods in Protein Evolution. Springer New York, New York, NY, 317-335.

Haas , L., Hofer, H., East, M., Wohlsein, P., Liess, B., Barrett, T., 1996. Canine distemper virus infection in Serengeti spotted hyaenas. Vet. Microbiol. 49, 147-152.

Han, Y., Gao, S., Muegge, K., Zhang, W., Zhou, B., 2015. Advanced Applications of RNA Sequencing and Challenges. Bioinform. Biol. Insights 9, 29-46.

Haralambieva, I.H., Ovsyannikova, I.G., Pankratz, V.S., Kennedy, R.B., Jacobson, R.M., Poland, G.A., 2013. The genetic basis for interindividual immune response variation to measles vaccine: new understanding and new vaccine approaches. Expert Rev. Vaccines 12, 57-70.

Harder, T.C., Kenter, M., Appel, M.J.G., Roelke-Parker, M.E., Barrett, T., Osterhaus, A.D., 1995. Phylogenetic evidence of canine distemper virus in Serengeti's lions. Vaccine 13, 521-523.

Harder, T.C., Osterhaus, A.D., 1997. Canine distemper virus - a morbillivirus in search of new hosts? Trends Microbiol. 5, 120-124.

Hashiguchi, T., Maenaka, K., Yanagi, Y., 2011. Measles virus hemagglutinin: structural insights into cell entry and measles vaccine. Front. Microbiol. 2, 247.

Headley, S.A., Oliveira, T.E.S., Pereira, A.H.T., Moreira, J.R., Michelazzo, M.M.Z., Pires, B.G., Marutani, V.H.B., Xavier, A.A.C., Di Santis, G.W., Garcia, J.L., Alfieri, A.A., 2018. Canine morbillivirus (canine distemper virus) with concomitant canine adenovirus, canine parvovirus-2, and Neospora caninum in puppies: a retrospective immunohistochemical study. Sci Rep 8, 13477.

Hedegaard, J., Thorsen, K., Lund, M.K., Hein, A.M., Hamilton-Dutoit, S.J., Vang, S., Nordentoft, I., Birkenkamp-Demtroder, K., Kruhoffer, M., Hager, H., Knudsen, B., Andersen, C.L., Sorensen, K.D., Pedersen, J.S., Orntoft, T.F., Dyrskjot, L., 2014. Next-generation sequencing of RNA and DNA isolated from paired fresh-frozen and formalin-fixed paraffin-embedded samples of human cancer and normal tissue. Plos One 9, e98187.

Hodge, M.J., Wolfson, C., 1997. Canine distemper virus and Multiple sclerosis. Neurology 49, S62-S69.

Hoeppner, M.P., Lundquist, A., Pirun, M., Meadows, J.R., Zamani, N., Johnson, J., Sundstrom, G., Cook, A., FitzGerald, M.G., Swofford, R., Mauceli, E., Moghadam, B.T., Greka, A., Alfoldi, J., Abouelleil, A., Aftuck, L., Bessette, D., Berlin, A., Brown, A., Gearin, G., Lui, A., Macdonald, J.P., Priest, M., Shea, T., Turner-Maier, J., Zimmer, A., Lander, E.S., di Palma, F., Lindblad-Toh, K., Grabherr, M.G., 2014. An improved canine genome and a comprehensive catalogue of coding genes and non-coding transcripts. Plos One 9, e91172.

Hoffman, J.M., Creevy, K.E., Franks, A., O'Neill, D.G., Promislow, D.E.L., 2018. The companion dog as a model for human aging and mortality. Aging Cell 17, e12737.

Hrdlickova, R., Toloue, M., Tian, B., 2017. RNA-Seq methods for transcriptome analysis. Wiley Interdiscip Rev RNA 8.

Huang da, W., Sherman, B.T., Lempicki, R.A., 2009. Bioinformatics enrichment tools: paths toward the comprehensive functional analysis of large gene lists. Nucleic Acids Res. 37, 1-13.

Humphrey, W., Dalke, A., Schulten, K., 1996. VMD: Visual Molecular Dynamics. J. Mol. Graph. 14, 33-38.

Iwatsuki, K., Okita, M., Ochikubo, E., Gemma, T., Shin, Y.S., Miyashita, N., Mikami, T., Kal, C., 1995. Immunohistochemical Analysis of the Lymphoid Organs of Dogs Naturally Infected with Canine Distemper Virus. J. Comp. Pathol. 113, 185-190.

Iwatsuki, K., Ikeda, Y., Ohashi, K., Nakamura, K., Kai, C., 1999. Establishment of a persistent mutant of canine distemper virus. Microbes Infect. 1, 987-991.

Jamieson, A.M., Pasman, L., Yu, S., Gamradt, P., Homer, R.J., Decker, T., Medzhitov, R., 2013. Role of tissue protection in lethal respiratory viral-bacterial coinfection. Science 340, 1230-1234.

Jardine, C.M., Buchanan, T., Ojkic, D., Campbell, G.D., Bowman, J., 2018. Frequency of Virus Coinfection in Raccoons (Procyon lotor) and Striped Skunks (Mephitis mephitis) During a Concurrent Rabies and Canine Distemper Outbreak. J. Wildlife Dis. 54, 622-625.

Jensen, T.H., Nielsen, L., Aasted, B., Blixenkrone-Moller, M., 2009. Early life DNA vaccination with the H gene of Canine distemper virus induces robust protection against distemper. Vaccine 27, 5178-5183.

Jensen, W.A., Totten, J.S., Lappin, M.R., Schultz, R.D., 2015. Use of serologic tests to predict resistance to Canine distemper virus-induced disease in vaccinated dogs. J. Vet. Diagn. Invest. 27, 576-580.

Kameo, Y., Nagao, Y., Nishio, Y., Shimoda, H., Nakano, H., Suzuki, K., Une, Y., Sato, H., Shimojima, M., Maeda, K., 2012. Epizootic canine distemper virus infection among wild mammals. Vet. Microbiol. 154, 222-229.

Kapil, S., Yeary, T.J., 2011. Canine distemper spillover in domestic dogs from urban wildlife. Vet. Clin. North Am. Small Anim. Pract. 41, 1069-1086.

Kapil, S., Neel, T., 2015. Canine distemper virus antigen detection in external epithelia of recently vaccinated, sick dogs by fluorescence microscopy is a valuable prognostic indicator. J. Clin. Microbiol. 53, 687-691.

Ke, G.M., Ho, C.H., Chiang, M.J., Sanno-Duanda, B., Chung, C.S., Lin, M.Y., Shi, Y.Y., Yang, M.H., Tyan, Y.C., Liao, P.C., Chu, P.Y., 2015. Phylodynamic analysis of the canine distemper virus hemagglutinin gene. BMC Vet. Res. 11, 164.

Kelley, L.A., Mezulis, S., Yates, C.M., Wass, M.N., Sternberg, M.J., 2015. The Phyre2 web portal for protein modeling, prediction and analysis. Nat. Protoc. 10, 845-858.

Khosravi, M., Bringolf, F., Rothlisberger, S., Bieringer, M., Schneider-Schaulies, J., Zurbriggen, A., Origgi, F., Plattet, P., 2015. Canine Distemper Virus Fusion Activation: Critical Role of Residue E123 of CD150/SLAM. J. Virol. 90, 1622-1637.

Kiefer, F., Arnold, K., Kunzli, M., Bordoli, L., Schwede, T., 2009. The SWISS-MODEL Repository and associated resources. Nucleic Acids Res. 37, D387-392.

Kim, M.Y., Shu, Y., Carsillo, T., Zhang, J., Yu, L., Peterson, C., Longhi, S., Girod, S., Niewiesk, S., Oglesbee, M., 2013. hsp70 and a novel axis of type I interferon-dependent antiviral immunity in the measles virus-infected brain. J. Virol. 87, 998-1009.

Konjević, D., Sabočanec, R., Grabarević, Ž., Zurbriggen, A., Bata, I., Beck, A., Kurilj, A.G., Cvitković, D., 2011. Canine distemper in Siberian tiger cubs from Zagreb ZOO: case report. Acta. Vet. Brno 80, 47-50.

Krakowka, S., Cork, I.L.C., Winkelstein, J.A., Axthelm, M.K., 1987a. Establishment of central nervous sytem infection by Canine distemper virus: breach of the blood-brain barrier and facilitation by antiviral antibody. Vet. Immunol. Immunop. 17, 471-482.

Krakowka, S., Ringler, S.S., Lewis, M., Olsen, R. G., Axtheim, M.K., 1987b. Immunosupression by Canine distemper virus: modulation of in vitro immunoglobulin synthesis, interleukin release and prostaglandin E2 production. Vet. Immunol. Immunop. 15, 181-201.

Krakowka, S., 1989. Canine distemper virus infectivity of various blood fractions for central nervous system vasculature. J. Neuroimmunol. 21, 75-80.

Kvam, V.M., Liu, P., Si, Y., 2012. A comparison of statistical methods for detecting differentially expressed genes from RNA-seq data. Am. J. Bot. 99, 248-256.

Langedijk, J.P., Janda, J., Origgi, F.C., Orvell, C., Vandevelde, M., Zurbriggen, A., Plattet, P., 2011. Canine distemper virus infects canine keratinocytes and immune cells by using overlapping and distinct regions located on one side of the attachment protein. J. Virol. 85, 11242-11254.

Langmead, B., Salzberg, S.L., 2012. Fast gapped-read alignment with Bowtie 2. Nat. Methods 9, 357-359.

Lassmann, H., 2013. Pathology and disease mechanisms in different stages of multiple sclerosis. J. Neurol. Sci. 333, 1-4.

Lassmann, H., Bradl, M., 2017. Multiple sclerosis: experimental models and reality. Acta Neuropathol. 133, 223-244.

Lempp, C., Spitzbarth, I., Puff, C., Cana, A., Kegler, K., Techangamsuwan, S., Baumgärtner, W., Seehusen, F., 2014. New aspects of the pathogenesis of canine distemper leukoencephalitis. Viruses 6, 2571-2601.

Li, S., Labaj, P.P., Zumbo, P., Sykacek, P., Shi, W., Shi, L., Phan, J., Wu, P.Y., Wang, M., Wang, C., Thierry-Mieg, D., Thierry-Mieg, J., Kreil, D.P., Mason, C.E., 2014a. Detecting and correcting systematic variation in large-scale RNA sequencing data. Nat. Biotechnol. 32, 888-895.

Li, S., Tighe, S.W., Nicolet, C.M., Grove, D., Levy, S., Farmerie, W., Viale, A., Wright, C., Schweitzer, P.A., Gao, Y., Kim, D., Boland, J., Hicks, B., Kim, R., Chhangawala, S., Jafari, N., Raghavachari, N., Gandara, J., Garcia-Reyero, N., Hendrickson, C., Roberson, D., Rosenfeld, J., Smith, T., Underwood, J.G., Wang, M., Zumbo, P., Baldwin, D.A., Grills, G.S., Mason, C.E., 2014b. Multi-platform assessment of transcriptome profiling using RNA-seq in the ABRF next-generation sequencing study. Nat. Biotechnol. 32, 915-925.

Liao, P., Guo, L., Wen, Y., Yang, Y., Cheng, S., 2015. Phylogenetic features of hemagglutin gene in canine distemper virus strains from different genetic lineages. Int. J. Clin. Exp. Med. 8, 6607-6612.

Lin, L.T., Richardson, C.D., 2016. The Host Cell Receptors for Measles Virus and Their Interaction with the Viral Hemagglutinin (H) Protein. Viruses 8.

Lindblad-Toh, K., Wade, C.M., Mikkelsen, T.S., Karlsson, E.K., Jaffe, D.B., Kamal, M., Clamp, M., Chang, J.L., Kulbokas, E.J., 3rd, Zody, M.C., Mauceli, E., Xie, X., Breen, M., Wayne, R.K., Ostrander, E.A., Ponting, C.P., Galibert, F., Smith, D.R., DeJong, P.J., Kirkness, E., Alvarez, P., Biagi, T., Brockman, W., Butler, J., Chin, C.W., Cook, A., Cuff, J., Daly, M.J., DeCaprio, D., Gnerre, S., Grabherr, M., Kellis, M., Kleber, M., Bardeleben, C., Goodstadt, L., Heger, A., Hitte, C., Kim, L., Koepfli, K.P., Parker, H.G., Pollinger, J.P., Searle, S.M., Sutter, N.B., Thomas, R., Webber, C., Baldwin, J., Abebe, A., Abouelleil, A., Aftuck, L., Ait-Zahra, M., Aldredge, T., Allen, N., An, P., Anderson, S., Antoine, C., Arachchi, H., Aslam, A., Ayotte, L., Bachantsang, P., Barry, A., Bayul, T., Benamara, M., Berlin, A., Bessette, D., Blitshteyn, B., Bloom, T., Blye, J., Boguslavskiy, L., Bonnet, C., Boukhgalter, B., Brown, A., Cahill, P., Calixte, N., Camarata, J., Cheshatsang, Y., Chu, J., Citroen, M., Collymore, A., Cooke, P., Dawoe, T., Daza, R., Decktor, K., DeGray, S., Dhargay, N., Dooley, K., Dooley, K., Dorje, P., Dorjee, K., Dorris, L., Duffey, N., Dupes, A., Egbiremolen, O., Elong, R., Falk, J., Farina, A., Faro, S., Ferguson, D., Ferreira, P., Fisher, S., FitzGerald, M., Foley, K., Foley, C., Franke, A., Friedrich, D., Gage, D., Garber, M., Gearin, G., Giannoukos, G., Goode, T., Goyette, A., Graham, J., Grandbois, E., Gyaltsen, K., Hafez, N., Hagopian, D., Hagos, B., Hall, J., Healy, C., Hegarty, R., Honan, T., Horn, A., Houde, N., Hughes, L., Hunnicutt, L., Husby, M., Jester, B., Jones, C., Kamat, A., Kanga, B., Kells, C., Khazanovich, D., Kieu, A.C., Kisner, P., Kumar, M., Lance, K., Landers, T., Lara, M., Lee, W., Leger, J.P., Lennon, N., Leuper, L., LeVine, S., Liu, J., Liu, X., Lokyitsang, Y., Lokyitsang, T., Lui, A., Macdonald, J., Major, J., Marabella, R., Maru, K., Matthews, C., McDonough, S., Mehta, T., Meldrim, J., Melnikov, A., Meneus, L., Mihalev, A., Mihova, T., Miller, K., Mittelman, R., Mlenga, V., Mulrain, L., Munson, G., Navidi, A., Naylor, J., Nguyen, T., Nguyen, N., Nguyen, C., Nguyen, T., Nicol, R., Norbu, N., Norbu, C., Novod, N., Nyima, T., Olandt, P., O'Neill, B., O'Neill, K., Osman,

S., Oyono, L., Patti, C., Perrin, D., Phunkhang, P., Pierre, F., Priest, M., Rachupka, A., Raghuraman, S., Rameau, R., Ray, V., Raymond, C., Rege, F., Rise, C., Rogers, J., Rogov, P., Sahalie, J., Settipalli, S., Sharpe, T., Shea, T., Sheehan, M., Sherpa, N., Shi, J., Shih, D., Sloan, J., Smith, C., Sparrow, T., Stalker, J., Stange-Thomann, N., Stavropoulos, S., Stone, C., Stone, S., Sykes, S., Tchuinga, P., Tenzing, P., Tesfaye, S., Thoulutsang, D., Thoulutsang, Y., Topham, K., Topping, I., Tsamla, T., Vassiliev, H., Venkataraman, V., Vo, A., Wangchuk, T., Wangdi, T., Weiand, M., Wilkinson, J., Wilson, A., Yadav, S., Yang, S., Yang, X., Young, G., Yu, Q., Zainoun, J., Zembek, L., Zimmer, A., Lander, E.S., 2005. Genome sequence, comparative analysis and haplotype structure of the domestic dog. Nature 438, 803-819.

Liszewski, M.K., Atkinson, J.P., 2015. Complement regulator CD46: genetic variants and disease associations. Human Genomics 9.

Litster, A.L., Pressler, B., Volpe, A., Dubovi, E., 2012. Accuracy of a point-of-care ELISA test kit for predicting the presence of protective canine parvovirus and canine distemper virus antibody concentrations in dogs. Vet. J. 193, 363-366.

Liu, D., Xiong, H., Ellis, A.E., Northrup, N.C., Dobbin, K.K., Shin, D.M., Zhao, S., 2015. Canine spontaneous head and neck squamous cell carcinomas represent their human counterparts at the molecular level. Plos Genet. 11, e1005277.

Liu, X., Harada, S., 2013. DNA isolation from mammalian samples. Curr. Protoc. Mol. Biol. Chapter 2, Unit2 14.

Liu, X., Rohr, J.R., Li, Y., 2013. Climate, vegetation, introduced hosts and trade shape a global wildlife pandemic. Proc. Biol. Sci. 280, 20122506.

Liu, Y., Zhou, J., White, K.P., 2014. RNA-seq differential expression studies: more sequence or more replication? Bioinformatics 30, 301-304.

Loots, A.K., Mitchell, E., Dalton, D.L., Kotzé, A., Venter, E.H., 2016. Advances in canine distemper virus (CDV) pathogenesis research: a wildlife perspective. J. Gen. Virol.

Loots, A.K., Mokgokong, P.S., Mitchell, E., Venter, E.H., Kotze, A., Dalton, D.L., 2018. Phylogenetic analysis of canine distemper virus in South African wildlife. Plos One 13, e0199993.

Ludlow, M., Rennick, L.J., Nambulli, S., de Swart, R.L., Duprex, W.P., 2014. Using the ferret model to study morbillivirus entry, spread, transmission and cross-species infection. Curr. Opin. Virol. 4, 15-23.

Luscombe, N.M., Austin, S.E., Berman, H.M., Thornton, J.M., 2000. An overview of the structures of protein-DNA complexes. Genome Biol. 1.

Luscombe, N.M., Thornton, J.M., 2002. Protein–DNA Interactions: Amino Acid Conservation and the Effects of Mutations on Binding Specificity. J. Mol Biol. 320, 991-1009.

Maes, R.K., Langohr, I.M., Wise, A.G., Smedley, R.C., Thaiwong, T., Kiupel, M., 2014. Beyond H&E: integration of nucleic acid-based analyses into diagnostic pathology. Vet. Pathol. 51, 238-256.

Magiorkinis, G., Sypsa, V., Magiorkinis, E., Paraskevis, D., Katsoulidou, A., Belshaw, R., Fraser, C., Pybus, O.G., Hatzakis, A., 2013. Integrating phylodynamics and epidemiology to estimate transmission diversity in viral epidemics. Plos Comput. Biol. 9, e1002876.

Mahad, D.H., Trapp, B.D., Lassmann, H., 2015. Pathological mechanisms in progressive multiple sclerosis. Lancet Neurol. 14, 183-193.

Malpica, J.M., Sacristan, S., Fraile, A., Garcia-Arenal, F., 2006. Association and host selectivity in multi-host pathogens. Plos One 1, e41.

Marescot, L., Benhaiem, S., Gimenez, O., Hofer, H., Lebreton, J., Olarte-Castillo, X.A., Kramer-Schadt, S., East, M.L., White, C., 2018. Social status mediates the fitness costs of infection with canine distemper virus in Serengeti spotted hyenas. Funct. Ecol. 32, 1237-1250.

Marioni, J.C., Mason, C.E., Mane, S.M., Stephens, M., Gilad, Y., 2008. RNA-seq: an assessment of technical reproducibility and comparison with gene expression arrays. Genome Res. 18, 1509-1517.

Markus, S., Failing, K., Baumgärtner, W., 2002. Increased expression of pro-inf lammatory cytokines and lack of up-regulation of anti-inf lammatory cytokines in early distemper CNS lesions. J. Neuroimmunol. 125, 30.

Martella, V., Elia, G., Buonavoglia, C., 2008. Canine distemper virus. Vet. Clin. North Am. Small Anim. Pract. 38, 787-797, vii-viii.

Martella, V., Bianchi, A., Bertoletti, I., Pedrotti, L., Gugiatti, A., Catella, A., Cordioli, P., Lucente, M.S., Elia, G., Buonavoglia, C., 2010. Canine Distemper Epizootic among Red Foxes, Italy,2009. Emerg. Infect. Dis.

Martella, V., Blixenkrone-Moller, M., Elia, G., Lucente, M.S., Cirone, F., Decaro, N., Nielsen, L., Banyai, K., Carmichael, L.E., Buonavoglia, C., 2011. Lights and shades on an historical vaccine canine distemper virus, the Rockborn strain. Vaccine 29, 1222-1227.

Martinez-Gutierrez, M., Ruiz-Saenz, J., 2016. Diversity of susceptible hosts in canine distemper virus infection: a systematic review and data synthesis. BMC Vet. Res. 12, 78.

McCallum, H., Dobson, A., 1995. Detecting disease and parasite threats to endangered species and ecosystems. Tree 10, 190-194.

McCarthy, A.J., Shaw, M.A., Goodman, S.J., 2007. Pathogen evolution and disease emergence in carnivores. Proc. Biol. Sci. 274, 3165-3174.

McCarthy, A.J., Shaw, M.A., Jepson, P.D., Brasseur, S.M., Reijnders, P.J., Goodman, S.J., 2011. Variation in European harbour seal immune response genes and susceptibility to phocine distemper virus (PDV). Infect. Genet. Evol. 11, 1616-1623.

McGavin, M.D., 2014. Factors affecting visibility of a target tissue in histologic sections. Vet. Pathol. 51, 9-27.

Mestas, J., Hughes, C.C.W., 2004. Of Mice and Not Men: Differences between Mouse and Human Immunology. J. Immunol. 172, 2731-2738.

Monne, I., Fusaro, A., Valastro, V., Citterio, C., Dalla Pozza, M., Obber, F., Trevisiol, K., Cova, M., De Benedictis, P., Bregoli, M., Capua, I., Cattoli, G., 2011. A distinct CDV genotype causing a major epidemic in Alpine wildlife. Vet. Microbiol. 150, 63-69.

Mooney, M., Bond, J., Monks, N., Eugster, E., Cherba, D., Berlinski, P., Kamerling, S., Marotti, K., Simpson, H., Rusk, T., Tembe, W., Legendre, C., Benson, H., Liang, W., Webb, C.P., 2013. Comparative RNA-Seq and microarray analysis of gene expression changes in B-cell lymphomas of Canis familiaris. Plos One 8, e61088.

Morens, D.M., Holmes, E.C., Davis, A.S., Taubenberger, J.K., 2011. Global rinderpest eradication: lessons learned and why humans should celebrate too. J. Infect. Dis. 204, 502-505.

Morozova, O., Marra, M.A., 2008. Applications of next-generation sequencing technologies in functional genomics. Genomics 92, 255-264.

Mortazavi, A., Williams, B.A., McCue, K., Schaeffer, L., Wold, B., 2008. Mapping and quantifying mammalian transcriptomes by RNA-Seq. Nat. Methods 5, 621-628.

Moss, W.J., Griffin, D.E., 2006. Global measles elimination. Nat Rev Microbiol 4, 900-908.

Nagao, Y., Nishio, Y., Shiomoda, H., Tamaru, S., Shimojima, M., Goto, M., Une, Y., Sato, A., Ikebe, Y., Maeda, K., 2012. An Outbreak of Canine Distemper Virus in Tigers (Panthera tigris): Possible Transmission from Wild Animals to Zoo Animals. J. Vet. Med. Sci. 74, 699-705.

Naumova, O.Y., Lee, M., Rychkov, S.Y., Vlasova, N.V., Grigorenko, E.L., 2013. Gene expression in the human brain: the current state of the study of specificity and spatiotemporal dynamics. Child. Dev. 84, 76-88.

Nemeth, N.M., Oesterle, P.T., Campbell, G.D., Ojkic, D., Jardine, C.M., 2018. Comparison of reverse-transcription real-time PCR and immunohistochemistry for the detection of canine distemper virus infection in raccoons in Ontario, Canada. J. Vet. Diagn. Invest. 30, 319-323.

Nguyen, D.T., 2014. Interactions between Paramyxoviruses and Bacteria: Implications for Pathogenesis and Intervention. Thesis.

Nielsen, L., Sogaard, M., Jensen, T.H., Andersen, M.K., Aasted, B., Blixenkrone-Moller, M., 2009. Lymphotropism and host responses during acute wild-type canine distemper virus infections in a highly susceptible natural host. J. Gen. Virol. 90, 2157-2165.

Nielsen, L., Jensen, T.H., Kristensen, B., Jensen, T.D., Karlskov-Mortensen, P., Lund, M., Aasted, B., Blixenkrone-Moller, M., 2012. DNA vaccines encoding proteins from wild-type and attenuated canine distemper virus protect equally well against wild-type virus challenge. Arch. Virol. 157, 1887-1896.

Nikolin, V.M., Osterrieder, K., von Messling, V., Hofer, H., Anderson, D., Dubovi, E., Brunner, E., East, M.L., 2012a. Antagonistic pleiotropy and fitness trade-offs reveal specialist and generalist traits in strains of canine distemper virus. Plos One 7, e50955.

Nikolin, V.M., Wibbelt, G., Michler, F.U., Wolf, P., East, M.L., 2012b. Susceptibility of carnivore hosts to strains of canine distemper virus from distinct genetic lineages. Vet. Microbiol. 156, 45-53.

Nikolin, V.M., Olarte-Castillo, X.A., Osterrieder, N., Hofer, H., Dubovi, E., Mazzoni, C.J., Brunner, E., Goller, K.V., Fyumagwa, R.D., Moehlman, P.D., Thierer, D., East, M.L., 2016. Canine distemper virus in the Serengeti ecosystem: molecular adaptation to different carnivore species. Mol. Ecol. .

Noel, D.D., Malerba, G., Ferarrini, A., Delledonne, M., 2014. Evaluation of microarray sensitivity and specificity in gene expression differential analysis by RNA-Seq and Quantitative RT-PRCR. J. Multidiscip. Sci. Res. 2, 5-9.

Noyce, R.S., Delpeut, S., Richardson, C.D., 2013. Dog nectin-4 is an epithelial cell receptor for canine distemper virus that facilitates virus entry and syncytia formation. Virology 436, 210-220.

O'Brien, S.J., 1999. The Promise of Comparative Genomics in Mammals. Science 286, 458-481.

Ohishi, K., Ando, A., Suzuki, R., Takishita, K., Kawato, M., Katsumata, E., Ohtsu, D., Okutsu, K., Tokutake, K., Miyahara, H., Nakamura, H., Murayama, T., Maruyama, T., 2010. Host-virus

specificity of morbilliviruses predicted by structural modeling of the marine mammal SLAM, a receptor. Comp. Immunol. Microbiol. Infect. Dis. 33, 227-241.

Ohishi, K., Suzuki, R., Maeda, T., Tsuda, M., Abe, E., Yoshida, T., Endo, Y., Okamura, M., Nagamine, T., Yamamoto, H., Ueda, M., Maruyama, T., 2014. Recent host range expansion of canine distemper virus and variation in its receptor, the signaling lymphocyte activation molecule, in carnivores. J. Wildlife Dis. 50, 596-606.

Ostrander, E.A., Comstock, K.E., 2004. The domestic dog genome. Curr. Biol. 14, R98-R99.

Ostrander, E.A., 2012. Franklin H. Epstein Lecture. Both ends of the leash--the human links to good dogs with bad genes. N. Engl. J. Med. 367, 636-646.

Otsuki, N., Nakatsu, Y., Kubota, T., Sekizuka, T., Seki, F., Sakai, K., Kuroda, M., Yamaguchi, R., Takeda, M., 2013. The V protein of canine distemper virus is required for virus replication in human epithelial cells. Plos One 8, e82343.

Ozsolak, F., Milos, P.M., 2011. RNA sequencing: advances, challenges and opportunities. Nat. Rev. Genet. 12, 87-98.

Pan, Y., Liu, X., Meng, L., Zhu, G., Xia, Y., Chen, J., Takashi, Y., 2013. Pathogenesis of Demyelinating Encephalopathy in Dogs with Spontaneous Acute Canine Distemper. J. Integr. Agr. 12, 334-343.

Pan, Y., Liu, X., Zhang, L., Sun, Y., Li, R., Liu, Z., Me, L., 2014. Alteration of T, B Cells Subsets Relating to Immunosuppression and Lymphoid Depletion in Dogs with Spontaneous Acute Distemper. Pak. Vet J. 34, 449-453.

Panzera, Y., Sarute, N., Carrau, L., Aldaz, J., Pérez, R., 2014. Genetic Diversity of Canine Distemper Virus in South America. Brit. J. Virol. 1, 48-53.

Panzera, Y., Sarute, N., Iraola, G., Hernandez, M., Perez, R., 2015. Molecular phylogeography of canine distemper virus: Geographic origin and global spreading. Mol. Phylogenet. Evol. 92, 147-154.

Park, J.Y., Shin, D.J., Lee, S.H., Lee, J.J., Suh, G.H., Cho, D., Kim, S.K., 2015. The anti-canine distemper virus activities of ex vivo-expanded canine natural killer cells. Vet. Microbiol. 176, 239-249.

Parker, H.G., Kim, L.V., Sutter, N.B., Carlson, S., Lorentzen, T.D., Malek, T.B., Johnson, G.S., DeFrance, H.B., Ostrander, E.A., Kruglyak, L., 2004. Genetic structure of the purebred domestic dog. Science 304, 1160-1164.

Parker, H.G., Meurs, K.M., Ostrander, E.A., 2006. Finding cardiovascular disease genes in the dog. J. Vet. Cardiol. 8, 115-127.

Parker, H.G., Shearin, A.L., Ostrander, E.A., 2010. Man's best friend becomes biology's best in show: genome analyses in the domestic dog. Annu. Rev. Genet. 44, 309-336.

Pedersen, N.C., 1999. A review of immunologic diseases of the dog. Vet. Immunol. Immunop. 69, 251-342.

Pedersen, R.O., Sandel, B., Svenning, J.C., 2014. Macroecological evidence for competitive regional-scale interactions between the two major clades of mammal carnivores (Feliformia and Caniformia). Plos One 9, e100553.

Pendleton, A.L., Shen, F., Taravella, A.M., Emery, S., Veeramah, K.R., Boyko, A.R., Kidd, J.M., 2018. Comparison of village dog and wolf genomes highlights the role of the neural crest in dog domestication. BMC Biol 16, 64.

Perri, A., 2016. A wolf in dog's clothing: Initial dog domestication and Pleistocene wolf variation. Journal of Archaeological Science 68, 1-4.

Perrone, D., Bender, S., Niewiesk, S., 2010. A comparison of the immune responses of dogs exposed to canine distemper virus (CDV) — Differences between vaccinated and wild-type virus exposed dogs. Can. J. Vet. Sci. 74, 214-217.

Pillet, S., von Messling, V., 2009. Canine distemper virus selectively inhibits apoptosis progression in infected immune cells. J. Virol. 83, 6279-6287.

Plattet, P., Rivals, J.P., Zuber, B., Brunner, J.M., Zurbriggen, A., Wittek, R., 2005. The fusion protein of wild-type canine distemper virus is a major determinant of persistent infection. Virology 337, 312-326.

Prager, K.C., 2010. An Investigation of Infectious Disease Dynamics in African Carnivores: Identifying Reservoirs and Risk Factors and Investigating Control Strategies. Thesis.

Prager, K.C., Woodroffe, R., Cameron, A., Haydon, D.T., 2011. Vaccination strategies to conserve the endangered African wild dog (Lycaon pictus). Biol. Conserv. 144, 1940-1948.

Prager, K.C., Mazet, J.A., Dubovi, E.J., Frank, L.G., Munson, L., Wagner, A.P., Woodroffe, R., 2012a. Rabies virus and canine distemper virus in wild and domestic carnivores in Northern Kenya: are domestic dogs the reservoir? Ecohealth 9, 483-498.

Prager, K.C., Mazet, J.A.K., Munson, L., Cleaveland, S., Donnelly, C.A., Dubovi, E.J., Szykman Gunther, M., Lines, R., Mills, G., Davies-Mostert, H.T., Weldon McNutt, J., Rasmussen, G., Terio, K.A., Woodroffe, R., 2012b. The effect of protected areas on pathogen exposure in endangered African wild dog (Lycaon pictus) populations. Biol. Conserv. 150, 15-22.

Pybus, O.G., Fraser, C., Rambaut, A., 2013. Evolutionary epidemiology: preparing for an age of genomic plenty. Philos. Trans. R. Soc. Lond. B. Biol. Sci. 368, 20120193.

Qeska, V., Barthel, Y., Herder, V., Stein, V.M., Tipold, A., Urhausen, C., Gunzel-Apel, A., Rohn, K., Baumgärtner, W., Beineke, A., 2014. Canine Distemper Virus Infection Leads to an Inhibitory Phenotype of Monocyte-Derived Dendritic Cells In Vitro with Reduced Expression of Co-Stimulatory Molecules and Increased Interleukin-10 Transcription. Plos One 9.

Qian, F., Chung, L., Zheng, W., Bruno, V., Alexander, R.P., Wang, Z., Wang, X., Kurscheid, S., Zhao, H., Fikrig, E., Gerstein, M., Snyder, M., Montgomery, R.R., 2013. Identification of genes critical for resistance to infection by West Nile virus using RNA-Seq analysis. Viruses 5, 1664-1681.

Raddatz, B.B., Hansmann, F., Spitzbarth, I., Kalkuhl, A., Deschl, U., Baumgärtner, W., Ulrich, R., 2014. Transcriptomic meta-analysis of multiple sclerosis and its experimental models. Plos One 9, e86643.

Ramsay, E., Sadler, R., Rush, R., Seimon, T., Tomaszewicz, A., 2016. Canine distemper virus antibody titers in domestic cats after delivery of a live attenuated virus vaccine. J. Zoo Wildlife Med. 47, 551-557.

Rapaport, F., Khanin, R., Liang, Y., Pirun, M., Krek, A., Zumbo, P., Mason, C.E., Socci, N.D., Betel, D., 2013. Comprehensive evaluation of differential gene expression analysis methods for RNA-seq data. Genome Biol. 14.

Rima, B.K., Baczko, K., Imagawa, D.T., Ter Meulen, V., 1987. Humoral Immune Response in Dogs with Old Dog Encephalitis and Chronic Distemper Meningo-encephalitis. J. Gen. Virol. 68, 1723-1735.

Rivals, J.P., Plattet, P., Currat-Zweifel, C., Zurbriggen, A., Wittek, R., 2007. Adaptation of canine distemper virus to canine footpad keratinocytes modifies polymerase activity and fusogenicity through amino acid substitutions in the P/V/C and H proteins. Virology 359, 6-18.

Riveros, C., Mellor, D., Gandhi, K.S., McKay, F.C., Cox, M.B., Berretta, R., Vaezpour, S.Y., Inostroza-Ponta, M., Broadley, S.A., Heard, R.N., Vucic, S., Stewart, G.J., Williams, D.W., Scott, R.J., Lechner-Scott, J., Booth, D.R., Moscato, P., Consortium, A.N.M.S.G., 2010. A transcription factor map as revealed by a genome-wide gene expression analysis of whole-blood mRNA transcriptome in multiple sclerosis. Plos One 5, e14176.

Robinson, M.D., McCarthy, D.J., Smyth, G.K., 2010. edgeR: a Bioconductor package for differential expression analysis of digital gene expression data. Bioinformatics 26, 139-140.

Robinson, M.D., Oshlack, A., 2010. A scaling normalization method for differential expression analysis of RNA-seq data. Genome Biol 11.

Roy, M., Kim, N., Kim, K., Chung, W.H., Achawanantakun, R., Sun, Y., Wayne, R., 2013. Analysis of the canine brain transcriptome with an emphasis on the hypothalamus and cerebral cortex. Mamm. Genome 24, 484-499.

Rudd, P.A., Cattaneo, R., von Messling, V., 2006. Canine distemper virus uses both the anterograde and the hematogenous pathway for neuroinvasion. J. Virol. 80, 9361-9370.

Rudd, P.A., Bastien-Hamel, L.E., von Messling, V., 2010. Acute canine distemper encephalitis is associated with rapid neuronal loss and local immune activation. J. Gen. Virol. 91, 980-989.

Ruiz-Lopez, M.J., Monello, R.J., Schuttler, S.G., Lance, S.L., Gompper, M.E., Eggert, L.S., 2014. Major Histocompatibility Complex, demographic, and environmental predictors of antibody presence in a free-ranging mammal. Infect. Genet. Evol. 28, 317-327.

Sadler, R.A., Ramsay, E., McAloose, D., Rush, R., Wilkes, R.P., 2016. Evaluation of two canine distemper vaccines in captive tigres (panthera tigris). J. Zoo Wildlife Med. 47, 558-563.

Sakai, K., Yoshikawa, T., Seki, F., Fukushi, S., Tahara, M., Nagata, N., Ami, Y., Mizutani, T., 2013. Canine Distemper Virus Associated with a Lethal Outbreak in Monkeys can Readily Adapt To Use Human Receptors. J. Virol. 87, 7170-7175.

Sarute, N., Calderon, M.G., Perez, R., La Torre, J., Hernandez, M., Francia, L., Panzera, Y., 2013. The fusion protein signal-peptide-coding region of canine distemper virus: a useful tool for phylogenetic reconstruction and lineage identification. PLoS One 8, e63595.

Sato, H., Yoneda, M., Honda, T., Kai, C., 2011. Recombinant vaccines against the mononegaviruses--what we have learned from animal disease controls. Virus Res. 162, 63-71.

Sattler, U., Khosravi, M., Avila, M., Pilo, P., Langedijk, J.P., Ader-Ebert, N., Alves, L.A., Plattet, P., Origgi, F.C., 2014. Identification of amino acid substitutions with compensational effects in the attachment protein of canine distemper virus. J. Virol. 88, 8057-8064.

Sawatsky, B., Cattaneo, R., von Messling, V., 2018. Canine Distemper Virus Spread and Transmission to Naive Ferrets: Selective Pressure on SLAM-Dependent Entry. J. Virol.

Schobesberger, M., Summerfield, A., Doherr, M.G., Zurbriggen, A., Griot, C., 2005. Canine distemper virus-induced depletion of uninfected lymphocytes is associated with apoptosis. Vet. Immunol. Immunop. 104, 33-44.

Seimon, T.A., Miquelle, D.G., Chang, T.Y., Newton, A.L., Korotkova, I., Ivanchuk, G., Lyubchenko, E., Tupikov, A., Slabe, E., McAloose, D., 2013. Canine distemper virus: an emerging disease in wild endangered Amur tigers (Panthera tigris altaica). MBio 4.

Sekulin, K., Hafner-Marx, A., Kolodziejek, J., Janik, D., Schmidt, P., Nowotny, N., 2011. Emergence of canine distemper in Bavarian wildlife associated with a specific amino acid exchange in the haemagglutinin protein. Vet. J. 187, 399-401.

Seyednasrollah, F., Laiho, A., Elo, L.L., 2015. Comparison of software packages for detecting differential expression in RNA-seq studies. Brief Bioinform. 16, 59-70.

Shen, Y., Wang, S., Ai, H., Min, C., Chen, Y., Zhang, S., 2011. Molecular structure, bioinformatics analysis, expression and bioactivity of BAFF (TNF13B) in dog (Canis familiaris). Vet. Immunol. Immunop. 142, 133-139.

Si, W., Zhou, S., Wang, Z., Cui, S.J., 2010. A multiplex reverse transcription-nested polymerase chain reaction for detection and differentiation of wild-type and vaccine strains of canine distemper virus. Virol. J. 7, 86.

Siebert, U., Gulland, F., Harder, T., Jauniaux, T., Seibel, H., Wohlsein, P., Baumgärtner, W., 2013. Epizootics in harbour seals (*Phoca vitulina*): clinical aspects. NAMMCO Sci. Pub. 8, 265-274.

Silva, A.P., Bodnar, L., Headley, S.A., Alfieri, A.F., Alfieri, A.A., 2014. Molecular detection of canine distemper virus (CDV), canine adenovirus A types 1 and 2 (CAdV-1 and CAdV-2), and canine parvovirus type 2 (CPV-2) in the urine of naturally infected dogs. Semina: Ciências Agrárias 35, 265-274.

Sips, G.J., Chesik, D., Glazenburg, L., Wilschut, J., De Keyser, J., Wilczak, N., 2007. Involvement of morbilliviruses in the pathogenesis of demyelinating disease. Rev. Med. Virol. 17, 223-244.

Soma, T., Uemura, T., Nakamoto, Y., Ozawa, T., Bandai, T., Oji, T., Une, S., 2013. Canine distemper virus antibody test alone increases misdiagnosis of distemper encephalitis. Vet. Rec. 173, 477.

Sorenson, C., Delorenzi, M., 2013. A comparison of methods for differential expression analysis of RNA-seq data. BMC Bioinformatics 14.

Spitzbarth, I., Lempp, C., Kegler, K., Ulrich, R., Kalkuhl, A., Deschl, U., Baumgärtner, W., Seehusen, F., 2016. Immunohistochemical and transcriptome analyses indicate complex breakdown of axonal transport mechanisms in canine distemper leukoencephalitis. Brain Behav. 6, e00472.

Starkey, M.P., Scase, T.J., Mellersh, C.S., Murphy, S., 2005. Dogs really are man's best friend — Canine genomics has applications in veterinary and human medicine! Brief. Funct. Genomics Proteom. 4, 112-128.

States, D.J., Gish, W., 1994. QGB: Combined Use of Sequence Similarity and Codon Bias for Coding Region Identification. J. Comput. Biol. 1, 39-50.

Stimmer, L., Siebert, U., Wohlsein, P., Fontaine, J.J., Baumgärtner, W., Beineke, A., 2010. Viral protein expression and phenotyping of inflammatory responses in the central nervous system of phocine distemper virus-infected harbor seals (Phoca vitulina). Vet. Microbiol. 145, 23-33.

Sugai, A., Sato, H., Yoneda, M., Kai, C., 2013. Phosphorylation of measles virus nucleoprotein affects viral growth by changing gene expression and genomic RNA stability. J. Virol. 87, 11684-11692.

Sulikhan, N.S., Gilbert, M., Blidchenko, E.Y., Naidenko, S.V., Ivanchuk, G.V., Gorpenchenko, T.Y., Alshinetskiy, M.V., Shevtsova, E.I., Goodrich, J.M., Lewis, J.C.M., Goncharuk, M.S., Uphyrkina, O.V., Rozhnov, V.V., Shedko, S.V., McAloose, D., Miquelle, D.G., 2018. Canine Distemper Virus in a Wild Far Eastern Leopard (Panthera Pardus Orientalis). J. Wildlife Dis. 54, 170-174.

Summers, B.A., Greisen, H.A., Appel, M.J.G., 1984. Canine distemper encephalomyelitis: variation with virus strain. J. Comp. Path. 94.

Summers, B.A., Appel, M.J.G., 1985. Syncytia formation: An aid in the diagnosis of canine distemper enchephalomyelitis. J. Comp. Path. 95, 425-435.

Suzuki, J., Nishio, Y., Kameo, Y., Terada, Y., Kuwata, R., Shimoda, H., Suzuki, K., Maeda, K., 2015. Canine distemper virus infection among wildlife before and after the epidemic. J. Vet. Med. Sci. 77, 1457-1463.

Svitek, N., Gerhauser, I., Goncalves, C., Grabski, E., Doring, M., Kalinke, U., Anderson, D.E., Cattaneo, R., von Messling, V., 2014. Morbillivirus control of the interferon response: relevance of STAT2 and mda5 but not STAT1 for canine distemper virus virulence in ferrets. J. Virol. 88, 2941-2950.

Takahashi, M., Wolf, A.M., Watari, E., Norose, Y., Ohta, S., Takahashi, H., 2013. Increased mitochondrial functions in human glioblastoma cells persistently infected with measles virus. Antiviral Res. 99, 238-244.

Takenaka, A., Sato, H., Ikeda, F., Yoneda, M., Kai, C., 2016. Infectious Progression of Canine Distemper Virus from Circulating Cerebrospinal Fluid into the Central Nervous System. J. Virol. 90, 9285-9292.

Tamura, K., Stecher, G., Peterson, D., Filipski, A., Kumar, S., 2013. MEGA6: Molecular Evolutionary Genetics Analysis version 6.0. Mol. Biol. Evol. 30, 2725-2729.

Tatsuo, H., Yusuke, Y., 2002. The Morbillivirus Receptor SLAM (CD150). Microbial Immunol. 46, 135-142.

Techangamsuwan, S., D'cundi, E.A.O., Imbschweiler, I., Gerhauser, I., Wewetzer, K., Baumgärtner, W., 2011. Cell-cell Interaction Appears to Represent a Pivotal Factor for Susceptibility of Adult Canine Schwann Cell-like Brain Glia to Canine Distemper Virus Infection in vitro. Tha.i J. Vet. Med. 41, 213-225.

Terio, K.A., Craft, M.E., 2013. Canine distemper virus (CDV) in another big cat: should CDV be renamed carnivore distemper virus? mBio 4, e00702-00713.

Terio, K.A., Craft, M.E., 2014. Canine distemper virus (CDV) in another big cat: Should CDV be renamed Carnivore Distemper Virus? . mBio 4, 1-3.

Thomson, S.A.M., Kennerrly, E., Olby, N., Mickelson, J.R., Hoffmann, D.E., Dickinson, P.J., Gibson, G., Breen, M., 2005. Microarray Analysis of Differentially Expressed Genes of Primary Tumors in the Canine Central Nervous System. Vet. Pathol. 42, 550-558.

Timm, S.F., Munson, L., Summers, B.A., Terio, K.A., Dubovi, E.J., Rupprecht, C.E., Kapil, S., Garcelon, D.K., 2009. A suspected canine distemper epidemic as the cause of a catastrophic decline in Santa Catalina Island foxes (Urocyon littoralis catalinae). J. Wildlife Dis. 45, 333-343.

Tipold, A., Vandelvelde, M., Wittek, R., Moore, P., Summerfield, A., Zurbriggen, A., 2001. Partial protection and intrathecal invasion of CD8+ T cells in acute canine distemper virus infection. Vet. Microbiol. 83, 189-203.

Tompkins, D.M., Dunn, A.M., Smith, M.J., Telfer, S., 2011. Wildlife diseases: from individuals to ecosystems. J. Anim. Ecol. 80, 19-38.

Trapnell, C., Pachter, L., Salzberg, S.L., 2009. TopHat: discovering splice junctions with RNA-Seq. Bioinformatics 25, 1105-1111.

Trapnell, C., Williams, B.A., Pertea, G., Mortazavi, A., Kwan, G., van Baren, M.J., Salzberg, S.L., Wold, B.J., Pachter, L., 2010. Transcript assembly and quantification by RNA-Seq reveals unannotated transcripts and isoform switching during cell differentiation. Nat. Biotechnol. 28, 511-515.

Trapnell, C., Roberts, A., Goff, L., Pertea, G., Kim, D., Kelley, D.R., Pimentel, H., Salzberg, S.L., Rinn, J.L., Pachter, L., 2012. Differential gene and transcript expression analysis of RNA-seq experiments with TopHat and Cufflinks. Nat. Protoc. 7, 562-578.

Tselis, A., 2011. Evidence for Viral Etiology of Multiple Sclerosis. Semin. Neurol. 31.

Ulrich, R., Imbschweiler, I., Kalkuhl, A., Lehmbecker, A., Ziege, S., Kegler, K., Becker, K., Deschl, U., Wewetzer, K., Baumgärtner, W., 2014a. Transcriptional profiling predicts overwhelming homology of Schwann cells, olfactory ensheathing cells, and Schwann cell-like glia. Glia 62, 1559-1581.

Ulrich, R., Puff, C., Wewetzer, K., Kalkuhl, A., Deschl, U., Baumgärtner, W., 2014b. Transcriptional changes in canine distemper virus-induced demyelinating leukoencephalitis favor a biphasic mode of demyelination. Plos One 9, e95917.

Van der Star, B.J., Y.S. Vogel, D., Kipp, M., Puentes, F., Baker, D., Amor, S., 2012. In Vitro and In Vivo Models of Multiple Sclerosis. CNS Neurol. Disord-DR 11, 570-588.

van Dijk, E.L., Auger, H., Jaszczyszyn, Y., Thermes, C., 2014. Ten years of next-generation sequencing technology. Trends Genet. 30, 418-426.

Van Moll, P., Alldinger, S., Baumgärtner, W., Adami, M., 1995. Distemper in wild carnivores: An epidemiological, histological and immunocytochemical study. Vet. Microbiol. 44, 193-199.

Vandevelde, M., Zurbriggen, A., 1995. The neurobiology of canine distemper virus infection. Vet. Microbiol. 44, 271-280.

Vandevelde, M., Zurbriggen, A., 2005. Demyelination in canine distemper virus infection: a review. Acta. Neuropathol. 109, 56-68.

Viana, M., Cleaveland, S., Matthiopoulos, J., Halliday, J., Packer, C., Craft, M.E., Hampson, K., 2015. Dynamics of a morbillivirus at the domestic–wildlife interface: Canine distemper virus in domestic dogs and lions. P. Natl. Acad. Sci. USA 112, 1464-1469.

Vijay, N., Poelstra, J.W., Kunstner, A., Wolf, J.B., 2013. Challenges and strategies in transcriptome assembly and differential gene expression quantification. A comprehensive in silico assessment of RNA-seq experiments. Mol. Ecol. 22, 620-634.

Vila, C., Savolainen, P., Maldonado, J.E., Amorim, I.R., Rice, J.E., Honeycutt, R.L., Crandall, K.A., Lundeberg, J., Wayne, R.K., 1997. Multiple and Ancient Origins of the Domestic Dog. Science 276, 1687-1689.

Volz, E.M., Koelle, K., Bedford, T., 2013. Viral phylodynamics. Plos Comput. Biol. 9, e1002947.

von Messling, V., Zimmer, G., Herrler, G., Haas, L., Cattaneo, R., 2001. The hemagglutinin of canine distemper virus determines tropism and cytopathogenicity. J. Virol. 75, 6418-6427.

von Messling, V., Springfeld, C., Devaux, P., Cattaneo, R., 2003. A Ferret Model of Canine Distemper Virus Virulence and Immunosuppression. J. Virol. 77, 12579-12591.

von Messling, V., Milosevic, D., Cattaneo, R., 2004. Tropism illuminated: lymphocyte-based pathways blazed by lethal morbillivirus through the host immune system. P. Natl. Acad. Sci. USA 101, 14216-14221.

von Messling, V., Oezguen, N., Zheng, Q., Vongpunsawad, S., Braun, W., Cattaneo, R., 2005. Nearby clusters of hemagglutinin residues sustain SLAM-dependent canine distemper virus entry in peripheral blood mononuclear cells. J. Virol. 79, 5857-5862.

von Messling, V., Svitek, N., Cattaneo, R., 2006. Receptor (SLAM [CD150]) recognition and the V protein sustain swift lymphocyte-based invasion of mucosal tissue and lymphatic organs by a morbillivirus. J. Virol. 80, 6084-6092.

Wahldén, L., Emanuelson, U., Møller, T., Wensman, J.J., 2018. Evaluation of Immunogenicity of a Commercially Available Live Attenuated Vaccine for Dogs Containing Canine Distemper Virus and Canine Parvovirus in African Wild Dog (Lycaon pictus pictus). Hosts and Viruses 5, 26-34.

Wang, C., Gong, B., Bushel, P.R., Thierry-Mieg, J., Thierry-Mieg, D., Xu, J., Fang, H., Hong, H., Shen, J., Su, Z., Meehan, J., Li, X., Yang, L., Li, H., Labaj, P.P., Kreil, D.P., Megherbi, D., Gaj, S., Caiment, F., van Delft, J., Kleinjans, J., Scherer, A., Devanarayan, V., Wang, J., Yang, Y., Qian, H.R., Lancashire, L.J., Bessarabova, M., Nikolsky, Y., Furlanello, C., Chierici, M., Albanese, D., Jurman, G., Riccadonna, S., Filosi, M., Visintainer, R., Zhang, K.K., Li, J., Hsieh, J.H., Svoboda, D.L., Fuscoe, J.C., Deng, Y., Shi, L., Paules, R.S., Auerbach, S.S., Tong, W., 2014. The concordance between RNA-seq and microarray data depends on chemical treatment and transcript abundance. Nat. Biotechnol. 32, 926-932.

Wang, J., Wang, J., Li, R., Liu, L., Yuan, W., 2017a. Rapid and sensitive detection of canine distemper virus by real-time reverse transcription recombinase polymerase amplification. BMC Vet. Res. 13, 241.

Wang, L., Feng, Z., Wang, X., Wang, X., Zhang, X., 2010. DEGseq: an R package for identifying differentially expressed genes from RNA-seq data. Bioinformatics 26, 136-138.

Wang, L.C., Kuo, Y.T., Chueh, L.L., Huang, D., Lin, J.H., 2017b. The detection and differentiation of canine respiratory pathogens using oligonucleotide microarrays. J. Virol. Methods 243, 131-137.

Wang, X., Ren, L., Tu, Q., Wang, J., Zhang, Y., Li, M., Liu, R., Wang, J., 2011. Magnetic protein microbead-aided indirect fluoroimmunoassay for the determination of canine virus specific antibodies. Biosens. Bioelectron. 26, 3353-3360.

Wang, Z., Gerstein, M., Snyder, M., 2009. RNA-Seq: A revolutionary tool for transcriptomics. Nat. Rev. Genet. 10.

Wayne, R.K., Ostrander, E.A., 2007. Lessons learned from the dog genome. Trends Genet. 23, 557-567.

Weckworth, J.K., 2018. Ecology, epidemiology, and evolutionary genetics of canine distemper virus spillover in African lions. ScholarWorks at University of Montana.

Weed, M.R., Gold, L.H., 2001. Paradigms for behavioural asessment of Viral pathogens. Adv. Virus Res. 56, 583-625.

Weis, S., Llenos, I.C., Dulay, J.R., Elashoff, M., Martinez-Murillo, F., Miller, C.L., 2007. Quality control for microarray analysis of human brain samples: The impact of postmortem factors, RNA characteristics, and histopathology. J. Neurosci. Methods 165, 198-209.

Wilkes, R.P., Sanchez, E., Riley, M.C., Kennedy, M.A., 2014. Real-time reverse transcription polymerase chain reaction method for detection of Canine distemper virus modified live vaccine shedding for differentiation from infection with wild-type strains. J. Vet. Diagn. Invest. 26, 27-34.

Williams, B.M., Berentsen, A.R., Shock, B.C., Teixiera, M., Dunbar, M.R., 2014a. Prevalence and diversity of *Babesia, Hepatozoon, Ehrlichia*, and *Bartonellain* wild and domestic carnivores from Zambia, Africa. Parasitol Res 113, 911-918.

Williams, D.M., Dechen Quinn, A.C., Porter, W.F., 2014b. Informing disease models with temporal and spatial contact structure among GPS-collared individuals in wild populations. Plos One 9, e84368.

Wilson, S., Siedek, E., Thomas, A., King, V., Stirling, C., Plevová, E., Salt, J., Sture, G., 2014. Influence of maternally-derived antibodies in 6-week old dogs for the efficacy of a new vaccine to protect dogs against virulent challenge with canine distemper virus, adenovirus or parvovirus. Trials in Vaccinology 3, 107-113.

Wimmer, I., Troscher, A.R., Brunner, F., Rubino, S.J., Bien, C.G., Weiner, H.L., Lassmann, H., Bauer, J., 2018. Systematic evaluation of RNA quality, microarray data reliability and pathway analysis in fresh, fresh frozen and formalin-fixed paraffin-embedded tissue samples. Sci Rep 8, 6351.

Woma, T.Y., van Vuuren, M., Bosman, A.M., Quan, M., Oosthuizen, M., 2010. Phylogenetic analysis of the haemagglutinin gene of current wild-type canine distemper viruses from South Africa: lineage Africa. Vet. Microbiol. 143, 126-132.

Woodroffe, R., Prager, K.C., Munson, L., Conrad, P.A., Dubovi, E.J., Mazet, J.A., 2012. Contact with domestic dogs increases pathogen exposure in endangered African wild dogs (Lycaon pictus). Plos One 7, e30099.

Wünschmann, A., Alldinger, S., Kremmer, E., Baumgärtner, W., 1999. Identification of CD4‡ and CD8‡ T cell subsets and B cells in the brain of dogs with spontaneous acute, subacute-, and chronic demyelinating distemper encephalitis. Vet. Immunol. Immunop. 67, 101-116.

Wünschmann, A., Kremmer, E., Baumgärtner, W., 2000. Phenotypical characterization of T and B cell areas in lymphoid tissues of dogs with spontaneous distemper. Vet. Immunol. Immunop. 73, 83-98.

Yang, D., Kim, H., Nah, J., Choi, S., Kim, J.S., Jeong, W., Song, J., 2013. Serologic Survey of Rabies Virus, Canine Distemper Virus and Parvovirus in Wild Raccoon Dogs (Nyctereutes procyonoides koreensis) in Korea. J. Bacteriol. Virol. 43, 204.

Yi, L., Cheng, S., 2015. Preparation and Identification of a Single-chain Variable Fragment Antibody Against Canine Distemper Virus. Monoclon. Antib. Immunodiagn. Immunother. 34, 228-232.

Yi, L., Cheng, Y., Zhang, M., Cao, Z., Tong, M., Wang, J., Zhao, H., Lin, P., Cheng, S., 2016. Identification of a novel canine distemper virus B-cell epitope using a monoclonal antibody against nucleocapsid protein. Virus research 213, 1-5.

Yuan, C., Liu, W., Wang, Y., Hou, J., Zhang, L., Wang, G., 2017. Homologous recombination is a force in the evolution of canine distemper virus. PLoS One 12, e0175416.

Zhang, H., Shan, F., Zhou, X., Li, B., Zhai, J.Q., Zou, S.Z., Wu, M.F., Chen, W., Zhai, S.L., Luo, M.L., 2017. Outbreak and genotyping of canine distemper virus in captive Siberian tigers and red pandas. Sci Rep 7, 8132.

Zhang, Z.H., Jhaveri, D.J., Marshall, V.M., Bauer, D.C., Edson, J., Narayanan, R.K., Robinson, G.J., Lundberg, A.E., Bartlett, P.F., Wray, N.R., Zhao, Q.Y., 2014. A comparative study of techniques for differential expression analysis on RNA-Seq data. PLoS One 9, e103207.

			Moderate severe chronic vs. controls		Mild subacute vs. controls		Moderate severe chronic vs. mild subacute	
Gene Symbol	**Gene Title**	**Ensembl**	**Fold change**	**p-value**	**Fold change**	**p-value**	**Fold change**	**p-value**
AADAC	arylacetamide deacetylase (esterase)	ENSG00000114771	-3.16	0.0167	-2.31	0.0011	-1.69	0.0030
ADCY1	adenylate cyclase 1 (brain)	ENSG00000164742	1.71	0.0317	2.01	0.0002	1.21	0.0041
CRISP1	cysteine-rich secretory protein 1	ENSG00000124812	-1.23	0.0465	-3.30	0.0023	1.53	0.0073
AFG3L1P	AFG3 ATPase family gene 3-like 1	ENSG00000223959	-1.57	0.6710	-2.12	0.0032	2.69	0.0013
ALDH1A1	aldehyde dehydrogenase 1 family, member A1	ENSG00000165092	1.32	0.0168	3.17	0.0000	2.19	0.0010
AMY2B	amylase, alpha 2B	ENSG00000240038	-1.63	0.1865	-3.72	0.3612	3.07	0.0710
ATP5G2	ATP synthase, H+ transporting, mitochondrial Fo complex, subunit C2 (subunit 9)	ENSG00000135390	3.52	0.0489	9.21	0.0342	-2.72	0.0004
AUH	AU RNA binding protein/enoyl-CoA hydratase	ENSG00000148090	2.45	0.0056	1.78	0.0046	1.82	0.0496
AZGP1	alpha-2-glycoprotein 1, zinc-binding	ENSG00000160862	-4.03	0.0075	-7.22	0.0081	2.24	0.0415
BTF3	basic transcription factor 3	ENSG00000145741	2.137	0.018	3.134	0.003	-1.087	0.001
CACNA1D	calcium channel, voltage-dependent, L type, alpha 1D subunit	ENSG00000157388	4.740	0.002	4.316	0.003	1.544	0.000
CALCB	calcitonin-related polypeptide beta	ENSG00000175868	-2.938	0.001	-2.377	0.002	7.445	0.000
CALM2	calmodulin 2 (phosphorylase kinase, delta)	ENSG00000143933	-13.388	0.007	-14.014	0.006	1.062	0.133
CAMK2B	calcium/calmodulin-dependent protein kinase II beta	ENSG00000058404	-2.740	0.002	-3.280	0.001	-1.631	0.000
CD1A	CD1a molecule	ENSG00000158477	-5.566	0.000	-6.283	0.000	-1.243	0.001
CD247	CD247 molecule	ENSG00000198821	-1.966	0.009	-2.253	0.004	-1.230	0.001
CD7	CD7 molecule	ENSG00000173762	-2.846	0.002	-2.762	0.002	-1.259	0.463
CDH18	cadherin 18, type 2	ENSG00000145526	3.249	0.002	3.522	0.002	1.079	0.740
CDKN1C	cyclin-dependent kinase inhibitor 1C (p57, Kip2)	ENSG00000129757	-2.034	0.007	-2.056	0.006	-1.375	0.136
CDR1	cerebellar degeneration-related protein 1, 34kDa	ENSG00000184258	-6.609	0.004	-9.135	0.002	-1.644	0.016
CEBPB	CCAAT/enhancer binding protein (C/EBP), beta	ENSG00000172216	-3.771	0.001	-3.308	0.001	-1.580	0.000
CETP	cholesteryl ester transfer protein, plasma	ENSG00000087237	-2.389	0.011	-2.681	0.007	1.463	0.000
CHIT1	chitinase 1 (chitotriosidase)	ENSG00000133063	3.350	0.007	2.319	0.028	1.841	0.000
COL8A1	collagen, type VIII, alpha 1	ENSG00000144810	-3.534	0.002	-4.809	0.001	1.533	0.004
COL15A1	collagen, type XV, alpha 1	ENSG00000204291	2.201	0.007	2.347	0.005	-1.344	0.000
CPE	carboxypeptidase E	ENSG00000109472	-2.450	0.004	-2.494	0.003	-1.582	0.018
CR1L	complement component (3b/4b) receptor 1-like	ENSG00000197721	-7.800	0.000	-10.664	0.000	-1.089	0.424
CRABP1	cellular retinoic acid binding protein 1	ENSG00000166426	-4.244	0.002	-5.058	0.001	-1.368	0.140
CRP	C-reactive protein, pentraxin-related	ENSG00000132693	-3.228	0.001	-2.349	0.003	-1.344	0.000
CSN1S1	casein alpha s1	ENSG00000126545	7.045	0.003	8.161	0.002	-1.624	0.002
CSNK1G3	casein kinase 1, gamma 3	ENSG00000151292	-4.667	0.000	-4.612	0.000	-1.044	0.002
CST4	cystatin S	ENSG00000101441	-3.589	0.019	-5.085	0.007	-1.363	0.000
CTBP2	C-terminal binding protein 2	ENSG00000175029	2.801	0.011	5.238	0.001	-1.027	0.052
CYP19A1	cytochrome P450, family 19, subfamily A, polypeptide 1	ENSG00000137869	21.397	0.000	13.830	0.000	-1.686	0.001
DGKA	diacylglycerol kinase, alpha 80kDa	ENSG00000065357	19.449	0.008	13.725	0.014	1.878	0.000
AKR1C1	aldo-keto reductase family 1, member C1 (dihydrodiol dehydrogenase 1; 20-alpha (3-alpha)-hydroxysteroid dehydrogenase)	ENSG00000187134	-5.387	0.017	-8.927	0.006	-1.903	0.646
AKR1C2	aldo-keto reductase family 1, member C2 (dihydrodiol dehydrogenase 2; bile acid binding protein; 3-alpha hydroxysteroid dehydrogenase, type III)	ENSG00000151632	-1.788	0.020	-2.333	0.004	-1.320	0.000
GADD45A	growth arrest and DNA-damage-inducible, alpha	ENSG00000116717	2.676	0.005	3.286	0.002	-1.037	0.973
DNASE1L2	deoxyribonuclease I-like 2	ENSG00000167968	2.980	0.025	4.157	0.009	-1.704	0.021
DPYD	dihydropyrimidine dehydrogenase	ENSG00000188641	3.193	0.002	3.964	0.001	1.834	0.000
EEF1A2	eukaryotic translation elongation factor 1 alpha 2	ENSG00000101210	-2.314	0.006	-2.142	0.010	-1.607	0.961
EVI2A	ecotropic viral integration site 2A	ENSG00000126860	-2.509	0.002	-2.488	0.002	1.135	0.000
GPC5	glypican 5	ENSG00000179399	-3.157	0.001	-3.237	0.001	-1.555	0.774
FOLR3	folate receptor 3 (gamma)	ENSG00000110203	-2.715	0.019	-3.587	0.007	-1.273	0.000

ADAM2	ADAM metallopeptidase domain 24	ENSG00000104755	3.502	0.002	2.840	0.005	-1.176	0.000
FUT2	fucosyltransferase 2 (secretor status included)	ENSG00000176920	-3.452	0.006	-3.754	0.004	4.435	0.006
GPT	glutamic-pyruvate transaminase (alanine aminotransferase)	ENSG00000167701	2.202	0.010	2.725	0.004	1.007	0.000
CXCL1	chemokine (C-X-C motif) ligand 1 (melanoma growth stimulating activity, alpha)	ENSG00000163739	2.292	0.003	3.420	0.000	-2.570	0.000
GSTM1	glutathione S-transferase mu 1	ENSG00000134184	5.143	0.002	6.163	0.001	3.082	0.000
GTF2H3	general transcription factor IIH, polypeptide 3, 34kDa	ENSG00000111358	-2.732	0.002	-2.891	0.001	2.186	0.000
HADHB	hydroxyacyl-CoA dehydrogenase/3-ketoacyl-CoA thiolase/enoyl-CoA hydratase	ENSG00000138029	-8.825	0.000	-8.145	0.000	-1.002	0.000
NRG1	neuregulin 1	ENSG00000157168	-2.086	0.006	-2.141	0.005	-1.659	0.008
HLA-A	major histocompatibility complex, class I, A	ENSG00000206503	-2.583	0.005	-3.485	0.001	1.131	0.027
HLA-DPA1	major histocompatibility complex, class II, DP alpha 1	ENSG00000231389	-4.746	0.000	-5.430	0.000	-2.276	0.004
HLA-DPB1	major histocompatibility complex, class II, DP beta 1	ENSG00000223865	-3.004	0.012	-4.391	0.003	1.132	0.613
HLA-DQA2	major histocompatibility complex, class II, DQ alpha 2	ENSG00000237541	-1.840	0.094	-4.090	0.004	1.050	0.458
NDST1	N-deacetylase/N-sulfotransferase (heparan glucosaminyl) 1	ENSG00000070614	-2.551	0.008	-3.661	0.002	-1.100	0.001
IFIT1	interferon-induced protein with tetratricopeptide repeats 1	ENSG00000185745	-2.092	0.005	-2.538	0.002	-1.074	0.029
IFNAR2	interferon (alpha, beta and omega) receptor 2	ENSG00000159110	-2.266	0.006	-2.688	0.002	1.146	0.000
IL9	interleukin 9	ENSG00000145839	-2.759	0.004	-3.695	0.001	1.607	0.000
KLRC1	killer cell lectin-like receptor subfamily C, member 1	ENSG00000134545	4.240	0.017	5.580	0.008	1.610	0.000
ITGB8	integrin, beta 8	ENSG00000105855	5.731	0.011	8.220	0.005	2.039	0.000
MB	myoglobin	ENSG00000198125	-1.918	0.008	-2.129	0.004	1.346	0.061
MECP2	methyl CpG binding protein 2	ENSG00000169057	2.586	0.007	2.556	0.007	-1.295	0.143
SCGB2A1	secretoglobin, family 2A, member 1	ENSG00000124939	-2.016	0.007	-2.401	0.002	-1.027	0.001
MGST1	microsomal glutathione S-transferase 1	ENSG00000008394	5.320	0.000	5.744	0.000	-2.103	0.001
CXCL9	chemokine (C-X-C motif) ligand 9	ENSG00000138755	6.886	0.001	6.122	0.001	-1.667	0.000
MNDA	myeloid cell nuclear differentiation antigen	ENSG00000163563	-2.997	0.007	-5.240	0.001	-1.546	0.499
MSRA	methionine sulfoxide reductase A	ENSG00000175806	14.576	0.002	20.136	0.001	-1.636	0.000
MT3	metallothionein 3	ENSG00000087250	-3.398	0.003	-4.102	0.001	-1.032	0.740
MUC3A	mucin 3A, cell surface associated	ENSG00000169894	-2.097	0.005	-2.424	0.002	3.373	0.000
NDUFA1	NADH dehydrogenase (ubiquinone) 1 alpha subcomplex, 1, 7.5kDa	ENSG00000125356	4.810	0.003	4.120	0.005	-2.268	0.046
NDUFA10	NADH dehydrogenase (ubiquinone) 1 alpha subcomplex, 10, 42kDa	ENSG00000130414	-7.074	0.008	-6.690	0.009	5.847	0.350
PABPC3	poly(A) binding protein, cytoplasmic 3	ENSG00000151846	-2.169	0.027	-3.125	0.006	-1.260	0.112
PAM	peptidylglycine alpha-amidating monooxygenase	ENSG00000145730	1.857	0.040	2.497	0.009	1.223	0.000
PCP4	Purkinje cell protein 4	ENSG00000183036	-3.302	0.002	-2.514	0.005	2.941	0.002
PDHA2	pyruvate dehydrogenase (lipoamide) alpha 2	ENSG00000163114	1.940	0.012	2.468	0.003	-1.124	0.008
ENPP2	ectonucleotide pyrophosphatase/phosphodiesterase 2	ENSG00000136960	1.864	0.092	3.357	0.009	-1.504	0.302
PDPK1	3-phosphoinositide dependent protein kinase-1	ENSG00000140992	-3.256	0.002	-4.265	0.001	-1.872	0.001
PFKFB1	6-phosphofructo-2-kinase/fructose-2,6-biphosphatase 1	ENSG00000158571	1.741	0.025	2.382	0.004	-1.741	0.001
PLD1	phospholipase D1, phosphatidylcholine-specific	ENSG00000075651	-13.663	0.014	-18.458	0.009	2.316	0.000
POLR2K	polymerase (RNA) II (DNA directed) polypeptide K, 7.0kDa	ENSG00000147669	6.062	0.000	5.700	0.000	-1.488	0.120
PPP1R1A	protein phosphatase 1, regulatory (inhibitor) subunit 1A	ENSG00000135447	-2.742	0.012	-2.968	0.009	-1.769	0.000
PPP2R5B	protein phosphatase 2, regulatory subunit B', beta	ENSG00000068971	-6.075	0.016	-7.738	0.010	1.033	0.000
MAOK11	mitogen-activated protein kinase 11	ENSG00000185386	1.921	0.013	2.317	0.004	-1.314	0.560
PTK6	PTK6 protein tyrosine kinase 6	ENSG00000101213	4.916	0.003	5.369	0.002	-2.051	0.777
RARRES1	retinoic acid receptor responder (tazarotene induced) 1	ENSG00000118849	-12.171	0.000	-13.193	0.000	-1.129	0.001
RGS13	regulator of G-protein signaling 13	ENSG00000127074	-2.142	0.005	-2.024	0.007	-2.426	0.001
RNASE2	ribonuclease, RNase A family, 2 (liver, eosinophil-derived neurotoxin)	ENSG00000169385	-2.818	0.002	-2.768	0.002	-1.278	0.737
ROBO2	roundabout, axon guidance receptor, homolog 2	ENSG00000185008	2.650	0.004	2.504	0.005	1.283	0.002
S100A1	S100 calcium binding protein A1	ENSG00000160678	-2.318	0.009	-2.259	0.010	-1.195	0.404
SAA2	serum amyloid A2	ENSG00000134339	-4.281	0.001	-4.308	0.001	-1.211	0.700

SAA3P	serum amyloid A3	ENSG00000166787	-2.020	0.012	-2.370	0.005	-2.979	0.030
SAA4	serum amyloid A4	ENSG00000148965	-4.730	0.006	-6.964	0.002	-1.663	0.000
ATXN1	ataxin 1	ENSG00000124788	-3.924	0.000	-3.844	0.000	-1.691	0.328
CCL11	chemokine (C-C motif) ligand 11	ENSG00000172156	-3.363	0.003	-2.495	0.010	-1.245	0.000
CXCL11	chemokine (C-X-C motif) ligand 11	ENSG00000169248	-2.168	0.004	-2.468	0.002	-2.406	0.007
SDC2	syndecan 2	ENSG00000169439	2.330	0.015	2.532	0.010	-1.043	0.191
SELENOP	selenoprotein P, plasma, 1	ENSG00000250722	-2.855	0.021	-3.532	0.010	2.121	0.001
ST6GAL1	ST6 beta-galactosamide alpha-2,6-sialyltransferase 1	ENSG00000073849	2.175	0.011	2.748	0.004	-1.701	0.005
ST8SIA1	ST8 alpha-N-acetyl-neuraminide alpha-2,8-sialyltransferase 1	ENSG00000111728	-2.397	0.002	-2.924	0.001	-1.152	0.640
SLC6A2	solute carrier family 6 (neurotransmitter transporter, noradrenalin), member 2	ENSG00000103546	-4.274	0.006	-3.981	0.007	1.292	0.000
SLC16A2	solute carrier family 16, member 2 (thyroid hormone transporter)	ENSG00000147100	-2.457	0.002	-2.558	0.002	1.862	0.000
SLC22A2	solute carrier family 22 (organic cation transporter), member 2	ENSG00000112499	-8.061	0.013	-10.056	0.008	1.707	0.000
SLP1	secretory leukocyte peptidase inhibitor	ENSG00000124107	-6.925	0.008	-9.979	0.004	-1.403	0.014
SMN1	survival of motor neuron 1, telomeric	ENSG00000172062	-2.354	0.004	-2.046	0.008	4.166	0.956
ST5	suppression of tumorigenicity 5	ENSG00000166444	-2.355	0.004	-2.355	0.004	1.225	0.000
STX3	syntaxin 3	ENSG00000166900	-2.496	0.004	-2.164	0.009	1.122	0.000
STXBP1	syntaxin binding protein 1	ENSG00000136854	15.021	0.001	18.566	0.001	1.760	0.000
STYX	serine/threonine/tyrosine interacting protein	ENSG00000198252	-2.863	0.035	-4.463	0.009	1.267	0.001
TCEA2	transcription elongation factor A (SII), 2	ENSG00000171703	-7.377	0.001	-6.401	0.001	-1.678	0.001
PHLDA2	pleckstrin homology-like domain, family A, member 2	ENSG00000181649	-4.385	0.001	-5.657	0.000	12.555	0.000
UBE2V2	ubiquitin-conjugating enzyme E2 variant 2	ENSG00000169139	6.745	0.001	8.832	0.000	1.425	0.250
VPREB1	pre-B lymphocyte 1	ENSG00000169575	1.986	0.015	2.311	0.006	1.351	0.000
WRB	tryptophan rich basic protein	ENSG00000182093	-4.446	0.001	-5.750	0.000	-1.523	0.024
CAVIN2	serum deprivation response	ENSG00000168497	-11.247	0.000	-11.801	0.000	1.270	0.000
APOL1	apolipoprotein L, 1	ENSG00000100342	12.244	0.000	13.705	0.000	1.020	0.002
PLA2G4C	phospholipase A2, group IVC (cytosolic, calcium-independent)	ENSG00000105499	-2.376	0.011	-2.575	0.007	1.318	0.001
NPFF	neuropeptide FF-amide peptide precursor	ENSG00000139574	-3.174	0.001	-3.027	0.001	-1.199	0.047
TNFRSF10B	tumor necrosis factor receptor superfamily, member 10b	ENSG00000120889	-2.630	0.032	-3.726	0.010	-1.815	0.000
ATP6V0E1	ATPase, H+ transporting, lysosomal 9kDa, V0 subunit e1	ENSG00000113732	2.594	0.003	3.094	0.001	1.441	0.000
MPZL1	myelin protein zero-like 1	ENSG00000197965	2.373	0.006	3.037	0.002	1.107	0.787
IL32	interleukin 32	ENSG00000008517	2.265	0.014	2.576	0.007	1.197	0.000
MED21	mediator complex subunit 21	ENSG00000152944	-12.618	0.000	-13.000	0.000	-1.931	0.000
HDAC9	histone deacetylase 9	ENSG00000048052	2.695	0.004	2.895	0.003	-1.313	0.043
BCL2L10	BCL2-like 10 (apoptosis facilitator)	ENSG00000137875	-2.942	0.002	-4.283	0.000	-1.600	0.001
PDCD7	programmed cell death 7	ENSG00000090470	-2.666	0.007	-2.618	0.008	1.038	0.001
LPAR6	lysophosphatidic acid receptor 6	ENSG00000139679	-10.110	0.000	-9.136	0.001	-1.368	0.001
MAEA	macrophage erythroblast attacher	ENSG00000090316	-2.953	0.002	-6.420	0.000	-1.258	0.310
SIRPB1	signal-regulatory protein beta 1	ENSG00000101307	-4.065	0.000	-3.398	0.001	1.254	0.000
BTN2A2	butyrophilin, subfamily 2, member A2	ENSG00000124508	-4.297	0.001	-5.671	0.000	1.554	0.012
BASP1	brain abundant, membrane attached signal protein 1	ENSG00000176788	-3.316	0.004	-2.868	0.007	-1.166	0.001
TAB1	TGF-beta activated kinase 1/MAP3K7 binding protein 1	ENSG00000100324	-3.568	0.010	-4.013	0.007	-1.368	0.008
GNLY	granulysin	ENSG00000115523	-2.844	0.001	-2.430	0.003	-1.379	0.340
MTHFS	5,10-methenyltetrahydrofolate synthetase (5-formyltetrahydrofolate cyclo-ligase)	ENSG00000136371	-6.016	0.005	-6.111	0.005	-1.124	0.743
none	trafficking protein particle complex 2 p	ENSG00000256060	3.292	0.005	4.239	0.002	-3.472	0.984
CDC42EP3	CDC42 effector protein (Rho GTPase binding) 3	ENSG00000163171	-1.881	0.018	-2.105	0.009	-1.059	0.003
ATP5L	ATP synthase, H+ transporting, mitochondrial Fo complex, subunit G	ENSG00000167283	8.281	0.000	10.892	0.000	-1.798	0.612
FTCD	formiminotransferase cyclodeaminase	ENSG00000160282	-2.130	0.021	-2.799	0.006	1.077	0.751
CFHR4	complement factor H-related 4	ENSG00000134365	-1.359	0.227	-2.681	0.006	-1.432	0.016

APLF	aprataxin and PNKP like factor	ENSG00000169621	-2.226	0.019	-2.859	0.006	-1.369	0.002
DHRS4	dehydrogenase/reductase (SDR family) member 4	ENSG00000157326	-4.883	0.020	-6.835	0.009	-1.452	0.805
GPR75	G protein-coupled receptor 75	ENSG00000119737	-1.621	0.044	-2.035	0.010	-1.127	0.000
TRIM31	tripartite motif containing 31	ENSG00000204616	6.514	0.001	5.211	0.001	-1.210	0.793
INMT	indolethylamine N-methyltransferase	ENSG00000241644	-3.462	0.013	-4.201	0.007	-1.555	0.628
MAN1B1	mannosidase, alpha, class 1B, member 1	ENSG00000177239	-3.059	0.007	-3.244	0.005	-3.733	0.000
SCN11A	sodium channel, voltage-gated, type XI, alpha subunit	ENSG00000168356	4.684	0.001	4.065	0.001	-1.133	0.001
NLGN1	neuroligin 1	ENSG00000169760	-2.859	0.002	-3.135	0.001	1.090	0.000
CARD8	caspase recruitment domain family, member 8	ENSG00000105483	2.457	0.003	1.896	0.012	-1.341	0.019
TMCC1	transmembrane and coiled-coil domain family 1	ENSG00000172765	2.127	0.012	2.340	0.007	-1.572	0.020
PDZRN3	PDZ domain containing ring finger 3	ENSG00000121440	-3.025	0.001	-2.730	0.001	1.518	0.000
MYT1L	myelin transcription factor 1-like	ENSG00000186487	-3.586	0.002	-3.608	0.001	-1.576	0.192
CDK19	cyclin-dependent kinase 19	ENSG00000155111	-1.722	0.029	-2.358	0.005	1.619	0.002
PASK	PAS domain containing serine/threonine kinase	ENSG00000115687	-1.917	0.014	-2.232	0.006	-1.613	0.106
ARC	activity-regulated cytoskeleton-associated protein	ENSG00000198576	5.241	0.011	6.676	0.006	-1.064	0.000
ITGB3BP	integrin beta 3 binding protein (beta3-endonexin)	ENSG00000142856	-3.587	0.002	-5.418	0.000	-1.371	0.012
CES3	carboxylesterase 3	ENSG00000172828	3.075	0.003	3.744	0.001	1.150	0.000
PHLDA3	pleckstrin homology-like domain, family A, member 3	ENSG00000174307	3.327	0.004	5.036	0.001	-1.046	0.152
APOL2	apolipoprotein L, 2	ENSG00000128335	5.005	0.003	6.001	0.002	-1.472	0.000
MTCH2	mitochondrial carrier 2	ENSG00000109919	2.339	0.025	4.315	0.002	1.289	0.005
ANAPC13	anaphase promoting complex subunit 13	ENSG00000129055	3.505	0.009	5.613	0.002	2.372	0.000
CNTNAP2	contactin associated protein-like 2	ENSG00000174469	6.079	0.003	5.009	0.005	-1.548	0.000
PHGDH	phosphoglycerate dehydrogenase	ENSG00000092621	3.378	0.020	4.226	0.010	1.219	0.000
SIGLEC7	sialic acid binding Ig-like lectin 7	ENSG00000168995	3.278	0.003	2.318	0.014	1.433	0.000
KCNH5	potassium voltage-gated channel, subfamily H (eag-related), member 5	ENSG00000140015	-10.999	0.001	-11.557	0.001	1.317	0.037
NAAA	N-acylethanolamine acid amidase [Source:HGNC Symbol;Acc:736]	ENSG00000138744	-5.303	0.000	-5.836	0.000	-1.371	0.000
SERP1	stress-associated endoplasmic reticulum protein 1	ENSG00000120742	18.126	0.001	18.910	0.001	1.182	0.181
BHLHE22	basic helix-loop-helix family, member e22	ENSG00000180828	3.302	0.001	4.028	0.000	-3.515	0.046
RGCC	regulator of cell cycle	ENSG00000102760	-1.766	0.124	-4.058	0.005	-1.021	0.037
CELA2B	chymotrypsin-like elastase family, member 2B	ENSG00000215704	8.364	0.000	15.211	0.000	-1.223	0.782
RNFT1	ring finger protein, transmembrane 1	ENSG00000189050	-2.396	0.037	-3.530	0.009	-1.159	0.000
SERPINA10	serpin peptidase inhibitor, clade A (alpha-1 antiproteinase, antitrypsin), member 10	ENSG00000140093	3.549	0.017	5.035	0.006	8.879	0.001
CKLF	chemokine-like factor	ENSG00000217555	1.834	0.043	2.536	0.008	1.295	0.000
GP6	glycoprotein VI (platelet)	ENSG00000088053	40.268	0.000	44.897	0.000	-2.353	0.897
IER5	immediate early response 5	ENSG00000162783	2.589	0.003	2.848	0.002	4.010	0.000
CEND1	cell cycle exit and neuronal differentiation 1	ENSG00000184524	2.053	0.007	1.746	0.020	1.058	0.001
POMP	proteasome maturation protein	ENSG00000132963	-2.266	0.006	-2.065	0.010	-1.253	0.002
NIP7	nuclear import 7 homolog	ENSG00000132603	-9.159	0.002	-8.552	0.002	1.469	0.217
MPC1	brain protein 44-like	ENSG00000060762	4.808	0.001	5.603	0.001	2.093	0.000
DNAJB11	DnaJ (Hsp40) homolog, subfamily B, member 11	ENSG00000090520	-6.606	0.002	-6.062	0.003	1.820	0.000
FTHL17	ferritin, heavy polypeptide-like 17	ENSG00000132446	-9.481	0.000	-9.150	0.000	-1.398	0.018
PCBP3	poly(rC) binding protein 3	ENSG00000183570	-6.378	0.002	-6.510	0.002	1.324	0.001
CRCT1	cysteine-rich C-terminal 1	ENSG00000169509	2.069	0.011	2.643	0.003	-2.115	0.000
LY6K	lymphocyte antigen 6 complex, locus K	ENSG00000160886	-4.484	0.000	-4.261	0.000	1.873	0.000
SAMD9	sterile alpha motif domain containing 9	ENSG00000205413	-3.381	0.002	-3.562	0.002	-1.272	0.033
UBE2R2	ubiquitin-conjugating enzyme E2R 2	ENSG00000107341	4.561	0.000	4.862	0.000	1.342	0.000
DUSP23	dual specificity phosphatase 23	ENSG00000158716	3.970	0.002	5.834	0.001	-2.343	0.000
PLEKHB2	pleckstrin homology domain containing, family B (evectins) member 2	ENSG00000115762	-2.581	0.006	-2.974	0.003	-1.565	0.616

NADSYN1	NAD synthetase 1	ENSG00000172890	-3.359	0.005	-3.623	0.003	-1.946	0.649
PNRC2	proline-rich nuclear receptor coactivator 2	ENSG00000189266	5.539	0.001	7.186	0.000	-1.249	0.288
DOK5	docking protein 5	ENSG00000101134	-4.801	0.000	-4.390	0.000	-1.006	0.195
ARHGAP15	Rho GTPase activating protein 15	ENSG00000075884	3.014	0.002	3.084	0.002	1.255	0.000
PDGFC	platelet derived growth factor C	ENSG00000145431	20.824	0.000	23.822	0.000	-1.000	0.527
NPDC1	neural proliferation, differentiation and control, 1	ENSG00000107281	-1.874	0.016	-2.173	0.007	2.000	0.000
LGALS14	lectin, galactoside-binding, soluble, 14	ENSG00000006659	13.234	0.000	12.709	0.000	-2.618	0.389
AGPAT3	1-acylglycerol-3-phosphate O-acyltransferase 3	ENSG00000160216	5.455	0.001	4.508	0.002	-1.377	0.000
CMC2	COX assembly mitochondrial protein 2 homolog	ENSG00000103121	-3.645	0.000	-4.138	0.000	1.638	0.000
PLSCR2	phospholipid scramblase 2	ENSG00000163746	-5.616	0.000	-4.786	0.000	1.020	0.029
CHMP1B	charged multivesicular body protein 1B	ENSG00000255112	5.249	0.002	5.490	0.002	1.381	0.348
ABHD6	abhydrolase domain containing 6	ENSG00000163686	2.342	0.002	2.533	0.002	-1.030	0.001
DISP3	patched domain containing 2	ENSG00000204624	1.493	0.081	2.233	0.006	1.726	0.000
CARNS1	carnosine synthase 1	ENSG00000172508	15.209	0.000	15.763	0.000	-2.220	0.002
DPP10	dipeptidyl-peptidase 10 (non-functional)	ENSG00000175497	-6.541	0.001	-7.747	0.001	-1.471	0.000
HMHB1	histocompatibility (minor) HB-1	ENSG00000158497	8.267	0.000	8.015	0.000	-1.039	0.959
CARD18	caspase recruitment domain family, member 18	ENSG00000255501	11.533	0.005	12.530	0.004	-1.698	0.000
TP53AIP1	tumor protein p53 regulated apoptosis inducing protein 1	ENSG00000120471	-3.000	0.002	-2.319	0.006	2.001	0.000
OXCT2	3-oxoacid CoA transferase 2	ENSG00000198754	-3.102	0.004	-4.446	0.001	1.430	0.000
CENPK	centromere protein K	ENSG00000123219	2.043	0.020	3.276	0.002	2.501	0.000
TFB2M	transcription factor B2, mitochondrial	ENSG00000162851	1.736	0.020	2.567	0.002	-2.415	0.000
NABP1	nucleic acid binding protein 1	ENSG00000173559	2.805	0.002	3.856	0.001	1.514	0.000
DUSP26	dual specificity phosphatase 26	ENSG00000133878	2.404	0.010	3.021	0.004	1.308	0.000
DHRS12	dehydrogenase/reductase (SDR family) member 12	ENSG00000102796	-4.719	0.004	-3.917	0.007	-1.010	0.009
MAP6D1	MAP6 domain containing 1	ENSG00000180834	4.013	0.000	4.072	0.000	-1.447	0.001
CNTD2	cyclin N-terminal domain containing 2	ENSG00000105219	-2.912	0.001	-2.859	0.001	7.313	0.447
TRPM3	transient receptor potential cation channel, subfamily M, member 3	ENSG00000083067	-3.741	0.001	-3.720	0.001	-1.295	0.287
CFHR5	complement factor H-related 5	ENSG00000134389	12.755	0.000	10.215	0.000	-1.151	0.010
SGPP1	sphingosine-1-phosphate phosphatase 1	ENSG00000126821	6.497	0.003	7.835	0.002	-1.052	0.000
LRRC3	leucine rich repeat containing 3	ENSG00000160233	-2.222	0.012	-2.330	0.010	1.652	0.000
SF3B5	splicing factor 3b, subunit 5, 10kDa	ENSG00000169976	-1.880	0.016	-2.089	0.008	1.057	0.001
DGAT2	diacylglycerol O-acyltransferase 2	ENSG00000062282	5.928	0.003	5.554	0.004	-2.781	0.003
RETNLB	resistin like beta	ENSG00000163515	-2.689	0.004	-3.072	0.002	-1.398	0.025
CAPS2	calcyphosine 2	ENSG00000180881	-2.710	0.002	-2.269	0.004	-1.314	0.845
TUBA1C	tubulin, alpha 1c	ENSG00000167553	-2.938	0.003	-2.788	0.004	-4.117	0.009
PARP10	poly (ADP-ribose) polymerase family, member 10	ENSG00000178685	7.828	0.000	6.393	0.000	1.144	0.000
ERI1	exoribonuclease 1	ENSG00000104626	3.447	0.014	4.766	0.005	4.636	0.470
DDX60L	DEAD (Asp-Glu-Ala-Asp) box polypeptide 60-like	ENSG00000181381	8.851	0.002	10.772	0.001	1.962	0.000
MYADM	myeloid-associated differentiation marker	ENSG00000179820	-7.106	0.000	-5.378	0.000	-2.130	0.000
CENPBD1	CENPB DNA-binding domains containing 1	ENSG00000177946	7.023	0.002	8.999	0.001	-1.063	0.000
TPTE2	transmembrane phosphoinositide 3-phosphatase and tensin homolog 2	ENSG00000132958	1.517	0.085	2.170	0.009	-1.072	0.769
POM121L2	POM121 transmembrane nucleoporin-like 2	ENSG00000158553	-10.567	0.005	-19.920	0.002	2.092	0.000
PHF21B	PHD finger protein 21B	ENSG00000056487	3.814	0.002	4.557	0.001	1.531	0.009
SAAL1	serum amyloid A-like 1	ENSG00000166788	-2.554	0.006	-2.938	0.003	1.057	0.231
CMTM1	CKLF-like MARVEL transmembrane domain containing 1	ENSG00000089505	-1.831	0.039	-3.208	0.003	-1.761	0.007
SLC22A9	solute carrier family 22 (organic anion transporter), member 9	ENSG00000149742	3.495	0.001	3.254	0.002	-1.701	0.005
TMEM123	transmembrane protein 123	ENSG00000152558	-3.541	0.002	-2.362	0.010	1.370	0.000
GBP4	guanylate binding protein 4	ENSG00000162654	-13.741	0.000	-10.315	0.000	-8.659	0.235

ACSM1	acyl-CoA synthetase medium-chain family member 1	ENSG00000166743	-2.661	0.003	-2.883	0.002	-1.717	0.000
TOP1MT	topoisomerase (DNA) I, mitochondrial	ENSG00000184428	10.700	0.000	11.553	0.000	1.014	0.469
SNAP47	synaptosomal-associated protein, 47kDa	ENSG00000143740	2.755	0.004	2.821	0.004	2.393	0.000
MUCL1	mucin-like 1	ENSG00000172551	9.291	0.002	4.782	0.008	1.063	0.001
IFI27L1	interferon, alpha-inducible protein 27-like 1	ENSG00000165948	-2.320	0.006	-2.459	0.004	-1.125	0.032
TDRD10	tudor domain containing 10	ENSG00000163239	2.549	0.014	2.832	0.009	-2.406	0.482
CMPK2	cytidine monophosphate (UMP-CMP) kinase 2, mitochondrial	ENSG00000134326	1.709	0.029	2.422	0.004	-1.020	0.000
DCAF8L1	DDB1 and CUL4 associated factor 8-like 1	ENSG00000226372	8.349	0.009	8.071	0.010	1.413	0.059
C2CD4A	C2 calcium-dependent domain containing 4A	ENSG00000198535	-3.157	0.004	-4.055	0.002	-1.264	0.001
SLC35G3	solute carrier family 35, member G3	ENSG00000164729	-3.723	0.005	-3.212	0.008	2.211	0.000
IGFL2	IGF-like family member 2	ENSG00000204866	-2.263	0.004	-2.175	0.005	-1.923	0.056
CDC42EP5	CDC42 effector protein (Rho GTPase binding) 5	ENSG00000167617	4.186	0.006	3.765	0.009	1.058	0.009
MGAT4D	Glycosyltransferase 54 domain-containing protein	ENSG00000205301	1.885	0.011	2.559	0.002	2.206	0.000
SLC2A7	solute carrier family 2 (facilitated glucose transporter), member 7	ENSG00000197241	4.452	0.001	6.960	0.000	-2.202	0.001
ANKRD46	ankyrin repeat domain 46	ENSG00000186106	12.552	0.005	15.817	0.003	-1.744	0.049
USP51	ubiquitin specific peptidase 51	ENSG00000247746	-4.937	0.001	-2.966	0.003	-1.123	0.000
CLEC12A	C-type lectin domain family 12, member A	ENSG00000172322	4.151	0.000	4.923	0.000	4.606	0.629
CLECL1	C-type lectin-like 1	ENSG00000184293	-3.004	0.005	-2.684	0.008	2.756	0.020
CITED4	Cbp/p300-interacting transactivator, with Glu/Asp-rich carboxy-terminal domain, 4	ENSG00000179862	4.101	0.002	4.368	0.002	-1.844	0.053
KLRC1	killer cell lectin-like receptor subfamily C, member 1	ENSG00000134545	-2.106	0.005	-2.089	0.005	-3.196	0.000
DDX53	DEAD (Asp-Glu-Ala-Asp) box polypeptide 53	ENSG00000184735	6.492	0.001	5.128	0.002	-2.782	0.103
SPIN3	spindlin family, member 3	ENSG00000204271	-5.569	0.002	-3.913	0.005	1.549	0.069
PTCRA	pre T-cell antigen receptor alpha	ENSG00000171611	-6.583	0.009	-8.198	0.005	-1.200	0.134
OXCT2P1	3-oxoacid CoA transferase 2	ENSG00000237624	-2.911	0.002	-3.008	0.001	-1.167	0.994
MLKL	mixed lineage kinase domain-like	ENSG00000168404	-2.006	0.014	-2.226	0.008	-2.122	0.001
NLRP7	NLR family, pyrin domain containing 7	ENSG00000167634	-7.030	0.000	-8.360	0.000	-1.384	0.000
PRPS1L1	phosphoribosyl pyrophosphate synthetase 1-like 1	ENSG00000229937	-2.178	0.004	-2.574	0.001	-1.440	0.494
CDHR3	cadherin-related family member 3	ENSG00000128536	-2.026	0.006	-2.115	0.004	-2.178	0.141
CADM2	cell adhesion molecule 2	ENSG00000175161	-5.785	0.000	-5.083	0.000	1.884	0.000
PCSK9	proprotein convertase subtilisin/kexin type 9	ENSG00000169174	-2.687	0.007	-2.732	0.007	-1.414	0.002
CNEP1R1	CTD nuclear envelope phosphatase 1 regulatory subunit 1	ENSG00000205423	2.179	0.044	3.777	0.005	-1.230	0.086
NPB	neuropeptide B	ENSG00000183979	-2.898	0.002	-2.963	0.002	1.905	0.000
PYDC1	PYD (pyrin domain) containing 1	ENSG00000169900	2.403	0.012	3.905	0.002	-2.227	0.000
FDCSP	follicular dendritic cell secreted protein	ENSG00000181617	2.826	0.004	2.540	0.007	1.773	0.457
DAOA	D-amino acid oxidase activator	ENSG00000182346	-4.528	0.002	-5.068	0.001	1.490	0.309
JAKMIP3	Janus kinase and microtubule interacting protein 3	ENSG00000188385	-2.789	0.001	-2.504	0.002	1.067	0.001
CES4A	carboxylesterase 4A	ENSG00000172824	-4.926	0.002	-5.221	0.001	1.878	0.000
TMEM114	transmembrane protein 114	ENSG00000232258	-4.222	0.001	-4.209	0.001	-1.802	0.000
CRIPAK	cysteine-rich PAK1 inhibitor	ENSG00000179979	-7.240	0.000	-9.642	0.000	-2.241	0.000
RNF212	ring finger protein 212	ENSG00000178222	-4.356	0.002	-5.300	0.001	-1.275	0.000
TREML4	triggering receptor expressed on myeloid cells-like 4	ENSG00000188056	3.610	0.001	4.254	0.000	-1.351	0.063
NKAIN3	Na+/K+ transporting ATPase interacting 3	ENSG00000185942	1.971	0.015	2.300	0.006	1.068	0.000
H2BFM	H2B histone family, member M	ENSG00000101812	-3.259	0.003	-4.877	0.001	-1.611	0.003
S100A7A	S100 calcium binding protein A7A	ENSG00000184330	4.922	0.004	6.005	0.002	-1.640	0.637
MS4A10	membrane-spanning 4-domains, subfamily A, member 10	ENSG00000172689	3.759	0.001	4.048	0.001	1.365	0.000
ARHGAP40	Rho GTPase activating protein 40	ENSG00000124143	16.538	0.000	18.390	0.000	-1.016	0.439
GPR148	G protein-coupled receptor 148	ENSG00000173302	8.521	0.000	5.817	0.000	-2.054	0.000
ECT2L	epithelial cell transforming sequence 2 oncogene-like	ENSG00000203734	-9.597	0.003	-10.153	0.002	-1.018	0.000

SLC10A5	solute carrier family 10 (sodium/bile acid cotransporter family), member 5	ENSG00000253598	9.778	0.000	14.201	0.000	-1.341	0.057
ADGRD2	G protein-coupled receptor 144	ENSG00000180264	-7.641	0.024	-14.558	0.008	1.684	0.001
IGFBPL1	insulin-like growth factor binding protein-like 1	ENSG00000137142	3.048	0.001	3.301	0.001	-1.235	0.583
RAB41	RAB41, member RAS oncogene family	ENSG00000147127	2.194	0.032	3.306	0.006	-1.612	0.005
TICAM2	toll-like receptor adaptor molecule 2	ENSG00000243414	-1.993	0.011	-2.211	0.006	2.090	0.472
NCR3LG1	natural killer cell cytotoxicity receptor 3 ligand 1	ENSG00000188211	13.641	0.000	17.146	0.000	4.216	0.758
PTPRQ	protein tyrosine phosphatase, receptor type, Q	ENSG00000139304	3.900	0.001	3.968	0.001	1.071	0.000
CA13	carbonic anhydrase XIII	ENSG00000185015	2.888	0.001	3.355	0.001	1.124	0.000
RNF148	ring finger protein 148	ENSG00000235631	-3.152	0.001	-2.426	0.005	1.003	0.917
CLEC2A	C-type lectin domain family 2, member A	ENSG00000188393	-2.490	0.004	-3.111	0.002	-1.820	0.023
SERPINA13P	serpin peptidase inhibitor, clade A (alpha-1 antiproteinase, antitrypsin), member 13	ENSG00000187483	4.774	0.000	5.621	0.000	2.676	0.000
C2CD4B	C2 calcium-dependent domain containing 4B	ENSG00000205502	2.139	0.014	2.819	0.004	-1.389	0.000
AATK-AS1	AATK antisense RNA 1 (non-protein coding)	ENSG00000225180	-2.623	0.001	-2.193	0.004	-1.251	0.001
GBP7	guanylate binding protein 7	ENSG00000213512	-4.200	0.001	-4.248	0.001	1.225	0.001
PLSCR5	phospholipid scramblase family, member 5	ENSG00000231213	8.410	0.001	8.589	0.001	1.632	0.000
PSMG4	proteasome (prosome, macropain) assembly chaperone 4	ENSG00000180822	-3.951	0.004	-3.516	0.006	-1.547	0.004
SAMD5	sterile alpha motif domain containing 5	ENSG00000203727	-5.061	0.000	-4.759	0.000	-1.636	0.001
FEZF1	FEZ family zinc finger 1	ENSG00000128610	-2.217	0.016	-2.432	0.010	-1.182	0.210
ACCSL	1-aminocyclopropane-1-carboxylate synthase homolog	ENSG00000205126	2.493	0.003	2.190	0.006	-1.305	0.075
C1QTNF8	C1q and tumor necrosis factor related protein 8	ENSG00000184471	-5.858	0.003	-10.924	0.001	-1.238	0.001
IGFL4	IGF-like family member 4	ENSG00000204869	2.929	0.003	2.560	0.005	-1.186	0.391
TCP10L2	t-complex 10-like 2 (mouse)	ENSG00000166984	2.652	0.011	2.805	0.008	-1.638	0.971
ACBD7	acyl-CoA binding domain containing 7	ENSG00000176244	2.624	0.011	3.451	0.004	-1.516	0.001
AARD	alanine and arginine rich domain containing protein	ENSG00000205002	-4.588	0.000	-3.272	0.001	-2.186	0.098
SDR16C6P	short chain dehydrogenase/reductase family 16C, member 6	ENSG00000253542	2.546	0.010	3.405	0.003	-2.319	0.046
ECSCR	endothelial cell surface expressed chemotaxis and apoptosis regulator	ENSG00000249751	-7.704	0.001	-6.838	0.001	-1.330	0.986
SYCE3	synaptonemal complex central element protein 3	ENSG00000217442	2.428	0.015	3.075	0.006	-1.236	0.177
S100A7L2	S100 calcium binding protein A7-like 2	ENSG00000197364	-3.719	0.007	-3.527	0.009	-1.525	0.000
NAP1L6	nucleosome assembly protein 1-like 6	ENSG00000204118	-3.175	0.008	-3.263	0.007	-1.883	0.091
HRCT1	histidine rich carboxyl terminus 1	ENSG00000196196	-2.419	0.009	-2.442	0.009	-1.312	0.075
SERPINE3	serpin peptidase inhibitor, clade E (nexin, plasminogen activator inhibitor type 1), member 3	ENSG00000253309	-2.345	0.006	-2.236	0.008	-1.953	0.177
PPP1RG3	protein phosphatase 1, regulatory subunit 3G	ENSG00000219607	3.287	0.002	4.559	0.001	-1.742	0.006
ASAH2B	N-acylsphingosine amidohydrolase (non-lysosomal ceramidase) 2B	ENSG00000204147	-4.957	0.002	-3.818	0.004	1.492	0.038
ACTR3C	ARP3 actin-related protein 3 homolog B	ENSG00000106526	-3.71	0.0188	-2.14	0.0368	3.58	0.0000
ANKDD1B	ankyrin repeat and death domain containing 1B	ENSG00000189045	-105.64	0.0301	-64.14	0.0117	16.15	0.0012
OAS2	2'-5'-oligoadenylate synthetase 2, 69/71kDa	ENSCAFG00000023107	36.46	0.0000	175.17	0.0000	-5.69	0.0001
PLA2G7	phospholipase A2, group VII (platelet-activating factor acetylhydrolase, plasma)	ENSCAFG00000002037	1.71	0.0329	2.90	0.0000	-1.70	0.0527
PNMA2	paraneoplastic Ma antigen 2	ENSCAFG00000008813	-1.07	0.8652	-2.65	0.0000	2.40	0.0017
DLA-79	MHC class Ib	ENSCAFG00000008234	9.73	0.0015	37.21	0.0000	-4.04	0.0254
CD274	CD274 molecule	ENSCAFG00000002120	1.44	0.1618	3.75	0.0000	-2.71	0.0098
GPNMB	glycoprotein (transmembrane) nmb	ENSCAFG00000002753	2.87	0.2114	23.12	0.0000	-8.15	0.0071
NSMCE4A	non-SMC element 4 homolog A (S. cerevisiae)	ENSCAFG00000012419	1.59	0.1227	2.03	0.0000	-1.66	0.0206
GPR65	G protein-coupled receptor 65	ENSCAFG00000017342	3.38	0.0111	6.31	0.0000	-1.85	0.2562
LOC100688660	microtubule-associated protein 9-like	---	-1.61	0.0668	-2.23	0.0001	1.96	0.0030
FTL	ferritin, light polypeptide	ENSCAFG00000003861 /	1.47	0.0736	2.22	0.0000	-1.51	0.0802
SLC6A12	solute carrier family 6 (neurotransmitter transporter, betaine/GABA), member 12	ENSCAFG00000015756	-1.27	0.6282	-5.12	0.0000	3.90	0.0005
STAT1 /// STAT4	signal transducer and activator of transcription 1, 91kDa /// signal transducer and activator of transcription 4	ENSCAFG00000009797	7.34	0.0000	20.15	0.0000	-2.84	0.0000
LOC100688091	uncharacterized LOC100688091	---	1.37	0.0423	2.31	0.0000	-1.47	0.0771

ACSBG1	acyl-CoA synthetase bubblegum family member 1	ENSCAFG00000014189	-1.81	0.0722	-3.76	0.0000	2.22	0.0192
RSAD2	radical S-adenosyl methionine domain containing 2	ENSCAFG00000003293	2.97	0.0075	25.01	0.0000	-8.12	0.0001
HERC6	HECT and RLD domain containing E3 ubiquitin protein ligase family member 6	ENSCAFG00000009781	12.06	0.0000	43.30	0.0000	-4.03	0.0000
DDX60	DEAD (Asp-Glu-Ala-Asp) box polypeptide 60	ENSCAFG00000009003	30.91	0.0000	40.15	0.0000	-1.95	0.3003
TIMP1	TIMP metallopeptidase inhibitor 1	ENSCAFG00000015155	19.15	0.0000	16.87	0.0000	1.51	0.6783
LGI2	leucine-rich repeat LGI family, member 2	ENSCAFG00000016480	-1.77	0.0279	-2.65	0.0001	1.50	0.2285
C4H10orf57	chromosome 4 open reading frame, human C10orf57	ENSCAFG00000015748	-1.16	0.4637	-2.34	0.0000	2.21	0.0024
CPED1	cadherin-like and PC-esterase domain containing 1	ENSCAFG00000003492	2.84	0.0001	1.62	0.0117	1.76	0.0182
ETV6	ets variant 6	ENSCAFG00000013371	3.07	0.0001	2.73	0.0000	1.31	0.5085
CXCL16	chemokine (C-X-C motif) ligand 16	ENSCAFG00000015892	4.04	0.0075	7.77	0.0000	-2.07	0.3714
ATP1A2	ATPase, Na+/K+ transporting, alpha 2 polypeptide	ENSCAFG00000012174	-3.64	0.0001	-2.33	0.0011	-1.64	0.1264
PNISR	PNN-interacting serine/arginine-rich protein	ENSCAFG00000003471	1.28	0.0776	2.44	0.0000	-1.90	0.0002
IDO1	indoleamine 2,3-dioxygenase 1	ENSCAFG00000005750	30.64	0.0000	64.12	0.0000	-2.46	0.0496
LY86	lymphocyte antigen 86	ENSCAFG00000009516	3.25	0.0730	10.01	0.0000	-3.33	0.0600
PCSK7	proprotein convertase subtilisin/kexin type 7	ENSCAFG00000013143	-2.05	0.0007	-1.60	0.0040	-1.29	0.2055
ADCY5	adenylate cyclase 5	---	-1.06	0.6710	-2.36	0.0000	2.56	0.0013
PTPRC	protein tyrosine phosphatase, receptor type, C	ENSCAFG00000011265	4.03	0.0016	3.74	0.0003	1.17	0.8200
APOF	apolipoprotein F	---	1.70	0.0145	2.64	0.0000	-1.73	0.0290
TAPBP	TAP binding protein (tapasin)	ENSCAFG00000000972	2.52	0.0013	8.33	0.0000	-4.78	0.0000
IGSF6	immunoglobulin superfamily, member 6	ENSCAFG00000017712	2.26	0.0904	5.76	0.0002	-2.28	0.1444
BIN2	bridging integrator 2	---	5.14	0.0004	3.89	0.0002	1.47	0.4982
none	none	---	141.17	0.0000	-1.17	0.6276	181.20	0.0000
EPAS1	endothelial PAS domain protein 1	---	-1.63	0.0257	-2.32	0.0001	1.34	0.2640
EMP3	epithelial membrane protein 3	ENSCAFG00000004034	5.05	0.0000	2.57	0.0005	1.90	0.0896
LOC100685792	interferon-activable protein 203-like	---	14.98	0.0000	15.29	0.0000	1.08	0.8363
GBP1	guanylate binding protein 1, interferon-inducible	ENSCAFG00000020204	55.46	0.0000	88.71	0.0000	-2.02	0.2641
SLC11A1	solute carrier family 11 (proton-coupled divalent metal ion transporters), member 1	---	5.02	0.0003	7.78	0.0000	-1.59	0.2796
PSAP	prosaposin	---	1.98	0.0004	1.91	0.0001	1.02	0.6277
SDC4	syndecan 4	---	2.32	0.0075	2.76	0.0001	-1.58	0.5659
none	none	ENSCAFG00000006557	25.01	0.0000	113.65	0.0000	-4.89	0.0001
IL10RB /// LOC10(	interleukin 10 receptor, beta /// interleukin-10 receptor subunit beta-like	ENSCAFG00000009071	2.04	0.0117	2.91	0.0000	-1.57	0.1376
BRCA2	breast cancer 2, early onset	ENSCAFG00000006383	2.17	0.0058	3.55	0.0000	-1.63	0.0940
PDPN	podoplanin	ENSCAFG00000016363	5.07	0.0007	5.39	0.0000	-1.12	0.8150
ADCY2	adenylate cyclase 2 (brain)	ENSCAFG00000010238	-1.53	0.1132	-3.04	0.0000	2.07	0.0084
OPTN	optineurin	ENSCAFG00000004769	1.55	0.0034	2.05	0.0000	-1.22	0.0849
TOMM34	translocase of outer mitochondrial membrane 34	ENSCAFG00000009591	-1.13	0.4289	-2.11	0.0000	1.86	0.0027
CTSZ	cathepsin Z	ENSCAFG00000012183	2.44	0.0001	1.93	0.0014	1.32	0.2237
CD180	CD180 molecule	ENSCAFG00000007594	2.07	0.0716	3.54	0.0003	-1.72	0.2141
PPM1M	protein phosphatase, Mg2+/Mn2+ dependent, 1M	---	2.30	0.0000	1.71	0.0004	1.36	0.1042
IGFBP4	insulin-like growth factor binding protein 4	---	2.02	0.0175	2.95	0.0000	-1.52	0.1573
LOC100856619	gamma-aminobutyric acid receptor subunit gamma-1-like	ENSCAFG00000001878	-3.57	0.0033	-3.75	0.0002	1.07	0.9003
EPB41L1	erythrocyte membrane protein band 4.1-like 1	---	-1.41	0.0713	-2.02	0.0000	1.46	0.0646
PARP14	poly (ADP-ribose) polymerase family, member 14	ENSCAFG00000011970	37.18	0.0000	68.18	0.0000	-1.83	0.1526
BATF	basic leucine zipper transcription factor, ATF-like	ENSCAFG00000017044	1.71	0.1087	3.39	0.0000	-2.05	0.0500
CHST10	carbohydrate sulfotransferase 10	ENSCAFG00000002235	-1.02	0.9278	-2.23	0.0001	2.18	0.0039
CD44	CD44 molecule (Indian blood group)	---	7.29	0.0001	5.07	0.0001	1.44	0.4567
CAV1	caveolin 1, caveolae protein, 22kDa	ENSCAFG00000003404	3.54	0.0003	2.30	0.0013	1.50	0.1941
HLA-DMB	major histocompatibility complex, class II, DM beta	ENSCAFG00000000844	4.91	0.0040	5.91	0.0001	-1.33	0.5254

S100P	S100 calcium binding protein P	ENSCAFG00000014333	1.36	0.3998	9.31	0.0000	-6.88	0.0000
LOC100855560	probable ATP-dependent RNA helicase DDX58-like	ENSCAFG00000001807	13.98	0.0000	44.11	0.0000	-3.78	0.0014
IL4I1	interleukin 4 induced 1	ENSCAFG00000003439	2.61	0.0047	3.55	0.0000	-1.36	0.3685
PAQR6	progestin and adipoQ receptor family member VI	ENSCAFG00000016844	-1.46	0.1935	-3.01	0.0000	2.07	0.0271
ARHGAP32	Rho GTPase activating protein 32	ENSCAFG00000010235	-1.59	0.0045	-2.23	0.0000	1.40	0.0461
FBXO2	F-box protein 2	ENSCAFG00000016590	-1.33	0.2066	-2.04	0.0003	1.53	0.0869
CSTB	cystatin B (stefin B)	---	2.24	0.0005	2.48	0.0000	-1.17	0.5015
PSMB9	proteasome (prosome, macropain) subunit, beta type, 9 (large multifunctional peptidase 2)	ENSCAFG00000000836	6.20	0.0000	11.61	0.0000	-1.87	0.0712
APOC1	apolipoprotein C-I	ENSCAFG00000004615	5.33	0.0027	17.27	0.0000	-4.34	0.0197
LGALS9	lectin, galactoside-binding, soluble, 9	ENSCAFG00000018641	7.23	0.0000	10.25	0.0000	-5.57	0.0001
LOC482088	WD repeat-containing protein KIAA1875-like	ENSCAFG00000001540	-2.52	0.0022	-2.21	0.0009	-1.14	0.6620
LTBP1	latent transforming growth factor beta binding protein 1	ENSCAFG00000005843	7.44	0.0001	2.59	0.0067	2.96	0.0246
SLC25A37	solute carrier family 25 (mitochondrial iron transporter), member 37	---	2.05	0.0018	2.00	0.0002	1.03	0.9069
SLC7A7	solute carrier family 7 (amino acid transporter light chain, y+L system), member 7	ENSCAFG00000011177	1.80	0.0433	3.10	0.0001	-1.55	0.1625
PI3	peptidase inhibitor 3, skin-derived	ENSCAFG00000009641	34.35	0.0000	43.32	0.0000	-1.26	0.7311
PDLIM4	PDZ and LIM domain 4	ENSCAFG00000000830	1.87	0.0053	2.08	0.0001	-1.11	0.6441
ERAP1	endoplasmic reticulum aminopeptidase 1	ENSCAFG00000007810	2.11	0.0011	2.57	0.0000	-1.22	0.3794
TNFRSF1A	tumor necrosis factor receptor superfamily, member 1A	---	2.35	0.0122	3.45	0.0001	-1.37	0.3691
CTTNBP2	cortactin binding protein 2	ENSCAFG00000003432	-1.59	0.0162	-2.05	0.0000	1.29	0.2087
LOC100856288 //	serine/threonine-protein kinase 19-like /// serine/threonine-protein kinase 19-like	ENSCAFG00000000695	2.23	0.0305	2.67	0.0004	-1.48	0.1014
LOC612135	Similar to Ig lambda chain V region 4A precursor	ENSCAFG00000023285 /	58.79	0.0000	-1.01	0.9720	59.58	0.0000
RARRES3	retinoic acid receptor responder (tazarotene induced) 3	ENSCAFG00000015087	55.02	0.0000	68.07	0.0000	-1.37	0.7162
PLEKHB1	pleckstrin homology domain containing, family B (evectins) member 1	ENSCAFG00000005594	-1.08	0.8319	-3.59	0.0001	3.33	0.0042
SIPA1L2	signal-induced proliferation-associated 1 like 2	ENSCAFG00000011665	-1.52	0.2625	-3.85	0.0001	2.53	0.0290
IFIT5	interferon-induced protein with tetratricopeptide repeats 5	ENSCAFG00000007151	1.92	0.0267	4.27	0.0000	-2.35	0.0052
XDH	xanthine dehydrogenase	ENSCAFG00000005609	2.50	0.0110	6.24	0.0000	-2.50	0.0192
PARP12	poly (ADP-ribose) polymerase family, member 12	ENSCAFG00000003997	5.12	0.0001	11.71	0.0000	-2.30	0.0461
FAM26F	family with sequence similarity 26, member F	ENSCAFG00000023345	1.65	0.0049	2.19	0.0000	-1.32	0.1270
SLC1A2	solute carrier family 1 (glial high affinity glutamate transporter), member 2	ENSCAFG00000006881	-2.09	0.0122	-2.79	0.0001	1.34	0.3381
TPM4	tropomyosin alpha-4 chain-like	---	2.09	0.0004	1.59	0.0027	1.32	0.1748
ANXA1	annexin A1	ENSCAFG00000001778	5.13	0.0000	3.86	0.0000	1.36	0.2992
PSMB10	proteasome (prosome, macropain) subunit, beta type, 10	ENSCAFG00000020333	5.27	0.0000	8.05	0.0000	-1.97	0.1407
none	none	---	-2.57	0.0001	-1.91	0.0003	-1.35	0.1764
CASP4	caspase 4, apoptosis-related cysteine peptidase	ENSCAFG00000014860	2.33	0.1768	12.88	0.0000	-5.52	0.0171
SAA1	serum amyloid A1	ENSCAFG00000009135	21.92	0.0003	18.47	0.0000	-2.20	0.1470
GFAP	glial fibrillary acidic protein	ENSCAFG00000013973	2.32	0.0015	1.89	0.0019	1.23	0.4355
DPP4	dipeptidyl-peptidase 4	---	3.15	0.0001	1.60	0.0194	1.97	0.0175
BTK	Bruton agammaglobulinemia tyrosine kinase	---	4.44	0.0000	2.67	0.0000	1.55	0.1234
LGALS3	lectin, galactoside-binding, soluble, 3	ENSCAFG00000015013	11.70	0.0000	4.72	0.0001	2.41	0.0662
TRIM21	tripartite motif containing 21	ENSCAFG00000006025	8.28	0.0000	41.94	0.0000	-5.10	0.0001
SERTAD1	SERTA domain containing 1	ENSCAFG00000005345	1.36	0.1643	2.22	0.0001	-1.62	0.0484
GBP7	guanylate binding protein 7	ENSCAFG00000020200	19.44	0.0000	27.36	0.0000	-1.30	0.4789
CD59	CD59 molecule, complement regulatory protein	ENSCAFG00000007187	3.36	0.0000	1.92	0.0007	1.75	0.0272
NR4A1	nuclear receptor subfamily 4, group A, member 1	ENSCAFG00000007338	-6.20	0.0091	-11.04	0.0000	1.78	0.3805
PSME1	proteasome (prosome, macropain) activator subunit 1 (PA28 alpha)	ENSCAFG00000011924	2.15	0.0002	3.73	0.0000	-1.86	0.0047
TMEM140	transmembrane protein 140-like	ENSCAFG00000003179	-1.01	0.9219	2.00	0.0000	-2.02	0.0000
RTP4	receptor (chemosensory) transporter protein 4	ENSCAFG00000013889	9.71	0.0000	27.91	0.0000	-3.08	0.0271
LOC100855689	spindlin-2B-like	ENSCAFG00000016514	1.08	0.7675	2.44	0.0001	-2.26	0.0070

LOC100856270	low affinity immunoglobulin gamma Fc region receptor II-b-like	ENSCAFG00000013035	12.97	0.0001	21.88	0.0000	-1.69	0.4064
CDKN1A	Cyclin-dependent kinase inhibitor 1A (p21, Cip1)	---	3.13	0.0032	4.64	0.0000	-1.49	0.1789
CD3D	CD3d molecule, delta (CD3-TCR complex)	ENSCAFG00000012791	23.23	0.0000	1.73	0.0385	13.57	0.0000
LOC100856329	perilipin-2-like	---	2.28	0.0032	2.41	0.0001	-1.68	0.0154
THBS1	thrombospondin 1	---	3.56	0.0002	4.73	0.0000	-1.49	0.2238
SNX13	sorting nexin 13	ENSCAFG00000002467	2.07	0.0000	-1.02	0.8441	2.11	0.0000
GADD45B	growth arrest and DNA-damage-inducible, beta	---	5.95	0.0001	11.41	0.0000	-1.92	0.1396
HLA-DQA1	major histocompatibility complex, class II, DQ alpha 1	ENSCAFG00000000812	16.93	0.0004	30.97	0.0000	-1.73	0.4756
none	none	---	1.18	0.7562	7.63	0.0001	-6.23	0.0056
CLIC2	chloride intracellular channel 2	---	11.43	0.0000	12.60	0.0000	-1.10	0.8562
SAT1	spermidine/spermine N1-acetyltransferase 1	ENSCAFG00000024917	2.03	0.0028	2.01	0.0003	1.01	0.9597
LOC612054 /// LC	uncharacterized LOC612054 /// ig lambda chain V-I region BL2-like	---	82.38	0.0000	-1.11	0.7440	89.65	0.0000
RAB20	RAB20, member RAS oncogene family	---	5.00	0.0006	6.01	0.0000	-2.12	0.6580
SMNDC1	survival motor neuron domain containing 1	ENSCAFG00000010720	1.03	0.8564	2.07	0.0000	-2.01	0.0010
BIRC3	baculoviral IAP repeat containing 3	ENSCAFG00000015105	20.82	0.0000	21.10	0.0000	-1.01	0.9769
RGS1	regulator of G-protein signaling 1	---	11.46	0.0001	10.15	0.0000	1.20	0.7600
TLR2	toll-like receptor 2	ENSCAFG00000008351	4.52	0.0004	2.84	0.0012	1.59	0.2596
CCR5	chemokine (C-C motif) receptor 5 (gene/pseudogene)	---	9.67	0.0000	4.67	0.0002	2.07	0.1528
MSN	moesin	---	4.31	0.0001	2.73	0.0003	1.58	0.1888
SLC44A1	solute carrier family 44, member 1	ENSCAFG00000002758	1.08	0.6778	2.30	0.0001	-2.01	0.0098
BAZ1A	bromodomain adjacent to zinc finger domain, 1A	ENSCAFG00000013302	2.18	0.0009	1.81	0.0010	1.20	0.4169
IFI35	interferon-induced protein 35	ENSCAFG00000014624	9.39	0.0000	17.19	0.0000	-2.49	0.0253
DMGDH	dimethylglycine dehydrogenase	ENSCAFG00000009138	-3.20	0.0026	-3.14	0.0001	1.08	0.8207
LOC612180	ig lambda chain V-I region BL2-like	ENSCAFG00000015393	2.71	0.0000	1.00	1.0000	2.73	0.0001
LTBR	lymphotoxin beta receptor (TNFR superfamily, member 3)	---	1.97	0.0033	2.10	0.0001	-1.07	0.7735
MAPK1	mitogen-activated protein kinase 1	---	6.94	0.0000	1.60	0.0333	4.34	0.0000
LOC100855594 //	uncharacterized LOC100855594 /// uncharacterized LOC100855788 /// uncharacterized LOC608320 /// uncharacterized LOC612054 /// uncharacterized LOC612122	---	157.36	0.0000	-1.01	0.9717	157.85	0.0000
ELOVL2	ELOVL fatty acid elongase 2	---	-1.13	0.5998	-2.29	0.0001	2.02	0.0101
NFKBIA	nuclear factor of kappa light polypeptide gene enhancer in B-cells inhibitor, alpha	ENSCAFG00000013418	1.44	0.0750	2.42	0.0000	-1.67	0.0255
LOC100855783	kinesin-like protein KIF1A-like	ENSCAFG00000012713	-2.08	0.0007	-1.79	0.0006	-1.16	0.4714
NR1H3	nuclear receptor subfamily 1, group H, member 3	ENSCAFG00000008824	2.88	0.0001	3.53	0.0000	-1.23	0.3994
LOC100685792	interferon-activable protein 203-like	---	15.43	0.0000	19.31	0.0000	1.31	0.5031
BCAN	brevican	ENSCAFG00000016712	-2.64	0.0001	-2.72	0.0000	1.03	0.8932
SERPING1	serpin peptidase inhibitor, clade G (C1 inhibitor), member 1	ENSCAFG00000007838	5.88	0.0005	11.82	0.0000	-2.01	0.1633
none	none	ENSCAFG00000023623	23.63	0.0002	1.31	0.6229	18.01	0.0010
UBA7	ubiquitin-like modifier activating enzyme 7	ENSCAFG00000011164	17.52	0.0000	55.11	0.0000	-4.11	0.0020
CCL19	chemokine (C-C motif) ligand 19	ENSCAFG00000001954	4.20	0.0145	8.43	0.0000	-2.00	0.2555
LOC607010 /// LC	Similar to Ig heavy chain V-III region VH26 precursor /// Similar to Ig heavy chain V-III region VH26 precursor /// Similar to Ig heavy chain V-III region VH26 precursor	ENSCAFG00000025006	11.81	0.0000	-1.03	0.9200	12.20	0.0000
LOC100855488	peroxisomal acyl-coenzyme A oxidase 2-like	ENSCAFG00000007261	1.78	0.1493	4.88	0.0000	-2.74	0.0266
MYOF	myoferlin	ENSCAFG00000007749	2.98	0.0046	3.19	0.0003	-1.07	0.8544
CD2	CD2 molecule	ENSCAFG00000009829	9.85	0.0005	13.86	0.0000	-1.41	0.5872
ACHE	acetylcholinesterase	ENSCAFG00000014054	-1.47	0.1304	-2.64	0.0000	1.80	0.0384
EIF2AK2	eukaryotic translation initiation factor 2-alpha kinase 2	ENSCAFG00000006051	6.90	0.0000	15.62	0.0000	-2.27	0.0175
LOC100856638 //	uridine phosphorylase 1-like /// uridine phosphorylase 1	ENSCAFG00000014262	8.07	0.0000	19.16	0.0000	-2.88	0.0117
SP100	SP100 nuclear antigen	ENSCAFG00000010717	6.84	0.0000	6.37	0.0000	1.07	0.8413
TLR1	toll-like receptor 1	ENSCAFG00000024010	1.84	0.1590	4.54	0.0001	-2.47	0.0604
FAM184B	family with sequence similarity 184, member B	ENSCAFG00000015078	-1.73	0.0081	-2.30	0.0000	1.33	0.1796

TCIRG1	T-cell, immune regulator 1, ATPase, H+ transporting, lysosomal V0 subunit A3	ENSCAFG00000010972	2.36	0.0006	2.92	0.0000	-1.26	0.4142
SELL	selectin L	ENSCAFG00000015177	6.13	0.0001	4.36	0.0000	1.41	0.4191
FERMT3	fermitin family member 3	ENSCAFG00000014609	6.38	0.0001	3.63	0.0003	1.75	0.2080
C1S	complement component 1, s subcomponent	ENSCAFG00000014346	9.20	0.0000	13.31	0.0000	-1.69	0.1417
PSMB8	proteasome (prosome, macropain) subunit, beta type, 8 (large multifunctional peptidase 7)	ENSCAFG00000000829	21.20	0.0000	45.76	0.0000	-2.81	0.0168
TAPBPL	TAP binding protein-like	ENSCAFG00000015143	2.90	0.0014	2.94	0.0001	-1.01	0.9738
none	none	---	-1.80	0.0202	-2.55	0.0000	1.42	0.1862
ARPC1B	actin related protein 2/3 complex, subunit 1B, 41kDa	ENSCAFG00000015081	2.39	0.0030	2.65	0.0001	-1.11	0.7182
TBCD	tubulin folding cofactor D	ENSCAFG00000013063	-1.11	0.6591	-2.36	0.0001	2.12	0.0065
EDEM1	ER degradation enhancer, mannosidase alpha-like 1	ENSCAFG00000005608	3.26	0.0000	-1.00	0.9836	3.27	0.0001
GDPD2	glycerophosphodiester phosphodiesterase domain containing 2	ENSCAFG00000016850	-2.45	0.0021	-2.10	0.0012	-1.17	0.5920
LOC100856330	transcription factor EC-like	---	8.74	0.0000	8.62	0.0000	1.01	0.9767
BAZ2B	bromodomain adjacent to zinc finger domain, 2B	---	1.14	0.4672	2.00	0.0000	-1.76	0.0066
XAF1	XIAP associated factor 1	---	16.69	0.0000	30.82	0.0000	-1.85	0.1354
FTL	ferritin, light polypeptide	---	2.13	0.0026	2.43	0.0000	-1.14	0.6098
LOC480493 /// LC	leucine-rich repeat-containing protein 37A3-like /// leucine-rich repeat-containing protein 37A2-like /// leucine rich repeat containing 37, member A2	ENSCAFG00000013742	2.31	0.1460	-9.49	0.0002	15.13	0.0002
GBP5	guanylate binding protein 5	ENSCAFG00000024540	6.28	0.0034	9.20	0.0000	-1.46	0.5437
RNF213	ring finger protein 213	ENSCAFG00000005675	5.04	0.0000	23.30	0.0000	-4.62	0.0000
BCL2L2 /// PABPN	BCL2-like 2 /// poly(A) binding protein, nuclear 1	ENSCAFG00000011482	-1.25	0.2319	-2.08	0.0000	1.67	0.0154
UBE2L6	ubiquitin-conjugating enzyme E2L 6	ENSCAFG00000007839	7.76	0.0000	21.99	0.0000	-2.84	0.0029
LOC612054	uncharacterized LOC612054	ENSCAFG00000015568 /	91.80	0.0000	1.17	0.6453	78.57	0.0000
C2 /// CFB	complement component 2 /// complement factor B	ENSCAFG00000000686	13.75	0.0000	16.61	0.0000	-1.60	0.1380
DLA-12 /// DLA-64	MHC class I DLA-12 /// MHC class I DLA-64	ENSCAFG00000000500	18.07	0.0000	37.51	0.0000	-2.15	0.0247
LOC492092	A-kinase anchor protein 17B-like	ENSCAFG00000018374	-1.48	0.1774	-3.35	0.0000	2.26	0.0147
none	none	ENSCAFG00000012303	2.17	0.0001	2.06	0.0000	1.06	0.7570
none	none	ENSCAFG00000012003	3.81	0.0092	6.67	0.0000	-1.75	0.2910
IRGM /// LOC481	immunity-related GTPase family M protein 1-like /// interferon-inducible GTPase 1-like	ENSCAFG00000000502	67.74	0.0000	170.24	0.0000	-2.51	0.0258
TTLL7	tubulin tyrosine ligase-like family, member 7	ENSCAFG00000020321	1.48	0.1013	-3.42	0.0000	5.06	0.0000
CTSH	cathepsin H	ENSCAFG00000014076	4.23	0.0001	8.61	0.0000	-3.06	0.0257
IFIT1	interferon-induced protein with tetratricopeptide repeats 1	ENSCAFG00000009617	47.07	0.0000	179.05	0.0000	-3.80	0.0222
PLGRKT	plasminogen receptor, C-terminal lysine transmembrane protein	ENSCAFG00000002116	2.69	0.0029	2.50	0.0006	1.08	0.8211
RPL36AL	ribosomal protein L36a-like	---	1.93	0.0199	3.18	0.0000	-1.65	0.0974
ICAM1	intercellular adhesion molecule 1	---	11.31	0.0000	19.72	0.0000	-1.74	0.2591
DTX3L	deltex 3-like (Drosophila)	ENSCAFG00000011948	12.59	0.0000	35.94	0.0000	-4.02	0.0008
APLP1	amyloid beta (A4) precursor-like protein 1	---	-1.13	0.5191	-2.11	0.0000	1.86	0.0066
LRRC25	leucine rich repeat containing 25	ENSCAFG00000014879	1.40	0.2824	3.08	0.0001	-2.20	0.0284
GRN	granulin	ENSCAFG00000014165	1.73	0.0420	2.54	0.0001	-1.46	0.1881
C1QC	complement component 1, q subcomponent, C chain	---	3.95	0.0323	17.78	0.0000	-8.52	0.0160
MAP3K13	mitogen-activated protein kinase kinase kinase 13	ENSCAFG00000013230	-2.44	0.0014	-2.18	0.0005	-1.12	0.6722
SP140	SP140 nuclear body protein	ENSCAFG00000010704	3.52	0.0001	8.62	0.0000	-2.45	0.0054
NCKAP1L	NCK-associated protein 1-like	ENSCAFG00000006413	4.49	0.0005	3.72	0.0001	1.21	0.6504
IFI44	interferon-induced protein 44	ENSCAFG00000020342	23.72	0.0000	78.05	0.0000	-3.29	0.0022
APOL5	apolipoprotein L, 5	ENSCAFG00000023063	2.04	0.0078	2.59	0.0000	-1.27	0.3811
C25H13orf33	chromosome 25 open reading frame, human C13orf33	ENSCAFG00000006579	6.61	0.0003	5.40	0.0001	1.22	0.6820
MORC3	MORC family CW-type zinc finger 3	ENSCAFG00000009660	1.34	0.1008	2.38	0.0000	-1.78	0.0048
LOC491492	Similar to Ig kappa chain V-II region RPMI 6410 precursor	ENSCAFG00000007351	188.09	0.0000	-1.03	0.9112	194.17	0.0000
FTSJD2 /// RNF8	FtsJ methyltransferase domain containing 2 /// ring finger protein 8, E3 ubiquitin protein ligase	ENSCAFG00000001477	1.69	0.0057	2.75	0.0000	-1.63	0.0171
TXNDC5	thioredoxin domain containing 5 (endoplasmic reticulum)	ENSCAFG00000009582	2.47	0.0000	-1.16	0.3232	2.70	0.0000

TRIM22	tripartite motif containing 22	ENSCAFG00000024867	8.33	0.0001	10.59	0.0000	-1.27	0.6415
HLA-DOB	major histocompatibility complex, class II, DO beta	ENSCAFG00000000819	1.07	0.7513	2.46	0.0000	-2.31	0.0008
NR4A2	nuclear receptor subfamily 4, group A, member 2	ENSCAFG00000009209	-6.47	0.0017	-9.01	0.0000	1.39	0.5710
TRAF3IP3	TRAF3 interacting protein 3	ENSCAFG00000011943	4.87	0.0000	1.71	0.0233	3.24	0.0002
CLEC2D	C-type lectin domain family 2, member D	ENSCAFG00000013605	8.71	0.0000	1.01	0.9653	8.64	0.0000
LOC100686179	midkine-like	ENSCAFG00000025124	1.65	0.0062	2.03	0.0000	-1.23	0.2589
C3	complement component 3	ENSCAFG00000018625	4.93	0.0000	3.19	0.0000	1.74	0.2164
SLC7A10	solute carrier family 7 (neutral amino acid transporter light chain, asc system), member 10	ENSCAFG00000007422	-2.96	0.0029	-4.92	0.0000	1.60	0.2013
PTGS2	prostaglandin-endoperoxide synthase 2 (prostaglandin G/H synthase and cyclooxygenase)	ENSCAFG00000013762	3.80	0.0217	4.95	0.0009	-1.30	0.6613
FAM111A	family with sequence similarity 111, member A	ENSCAFG00000007655	3.40	0.0001	1.71	0.0168	1.99	0.0296
TRPM3	transient receptor potential cation channel, subfamily M, member 3	---	-2.81	0.0002	-2.84	0.0000	-1.31	0.3078
MSR1	macrophage scavenger receptor 1	ENSCAFG00000006830	3.57	0.0207	9.60	0.0000	-2.69	0.0910
OAS1	2'-5'-oligoadenylate synthetase 1, 40/46kDa	ENSCAFG00000023556	13.22	0.0000	40.82	0.0000	-3.09	0.0012
DNASE2	deoxyribonuclease II, lysosomal	ENSCAFG00000017115	3.02	0.0002	4.24	0.0000	-1.73	0.1854
LOC100686047	CMRF35-like molecule-like	---	3.99	0.0134	16.12	0.0000	-4.03	0.0217
DHX58	DEXH (Asp-Glu-X-His) box polypeptide 58	ENSCAFG00000015720	4.49	0.0007	31.31	0.0000	-6.97	0.0001
MAP1A	microtubule-associated protein 1A	ENSCAFG00000012673	-1.70	0.0188	-3.18	0.0000	1.87	0.0121
RNASEL	ribonuclease L (2',5'-oligoisoadenylate synthetase-dependent)	ENSCAFG00000013121	3.49	0.0000	9.07	0.0000	-2.76	0.0003
LGMN	legumain	ENSCAFG00000010995	1.47	0.2538	2.52	0.0000	-1.91	0.0197
FGD2	FYVE, RhoGEF and PH domain containing 2	ENSCAFG00000001444	3.06	0.0012	2.29	0.0018	1.34	0.3906
NEK6	NIMA (never in mitosis gene a)-related kinase 6	ENSCAFG00000020225 /	2.50	0.0001	2.10	0.0000	1.19	0.4293
NPEPPS	aminopeptidase puromycin sensitive	ENSCAFG00000016644	-1.46	0.1801	-3.15	0.0000	2.16	0.0159
C20H19orf66	chromosome 20 open reading frame, human C19orf66	ENSCAFG00000017921	2.75	0.0000	7.38	0.0000	-2.69	0.0002
CENPF	centromere protein F, 350/400kDa (mitosin)	ENSCAFG00000012593	3.34	0.0001	-1.00	1.0000	3.34	0.0003
LOC100856585 //	protein SON-like /// SON DNA binding protein	---	143.07	0.0000	351.72	0.0000	-2.51	0.0125
XPO4	exportin 4	ENSCAFG00000007222	1.16	0.4077	2.01	0.0000	-1.73	0.0109
LOC475935 /// LO	interferon-induced transmembrane protein 1-like /// interferon-induced transmembrane protein 1-like	ENSCAFG00000006485	20.62	0.0000	2.05	0.1189	10.04	0.0012
TLR3	toll-like receptor 3	ENSCAFG00000007406	8.00	0.0001	5.87	0.0000	1.36	0.5310
FCGRT	Fc fragment of IgG, receptor, transporter, alpha	ENSCAFG00000003625	2.68	0.0026	3.24	0.0001	-1.40	0.4042
MOV10	Mov10, Moloney leukemia virus 10, homolog (mouse)	ENSCAFG00000013454	3.25	0.0000	5.21	0.0000	-1.71	0.0407
PHF11	PHD finger protein 11	ENSCAFG00000004351	1.37	0.0318	2.68	0.0000	-1.95	0.0002
TAP2	transporter 2, ATP-binding cassette, sub-family B (MDR/TAP)	ENSCAFG00000000823	2.09	0.0007	5.36	0.0000	-2.60	0.0007
MOBP	myelin-associated oligodendrocyte basic protein	---	-1.65	0.3265	-7.26	0.0000	4.61	0.0128
CTSC	cathepsin C	ENSCAFG00000004384 /	3.77	0.0043	6.62	0.0000	-1.76	0.2330
SLC1A1	solute carrier family 1 (neuronal/epithelial high affinity glutamate transporter, system Xag), member 1	ENSCAFG00000002067	2.43	0.0001	1.84	0.0005	1.33	0.1997
BCL2A1	BCL2-related protein A1	---	36.12	0.0000	77.17	0.0000	-2.46	0.1577
CMTM7	CKLF-like MARVEL transmembrane domain containing 7	ENSCAFG00000005397	1.75	0.0237	2.02	0.0006	-1.16	0.5719
SAA1	serum amyloid A1	---	99.99	0.0000	472.14	0.0000	-6.71	0.0002
IFI44L	interferon-induced protein 44-like	ENSCAFG00000020343	109.23	0.0000	419.93	0.0000	-4.40	0.0001
COL11A2	collagen, type XI, alpha 2	ENSCAFG00000000903	-2.35	0.0020	-3.05	0.0000	1.48	0.1580
NMI	N-myc (and STAT) interactor	ENSCAFG00000005659	2.15	0.0015	5.14	0.0000	-2.91	0.0021
C1R	complement component 1, r subcomponent	ENSCAFG00000014220	4.86	0.0000	11.76	0.0000	-2.42	0.0070
BATF2	basic leucine zipper transcription factor, ATF-like 2	ENSCAFG00000014017	1.04	0.8461	3.25	0.0000	-3.12	0.0000
MPDZ	multiple PDZ domain protein	ENSCAFG00000001498	-1.31	0.2230	2.28	0.0001	-2.99	0.0001
LOC100855762	E3 ubiquitin ligase RNF4-like	ENSCAFG00000013638	2.13	0.0007	2.94	0.0000	-1.38	0.1415
CD163	CD163 molecule	ENSCAFG00000013968	1.34	0.5525	10.76	0.0000	-8.91	0.0014
BACE1	beta-site APP-cleaving enzyme 1	ENSCAFG00000013069	-1.62	0.0152	-2.07	0.0000	1.28	0.2333
FCGR3A	Fc fragment of IgG, low affinity IIIa, receptor (CD16a)	---	11.38	0.0012	62.16	0.0000	-5.66	0.0227

SLC26A11	solute carrier family 26, member 11	ENSCAFG00000005654	-1.39	0.0371	-2.55	0.0000	1.94	0.0047
VIM	vimentin	ENSCAFG00000004529	4.96	0.0000	2.68	0.0001	1.72	0.0852
IGJ	immunoglobulin J polypeptide, linker protein for immunoglobulin alpha and mu polypeptides	ENSCAFG00000002911	3.82	0.0000	-1.17	0.3760	4.45	0.0000
BMP5	bone morphogenetic protein 5	ENSCAFG00000002345	3.38	0.0001	-1.31	0.1948	4.42	0.0000
DDO	D-aspartate oxidase	ENSCAFG00000003882	-1.19	0.3039	-2.12	0.0000	1.78	0.0034
WDR90	WD repeat domain 90	ENSCAFG00000019654	-2.08	0.0005	-1.79	0.0018	-1.27	0.2435
C1QA	complement component 1, q subcomponent, A chain	---	2.68	0.0893	9.06	0.0000	-3.50	0.0437
ISG20	interferon stimulated exonuclease gene 20kDa	ENSCAFG00000011525	2.87	0.0270	8.05	0.0000	-2.99	0.0465
LCK	lymphocyte-specific protein tyrosine kinase	ENSCAFG00000010625	2.28	0.0009	2.12	0.0003	1.14	0.6234
CTLA4	cytotoxic T-lymphocyte-associated protein 4	ENSCAFG00000012876	2.80	0.0000	1.02	0.8987	2.75	0.0000
C4A	complement component 4A (Rodgers blood group)	ENSCAFG00000000701	3.17	0.0002	5.25	0.0000	-3.23	0.0044
SYT7	synaptotagmin VII	ENSCAFG00000016121	-2.03	0.0237	-3.91	0.0000	1.67	0.1216
TMOD2	tropomodulin 2 (neuronal)	---	1.02	0.9344	-2.27	0.0001	2.32	0.0023
IFI6	interferon, alpha-inducible protein 6	---	2.57	0.0000	6.45	0.0000	-2.57	0.0000
CCL5	chemokine (C-C motif) ligand 5	ENSCAFG00000018171	71.11	0.0000	150.39	0.0000	-2.65	0.0485
MAN1A1	mannosidase, alpha, class 1A, member 1	ENSCAFG00000000945	2.86	0.0013	2.24	0.0014	1.28	0.4466
CXHXorf21	chromosome X open reading frame, human CXorf21	ENSCAFG00000013673	7.27	0.0000	4.11	0.0001	1.72	0.2142
TDRD7	tudor domain containing 7	ENSCAFG00000002416	1.83	0.0071	3.23	0.0000	-1.16	0.0187
CLIC1	chloride intracellular channel 1	ENSCAFG00000000621 /	2.61	0.0014	2.93	0.0000	-1.12	0.6913
FCGR1A	Fc fragment of IgG, high affinity Ia, receptor (CD64)	ENSCAFG00000011504	1.98	0.1743	5.24	0.0002	-2.65	0.0810
ATP1B2	ATPase, Na+/K+ transporting, beta 2 polypeptide	ENSCAFG00000016703	-2.17	0.0003	-1.66	0.0009	-1.24	0.2719
ASCL1	achaete-scute complex homolog 1 (Drosophila)	ENSCAFG00000007324	-2.37	0.0039	-4.16	0.0000	1.72	0.0634
NEFH	neurofilament, heavy polypeptide	---	-1.29	0.3628	-3.13	0.0000	2.42	0.0079
TEX14	testis expressed 14	ENSCAFG00000017556	2.69	0.0047	6.34	0.0000	-2.84	0.0083
LOC484897	EGF-like module-containing mucin-like hormone receptor-like 2-like	---	8.95	0.0000	11.01	0.0000	-1.25	0.6312
TGIF1	TGFB-induced factor homeobox 1	---	2.90	0.0023	2.67	0.0005	1.09	0.8048
STAT3	signal transducer and activator of transcription 3 (acute-phase response factor)	ENSCAFG00000015213	1.56	0.0213	2.10	0.0000	-2.08	0.0012
IRGM	immunity-related GTPase family, M	ENSCAFG00000012662	3.09	0.0157	12.71	0.0000	-4.10	0.0068
SP100	SP100 nuclear antigen	ENSCAFG00000010717	14.20	0.0000	9.77	0.0000	1.40	0.4833
CFI	complement factor I	ENSCAFG00000011462	10.06	0.0000	5.08	0.0000	1.96	0.1224
SLC25A48	solute carrier family 25, member 48	---	1.37	0.1697	3.03	0.0000	-2.22	0.0030
RASA3	RAS p21 protein activator 3	---	1.59	0.0210	2.13	0.0000	-1.34	0.1704
NT5C3	5'-nucleotidase, cytosolic III	---	1.43	0.1495	2.93	0.0000	-2.16	0.0048
SPTBN2	spectrin, beta, non-erythrocytic 2	ENSCAFG00000012306	-3.63	0.0007	-2.73	0.0006	-1.33	0.4384
EOMES	eomesodermin	ENSCAFG00000005510	-2.56	0.0130	-3.97	0.0000	1.55	0.2674
IER3	immediate early response 3	---	3.07	0.0002	3.36	0.0000	-2.33	0.0800
DNPEP	aspartyl aminopeptidase	ENSCAFG00000015399	1.20	0.2318	2.02	0.0000	-1.69	0.0035
LOC100856347	apoptosis-associated speck-like protein containing a CARD-like	ENSCAFG00000016865	2.67	0.0737	6.10	0.0008	-2.28	0.1655
GCH1	GTP cyclohydrolase 1	ENSCAFG00000014965	3.01	0.0132	4.19	0.0002	-1.39	0.4689
LAP3	leucine aminopeptidase 3	ENSCAFG00000015095	2.73	0.0001	3.34	0.0000	-1.22	0.3898
C5AR1	complement component 5a receptor 1	ENSCAFG00000004175	1.97	0.0422	4.28	0.0000	-2.17	0.0444
PLSCR1	phospholipid scramblase 1	ENSCAFG00000008181	1.95	0.0251	5.02	0.0000	-2.74	0.0014
GMFG	glia maturation factor, gamma	ENSCAFG00000005577	1.78	0.0215	2.15	0.0003	-1.21	0.4661
STOM	stomatin	---	2.75	0.0011	4.33	0.0000	-1.57	0.1441
RRBP1	ribosome binding protein 1 homolog 180kDa (dog)	ENSCAFG00000005479	2.50	0.0088	3.99	0.0000	-1.44	0.3085
TIMD4	T-cell immunoglobulin and mucin domain containing 4	---	3.51	0.0276	7.08	0.0001	-2.02	0.2429
MOXD1	monooxygenase, DBH-like 1	ENSCAFG00000000184	4.01	0.0007	3.33	0.0002	1.18	0.6767
IL7R	interleukin 7 receptor	---	5.85	0.0023	8.49	0.0000	-2.17	0.0958

HCLS1	hematopoietic cell-specific Lyn substrate 1	---	3.66	0.0007	3.93	0.0000	-1.07	0.8487
TNFSF10	tumor necrosis factor (ligand) superfamily, member 10	ENSCAFG00000015383	6.39	0.0000	7.07	0.0000	-1.33	0.5050
CYBB	cytochrome b-245, beta polypeptide (chronic granulomatous disease)	ENSCAFG00000013933	3.31	0.0109	5.71	0.0000	-1.90	0.1910
HLA-DMA	major histocompatibility complex, class II, DM alpha	ENSCAFG00000000848	4.48	0.0017	6.35	0.0000	-1.83	0.2566
AIFM3	apoptosis-inducing factor, mitochondrion-associated, 3	---	-1.73	0.0924	-2.60	0.0001	1.62	0.1145
CASP12	caspase 12 (gene/pseudogene)	ENSCAFG00000014864	7.63	0.0001	5.86	0.0000	1.30	0.5675
none	none	---	19.31	0.0000	-1.23	0.6530	23.76	0.0001
SAMD9L	sterile alpha motif domain containing 9-like	---	32.84	0.0000	54.14	0.0000	-1.79	0.1350
FYB	FYN binding protein	ENSCAFG00000023062	2.92	0.0009	3.16	0.0000	-1.08	0.7999
EFEMP2	EGF containing fibulin-like extracellular matrix protein 2	ENSCAFG00000013195	2.15	0.0002	1.69	0.0002	1.33	0.1510
EPSTI1	epithelial stromal interaction 1 (breast)	---	14.07	0.0000	20.63	0.0000	-1.85	0.3736
TOP2A	topoisomerase (DNA) II alpha 170kDa	ENSCAFG00000016090	18.38	0.0000	14.03	0.0000	1.31	0.5604
HLA-DQB1 /// LO	major histocompatibility complex, class II, DQ beta 1 /// HLA class II histocompatibility antigen, DQ beta 2 chain-like	ENSCAFG00000000814	14.09	0.0003	22.98	0.0000	-1.63	0.4813
ADA	adenosine deaminase	ENSCAFG00000009498	5.02	0.0000	2.93	0.0001	1.71	0.1073
IFIT2	interferon-induced protein with tetratricopeptide repeats 2	ENSCAFG00000009612	9.11	0.0000	24.02	0.0000	-2.64	0.0435
GNS	glucosamine (N-acetyl)-6-sulfatase	ENSCAFG00000000359	1.82	0.0151	2.35	0.0004	-1.42	0.2441
LCP1	lymphocyte cytosolic protein 1 (L-plastin)	ENSCAFG00000004491	3.37	0.0005	5.45	0.0004	-1.94	0.2688
LOC100855809	carbonic anhydrase 14-like	ENSCAFG00000011762	-1.50	0.2739	-4.50	0.0000	2.68	0.0195
EVI2B	ecotropic viral integration site 2B	ENSCAFG00000018623	3.29	0.0235	5.46	0.0002	-1.66	0.3589
LOC606875	interferon-inducible GTPase 1-like	---	29.82	0.0000	107.80	0.0000	-3.83	0.0052
LOC100855737	suppressor of cytokine signaling 2-like	ENSCAFG00000006180	1.20	0.4592	-2.50	0.0000	2.99	0.0003
none	none	---	3.53	0.0001	1.95	0.0027	1.81	0.0469
ACSL5	acyl-CoA synthetase long-chain family member 5	ENSCAFG00000010928	6.74	0.0000	6.97	0.0000	1.25	0.3712
LOC100856263	cholesterol 25-hydroxylase-like	---	2.48	0.0356	4.68	0.0001	-1.89	0.1684
CTRL	chymotrypsin-like	ENSCAFG00000020334	1.00	0.9996	3.78	0.0000	-4.18	0.0009
USP18	ubiquitin specific peptidase 18	ENSCAFG00000016252	15.92	0.0000	39.68	0.0000	-2.49	0.0103
CXCL10	chemokine (C-X-C motif) ligand 10	ENSCAFG00000008584	226.67	0.0000	385.62	0.0000	-1.75	0.3197
IL18BP	interleukin 18 binding protein	ENSCAFG00000005829	3.99	0.0004	4.57	0.0000	-1.20	0.6330
STAT2	signal transducer and activator of transcription 2, 113kDa	ENSCAFG00000000121	2.63	0.0003	4.57	0.0000	-1.74	0.0380
PNPT1	polyribonucleotide nucleotidyltransferase 1	ENSCAFG00000002891	1.73	0.0004	2.71	0.0000	-1.71	0.0058
SERPINA1	serpin peptidase inhibitor, clade A (alpha-1 antiproteinase, antitrypsin), member 1	ENSCAFG00000017646	3.26	0.0183	27.16	0.0000	-8.33	0.0004
GPC4	glypican 4	ENSCAFG00000018857	2.94	0.0003	1.59	0.0129	1.61	0.0641
DHRS3	dehydrogenase/reductase (SDR family) member 3	ENSCAFG00000016376	3.05	0.0000	2.59	0.0000	1.17	0.4886
HLA-DRB1	MHC class II DLA DRB1 beta chain	---	7.64	0.0005	10.27	0.0000	-1.28	0.6611
LOC100855667	ubiquitin-like protein ISG15-like	ENSCAFG00000019348	245.71	0.0000	928.35	0.0000	-3.78	0.0002
SHISA5	shisa homolog 5 (Xenopus laevis)	ENSCAFG00000012529	2.49	0.0001	3.99	0.0000	-1.81	0.0040
WARS	tryptophanyl-tRNA synthetase	ENSCAFG00000017906	1.95	0.0009	2.08	0.0000	-1.18	0.4073
LOC100856206	zinc finger CCCH-type antiviral protein 1-like	ENSCAFG00000004102	3.68	0.0001	7.07	0.0000	-2.20	0.0094
C1QB	complement component 1, q subcomponent, B chain	ENSCAFG00000014639	4.60	0.0169	27.47	0.0000	-6.09	0.0112
LOC606869 /// LC	Similar to Ig heavy chain V-III region VH26 precursor /// Similar to Ig heavy chain V-III region VH26 precursor /// Similar to Ig heavy chain V-III region VH26 precursor /// Similar to Ig heavy chain V-III region VH26 precursor /// Similar to Ig heavy chain V-III region VH26 precursor /// Similar to Ig heavy chain V-III region VH26 precursor /// Similar to Ig heavy chain V-III region VH26 precursor	---	6.95	0.0000	1.00	1.0000	6.95	0.0000
DAPP1	dual adaptor of phosphotyrosine and 3-phosphoinositides	ENSCAFG00000010571	2.48	0.0001	1.05	0.8683	2.42	0.0003
MX2	myxovirus (influenza virus) resistance 2 (mouse)	ENSCAFG00000010167	38.43	0.0000	147.59	0.0000	-3.84	0.0017
SLC2A5	solute carrier family 2 (facilitated glucose/fructose transporter), member 5	ENSCAFG00000019714	3.79	0.0096	8.10	0.0000	-2.14	0.1564
none	none	---	24.15	0.0000	-1.08	0.8526	26.17	0.0000
SP110	SP110 nuclear body protein	ENSCAFG00000010682	4.05	0.0002	4.60	0.0000	-1.74	0.0102
SERPINA3 /// SER	serpin peptidase inhibitor, clade A (alpha-1 antiproteinase, antitrypsin), member 3 /// serpin peptidase inhibitor, clade A (alpha-1 antiproteinase, antitrypsin), member 5	ENSCAFG00000017675	39.55	0.0000	74.03	0.0000	-2.07	0.3183

LOC476669	gamma-interferon-inducible-lysosomal thiol reductase-like	ENSCAFG00000014956	2.99	0.0144	4.50	0.0001	-1.50	0.3799
LOC100682747	transmembrane protein 229A-like	ENSCAFG00000001762	-2.66	0.0111	-3.73	0.0000	1.47	0.3116
CD48	CD48 molecule	ENSCAFG00000012585	10.22	0.0001	15.69	0.0000	-2.61	0.1350
LOC100856220	neurofilament light polypeptide-like	---	-1.19	0.4799	-3.00	0.0000	2.52	0.0018
none	none	---	4.21	0.0000	1.09	0.4218	3.56	0.0000
MBP	myelin basic protein	---	-1.14	0.7158	-4.34	0.0000	3.80	0.0024
CHRNB1	cholinergic receptor, nicotinic, beta 1 (muscle)	ENSCAFG00000016315	1.40	0.2632	4.34	0.0000	-3.09	0.0018
CD74	CD74 molecule, major histocompatibility complex, class II invariant chain	---	7.80	0.0004	9.89	0.0000	-1.63	0.4610
PSME2	proteasome (prosome, macropain) activator subunit 2 (PA28 beta)	ENSCAFG00000011966	2.09	0.0000	3.99	0.0000	-2.04	0.0010
GLDN	gliomedin	ENSCAFG00000015360	63.21	0.0000	22.62	0.0000	2.78	0.1181
CHI3L1	chitinase 3-like 1 (cartilage glycoprotein-39)	ENSCAFG00000010274	45.33	0.0000	113.98	0.0000	-4.11	0.0219
ANXA2	annexin A2	ENSCAFG00000016686	6.99	0.0000	5.27	0.0000	1.37	0.3525
IRAK3	interleukin-1 receptor-associated kinase 3	ENSCAFG00000000374	2.38	0.0000	1.02	0.0002	1.38	0.0713
HERC5	HECT and RLD domain containing E3 ubiquitin protein ligase 5	ENSCAFG00000009800	14.71	0.0000	51.33	0.0000	-3.49	0.0099
TRANK1	tetratricopeptide repeat and ankyrin repeat containing 1	ENSCAFG00000004776	1.27	0.4150	4.22	0.0000	-3.23	0.0008
MOCOS	molybdenum cofactor sulfurase	ENSCAFG00000017801	1.43	0.0942	2.43	0.0001	-1.48	0.0932
LOC100855872	interferon regulatory factor 1-like	ENSCAFG00000000851	14.07	0.0000	30.13	0.0000	-3.17	0.0047
LGALS3BP	lectin, galactoside-binding, soluble, 3 binding protein	ENSCAFG00000005537	-1.01	0.9752	3.11	0.0000	-2.95	0.0008
LOC474866	Similar to Antigen peptide transporter 1	ENSCAFG00000000832	5.57	0.0000	12.97	0.0000	-3.10	0.0035
DLA-12 /// DLA-64	MHC class I DLA-12 /// MHC class I DLA-64 /// MHC class I DLA-88	ENSCAFG00000000487 /	8.82	0.0000	19.16	0.0000	-2.77	0.1599
KIAA1456	KIAA1456 ortholog	ENSCAFG00000006759	-4.18	0.0005	-2.89	0.0008	-1.45	0.3502
PARP15	poly (ADP-ribose) polymerase family, member 15	ENSCAFG00000011953	10.45	0.0000	8.80	0.0000	1.19	0.7355
CTSB	cathepsin B	ENSCAFG00000007934	2.10	0.0033	3.74	0.0000	-2.36	0.0276
MARCH11	membrane-associated ring finger (C3HC4) 11	ENSCAFG00000019105	-1.26	0.0086	-2.21	0.0000	1.12	0.3567
CHEK2	checkpoint kinase 2	ENSCAFG00000011919	-1.00	0.9949	-2.41	0.0001	2.38	0.0039
IGF2BP3	insulin-like growth factor 2 mRNA binding protein 3	ENSCAFG00000002766	1.01	0.2832	1.24	0.1024	-1.44	0.8440
GCA	grancalcin, EF-hand calcium binding protein	ENSCAFG00000010470	3.97	0.0010	6.12	0.0000	-1.54	0.2944
MT1H	metallothionein 1H	ENSCAFG00000023759	1.72	0.0078	2.06	0.0000	-1.19	0.3979
FADS1 /// LOC612	fatty acid desaturase 1 /// fatty acid desaturase 1-like	ENSCAFG00000025083	-1.54	0.0472	-2.24	0.0001	1.46	0.1241
BPI	bactericidal/permeability-increasing protein	ENSCAFG00000008901	2.14	0.0898	8.64	0.0000	-6.13	0.0029
FAM54A	family with sequence similarity 54, member A	ENSCAFG00000000244	2.76	0.0000	2.13	0.0000	1.18	0.4403
RAC2	ras-related C3 botulinum toxin substrate 2 (rho family, small GTP binding protein Rac2)	---	11.04	0.0000	5.24	0.0000	2.18	0.0920
CFLAR	CASP8 and FADD-like apoptosis regulator	---	2.08	0.0036	6.05	0.0000	-2.84	0.0508
RALGPS2	Ral GEF with PH domain and SH3 binding motif 2	ENSCAFG00000013981	-2.85	0.0001	-1.61	0.0008	-1.48	0.1219
LOC609880	Similar to Kinesin-like protein KIFC2	---	-1.96	0.0044	-2.04	0.0002	1.04	0.8683
SLC16A13	solute carrier family 16, member 13 (monocarboxylic acid transporter 13)	---	1.96	0.0016	2.48	0.0000	-1.27	0.2617
MX1	myxovirus (influenza virus) resistance 1, interferon-inducible protein p78 (mouse)	ENSCAFG00000010172	7.55	0.0000	15.98	0.0000	-2.17	0.0015
LOC612422	guanylate-binding protein 4-like	---	4.91	0.0001	3.85	0.0000	1.27	0.5308
WDFY4	WDFY family member 4	ENSCAFG00000006576	7.47	0.0000	3.17	0.0001	2.35	0.0243
TRIM21	tripartite motif containing 21	---	1.84	0.1127	6.87	0.0000	-3.74	0.0034
CCL2	chemokine (C-C motif) ligand 2	ENSCAFG00000018349	8.28	0.0004	14.61	0.0000	-1.76	0.3281
LOC612521	uncharacterized LOC612521	---	-2.42	0.0010	-2.25	0.0002	-1.07	0.7879
JAK2	Janus kinase 2	---	2.17	0.0005	2.34	0.0000	-1.08	0.7224
OAS1	2'-5'-oligoadenylate synthetase 1, 40/46kDa	ENSCAFG00000023556	13.57	0.0000	46.01	0.0000	-4.42	0.0003
LOC100684769	immunity-related GTPase family M protein 1-like	ENSCAFG00000000497	37.83	0.0000	64.69	0.0000	-1.82	0.1784
FGG	fibrinogen gamma chain	ENSCAFG00000008440	123.91	0.0000	59.51	0.0000	2.22	0.1979
GSDMD	gasdermin D	ENSCAFG00000001301	1.60	0.0685	2.72	0.0000	-1.70	0.0594
LOC100855594 //	uncharacterized LOC100855594 /// uncharacterized LOC100855788	ENSCAFG00000023190	49.54	0.0000	1.13	0.7224	45.59	0.0000

NEFM	neurofilament, medium polypeptide	---	-1.32	0.5179	-3.78	0.0000	3.13	0.0014
DLA-DRA	MHC class II DR alpha chain	ENSCAFG00000000803	6.78	0.0023	8.44	0.0001	-1.23	0.7395
LOC612054	uncharacterized LOC612054	---	42.16	0.0000	-1.10	0.5666	45.87	0.0000
LOC100682772 //	uncharacterized LOC100682772 /// leucine-rich repeat-containing protein 37A3-like /// leucine-rich repeat-containing protein 37A2-like	ENSCAFG00000013742	1.58	0.3538	-8.10	0.0000	12.46	0.0001
LOC100855741	beta-2-microglobulin-like	ENSCAFG00000013633	4.93	0.0000	6.33	0.0000	-1.28	0.2175
LOC100683822 //	immunoglobulin lambda-like polypeptide 5-like /// uncharacterized LOC100856278 /// immunoglobulin lambda-like polypeptide 5-like /// immunoglobulin lambda-like polypeptide 5-like /// immunoglobulin lambda-like polypeptide 5-like /// immunoglobulin lambda-like polypeptide 5-like /// immunoglobulin lambda-like polypeptide 5-like	ENSCAFG00000014139 /	572.06	0.0000	-1.61	0.6150	710.04	0.0001
C30H15orf48	chromosome 30 open reading frame, human C15orf48	---	9.77	0.0009	12.28	0.0000	-1.75	0.7321
CMBL	carboxymethylenebutenolidase homolog (Pseudomonas)	ENSCAFG00000010064	-1.71	0.0497	-2.86	0.0000	1.75	0.0425
LRMP	lymphoid-restricted membrane protein	ENSCAFG00000011458	3.15	0.0001	1.10	0.6192	2.87	0.0004
CDKN2C	cyclin-dependent kinase inhibitor 2C (p18, inhibits CDK4)	ENSCAFG00000003898	1.81	0.0060	2.94	0.0000	-1.63	0.0323
CRIP1	cysteine-rich protein 1 (intestinal)	ENSCAFG00000018440	2.78	0.0038	2.96	0.0002	-1.98	0.3421
MYD88	myeloid differentiation primary response gene (88)	---	2.56	0.0002	5.95	0.0000	-2.46	0.0012
STX11	syntaxin 11	ENSCAFG00000000322	2.26	0.0228	4.00	0.0000	-1.77	0.1341
CTSS	cathepsin S	ENSCAFG00000012086	2.48	0.0018	4.81	0.0000	-2.22	0.0736
LY96	lymphocyte antigen 96	---	10.79	0.0000	13.15	0.0000	-1.22	0.7032
SETD7	SET domain containing (lysine methyltransferase) 7	ENSCAFG00000003703	-1.29	0.0038	-2.01	0.0000	1.26	0.1594
TNFRSF14	tumor necrosis factor receptor superfamily, member 14	---	4.11	0.0006	3.98	0.0000	-1.08	0.8335
PLCD1	phospholipase C, delta 1	ENSCAFG00000004931	4.24	0.0006	3.58	0.0005	1.35	0.4696
CD86	CD86 molecule	ENSCAFG00000011751	1.90	0.1514	4.03	0.0004	-2.12	0.1266
LOC100856258	golgi-associated plant pathogenesis-related protein 1-like	ENSCAFG00000002284	6.40	0.0001	6.43	0.0000	1.05	0.9138
LOC606869 /// LC	Similar to Ig heavy chain V-III region VH26 precursor /// Similar to Ig heavy chain V-III region VH26 precursor /// Similar to Ig heavy chain V-III region VH26 precursor /// Similar to Ig heavy chain V-III region VH26 precursor /// Similar to Ig heavy chain V-III region VH26 precursor	---	3.35	0.0000	1.00	1.0000	3.35	0.0001
GSK3B	glycogen synthase kinase 3 beta	ENSCAFG00000011122	-1.89	0.0052	-2.02	0.0002	1.07	0.7742
GPR180	G protein-coupled receptor 180	ENSCAFG00000005334	-1.45	0.0982	-2.49	0.0000	1.72	0.0298
CD40	CD40 molecule, TNF receptor superfamily member 5	---	2.71	0.0005	4.13	0.0000	-1.46	0.1759
SHC2	SHC (Src homology 2 domain containing) transforming protein 2	ENSCAFG00000019724	-1.77	0.0000	-2.17	0.0000	1.22	0.1187
SMPDL3A	sphingomyelin phosphodiesterase, acid-like 3A	ENSCAFG00000001002	6.17	0.0000	10.03	0.0000	-1.66	0.1812
GRM3	glutamate receptor, metabotropic 3	---	-1.62	0.0096	-2.04	0.0000	1.25	0.2420
OASL	2'-5'-oligoadenylate synthetase-like	ENSCAFG00000010511	33.62	0.0000	118.26	0.0000	-4.45	0.0021
DGKZ	diacylglycerol kinase, zeta	ENSCAFG00000009248	-2.30	0.0008	-1.85	0.0012	-1.24	0.3674
BTG3	BTG family, member 3	ENSCAFG00000008295	2.83	0.0087	3.98	0.0001	-1.41	0.3984
NLRC5	NLR family, CARD domain containing 5	ENSCAFG00000008933	1.01	0.0127	3.92	0.0000	-2.06	0.0106
CMPK2	cytidine monophosphate (UMP-CMP) kinase 2, mitochondrial	---	12.12	0.0000	46.23	0.0000	-4.78	0.0015
IRF9	interferon regulatory factor 9	ENSCAFG00000012007	3.38	0.0000	11.44	0.0000	-3.38	0.0000
SCD	stearoyl-CoA desaturase (delta-9-desaturase)	---	-2.32	0.0164	-3.48	0.0000	1.90	0.0016
LOC100856405	tubulin alpha-1C chain-like	---	4.39	0.0000	3.23	0.0000	1.36	0.2200
ZNFX1	zinc finger, NFX1-type containing 1	ENSCAFG00000011408	1.72	0.0017	3.96	0.0000	-3.20	0.0004
FOLR2	folate receptor 2 (fetal)	ENSCAFG00000005768	2.60	0.0002	2.66	0.0000	-1.20	0.5302
RASGRP2	RAS guanyl releasing protein 2 (calcium and DAG-regulated)	ENSCAFG00000014309	1.09	0.6349	-2.14	0.0000	2.44	0.0001
RAB13	RAB13, member RAS oncogene family	ENSCAFG00000017389	2.00	0.0016	2.11	0.0011	1.19	0.5414
AGFG2	ArfGAP with FG repeats 2	ENSCAFG00000014351	1.25	0.4100	2.88	0.0000	-2.42	0.0083
VCAM1	vascular cell adhesion molecule 1	ENSCAFG00000020004	3.52	0.0007	3.15	0.0002	1.15	0.7077
PARP9	poly (ADP-ribose) polymerase family, member 9	ENSCAFG00000011940	9.32	0.0000	29.63	0.0000	-3.18	0.0049
MZB1	marginal zone B and B1 cell-specific protein	ENSCAFG00000005693	9.56	0.0000	-1.02	0.9344	10.01	0.0000
PARP4	poly (ADP-ribose) polymerase family, member 4	ENSCAFG00000007375	4.29	0.0000	3.91	0.0000	-1.46	0.0893
IFIH1	interferon induced with helicase C domain 1	ENSCAFG00000010438	20.76	0.0000	34.08	0.0000	-1.63	0.2355

TLR8	toll-like receptor 8	ENSCAFG00000023498	1.64	0.1233	4.44	0.0000	-2.72	0.0068
FLNC	filamin C, gamma	---	8.16	0.0000	5.71	0.0000	1.91	0.0014
none	none	---	2.60	0.0779	2.83	0.0004	-1.36	0.8086
EGOT	eosinophil granule ontogeny transcript (non-protein coding)	ENSG00000235947	3.70	0.0000	3.28	0.0490	-0.26	0.0026
CD300LD	CD300 molecule-like family member d	ENSG00000204345	1.24	0.0125	2.83	0.0004	-1.36	0.8084
C2CD4D	C2 calcium-dependent domain containing 4D	ENSG00000225556	2.72	0.0327	1.83	0.0043	-1.60	0.0066
GLYATL1	glycine-N-acyltransferase-like 1	ENSG00000166840	7.62	0.0231	6.2345	0.0004	-3.11	0.0096
AGAP1-IT1	AGAP1 intronic transcript 1 (non-protein coding)	ENSG00000235529	1.05	0.0779	1.23	0.0634	-1.09	0.0083
MICA	MHC class I polypeptide-related sequence A	ENSG00000204520	-7.51	0.0301	-9.41	0.0231	2.53	0.0246
ATF5	activating transcription factor 5	ENSG00000169136	2.79	0.0779	-3.52	0.0044	1.87	0.0085
CADM2-AS1	CADM2 antisense RNA 1 (non-protein coding)	ENSG00000239519	1.47	0.0976	1.02	0.0065	1.86	0.0496
AOAH-IT1	AOAH intronic transcript 1 (non-protein coding)	ENSG00000230539	-2.45	0.0499	1.85	0.0004	-1.09	0.0000
TNFRSF1B	tumor necrosis factor receptor superfamily, member 1B	ENSG00000028137	12.60	0.0541	26.73	0.0003	-6.48	0.0216
MTPAP	mitochondrial poly(A) polymerase	ENSG00000107951	-2.62	0.0031	-1.88	0.0006	-1.33	0.0264
MTRR	5-methyltetrahydrofolate-homocysteine methyltransferase reductase	ENSG00000124275	2.22	0.0123	2.14	0.0735	-1.04	0.0062